RESISTANCE TO SALINITY AND WATER SCARCITY IN HIGHER PLANTS. INSIGHTS FROM EXTREMOPHILES AND STRESS-ADAPTED PLANTS: TOOLS, DISCOVERIES AND FUTURE PROSPECTS

EDITED BY: Ruth Grene, Nicholas J. Provart and José M. Pardo

PUBLISHED IN: Frontiers in Plant Science

frontiers Research Topics

frontiers

ISSN 1664-8714
ISBN 978-2-88945-961-2
DOI 10.3389/978-2-88945-961-2

About Frontiers

Frontiers is more than just an open-access publisher of scholarly articles: it is a pioneering approach to the world of academia, radically improving the way scholarly research is managed. The grand vision of Frontiers is a world where all people have an equal opportunity to seek, share and generate knowledge. Frontiers provides immediate and permanent online open access to all its publications, but this alone is not enough to realize our grand goals.

Frontiers Journal Series

The Frontiers Journal Series is a multi-tier and interdisciplinary set of open-access, online journals, promising a paradigm shift from the current review, selection and dissemination processes in academic publishing. All Frontiers journals are driven by researchers for researchers; therefore, they constitute a service to the scholarly community. At the same time, the Frontiers Journal Series operates on a revolutionary invention, the tiered publishing system, initially addressing specific communities of scholars, and gradually climbing up to broader public understanding, thus serving the interests of the lay society, too.

Dedication to Quality

Each Frontiers article is a landmark of the highest quality, thanks to genuinely collaborative interactions between authors and review editors, who include some of the world's best academicians. Research must be certified by peers before entering a stream of knowledge that may eventually reach the public - and shape society; therefore, Frontiers only applies the most rigorous and unbiased reviews.
Frontiers revolutionizes research publishing by freely delivering the most outstanding research, evaluated with no bias from both the academic and social point of view. By applying the most advanced information technologies, Frontiers is catapulting scholarly publishing into a new generation.

What are Frontiers Research Topics?

Frontiers Research Topics are very popular trademarks of the Frontiers Journals Series: they are collections of at least ten articles, all centered on a particular subject. With their unique mix of varied contributions from Original Research to Review Articles, Frontiers Research Topics unify the most influential researchers, the latest key findings and historical advances in a hot research area! Find out more on how to host your own Frontiers Research Topic or contribute to one as an author by contacting the Frontiers Editorial Office: researchtopics@frontiersin.org

RESISTANCE TO SALINITY AND WATER SCARCITY IN HIGHER PLANTS. INSIGHTS FROM EXTREMOPHILES AND STRESS-ADAPTED PLANTS: TOOLS, DISCOVERIES AND FUTURE PROSPECTS

Topic Editors:
Ruth Grene, Virginia Tech, United States
Nicholas J. Provart, University of Toronto, Canada
José M. Pardo, Instituto de Bioquímica Vegetal y Fotosíntesis, Spain

Citation: Grene, R., Provart, N. J., Pardo, J. M., eds. (2019). Resistance to Salinity and Water Scarcity in Higher Plants. Insights From Extremophiles and Stress-Adapted Plants: Tools, Discoveries and Future Prospects. Lausanne: Frontiers Media. doi: 10.3389/978-2-88945-961-2

Table of Contents

frontiers in Plant Science

EDITORIAL
published: 02 April 2019
doi: 10.3389/fpls.2019.00373

Editorial: Resistance to Salinity and Water Scarcity in Higher Plants. Insights From Extremophiles and Stress-Adapted Plants: Tools, Discoveries and Future Prospects

Ruth Grene[1]*, *Nicholas J. Provart*[2] *and José M. Pardo*[3]

[1] Department of Plant Pathology, Physiology, and Weed Science, College of Agriculture and Life Sciences, Virginia Tech, Blacksburg, VA, United States, [2] Department of Cell and Systems Biology, University of Toronto, Toronto, ON, Canada, [3] Instituto de Bioquímica Vegetal y Fotosíntesis, Seville, Spain

Keywords: salinity, water stress, resistance, adaptation, extremophiles

OPEN ACCESS

Edited by:
Lam-Son Tran,
RIKEN, Japan

Reviewed by:
Kentaro Nakaminami,
RIKEN, Japan
Paul Mike Hasegawa,
Purdue University, United States

***Correspondence:**
Ruth Grene
grene@vt.edu

Specialty section:
This article was submitted to Plant Abiotic Stress, a section of the journal Frontiers in Plant Science

Received: *30 January 2019*
Accepted: *11 March 2019*
Published: *02 April 2019*

Citation:
Grene R, Provart NJ and Pardo JM (2019) Editorial: Resistance to Salinity and Water Scarcity in Higher Plants. Insights From Extremophiles and Stress-Adapted Plants: Tools, Discoveries and Future Prospects. Front. Plant Sci. 10:373. doi: 10.3389/fpls.2019.00373

Editorial on the Research Topic

Resistance to Salinity and Water Scarcity in Higher Plants. Insights From Extremophiles and Stress-Adapted Plants: Tools, Discoveries and Future Prospects

Abiotic stresses, such as excessive salinity and low water availability, have always presented major barriers to achieving high biomass and full yield potential in crops. Global climate change, with attendant increases in the severity of these abiotic stresses, will require directed adaptations of crop species on an unprecedented scale in order to sustain agricultural productivity. Current, and rapidly expanding, information on genome structure and function, primarily, but not exclusively, in model angiosperms, provides a starting point for a heightened understanding of genomic responses to drought and/or salt stress, within and across species. A crucial component that is leading to an acceleration in our understanding of stress responses is the ability to sequence whole genomes more rapidly and relatively inexpensively, and to begin to interpret the data that are accumulating, although such analyses are still very much in the beginning stages.

Superior stress tolerance may be due to the nature of defense-related protein-coding genes, expanded gene families of stress proteins, or the "stress-readiness" of tolerant species/ecotypes. This last mechanism—stress-readiness—may be due to stress-independent, constitutively higher expression of key "defense" genes through primed signaling networks or due to specific transcription factors, the role of post-transcriptional processes, such as alternative splicing, and combinations thereof (Haak et al., 2018). Lest this field fall into the trap of the "drunk looking under the streetlight for his keys" (that is, searching in easily studied areas), we must keep in mind that the discovery of novel mechanisms, novel gene family members, and novel signaling pathways is a distinct possibility as the combined analytical power of sequencing and data mining increases.

Filichkin et al. have conducted a comprehensive study, using both RNA-Seq and Iso-Seq, of alternative splicing events that occur in response to drought, heat and temperature stress in root, xylem and leaf tissue of poplar. They identified both stress-responsive isoforms that responded to each of the stresses that were tested, and isoforms that were unique to each of the three abiotic stresses. Interestingly, extensive stress-induced intron retention was detected in the data set, with the imposition of specific stresses being associated, in some cases, with an increase in fully spliced

mRNAs, at the expense of isoforms that had retained introns, or the converse. Tissue specificity with respect to splicing events was also found. Isoforms encoding regulatory proteins showed differential intron retention (DIR), including some known poplar splicing factors. Additionally, co-regulation of DIR events occurred as a result of stress imposition. Non-coding mRNAs were also spliced, which brings the question of whether the differential splicing aims to enlarge the repertoire of cellular proteins or the physical presence of introns in the genome promotes survival under stress conditions by alternative mechanisms, as recently shown for the starvation response of the yeast *Saccharomyces cerevisiae* (Parenteau et al., 2019). Potentially, much more information lies in this large and very valuable dataset concerning the role of specific splice variants in known and novel stress response pathways. The data set is available to the public at Poplar Interactome GBrowse.

In another molecular study in this special topic, Mo et al. studied cassava (*Manihot esculenta*), which is an important staple food for around 800 million people. It is tolerant to environmental stresses such as drought and heat. Specifically, the authors cloned gene family members from the CBLs and CIPKs (calcineurin B-like proteins and CBL-interacting protein kinases, respectively, which are known to be involved in calcium-mediated stress signaling) and examined their expression patterns in response to different environmental stresses. The authors also tested whether pairs of the 8 CBLs and 25 CIPKs cloned for yeast two-hybrid analysis could interact in a yeast two-hybrid system. The authors also elegantly used a yeast-based system to reconstitute a functional SOS pathway (Quintero et al., 2002) and to show that co-expression of the cassava proteins SOS1, CBL10, and CIPK24 restored salt tolerance in transgenic yeast. These data recall previous findings in *A. thaliana* (Quan et al., 2007) and provide further evidence of the high degree of evolutionary conservation in stress-related signaling across plant species.

In the case of species that are closely related to mesophytes (plants that do not possess specific adaptation mechanisms for survival in extreme conditions) or ecotypes within species, their relatedness to better-studied close relatives increases the likelihood of discovering the genetic bases for their relatively superior stress resistance. Thus, these species or ecotypes present a rich potential resource for the identification of genes, processes, and pathways that confer this superior stress resistance. The coming together of more "classical" approaches such as QTL analysis with our increasing understanding of the genes and associated mechanisms that underlie stress responses in plants has made possible the identification of specific genes that contribute to stress tolerance, insights into details of known pathways, and, sometimes, the discovery of novel stress resistance phenomena. One approach to uncovering the mechanisms that underlie superior stress resistance lies in the study of these "extremophile" species, and ecotypes within species, that are adapted to thrive in more stressful environments than their near relatives.

Extremophiles have emerged in many plant families, often, in the case of crop plants, ecotypes or species that are closely related to less tolerant species of agronomic importance. The focus of Quan et al.'s study was to show that wild rice, in this case, a salt-tolerant line of *Oryza rufipogon* Griff, could be used as a source to improve the salt tolerance of a cultivated variety of *O. sativa* ssp. Japonica, using genome resequencing of sensitive and tolerant lines, as well as tolerant hybrid offspring combined with QTL analysis to identify, where possible, the basis for increased tolerance. Since salt tolerance is a polygenic trait, much remains to be understood about its mechanistic basis. Nine QTLs for salt tolerance were identified by Quan et al. which included, for example, candidate genes such as *OsSKC1,* a sodium ion transporter, in addition to other ion transporters and many transcription factors whose role in salt tolerance is not yet well understood. Such data constitute a rich source for further exploration of the complexity of salt tolerance at the mechanistic level.

The work of Prusty et al. reveals an interesting, and perhaps unexpected mechanism, of "tissue tolerance" in some wild relatives of cultivated rice that exhibited relatively high salt tolerance. A tolerant tissue is defined as one which continues to function even in the presence of high levels of sodium, as opposed to sensitive tissues, which may co-exist in the same organism, which lack this capacity. Those cultivated rice cultivars that scored as salt tolerant were shown by Prusty et al. not to possess tissue tolerance, by this definition, whereas the tolerant wild rice species were tissue tolerant, specifically with respect to their shoots, but not their roots. The cells of the shoots of the wild rice species appeared to be able to sequester large amounts of sodium in their vacuoles, thus protecting the cytosol from toxic effects. This ability may be due to the action of specific members of the *NHX* gene family that evolved in wild rice, and were lost with cultivation, or to hitherto undiscovered mechanisms that bring about the sequestration of large amounts of sodium in the vacuole of the shoots of these wild rice genotypes. Another example of tissue tolerance is the extremophile xerophytic Asiatic shrub *Zygophyllum xanthoxylum,* studied by Xi et al. Like the salt tolerant wild rice studied by Prusty et al., this plant also accumulates sodium ion in its leaves, and in fact, under salt stress, tolerance increased, as measured by physiological traits, among them, expanded mesophyll cell size and increased ability to store water. More work is needed to pinpoint the genetic bases of the phenomenon of tissue tolerance, but these findings illustrate the possibility of discovering additional potential sources of salt tolerance.

Chen et al. also used a wild relative, in their case, of soybean, to identify potential regulators of alkali and salt stresses. This wild relative, *Glycine soja*, has the favorable trait of exhibiting superior tolerance to salt-alkali stress. The authors looked at 56 "response regulator" genes (GsRRs), which in previous studies were shown to be involved in diverse abiotic stresses. After grouping the genes into 5 subclasses, the authors examined transcriptional profiles of the genes in response to alkali stress and showed that the A1 and A2 subclass genes exhibit higher transcriptional levels than the B subclass genes. The response of GsRR2a in the A1 subclass was opposite for salt stress, however. In a nice use of Arabidopsis to test the function of the GsRRs, Chen et al. overexpressed GsRR2a in

Arabidopsis and found that tolerance to alkali, but not salt, was increased.

Moving more into the genome-environment association field, Cortés and Blair used genotyping by sequencing of 86 geo-referenced wild accession of common bean, *Phaseolus vulgaris*, to discover single nucleotide polymorphisms. The authors then quantified allelic associations with a bioclimatic-based drought index under different models. For their optimum model, 115 SNPs in 90 regions across all 11 common bean chromosomes were associated with the bioclimatic-based drought index. A phototropic-responsive *NPH3* gene and a gene coding for an ankyrin repeat-containing protein were identified as potential drought tolerance candidates, but signatures of natural selection in these and other SNP-associated regions suggest that while drought tolerance might obviously be advantageous under drought conditions, it could be detrimental under humid conditions. It's complicated!

Last, Ulrike Bechtold from the University of Essex provides a mini-review on improving drought tolerance for this research topic. She points out that in spite of the identification of many desiccation inducible genes in dozens of studies in xerophytes or model species, there are few "gene-to-field" translational examples of genes that have resulted in improved crop performance under drought. She addresses the longstanding arguments between ecophysiologists who are studying drought tolerant extremophiles and molecular biologists who work with model species on how to "drought-proof" crops in the future. Also discussed are the different kinds of strategies (tolerance or avoidance) that plants use to survive drought and the occurrence of lineage-specific genes and non-coding RNAs in some of the extremophiles.

We feel that this collection of eight articles highlights a number of interesting avenues for exploration in the context of using natural variation and extremophiles to better understand how we can improve crops to be less thirsty and more tolerant of salt stress. Further improvements and price decreases in next generation sequencing technologies will enable more genome-environment kinds of studies with wild relatives of crop plants to be undertaken. Networks of interactions can be determined using other high throughput technologies. Better understanding of physiological responses will also play a key role.

AUTHOR CONTRIBUTIONS

All authors listed edited the manuscript, contributed to the Research Topic and wrote the Editorial.

ACKNOWLEDGMENTS

NSF grants DBI-1062472 and MCB-1052145 and the Genomics, Bioinformatics, and Computational Biology doctoral program at Virginia Tech (RG); The Virginia Agricultural Experiment Station and the Hatch Program of NIFA, USDA (RG); grants BFU2015-64671-R and BIO2016-81957-REDT from AEI-MINECO, co-financed by the European Regional Development Fund (JP); SSAC grant PJ01318205 from the Rural Development Administration, Republic of Korea (JP); NP was funded by a grant from NSERC.

REFERENCES

Haak, D. C., Fukao, T., Grene, R., Hua, Z., Ivanov, R., Perrella, G., et al. (2018). Multilevel regulation of abiotic stress responses in plants. *Front Plant Sci.* 8:1564. doi: 10.3389/fpls.2017.01564

Parenteau, J., Maignon, L., Berthoumieux, M., Catala, M., Gagnon, V., and Abou Elela, S. (2019). Introns are mediators of cell response to starvation. *Nature* 565, 612–617 doi: 10.1038/s41586-018-0859-7

Quan, R., Lin, H., Mendoza, I., Zhang, Y., Cao, W., Yang, Y., et al. (2007). SCABP8/CBL10, a putative calcium sensor, interacts with the protein kinase SOS2 to protect Arabidopsis shoots from salt stress. *Plant Cell* 19, 1415–1431. doi: 10.1105/tpc.106.042291

Quintero, F. J., Ohta, M., Shi, H., Zhu, J. K., and Pardo, J. M. (2002). Reconstitution in yeast of the Arabidopsis SOS signaling pathway for Na^+ homeostasis. *Proc. Natl. Acad. Sci. U.S.A.* 99, 9061–9066. doi: 10.1073/pnas.132092099

Conflict of Interest Statement: The authors declare that the research was conducted in the absence of any commercial or financial relationships that could be construed as a potential conflict of interest.

frontiers in Plant Science

ORIGINAL RESEARCH
published: 20 November 2018
doi: 10.3389/fpls.2018.01678

Sodium-Related Adaptations to Drought: New Insights From the Xerophyte Plant *Zygophyllum xanthoxylum*

Jie-Jun Xi[1], Hong-Yu Chen[1], Wan-Peng Bai[1], Rong-Chen Yang[1], Pei-Zhi Yang[1], Ru-Jin Chen[2], Tian-Ming Hu[1] and Suo-Min Wang[3]**

[1] College of Grassland Agriculture, Northwest A&F University, Xianyang, China, [2] Noble Research Institute, Ardmore, OK, United States, [3] State Key Laboratory of Grassland Agro-Ecosystems, College of Pastoral Agriculture Science and Technology, Lanzhou University, Lanzhou, China

Understanding the unusual physiological mechanisms that enable drought tolerance in xerophytes will be of considerable benefit because of the potential to identify novel and key genetic elements for future crop improvements. These plants are interesting because they are well-adapted for life in arid zones; *Zygophyllum xanthoxylum*, for example, is a typical xerophytic shrub that inhabits central Asian deserts, accumulating substantial levels of sodium (Na^+) in its succulent leaves while growing in soils that contain very low levels of this ion. The physiological importance of this unusual trait to drought adaptations remains poorly understood, however. Thus, 2-week-old *Z. xanthoxylum* plants were treated with 50 mM NaCl (Na) for 7 days in this study in order to investigate their drought tolerance, leaf osmotic potential (Ψ_S) related parameters, anatomical characteristics, and transpiration traits. The results demonstrated that NaCl treatment significantly enhanced both the survivability and durability of *Z. xanthoxylum* plants under extreme drought conditions. The bulk of the Na^+ ions encapsulated in plants was overwhelmingly allocated to leaves rather than roots or stems under drought conditions; thus, compared to the control, significantly more Na^+ compared to other solutes such as K^+, Ca^{2+}, Cl^-, sugars, and proline accumulated in the leaves of NaCl-treated plants and led to a marked decrease (31%) in leaf Ψ_S. In addition, the accumulation of Na^+ ions also resulted in mesophyll cell enlargement and leaf succulence, enabling the additional storage of water; Na^+ ions also reduced the rate of water loss by decreasing stomatal density and down-regulating stomatal aperture size. The results of this study demonstrate that *Z. xanthoxylum* has evolved a notable ability to utilize Na^+ ions to lower Ψ_S, swell its leaves, and decrease stomatal aperture sizes, in order to enable the additional uptake and storage of water and mitigate losses. These distinctive drought adaption characteristics mean that the xerophytic plant *Z. xanthoxylum* presents a fascinating case study for the potential identification of important and novel genetic elements that could improve crops. This report provides insights on the eco-physiological role of sodium accumulation in xerophytes adapted to extremely arid habitats.

Keywords: drought, leaf succulence, sodium, xerophyte, *Zygophyllum xanthoxylum*

OPEN ACCESS

Edited by:
Oscar Vicente, Universitat Politècnica de València, Spain

Reviewed by:
Jose M. Pardo, Instituto de Bioquímica Vegetal y Fotosíntesis (IBVF), Spain
Ratna Karan, University of Florida, United States

***Correspondence:**
Tian-Ming Hu
hutianming@126.com
Suo-Min Wang
smwang@lzu.edu.cn

Specialty section:
This article was submitted to Plant Abiotic Stress, a section of the journal Frontiers in Plant Science

Received: *22 September 2017*
Accepted: *29 October 2018*
Published: *20 November 2018*

Citation:
Xi J-J, Chen H-Y, Bai W-P, Yang R-C, Yang P-Z, Chen R-J, Hu T-M and Wang S-M (2018) Sodium-Related Adaptations to Drought: New Insights From the Xerophyte Plant Zygophyllum xanthoxylum. Front. Plant Sci. 9:1678. doi: 10.3389/fpls.2018.01678

INTRODUCTION

Drought is the most devastating and commonly occurring global environmental stress that severely impairs food productivity in agriculture and grassland systems (Boyer, 1982; Glantz, 1994; Lambers et al., 2008; Zhao and Running, 2010; Nuccio et al., 2015). This stress is likely to cause more and more issues for food security because predictions suggest that droughts will increase in both severity and frequency given current scenarios for ongoing global climate warming (Li et al., 2009; FAO, 2010; Mishra and Singh, 2010; IPCC, 2014). Thus, understanding the resistance mechanisms used by plants in response to drought is extremely important in light of global and regional changes, not just to forecast the population dynamics of natural ecosystems, but also to enhance agricultural management practices (De Micco and Aronne, 2012).

Species adapted to arid environments tend to survive and grow better during droughts than mesic-adapted counterparts when cultivated together in garden experiments or in natural ecotones (Splunder et al., 1996; Allen and Breshears, 1998; Volaire et al., 1998; McDowell et al., 2008). This attribute is indicative of an underlying difference in the genetic inheritance of drought-resistant traits, as well as the fact that plants with the ability to tolerate conditions where water is scare probably evolved novel mechanisms and key genetic resources which are absent in mesophytes. In light of this background, there has been increasing research interest in revealing the physiological behaviors and mechanisms that underpin the drought adaptations and strategies seen in xerophytes (Yoshimura et al., 2008; Esen et al., 2012; Shi et al., 2013; Yuan et al., 2015), plants that live in arid regions such as the Gobi Desert. Developing a deeper understanding of how these plants manage to resist drought at the physiological level will not only be very beneficial in itself but will also capitalize on the increasing availability of bioinformatics data (Ma et al., 2016; Wu and Su, 2016) and will help to identify the genetic components that are key to crop improvements.

The xerophyte *Zygophyllum xanthoxylum*, a member of the Zygophyllaceae, is a perennial and deciduous succulent shrub that is mainly distributed in the extremely arid regions of northwestern China (Chinese Vegetation Editorial Board, 1980; Ma, 1989; Sheahan and Chase, 2000). The annual precipitation in these areas ranges between 50 and 200 mm, evaporation is more than 2,000 mm per year (Liu and Qiu, 1982), and summer ground temperatures can reach as high as 70°C (Liu et al., 1987); under these conditions, any occasional light rainfall rapidly evaporates. Previous research has shown that *Z. xanthoxylum* accumulates large amounts of Na^+ ions from the soils where it grows containing extremely low levels of salt (Wang et al., 2004). Therefore, in terms of drought resistance, the function of accumulated Na^+ in *Z. xanthoxylum* has mostly been attributed to the fact that an increased amount of these ions will contribute significantly to reducing the osmotic potential (Ψ_s) of leaves (Ma et al., 2012; Yue et al., 2012), thus enhancing the uptake of water during droughts. At the same time, however, the root system of *Z. xanthoxylum* tends to be shallow, distributed in sandy loams within the top 100 cm of the soil profile, mainly at depths between 20 and 40 cm (Chen et al., 2001; Zhou et al., 2006; Kuang et al., 2016); the water content at soil depths between 10 and 20 cm is less than 1%, whereas it ranges between 2 and 3% at depths between 20 and 100 cm (Feng and Cheng, 1999; Sheng et al., 2004). As the matric potential of soils with such an extremely low water content is significantly less than −2.0 MPa (Richards and Weaver, 1944; Wadleigh et al., 1946; Serraj and Sinclair, 2002) and the matric potential decreases approximately vertically in such dry soils if soil water is continuing to be consumed (Serraj and Sinclair, 2002), water absorption by *Z. xanthoxylum* would normally be expected to be impossible via lowering Ψ_s by Na^+ accumulation in its extreme dry habitat. The ability to enhance water uptake via osmotic adjustments due to Na^+ accumulation may make a limited, though perhaps critical, contribution that enables *Z. xanthoxylum* to live in such extreme habitats. Eco-physiologically, however, why *Z. xanthoxylum* accumulate large quantities of Na^+ from their natively low Na^+ content soils or how the accumulated Na^+ benefits their drought adaptations remains unclear.

This study aims to elucidate the precise role of accumulated Na^+ in the drought adaptations of *Z. xanthoxylum*. Thus, the effects of these ions on mortality under extreme drought, and on leaf succulence, rate of water loss by transpiration, and stomatal aperture size were all investigated and discussed to elucidate the possible eco-physiological role of the accumulated sodium in *Z. xanthoxylum*.

MATERIALS AND METHODS

Plant Growth Conditions and NaCl Treatments

Seeds of *Z. xanthoxylum* were collected from wild plants within the Alxa League (39°05′N, 105°34′E at an elevation of 1,360 m) in the Inner-Mongolia Autonomous Region, China. Healthy seeds were washed several times under running water using magnetic stirrers to remove any substances that might inhibit their germination, soaked in distilled water for 1 day at 4°C, and germinated for 2 days in the dark at 25°C. Vigorous germinating seeds with uniform radicle length were selected and transplanted into plastic trays (15 cm × 24 cm × 11 cm; 12 seedlings per container) filled with 2-mm diameter white quartz grits. The quartz grits were washed with standard procedure to remove Na^+ as much as possible: firstly, soaked in 2N sulfuric acid and 1N hydrochloric acid for 2 days, then washed with running water four times, and lastly with distilled water six times. It should be noted that there was still trace amounts of Na^+ left in washed quartz grits (0.8 ± 0.1 micromoles·g^{-1} dry wt.). And this size of grit is too coarse to maintain or absorb water. The plants were irrigated with modified half-strength Hoagland nutrient solution containing 2 mM KNO_3, 0.5 mM $NH_4H_2PO_4$, 0.25 mM $MgSO_4{\cdot}H_2O$, 0.1 mM Ca $(NO_3)_2{\cdot}4H_2O$, 50 μM Fe-citrate, 92 μM H_3BO_3, 18 μM $MnCl_2{\cdot}4H_2O$, 1.6 μM $ZnSO_4{\cdot}7H_2O$, 0.6 μM $CuSO_4{\cdot}5H_2O$, and 0.7 μM $(NH_4)_6Mo_7O_{24}{\cdot}4H_2O$. Prior to planting, the weight of each grit-filled container was recorded using an electronic scale to control and record the proper amount of solution added to each tray daily. In order to prevent drowning

damage to roots, the amount of culture solution was limited to depths of between 1 and 2 cm, approximately one-seventh the height of each cultivation tray. Seedlings were grown in a culture room at 32°C/26°C (day/night) under a light/dark cycle of 16 h/8 h and at a light intensity of 400 μm mol m^{-2} s^{-1}. Relative humidity was maintained at approximately 65% in growth room.

The culture boxes containing 2-week-old *Z. xanthoxylum* seedlings were randomly separated into two groups and treated for 1 week with modified half-strength Hoagland nutrient solution supplemented with, or without, 50 mM NaCl. The NaCl concentration used in this study was based on previous work where 50 mM NaCl was shown to be optimum among a series of concentration gradients to promote growth and alleviate the deleterious impacts of drought stress (Ma et al., 2012; Yue et al., 2012). Distilled water was supplemented every day to maintain a relatively constant culture solution concentration.

Survival Rate and Evapotranspiration Assays

In order to determine whether or not NaCl treatment had a positive effect on drought tolerance in *Z. xanthoxylum*, plant watering was curtailed after each treatment. The culture solutions quickly became dried out within 2 days through evapotranspiration, plant deaths occurred following unrecoverable wilt, and the survival rate was calculated as (live plants/total plants) × 100%. In addition, the amount of evapotranspiration was recorded in each case on the 7th day of treatment, calculated as the total weight of each tray containing plants following water supplementation at the end of the sixth treatment day minus the total weight of the tray containing plants at the end of the seventh treatment day.

Leaf Cell Damage and Antioxidant Systems Assays

In order to further verify the effects of NaCl, a mimic water deficit experiment was performed using −0.5 MPa mannitol (Michel et al., 1983) prepared with half-strength Hoagland nutrient solution. This combination was applied over a 24-h period to plants that had been treated with NaCl for 7 days, and a number of biochemical indicators were assayed using leaves from the third and fourth nodes counted from the bottom of plants (the same below). Thus, the superoxide radical was determined using hydroxylamine oxidation (Elstner and Heupel, 1976), and lipid peroxidation was assessed by monitoring malondialdehyde (MDA) production in leaves, quantified as thiobarbituric acid reactive substances (Dhindsa et al., 1981). Leaf electrolyte leakage was determined by means of relative membrane permeability as measured using a conductivity meter (Murray et al., 1989), while superoxide dismutase (SOD) was assayed using the nitroblue tetrazolium method (Dhindsa et al., 1981), and catalase (CAT) and peroxidase (POD) activities were measured following the method outlined by Cakmak et al. (1993). The ascorbate peroxidase (APX) activity was determined by Nakano and Asada (1981). Glutathione reductase (GR) activity was determined as described by Rao et al. (1996). The Reduced glutathione (GSH) and oxidized glutathione (GSSG) were determined according to Nagalakshmi and Prasad (2001). Briefly, 0.2 g fresh leaves were homogenized by grinder (BioSpec Mini-Beadbeater-96, United States) in liquid N_2. For MDA, 5 ml 0.1% (w/v) trichloroacetic acid was used to extract the sample and then centrifuged; the resulted supernatant was added 5 ml of 0.5% thiobarbituric acid solution and heated for 10 min at 100°C. After cooling, the precipitate was removed by centrifugation. The absorbance of the sample was measured at 450, 535, and 600 nm. For SOD, CAT, POD, and APX, 8 ml 50 mM sodium phosphate buffer (pH 7.8) was used to extract the sample, centrifuged to get the crude enzyme solution, and then measured accordingly. For GR, the sample extracted by 1.5 ml 100 mM potassium phosphate buffer (pH 7.8), 0.1% (v/v) Triton X-100 and 2 mM $MgCl_2$ was centrifuged 10 min at 12,000 *g*. The supernatant was crude extract. For GSH and GSSG, 5 ml of 5% (w/v) sulphosalicylic acid was used to extract and then centrifuged.

Inorganic and Organic Leaf Solutes and Their Contributions to Ψ_s

Contents of Na^+, K^+, and Ca^{2+} were measured following the method outlined by Wang et al. (2007). Briefly, these ions were extracted from dried plant samples soaked in 100 mM acetic acid at 99°C for 4 h; ion analysis was then performed using a polarization Zeeman atomic absorption spectrophotometer (Hitachi Z-2000, Hitachi High-Technologies Co., Japan). As for chloride (Cl^-), 0.2 g fresh leaves oven-dried were grinded (BioSpec Mini-Beadbeater-96, United States) into powder, extracted by 1.2 ml ddH_2O twice within boiled water bath for 2 h, and determined by Mohr titration (Korkmaz, 2001).

Total soluble sugar content was measured using the anthrone method (Dubois et al., 1956; Chow and Landhäusser, 2004). Briefly, 0.2 g samples of fresh leaves were dried, ground in liquid nitrogen, and double-extracted using 4 ml of 80% ethanol by boiling in capped polypropylene tubes at 95°C for 30 min. Extraction supernatants were then centrifuged at 12,000 rpm for 10 min and combined for sugar analysis; each 0.5 ml extraction was diluted in 1.5 ml of distilled water, and 0.5 ml of 2% (w/v) anthrone ethyl acetate reagent was rapidly added, followed by 2.5 ml of concentrated sulfuric acid (H_2SO_4). Absorbance was then measured at 630 nm (Hitachi ultraviolet spectrophotometer U-3900, Hitachi High-Technologies Co., Japan) following 10 min of color development in the dark.

The content of free proline was determined using the sulphosalicylic acid method (Bates et al., 1973). Briefly, 0.2 g samples of fresh leaves were dried and homogenized (Mini-Beadbeater-96, Bio Spec Products Inc. United States) in 5 ml of 3% (w/v) sulphosalicylic acid and centrifuged; ninhydrin and glacial acetic acid were then added to the supernatants, and the mixture was heated at 95°C for 60 min in a water bath. Reactions were then stopped using an ice bath, the mixture was extracted using toluene, and the absorbance was read at 520 nm.

The variable Ψ_s was measured using a freezing-point osmometer (FM-8P, Shanghai Yida Instrument Co., Japan). Briefly, fresh leaves were frozen and thawed several times in liquid N and then squeezed using a syringe. Leaf sap was then collected,

centrifuged, and then used for Ψ_s determination at 25°C. These readings (mmol kg^{-1}) were used to calculate Ψ_s in Mpa, as follows:

$$\Psi_s = \text{-moles of solute} \times R \times K.$$

In this expression, $R = 0.008314$ and $K = 298.8$. Similarly, Ψ_s values for each inorganic and organic solute were calculated using the Van't Hoff equation, as follows:

$$\text{Calculated } \Psi_s \text{ (COP)} = -nRT.$$

In this expression, n denotes the number of solute molecules, while $R = 0.008314$, and $T = 298.8$. The contributions of each solute to leaf Ψ_s were then estimated, as follows:

$$C = \text{COP}/\Psi_s \times 100\% \text{ (Guerrier, 1996).}$$

Fresh and Dry Weights, Water and Absolute Water Contents, Leaf Volume, and Water Loss Rate Assays

At the end of treatments, whole plants were washed with distilled water and tissue samples were rapidly taken and immediately weighed to determine fresh weight (FW). Additional tissues were oven-dried at 80°C for 72 h and dry weight (DW) was determined. Thus, tissue and absolute water contents were calculated as follows:

$$\text{Water content} = (\text{FW} - \text{DW})/\text{FW} \times 100\%, \text{ and;}$$

$$\text{Absolute water content} = \text{FW} - \text{DW}.$$

The measurement method used to calculate leaf volume was as follows:

$$V_{leaf} = (M_{leaf} + M_1 - M_2)/\rho_{water}.$$

This equation was taken from the manual of a patented volumenometer (ZL 2015207858757) with a measurement precision of 0.1 mm^3; in this expression, V_{leaf} refers to leaf volume, while M_{leaf} is leaf FW, M_1 is the weight of the volumenometer fully filled with pure water, M_2 denotes the weight of this instrument fully filled with pure water plus the leaf, and ρ_{water} is the density of pure water at ambient temperature.

In order to assess the water loss rate, leaves from the same position as those sampled above were carefully excised from the plant with a scalpel and the cut petiole section was sealed with white vaseline to prevent water loss. These cut leaves were then placed on filter paper in plastic dishes in a dark chamber at constant temperature and humidity and their weights were recorded every 4 h. Water loss rates were calculated as follows:

$$\text{Water loss rate} = (FW_{Tn} - FW_{Tn+1})/(\Delta T^* FW_{Tn}).$$

In this expression, FW_{Tn} is the weight at each time point, while ΔT denotes the time interval between consecutive measurements.

Abscisic Acid (ABA) Content Assay

The extraction and purification of ABA from leaves was carried out following previously described procedures (Dobrev and Vankova, 2012). Briefly, an approximately 1 g sample of fresh leaves was homogenized and extracted using a methanol/double-distilled water/formic acid (15:4:1, v:v:v) mixture. This extract was then passed through a SPE C18 column (T1616-2008, Tianjin BoJin Technology Co., Japan) and the eluate was collected and evaporated using a N_2-pressure blowing concentrator at room temperature in the dark to about one-tenth of its original volume. The residue was then dissolved in 2 mL of 80% methanol and filtered through a 0.45-μm filter, prior to the determination of ABA content using liquid chromatography mass spectrometry (Applied Biosystems PE Sciex API 2000, ABSciex, United States).

Light and Scanning Electron Microscope (SEM) Observations

Leaves from Control and Na treatments were fixed using 2.5% (v/v) glutaraldehyde in phosphate-buffered saline (PBS, pH 7.4) for 12 h at 4°C. Samples were then washed with PBS, dehydrated using a graded ethanol series, and embedded in LR White resin (London Resin Co., United Kingdom). The resin was then polymerized at 55°C for 3 days, and 0.5 and 0.1 μm sections were cut with a diamond knife using a Leica EM UC7 ultramicrotome (Leica Mikrosysteme GmbH, Austria).

Semi-thin 0.5 μm sections were placed onto glass slides for light microscope observations, stained with 1% (w/v) Toluidine Blue O (with 1% [wt/vol] sodium borate) for 5 min, and observed using an OLYMPUS BX51 system (Olympus Corporation, Japan).

Leaves were fixed with 2.5% (v/v) glutaraldehyde in pH 7.4 PBS for 12 h at 4°C before being re-washed with PBS, dehydrated using a graded ethanol series, immersed in isoamyl acetate, and fully dried with a critical point dryer for SEM observations. Treated samples were then mounted on copper stubs and sputter-coated with gold-palladium; specimens were observed and photographed using a field emission (FE) SEM (S-4800, HITACHI, Japan) at 10 kV.

Statistical Analysis

Each experiment was repeated at least twice and comprised three replicates. All values are reported in this study as means ± standard deviation (SD); analysis of variance (ANOVA) was performed for experiments using the software Excel 2016 applying the Student's *t*-test for simple one-way comparisons of two samples.

RESULTS

Application of 50 mM NaCl Enhanced Survival Rate and Durability Under Extreme Drought Conditions

Two-week-old *Z. xanthoxylum* seedlings were randomly treated either with NaCl, or without NaCl (control), for 1 week. The results revealed that water loss by evapotranspiration from trays of NaCl-treated plants was significantly less than from control plants on the 7th day after treatment (**Figure 1A**). Watering was stopped following treatment and time-course analyses of survival rate and durability were performed. These experiments showed

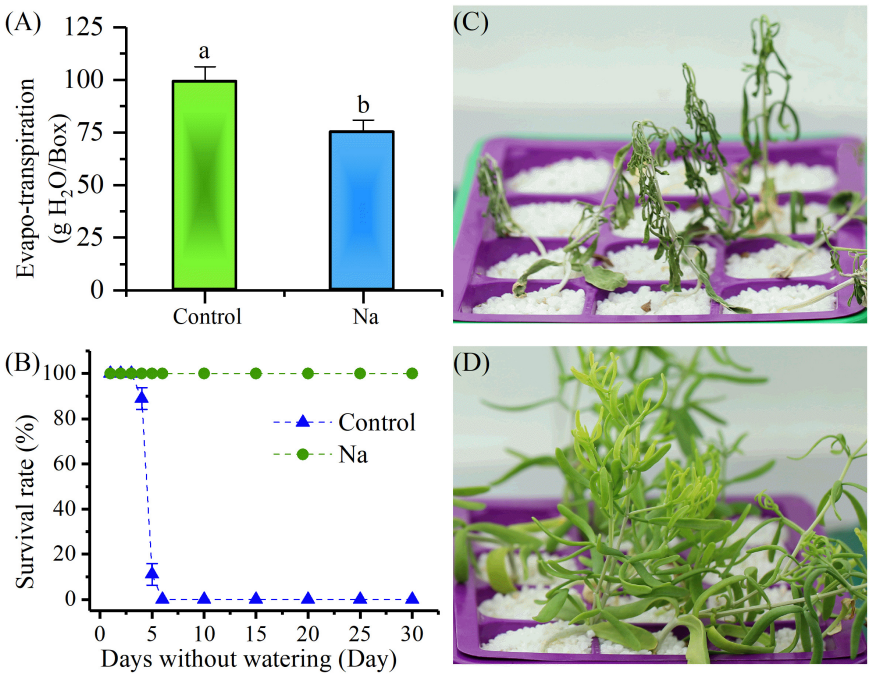

FIGURE 1 | NaCl treatment (50 mM) for 7 days increased the survival rate and durability of 2-week-old *Zygophyllum xanthoxylum* seedlings compared to controls when water was withheld. **(A)** Water lost by evapotranspiration per box on the 7th day of NaCl treatment. **(B)** Survival rate versus days that water was withheld; **(C,D)** show representative photographs of control and NaCl-treated plants taken after 19 days without water, respectively. Bars denote the mean ± SD of between three and four replicates; each replicate in **(A)** involved 12 plants. Bars with different letters are significantly different at the level of 0.05.

that because of rapid evapotranspiration and the fact that large quartz grit particles cannot retain moisture, the solution quickly ran out in the culture trays within 2 days or less. On the 3rd day after watering was stopped, the control plants started to visibly wilt; as shown in **Figure 1B**, the survival rate of this group also sharply decreased between the 4th and 6th day after watering was stopped because of unrecoverable wilt, while this rate did not change in the NaCl- treated group. It is also noteworthy that the plants in the control group were totally dried out by between 6 and 8 days after watering was stopped, while this took between 35 and 45 days in the treatment group (**Figures 1C,D**). The results corroborated the fact that NaCl treatment enhanced the survival rate and durability of *Z. xanthoxylum* under absolute drought conditions.

Treatment With 50 mM NaCl Enhanced Adaptability to Short-Term Osmotic Stress

In order to test whether, or not, NaCl treatment enhances osmotic stress resistance, plants that had been subject to 7 days of treatment were exposed for 24 h to a further culture solution containing an additional −0.5 MPa of mannitol. Observations revealed that less of this solution remained in the control trays than in those treated with NaCl, while visible wilt wrinkles appeared on the leaves of control plants but not on treated individuals. Consistent with these observations, biochemical assays demonstrated that the content of the superoxide radical ($O_2^-\cdot$), a reactive oxygen species (ROS) produced in plants under stress, was significantly less in NaCl-treated plants than in the control group (**Figure 2A**). In addition, the content of MDA, an end product of lipid peroxidation that is stimulated by ROS, was also significantly lower in NaCl-treated plants (**Figure 2B**), while the relative conductivity or electrolyte leakage, proxy for the degree of cell membrane damage due to stress, was also markedly reduced in NaCl-treated plants (**Figure 2C**). The activity of enzymes involved in removing ROS, such as SOD, POD, CAT, APX, and GR were also significantly reduced in NaCl-treated plants (**Figures 2D–H**). The Ratio of the non-enzymatic antioxidant reduced/oxidized glutathione (GSH/GSSG) was lower in NaCl-treated plants, too, indicating the treated leaves with more efficiency to use reduced glutathione (**Figure 2I**). All of these results demonstrated that treatment with NaCl reduced the damage caused by osmotic stress.

Na^+ Contributed to, and Significantly Decreased, Leaf Ψ_s

In order to investigate the function of Na^+ in drought tolerance, leaf solute potential (Ψ_s) and the contents of Na^+, K^+, Ca^{2+}, Cl^-, soluble sugar, and proline in leaves were measured. The concentration of each solute, as well as its relative contribution to Ψ_s, were also calculated. Results showed (**Figure 3A**) that Ψ_s was significantly lowered in NaCl-treated plants compared to the control group and the same was true for K^+, Ca^{2+}, soluble sugar, and proline, while opposite pattern was seen in Na^+ and

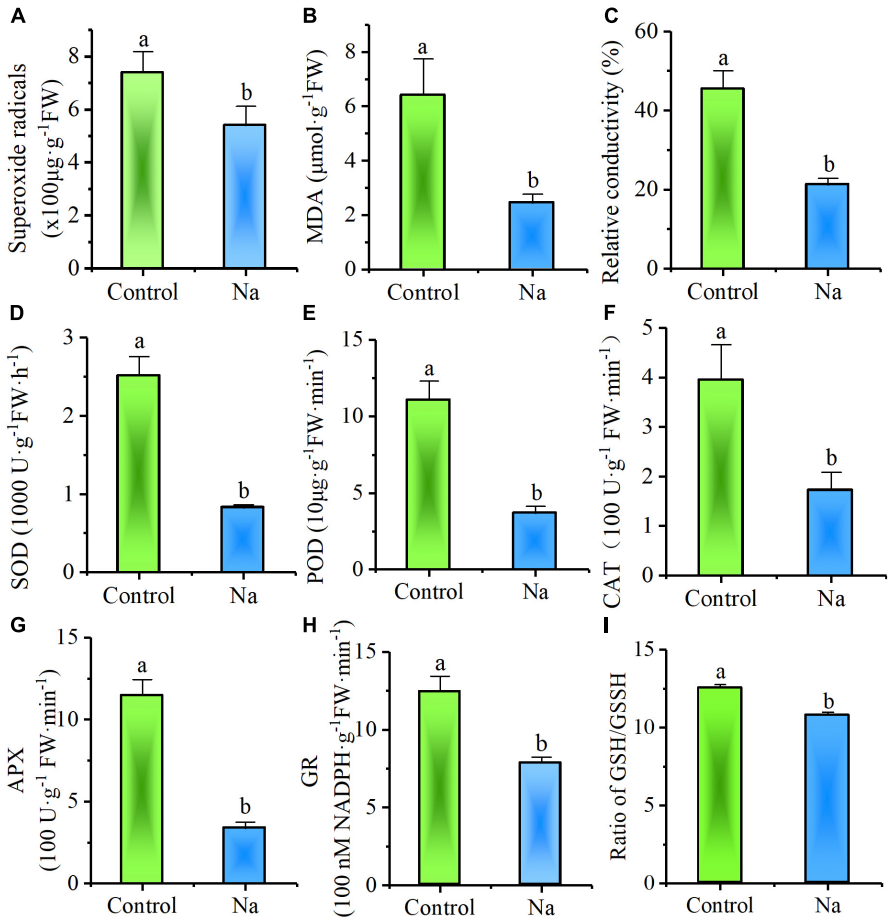

FIGURE 2 | NaCl treatment reduced *Z. xanthoxylum* leaf damage from short-term osmotic stress induced with -0.5 MPa mannitol. Relative biochemical content of **(A)** superoxide radicals, **(B)** MDA, **(C)** electrolyte leakage and antioxidase activity of **(D)** SOD, **(E)** POD, **(F)** CAT, **(G)** APX, **(H)** GR as well as **(I)** Ratio of GSH/GSSH were all analyzed in leaves harvested after 24 h of –0.5 MPa mannitol stress from third and fourth nodes of 2-week-old *Z. xanthoxylum* seedlings treated with 50 mM NaCl or without (control) for 7 days. Bars denote the mean ± SD (n = 8), with different letters indicating significantly different at the level of 0.05.

Cl^- content (**Figure 3B**). Na^+ was greatly accumulated to more than 50 mM in control group plants (**Figure 3B**), even though these ions were not added to the culture solution and a great deal of effort was expended to clean the quartz grit used in these experiments. At the same time, the contribution of inorganic solutes, such as Na^+, K^+, Ca^{2+}, and Cl^-, to Ψ_s was as high as 87.36% in the control plants, while the contribution of Na^+ was just 11.2% ± 1.1%. In treated plants, the contribution of inorganic solutes was 76.37%, and the Na^+ contribution was definitely higher, 63.9% ± 10.4% (**Figure 3C**). These results suggested that inorganic solutes of Na^+, K^+, Ca^{2+}, and Cl^- are the preferred osmolytes of *Z. xanthoxylum* and that the first of them is favored overall. Thus, when available, Na^+ is rapidly accumulated in leaves, significantly decreasing their solute potential.

Treatment With 50 mM NaCl Enhanced Leaf Succulence and Water Storage

In order to further determine the effects of accumulated Na^+ on leaf growth, mature leaf characteristics pruned from the third and fourth nodes of plants were examined. The results showed that leaf FW and DW, absolute water content, leaflet length, thickness, and volume all markedly increased in treated plants (**Figures 4A–F**). Results also suggested that NaCl treatment had a great impact on promoting leaf succulence.

Further, to examine the effect of NaCl on leaf succulence at the cellular level, semi-thin cross-sections of mature leaves from the same positions on plants were investigated. Compared with the control, both palisade and spongy cells were enlarged dramatically in NaCl-treated plants (**Figure 5**); because of cell enlargement, morphological differences between palisade and spongy tissues became less obvious in treated plants (**Figures 5A,B**). Thus, to quantify the effect of Na^+ on cell enlargement, areas of the three largest palisade and spongy cells in each different section were measured. These results demonstrated that the areas of these cells were significantly increased by 91.3% ± 18.8% and 89.2% ± 19.5% in NaCl-treated plants compared with the control, respectively (**Figures 4G,H**, **5C–F**). Because the number of leaf cell layers did not differ between the control and treatment (**Figure 4I**),

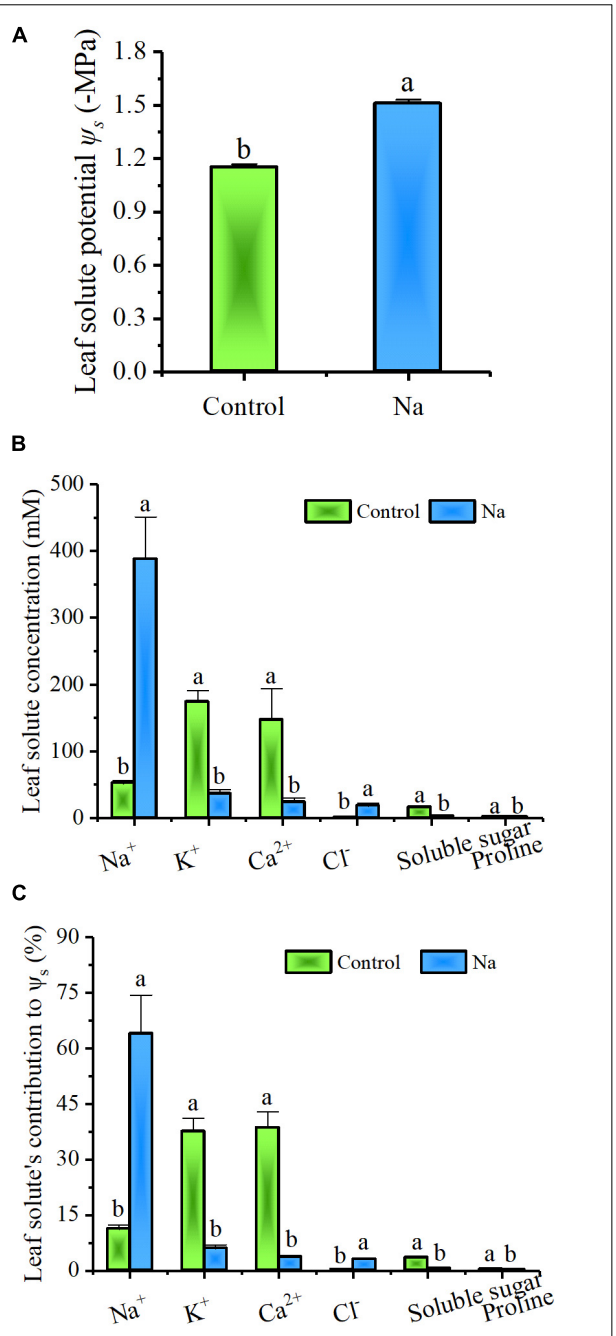

FIGURE 3 | Na^+ not only significantly decreased Ψs but made a large contribution to Ψs in leaves from the third and fourth nodes in 2-week-old *Z. xanthoxylum* seedlings treated with 50 mM NaCl or without (control) for 7 days. **(A)** (Ψs). **(B)** Solute concentration in leaves. **(C)** Solute contributions to Ψs. Bars denote the mean ± SD (n = 8), with different letters indicating significantly different at the level of 0.05.

these results suggested that succulence promoted by Na^+ was mainly the result of cell enlargement rather than cell division.

In order to gain a deeper understanding of the significance of Na^+ in *Z. xanthoxylum*, the distributions of both water and Na^+ at the organ level in plants were also investigated. These results showed that Na^+ sequestered in plants was overwhelmingly allocated to leaves, irrespective of treatment or control (**Figure 6A**), and that the same distribution pattern was seen for water in different organs (**Figure 6B**). And the Na^+ concentration was the highest in leaves (**Figure 6C**). Correlation analysis showed that the Na^+ distribution varies across organs at the whole plant level, but was positively correlated with the corresponding water distribution (**Figure 6D**). Thus, absolute plant water content increased by 188.0% ± 33. 5% in NaCl-treated plants compared to the control and that this increment comprised as much as a 99.4% ± 19.0% increase in leaves. These results also showed strongly that Na^+ absorbed by *Z. xanthoxylum* was mainly allocated to leaves so that cells could be enlarged for water storage.

Treatment With 50 mM NaCl Decreased Leaf Water Loss and Stomatal Aperture Size

Because the results of this study showed that water loss via evapotranspiration at the plant tray level was reduced by NaCl treatment (**Figure 1A**), it was further hypothesized that this might also act to reduce the plant water loss rate. Thus, to test this, the water loss rates of detached third and fourth node leaves from 2-week-old seedlings treated for 7 days with NaCl and without NaCl (control) were investigated (**Figure 7**). The results of this comparison showed that when leaves were detached from their parent plant their water content generally declined; however, the rate of water content loss was clearly less in NaCl-treated leaves than in those from control plants (**Figure 7A**). Results showed that the water loss rate of detached leaves from NaCl-treated plants was only about one eighth of that from their control counterparts after a period of up to 4 h (**Figure 7B**) and that the rate in leaves from the latter remained significantly higher throughout this period even though overall water content was lower (**Figure 7A,B**). This suggested that the water loss rate of detached leaves was independent of cell sap concentration; this rate also fell to almost zero in NaCl-treated detached leaves within 12 h, while that in control leaves continued to decline (**Figure 7B**). This suggested that NaCl treatment promoted water retention and greatly reduced leaf water losses.

To further understand how this treatment influences water loss, leaf stomata from the third and fourth nodes of 2-week-old plants subjected to treatment with, and without, NaCl for 7 days were examined via SEM. These observations showed that although the stomata of control group leaves were mostly open, those on both the adaxial and abaxial surfaces of treatment group plants were closed (**Figure 8**). Further SEM analysis revealed that 69.5 and 94.4% of adaxial and abaxial epidermal stomata were open in control plants, respectively, while just 5.7 and 6.1% were open in their NaCl-treated counterparts (**Supplementary Table S1**). Statistical analysis also showed that stomatal density on both the adaxial and abaxial surfaces of NaCl-treated plants was significantly reduced compared to the control (**Figure 7C**); however, as these leaves were completely developed on the third and fourth nodes of 2-week old-seedlings,

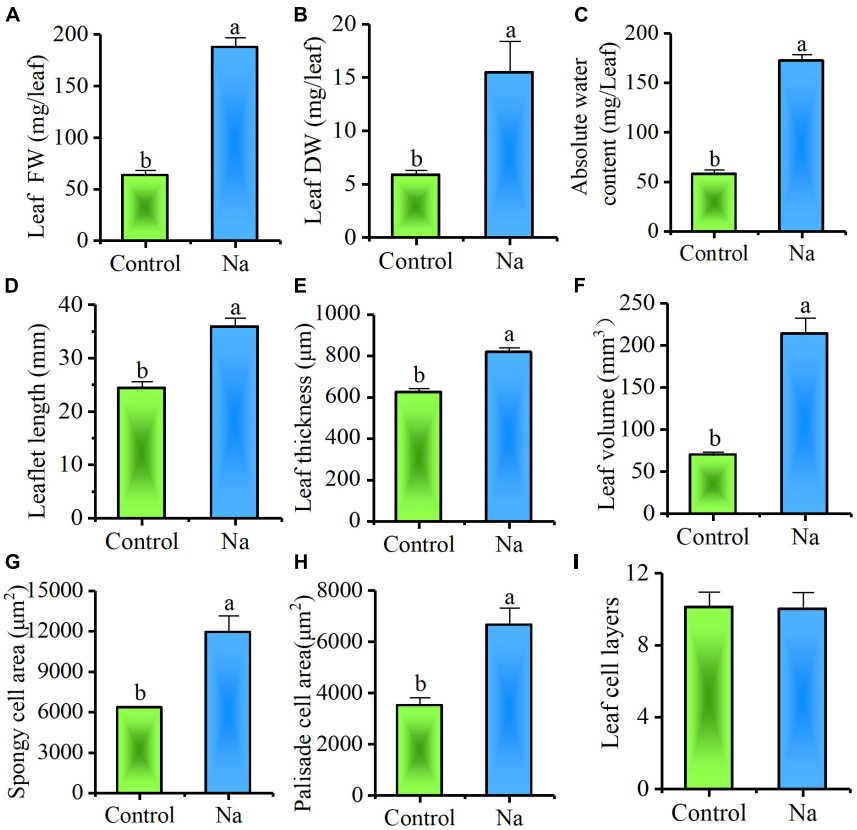

FIGURE 4 | Treatment with NaCl promotes leaf succulence. The samples for this experiment were third- and fourth-node leaves from 2-week-old *Z. xanthoxylum* seedlings treated with 50 mM NaCl or without (control) for 7 days. These results show that NaCl treatment stimulated **(A)** leaf FW, **(B)** DW, and **(C)** absolute water content **(D)**, as well as leaflet length **(E)**, leaf thickness **(F)** and volume **(G)**, and spongy **(H)** and palisade cell area, but not **(I)** leaf cell layers. Bars denote the mean ± SD (n = 8), with different letters indicating significantly different at the level of 0.05.

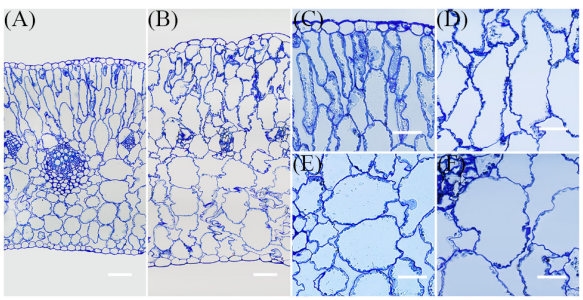

FIGURE 5 | Representative transverse semi-thin sections of leaves. The samples for this experiment were third- and fourth-node leaves from 2-week-old *Z. xanthoxylum* seedlings treated with 50 mM NaCl or without (control) for 7 days. All these sections were stained with toluidine blue. Semi-thin section of leaf from control **(A)** and NaCl treatment **(B)**. Palisade cells from control **(C)** and NaCl treatment **(D)**. Spongy cells from control **(E)** and NaCl treatment **(F)**. The scale bars in **(A,B)** are 100 μm, while those in **(C–F)** are 50 μm.

this decrease in stomatal density might also be due to the enlargement of epidermal cells in treated plants (**Figures 5A,B**, **8A–D**). Taken together, these results demonstrated that NaCl treatment influenced water loss reduction mainly via stomatal closure and decreases in the density of these structures.

It is likely that levels of the stress signaling molecule ABA, which promotes stomatal closure, increase when plants are subject to water stress. Thus, to detect whether, or not, reductions in stomatal aperture size can be linked to changes in the proportions of this molecule, ABA content was measured. The data showed that ABA content did not vary significantly between the control and NaCl-treated plants (**Figure 7D**); this suggested that the leaves of NaCl-treated plants may not suffer stress and that stomatal closure was probably independent of ABA.

DISCUSSION

Droughts occurring in arid regions, or generally because of insufficient rainfall, have always been the main factor limiting crop production across most of the world (Steduto et al., 2012). However, in extremely arid environments, such as the deserts of northwestern China, succulent xerophytes such as *Z. xanthoxylum* manage to grow well. These plants are important because they possess outstanding ability to thrive in arid areas in which model and agronomic plant species cannot survive,

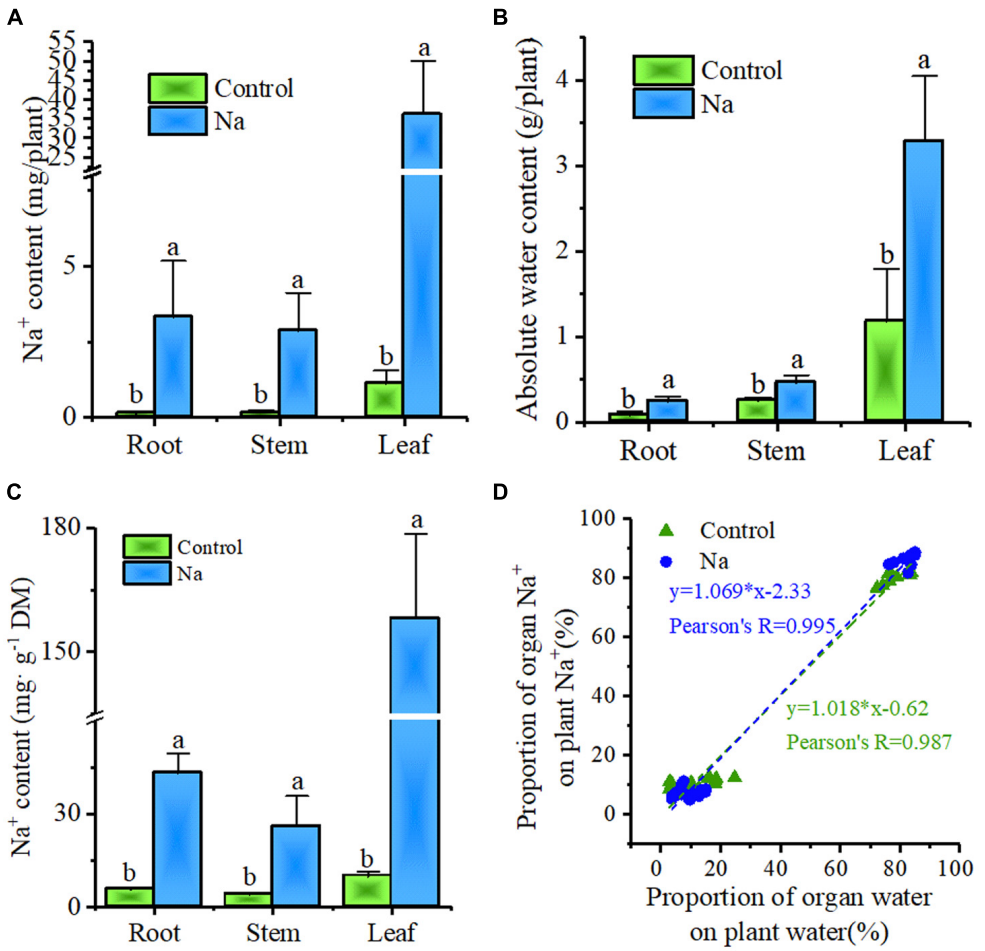

FIGURE 6 | Plant water distribution is positively correlated with plant Na^+ distribution in root, stem, and leaf organs. The samples for this experiment were third- and fourth-node leaves from 2-week-old *Z. xanthoxylum* seedlings treated with 50 mM NaCl or without (control) for 7 days. **(A)** Na^+ content in root, stem, and leaf organs. **(B)** Absolute water content in root, stem, and leaf organs. **(C)** Na^+ concentration in root, stem, and leaf organs. **(D)** Correlation analysis between the proportional distribution of Na^+ and water in different organs across the whole plant. Bars represent the mean ± SD (n = 8), with different letters indicating significantly different at the level of 0.05.

and thus they may have evolved a range of novel strategies to cope with drought. Unfortunately, most of the plants that have been the focus of detailed research to date have limited tolerance to drought, including *Arabidopsis* (Clauw et al., 2016), tobacco (Xie et al., 2016), rice (Todaka et al., 2017), wheat (Sukumaran et al., 2016), and maize (Wang et al., 2016). Thus far, relatively little attention has been focused on plants which are already adapted for growth in conditions of severe drought, due largely to the difficulties of working with these slow-growing species. As a result, however, the precise physiological mechanisms exhibited by these drought-tolerant plants remain to be elucidated.

The subject of this paper, the xerophyte *Z. xanthoxylum,* possesses this ability as it could live in the Gobi Desert of northwestern China (Liu et al., 1987). In earlier work, Wang et al. (2004) noted that this plant accumulates abundant Na^+ from non-saline soils even though its natural habitats are characterized by very low salt content; this suggests that this ion might exert a positive influence on drought tolerance in this species. The results of this study showed that treatment with 50 mM NaCl not only enhanced the survival rate and durability of *Z. xanthoxylum* under extreme drought conditions, but that the presence of this ion also increased the adaptability of this plant to short-term osmotic stress (**Figures 1**, **2**). These results highlighted the fact that Na^+ is an important component of the desert adaptations seen in *Z. xanthoxylum*.

Increased water uptake in plants can be achieved by decreasing Ψ_s via the enhanced accumulation of solutes during droughts or periods of salinity, a process termed osmotic adjustment (Turner and Jones, 1980; Verslues et al., 2006). This adaptation is seen in numerous plant species and is well known to play a role in combating dehydration (Blum, 2017). Indeed, the treatment with 50 mM NaCl applied in this study to *Z. xanthoxylum* significantly decreased leaf Ψ_s compared to the control (**Figure 3A**), a reduction that was overwhelmingly due to increased Na^+ accumulation (**Figures 3B,C**). Halophyte

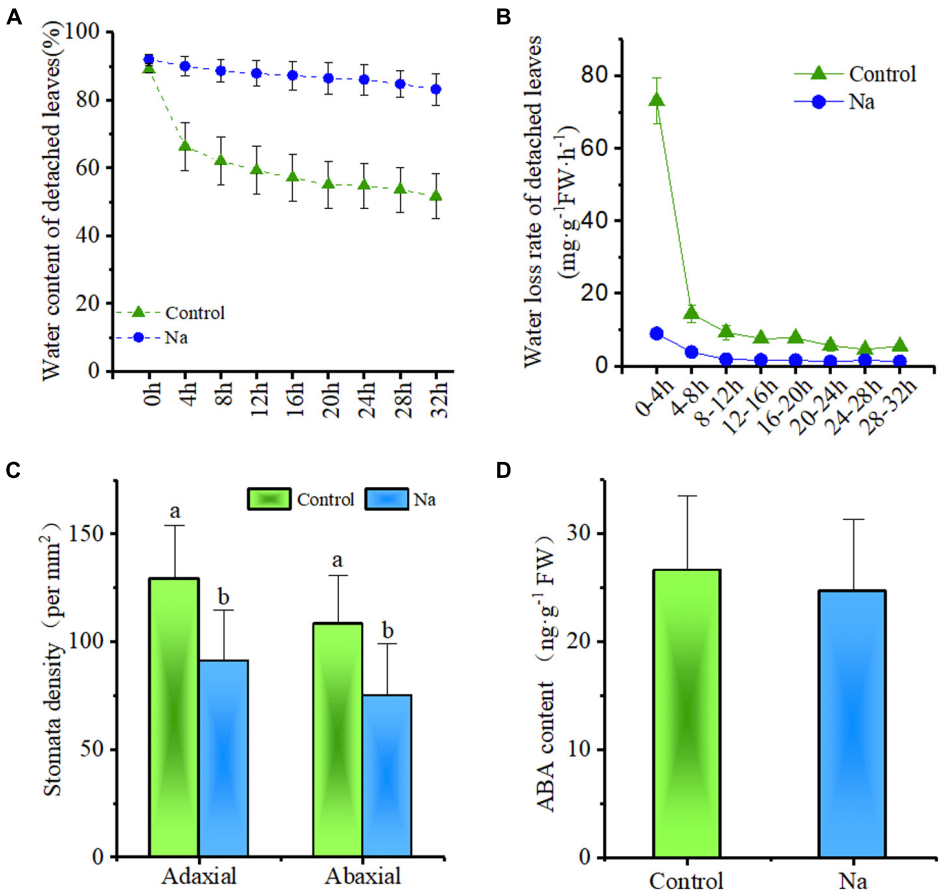

FIGURE 7 | Treatment with NaCl reduced the rate of water loss and stomatal density in detached leaves but did not influence ABA content. The samples for this experiment were third- and fourth-node leaves from 2-week-old *Z. xanthoxylum* seedlings treated with 50 mM NaCl or without (control) for 7 days. **(A)** Water content of detached leaves versus length of time (h) detached (n = 8). **(B)** Water loss rate of detached leaves (n = 8). **(C)** Stomatal density on adaxial and abaxial leaf surface (n = 18). **(D)** Leaf ABA content (n = 4). Bars denote the mean ± SD (n = 8), with different letters indicating significantly different at the level of 0.05.

plants that live on seacoasts or in saltmarshes, like *Suaeda maritima* (Yeo and Flowers, 1980) and *Atriplex vesicaria* (Black, 1960), also accumulate large quantities of this ion in their leaves to enable enhanced water uptake so as to counteract the external osmotic stresses imposed by the high salt concentrations in their environments (Flowers et al., 1977). However, unlike halophytes that live in habitats where there is plenty of water, this resource is almost entirely absent from the upper desert layer and thus increasing water uptake via Na^+ accumulation cannot play a great role in the adaptations of *Z. xanthoxylum* in deserts. It is because that water uptake via osmotic adjustments can only function at the onset of drought or during mild-to-moderate events of this kind, in the first place because soil water potentials become far too low to extract additional water during long periods of drought. This is especially the case in soil horizons below depths of 100 cm in arid regions (Nobel, 1977; von Willert et al., 1992). In addition, it is also possible that water potential can drop sharply in severely arid soils if any depletion occurs which further acts to limit the uptake of plants (Serraj and Sinclair, 2002). This conclusion is corroborated by the results of this study because in experiments in which watering was withheld, the Ψ_s in control plants fell to lower levels than in NaCl-treated individuals because of the passive decrease associated with wilting. Nevertheless, plants in the control group still died faster and earlier because of no water available (**Figure 1**). Our results also showed that at the start of the short-term osmotic stress experiment reported in this study, the total calculated Ψ_s values of the culture solutions were −0.52 and −0.76 MPa for the control and treatment, respectively; data showed that although control plants should tend to suffer less, they were nevertheless damaged to a greater extent because of a rapid decrease in the Ψ_s of the culture solution due to fast water depletion (**Figure 2**). Thus, in terms of long-term survival, the role of Na^+ in osmotic adjustment may only contribute to the desert adaptations of *Z. xanthoxylum* to a limited extent because most of the growing season for this plant coincides with extreme drought conditions.

The swelling of tissues and organs for water storage, a process known as succulence, is another important adaptation seen in a diverse range of plant species that cope with semi-arid and arid environments (Ogburn and Edwards, 2010; Males,

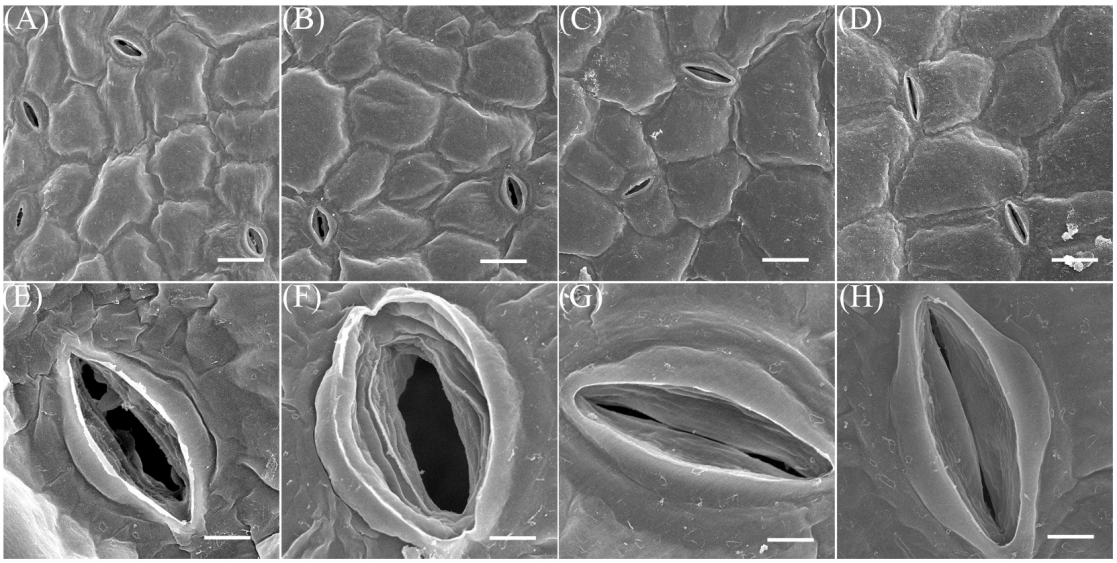

FIGURE 8 | SEM images. The samples for this experiment were third- and fourth-node leaves from 2-week-old *Z. xanthoxylum* seedlings treated with 50 mM NaCl or without (control) for 7 days. **(A,E)** Adaxial stomata in control plants. **(B,F)** Abaxial stomata in control plants. **(C,G)** Adaxial stomata in NaCl-treated plants. **(D,H)** Abaxial stomata in NaCl-treated plants. Scale bars in **(A–C)**, and **(D)** are 20 μm, while those in **(E–H)** are 4 μm. Scanning electron microscope (SEM) analysis of leaves on the 3rd–4th nodes of 2-week *Z. xanthoxylum* seedlings treated without (Control) or with 50 mM NaCl (Na) for 7 days. **(A,E)** Adaxial stomata in control plants. **(B,F)** Abaxial stomata in control plants. **(C,G)** Adaxial stomata in Na treatment plants. **(D,H)** Abaxial stomata in Na treatment plants. Scale bar: **(A–D)** 20 μm; **(E–H)** 4 μm.

2017). This process of tissue and organ swelling involves an increase in cell volume accompanied by the intake of vast amounts of water. Water uptake by cells is generally associated with, or modulated by, cell wall relaxation to reduce turgor pressure (Ψ_p), modification of cell solute content, and changes in plant hydraulic conductance; the last of these factors, however, only works in cells that are far from their water potential equilibrium (Cosgrove, 1993). This means that water uptake into a cell is mainly controlled by cell wall elasticity and solute content, themselves affected by the Ψ_p and Ψ_s, respectively (Steudle et al., 1977). In a rigid plant cell, Ψ_p is primarily dependent on cell solute content; thus, any increase in this variable will result in a concomitant Ψ_p increase, leading to a large tensile stress on the cell wall. If a cell wall is in an "extensible" state, it will undergo turgor-driven expansion and water uptake (Cosgrove, 2000). The Ψ_s values measured in this study (**Figure 3A**) showed that total solute content by concentration increased by around 31.3% in leaves of NaCl-treated plants, compared to the control group, a result that was consistent with a previously reported 28.8% increase in cell Ψ_p in similarly treated plants (Ma et al., 2012). In contrast, if the leaf cell size of NaCl-treated plants is reduced to the same size as the control group (**Figure 5**), between two and four times more solute concentration is generated, based on estimates for cell wall increases (**Figures 4G,H**). This result suggested that cells in the leaves of NaCl-treated plants underwent both turgor-driven expansion and water uptake. The data presented in this study also showed that of the accumulated solutes analyzed, Na^+ comprised 86.2% of the total in leaves of plants treated in this way (**Figures 3B,C**); this means that this ion made a major contribution to the increase in Ψ_p and cell size. The NaCl treatment therefore notably enhanced water storage by promoting leaf succulence in *Z. xanthoxylum* through cell enlargement (**Figures 4**, **5**). This leads to a number of inevitable conclusions, including that the majority of Na^+ contained in plants is allocated to leaves, the water distribution at the individual level is tightly positively correlated to the distribution of this ion in different organs, and the prominent rise in absolute water content in NaCl-treated plants was nearly all the result of water increase from leaves (**Figure 6**). We therefore concluded that the role of absorbed Na^+ in *Z. xanthoxylum* is mainly to promote leaf succulence by enlarging cells for enhanced water storage. This resource, once stored, helps to mitigate drought stress in tissues and buffer stomatal conductance and photosynthesis over a period of days in the face of soil water deficits (Sinclair, 1983; Martin, 1994). The resultant increase in leaf hydration recorded in this study was also partially responsible for enhanced durability and reduced cell damage (**Figures 1**, **2**) and in addition improved photosynthetic performance under drought stress (Ma et al., 2012; Yue et al., 2012).

Water retention by down-regulating transpiration is another common strategy utilized by plants to sustain the balance of water resource as a drought resistance adaption. This can be achieved via the formation of xeromorphic traits including leaf shedding, a lower leaf number, smaller leaf size, and the presence of xeromorphic leaves with features such as thick cuticles, and stiff or sunken stomata in plants that live in arid and semiarid environments (De Micco and Aronne, 2012). This adaptation can also result from instant adjustments in

the stomatal aperture of most plants when subject to water shortages (Sperry, 2000; Liu et al., 2005). This water-saving process could be fulfilled in our study via intensive accumulation of Na^+ in leaves which consequently resulted in a marked decrease in water loss rate the via down-regulation of stomatal aperture size and decrease in density (**Figures 7**, **8**). This is perhaps one major reason why *Z. xanthoxylum* plants are able to withstand many days under conditions of extreme drought (**Figure 1**) or are adapted to their desert habitats because of lower water demand and expenditure. As regards stomatal closure, various studies demonstrated that ABA produced in root tips in response to drought in drying soils is a major signaling molecule transported into leaves via the transpiration stream. When this molecule reaches a leaf it leads to an increase in ABA and reduced stomatal conductance (Davies and Zhang, 1991; Davies et al., 1994). The NaCl-treated plants in our study, however, did not suffer from water shortage and so the content of this stress signaling molecule (ABA) was not difference in control and treated plant leaves (**Figure 7D**); this indicated that stomatal closure in NaCl-treated plants did not result in detectable ABA changes. Additional studies on the stomatal behavior of isolated epidermis have shown that Na^+ can directly inhibit the opening of these structures in the non-succulent halophyte *Aster tripolium*, and that this process is not mediated by ABA (Perera et al., 1994). Compared to the contrasting and unusual stomatal response of *A. tripolium*, Na^+ appears to promote opening in non-halophyte and glycophyte species such as *Commelina communis* and *A. amellus* (a relative of *A. tripolium*), finally leading to irreversible opening, disrupting the ability of stomata to close in response to both environmental signals (i.e., darkness and CO_2) and ABA (Jarvis and Mansfield, 1980; Zeiger, 1983; Perera et al., 1994). The presence of this notable distinction in Na^+ effects on stomatal behavior between halophytes and glycophytes mainly relies on the fact that the former has evolved a novel mechanism to sense Na^+ signaling and then to downregulate K^+ uptake, as the latter is the main ion involving in stomatal opening (Perera et al., 1997; Véry et al., 1998). The mechanism by which Na^+ downregulates stomatal aperture size could also decrease transpiration and limit the excessive upward passage of this ion in the xylem to the shoots, enabling *A. tripolium* to avoid toxicity in its saline habitat (Kerstiens et al., 2002). It is likely that a similar mechanism has also evolved in the xerophyte *Z. xanthoxylum*. However, unlike halophytes that inhabit saline environments, the species studied in this research lives in soils that contain very low Na^+ concentrations and also has a marked ability to absorb and distribute large concentrations of this element in its leaves. This means that the active accumulation of larger quantities of Na^+ in leaves acts to downregulate water loss by transpiration, an additional arid habitat adaptation. This result implies that the xerophyte *Z. xanthoxylum* possesses some unique molecular systems that are distinct from both halophytes and glycophytes.

An ever-increasing body of research demonstrates that, in addition to reduced transpiration, decreased stomatal opening could also result in a lower influx of stomatal CO_2 and increased temperatures inside leaves, limiting photosynthesis (Sharkey, 2005; Allakhverdiev et al., 2008; Farooq et al., 2012). The results of this study show, however, that both the FW and DW of NaCl-treated plants, and especially of their leaves, increased markedly in comparison to control plants (data not shown). Similar results also have been reported in other studies (Ma et al., 2012; Yue et al., 2012), and provide insights into the presence of possible additional mechanisms in *Z. xanthoxylum* that might act to neutralize the adverse effects on photosynthesis of reduced stomatal opening. One critical mechanism to separate the excess Na^+ form cytosol in leaf cell should exist, because lots of important metabolic enzymes like malate dehydrogenase, aspartate transaminase, glucose-6-phosphate dehydrogenase, isocitrate dehydrogenase, phosphoribose isomerase, lactate dehydrogenase, nitrate reductase, and 6-phosphogluconate dehydrogenase are all sensitive to high Na^+ concentrations (Flowers et al., 1977). And most likely, the much Na^+ accumulated in leave of *Z. xanthoxylum* is localized in vacuole (Flowers et al., 1977; Wu et al., 2011).

Drought tolerance in plants depends on the maximization of water uptake and storage and the minimization of water loss (De Micco and Aronne, 2012). The results presented in this study showed that the xerophyte *Z. xanthoxylum* achieves these three aims simultaneously by accumulating Na^+ in its leaves by decreasing cell Ψ_s, enhancing leaf succulence, and down-regulating transpiration (**Figure 9**). Similar strategies may also be employed by leaf-succulent shrubs including *Nolana mollis*, *Heliotropium pycnophyllum*, and *Tetragonia maritima* that are native to the Atacama Desert, as they also accumulate extremely high levels of Na^+ in their leaves (Rundel et al., 1980). These strategies are important because this desert in northern Chile in one of the two most arid regions globally, with a mean precipitation of less than 25 mm $year^{-1}$. Acquiring and storing water using these approaches is optimal and adaptive because

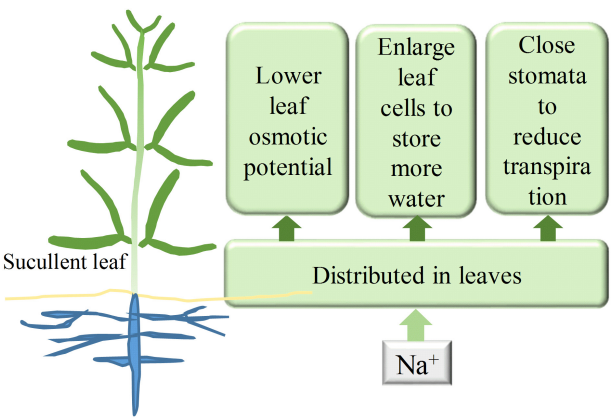

FIGURE 9 | The probable roles of Na^+ in *Z. xanthoxylum* drought tolerance. A great deal of Na^+ resulted in a decrease in leaf Ψ_s and facilitated more water uptake. Accumulated Na^+ in leaves enhances water storage by enlarging leaf cells and reduces transpiration by closing stomata. The three possible physiological roles of Na^+ shown in this figure are likely to enable the xerophyte *Z. xanthoxylum* to thrive in extremely arid habitats.

brief precipitation is exhausted quickly, usually within 2 or 3 days, by the scorching summer desert sun (Feng and Cheng, 1999).

CONCLUSION

The results of this study demonstrated that Na^+ can significantly increase the survivability and durability of the xerophyte *Z. xanthoxylum* under drought conditions. These drought adaptations are physiologically most likely the result of high concentrations of Na^+ distributed in leaves that act to lower Ψ_s, swell leaf organs, and decrease stomatal aperture size, enabling enhanced water uptake and storage and reducing losses. This intriguing ability to utilize Na^+ to balance the water budget as an adaptation to life in arid areas suggests that the xerophyte *Z. xanthoxylum* will be a key species for further study, especially in light of increasing global warming and frequent drought scenarios. This species presents a number of novel physiological mechanisms for drought resistance, as well as putatively related key genetic characteristics for the improvement of crops and pastures.

AUTHOR CONTRIBUTIONS

J-JX, R-JC, S-MW, and T-MH planned and designed the research. H-YC, W-PB, R-CY, and P-ZY performed the experiments. J-JX analyzed the data. J-JX and R-JC wrote the manuscript. All authors read and approved the final manuscript.

FUNDING

This study was supported by the National Natural Science Foundation of China (31402127), the Key R&D Plan of Shaanxi Province of China (2018ZDXM-NY-040), the Natural Science Foundation of Shaanxi Province of China (2015JQ3079), Ph.D. Research Start-Up Funds (2013BSJJ004) from Northwest A&F University, and the Fundamental Research Funds for the Central Universities (2452015028) of Northwest A&F University.

ACKNOWLEDGMENTS

We thank S. J. Chen, X. Li, Y. L. Jiang, and X. R. Song for their help with the experiments presented in this paper.

SUPPLEMENTARY MATERIAL

The Supplementary Material for this article can be found online at: https://www.frontiersin.org/articles/10.3389/fpls.2018.01678/full#supplementary-material

REFERENCES

Allakhverdiev, S. I., Kreslavski, V. D., Klimov, V. V., Los, D. A., Carpentier, R., and Mohanty, P. (2008). Heat stress: an overview of molecular responses in photosynthesis. *Photosynth. Res.* 98, 541. doi: 10.1007/s11120-008-9331-0

Allen, C. D., and Breshears, D. D. (1998). Drought-induced shift of a forest-woodland ecotone: rapid landscape response to climate variation. *Pro. Natl. Acad. Sci. U.S.A.* 95, 14839–14842.

Bates, L., Waldren, R., and Teare, I. (1973). Rapid determination of free proline for water-stress studies. *Plant Soil* 39, 205–207. doi: 10.1016/j.dental.2010.07.006

Black, R. (1960). Effects of NaCI on the ion uptake and growth of *Atriplex vesicaria* Heward. *Aust. J. Biol. Sci.* 13, 249–266. doi: 10.1071/BI9600249

Blum, A. (2017). Osmotic adjustment is a prime drought stress adaptive engine in support of plant production. *Plant Cell Environ.* 40, 4–10. doi: 10.1111/pce.12800

Boyer, J. S. (1982). Plant productivity and environment. *Science* 218, 443–448. doi: 10.1126/science.218.4571.443

Cakmak, I., Strbac, D., and Marschner, H. (1993). Activities of hydrogen peroxide-scavenging enzymes in germinating wheat seeds. *J. Exp. Bot.* 44, 127–132. doi: 10.1093/jxb/44.1.127

Chen, S., Zhang, H., Wang, L., Bu, Z., and Zhao, M. (2001). *Root Systems of Grassland Plants in the North of China*. Changchun: Jilin University Press.

Chinese Vegetation Editorial Board. (1980). *China Vegetation*. Beijing: Science Press.

Chow, P. S., and Landhäusser, S. M. (2004). A method for routine measurements of total sugar and starch content in woody plant tissues. *Tree Physiol.* 24, 1129–1136.

Clauw, P., Coppens, F., Korte, A., Herman, D., Slabbinck, B., Dhondt, S., et al. (2016). Leaf growth response to mild drought: natural variation in Arabidopsis sheds light on trait architecture. *Plant Cell* 28, 2417–2434. doi: 10.1105/tpc.16.00483

Cosgrove, D. J. (1993). Water uptake by growing cells: an assessment of the controlling roles of wall relaxation, solute uptake, and hydraulic conductance. *Int. J. Plant Sci.* 154, 10–21. doi: 10.1086/297087

Cosgrove, D. J. (2000). Loosening of plant cell walls by expansins. *Nature* 407, 321–326.

Davies, W. J., Tardieu, F., and Trejo, C. L. (1994). How do chemical signals work in plants that grow in drying soil? *Plant Physiol.* 104:309. doi: 10.1104/pp.104.2.309

Davies, W. J., and Zhang, J. (1991). Root signals and the regulation of growth and development of plants in drying soil. *Annu. Rev. Plant Biol.* 42, 55–76. doi: 10.1146/annurev.pp.42.060191.000415

De Micco, V., and Aronne, G. (2012). "Morpho-anatomical traits for plant adaptation to drought," in *Plant Responses to Drought Stress*, ed. R. Aroca (Berlin: Springer), 37–61. doi: 10.1007/978-3-642-32653-0

Dhindsa, R. S., Plumb-Dhindsa, P., and Thorpe, T. A. (1981). Leaf senescence: correlated with increased levels of membrane permeability and lipid peroxidation, and decreased levels of superoxide dismutase and catalase. *J. Exp. Bot.* 32, 93–101. doi: 10.1093/jxb/32.1.93

Dobrev, P. I., and Vankova, R. (2012). "Quantification of abscisic acid, cytokinin, and auxin content in salt-stressed plant tissues," in *Plant Salt Tolerance: Methods and Protocols*, eds S. Shabala and T. A. Cuin (Berlin: Springer), 251–261.

Dubois, M., Gilles, K. A., Hamilton, J. K., Rebers, P., and Smith, F. (1956). Colorimetric method for determination of sugars and related substances. *Anal. Chem.* 28, 350–356. doi: 10.1007/978-1-61779-986-0

Elstner, E. F., and Heupel, A. (1976). Inhibition of nitrite formation from hydroxylammoniumchloride: a simple assay for superoxide dismutase. *Anal. Chem.* 70, 616–620.

Esen, A. H. S., Özgür, R., Uzilday, B., Tanyolaç, Z. Ö, and Dinc, A. (2012). The response of the xerophytic plant *Gypsophila aucheri* to salt and drought stresses: the role of the antioxidant defence system. *Turk. J. Bot.* 36, 697–706.

FAO. (2010). *Climate Change Implications for Food Security and Natural Resources Management in Africa*. Luanda: Food and Agriculture Organization of the United Nations.

Farooq, M., Hussain, M., Wahid, A., and Siddique, K. (2012). "Drought stress in plants: an overview," in *Plant Responses to Drought Stress*, ed. R. Aroca (Berlin: Springer), 1–33. doi: 10.1007/978-3-642-32653-0

Feng, Q., and Cheng, G. D. (1999). Moisture distribution and movement in sandy lands of China. *Acta Pedol. Sin.* 36, 225–236.

Flowers, T., Troke, P., and Yeo, A. (1977). The mechanism of salt tolerance in halophytes. *Ann. Rev. Plant Physio.* 28, 89–121. doi: 10.1146/annurev.pp.28.060177.000513

Glantz, M. H. (1994). "Drought, desertification and food production," in *Drought Follows the Plow*, ed. M. H. Glantz (Denver, CO: Cambridge University Press), 9–30.

Guerrier, G. (1996). Fluxes of Na^+, K^+ and Cl^-, and osmotic adjustment in *Lycopersicon pimpinellifolium* and L. *esculentum* during short- and long-term exposures to NaCl. *Physiol. Plantarum* 97, 583–591. doi: 10.1111/j.1399-3054.1996.tb00519.x

IPCC. (2014). "In: climate change 2014: synthesis report. contribution of working groups I, II and III to the fifth assessment report of the intergovernmental panel on climate change," in *The Core Writing Team*, eds R. K. Pachauri and L. Meyer (Geneva: IPCC).

Jarvis, R., and Mansfield, T. (1980). Reduced stomatal responses to light, carbon dioxide and abscisic acid in the presence of sodium ions. *Plant Cell Environ.* 3, 279–283.

Kerstiens, G., Tych, W., Robinson, M. F., and Mansfield, T. A. (2002). Sodium-related partial stomatal closure and salt tolerance of *Aster tripolium*. *New Phytol.* 153, 509–515. doi: 10.1046/j.0028-646X.2001.00330.x

Korkmaz, D. (2001). *Precipitation Titration:Determination of Chloride by the Mohr Method*. Available at: http://academic.brooklyn.cuny.edu/esl/gonsalves/tutorials/Writing_a_Lab_Report/xPrecipitation%20Titration%20edited%203.pdf

Kuang, W., Qian, J., Ma, Q., and Liu, Z. (2016). Vertical distribution of soil organic carbon and its relation to root distribution in five desert shrub communities. *Chin. J. Ecol.* 35, 275–281.

Lambers, H., Chapin, F. S. III, and Pons, T. L. (2008). "Plant water relations," in *Plant Physiological Ecology*, ed. I. Forseth (New York, NY: Springer), 163–223. doi: 10.1007/978-0-387-78341-3

Li, Y., Ye, W., Wang, M., and Yan, X. (2009). Climate change and drought: a risk assessment of crop-yield impacts. *Clim. Res.* 39, 31–46. doi: 10.3354/cr00797

Liu, F., Andersen, M. N., Jacobsen, S.-E., and Jensen, C. R. (2005). Stomatal control and water use efficiency of soybean (*Glycine max* L. Merr.) during progressive soil drying. *Environ. Exp. Bot.* 54, 33–40. doi: 10.1016/j.envexpbot.2004.05.002

Liu, J. Q., Pu, J. C., and Liu, X. M. (1987). Comparative studies on water relations and xeromorphic structures of some plant species in the middle part of the desert zone in China. *Acta Bot. Sin.* 29, 662–673.

Liu, J. Q., and Qiu, M. X. (1982). Ecological, physiological and anatomical traits of *Ammopiptanthus mongolicus* grown in desert of China. *Acta Bot. Sin.* 24, 568–574.

Ma, Q., Bao, A.-K., Chai, W. W., Wang, W.-Y., Zhang, J. L., Li, Y. X., et al. (2016). Transcriptomic analysis of the succulent xerophyte *Zygophyllum xanthoxylum* in response to salt treatment and osmotic stress. *Plant Soil* 402, 343–361. doi: 10.1007/s11104-016-2809-1

Ma, Q., Yue, L. J., Zhang, J. L., Wu, G. Q., Bao, A. K., and Wang, S. M. (2012). Sodium chloride improves photosynthesis and water status in the succulent xerophyte *Zygophyllum xanthoxylum*. *Tree Physiol.* 32, 4–13. doi: 10.1093/treephys/tpr098

Ma, Y. (1989). *Inner Mongolia Flora*. Hohhot: Inner Mongolia People's Publishing House.

Males, J. (2017). Secrets of succulence. *J. Exp. Bot.* 68, 2121–2134. doi: 10.1093/jxb/erx096

Martin, C. E. (1994). Physiological ecology of the Bromeliaceae. *Bot. Rev.* 60, 1–82. doi: 10.1007/BF02856593

McDowell, N., Pockman, W. T., Allen, C. D., Breshears, D. D., Cobb, N., Kolb, T., et al. (2008). Mechanisms of plant survival and mortality during drought: why do some plants survive while others succumb to drought? *New Phytol.* 178, 719–739. doi: 10.1111/j.1469-8137.2008.02436.x

Michel, B. E., Wiggins, O. K., and Outlaw, W. H. (1983). A guide to establishing water potential of aqueous two-phase solutions (Polyethylene Glycol plus Dextran) by amendment with mannitol. *Plant Physiol.* 72, 60–65.

Mishra, A. K., and Singh, V. P. (2010). A review of drought concepts. *J. Hydrol.* 391, 202–216. doi: 10.1016/j.jhydrol.2010.07.012

Murray, M., Cape, J., and Fowler, D. (1989). Quantification of frost damage in plant tissues by rates of electrolyte leakage. *New Phytol.* 113, 307–311. doi: 10.1111/j.1469-8137.1989.tb02408.x

Nagalakshmi, N., and Prasad, M. N. V. (2001). Responses of glutathione cycle enzymes and glutathione metabolism to copper stress in *Scenedesmus bijugatus*. *Plant Sci.* 160, 291–299. doi: 10.1016/S0168-9452(00)00392-7

Nakano, Y., and Asada, K. (1981). Hydrogen peroxide is scavenged by ascorbate-specific peroxidase in spinach chloroplasts. *Plant Cell Physiol.* 22, 867–880. doi: 10.1093/oxfordjournals.pcp.a076232

Nobel, P. S. (1977). Water relations and photosynthesis of a barrel cactus, *Ferocactus acanthodes*, in the Colorado Desert. *Oecologia* 27, 117–133. doi: 10.1007/BF00345817

Nuccio, M. L., Wu, J., Mowers, R., Zhou, H. P., Meghji, M., Primavesi, L. F., et al. (2015). Expression of trehalose-6-phosphate phosphatase in maize ears improves yield in well-watered and drought conditions. *Nat. Biotechnol.* 33:862. doi: 10.1038/nbt.3277

Ogburn, R., and Edwards, E. J. (2010). The ecological water-use strategies of succulent plants. *Adv. Bot. Res.* 55, 179–225. doi: 10.1016/S0065-2296(10)55004-3

Perera, L., De Silva, D., and Mansfield, T. (1997). Avoidance of sodium accumulation by the stomatal guard cells of the halophyte *Aster tripolium*. *J. Exp. Bot.* 48, 707–711. doi: 10.1093/jxb/48.3.707

Perera, L., Mansfield, T., and Malloch, A. (1994). Stomatal responses to sodium ions in *Aster tripolium*: a new hypothesis to explain salinity regulation in above-ground tissues. *Plant Cell Environ.* 17, 335–340. doi: 10.1111/j.1365-3040.1994.tb00300.x

Rao, M. V., Paliyath, G., and Ormrod, D. P. (1996). Ultraviolet-B-and ozone-induced biochemical changes in antioxidant enzymes of *Arabidopsis thaliana*. *Plant Physiol.* 110, 125–136. doi: 10.1104/pp.110.1.125

Richards, L., and Weaver, L. (1944). Moisture retention by some irrigated soils as related to soil moisture tension. *J. Agric. Res.* 69, 215–235.

Rundel, P., Ehleringer, J., Mooney, H., and Gulmon, S. (1980). Patterns of drought response in leaf-succulent shrubs of the coastal Atacama Desert in northern Chile. *Oecologia* 46, 196–200. doi: 10.1007/BF00540126

Serraj, R., and Sinclair, T. (2002). Osmolyte accumulation: can it really help increase crop yield under drought conditions? *Plant Cell Environ.* 25, 333–341. doi: 10.1046/j.1365-3040.2002.00754.x

Sharkey, T. D. (2005). Effects of moderate heat stress on photosynthesis: importance of thylakoid reactions, rubisco deactivation, reactive oxygen species, and thermotolerance provided by isoprene. *Plant Cell Environ.* 28, 269–277. doi: 10.1111/j.1365-3040.2005.01324.x

Sheahan, M. C., and Chase, M. W. (2000). Phylogenetic relationships within Zygophyllaceae based on DNA sequences of three plastid regions, with special emphasis on Zygophylloideae. *Syst. Bot.* 25, 371–384. doi: : 10.2307/2666648

Sheng, J., Qiao, Y., Liu, H., Zhai, Z., and Guo, Y. (2004). A study of the root system of *Haloxylon ammodendron*. *Acta Agrestia. Sin.* 12, 91–94. doi: 10.1371/journal.pone.0180875

Shi, Y., Yan, X., Zhao, P., Yin, H., Zhao, X., Xiao, H., et al. (2013). Transcriptomic analysis of a tertiary relict plant, extreme xerophyte *Reaumuria soongorica* to identify genes related to drought adaptation. *PLoS One* 8:e63993. doi: 10.1371/journal.pone.0063993

Sinclair, R. (1983). Water relations of tropical epiphytes: II. Performance during droughting. *J. Exp. Bot.* 34, 1664–1675. doi: 10.1007/s004420100714

Sperry, J. S. (2000). Hydraulic constraints on plant gas exchange. *Agr. For. Meteorol.* 104, 13–23. doi: 10.1016/S0168-1923(00)00144-1

Splunder, I. V., Voesenek, L., Vries, X. D., Blom, C., and Coops, H. (1996). Morphological responses of seedlings of four species of Salicaceae to drought. *Can. J. Bot.* 74, 1988–1995. doi: 10.1139/b96-238

Steduto, P., Hsiao, T. C., Fereres, E., and Raes, D. (2012). *Crop Yield Response to Water*. Rome: FAO.

Steudle, E., Zimmermann, U., and Lüttge, U. (1977). Effect of turgor pressure and cell size on the wall elasticity of plant cells. *Plant Physiol.* 59, 285–289.

Sukumaran, S., Cossani, C., Molero, G., Valluru, R., Tattaris, M., and Reynolds, M. (2016). *Genetic Mapping and Physiological Breeding Towards Heat and Drought Tolerance in Spring Wheat*. Mexico City: CIMMYT.

Todaka, D., Zhao, Y., Yoshida, T., Kudo, M., Kidokoro, S., Mizoi, J., et al. (2017). Temporal and spatial changes in gene expression, metabolite accumulation and phytohormone content in rice seedlings grown under drought stress conditions. *Plant J.* 90, 61–78. doi: 10.1111/tpj.13468

Turner, N., and Jones, M. (1980). "Turgor maintenance by osmotic adjustment: a review and evaluation," in *Adaptation of Plants to Water and High Temperature*

Stress, eds N. C. Turner and P. J. Kramer (New York, NY: John Wiley & Sons), 87–103.

Verslues, P. E., Agarwal, M., Katiyar-Agarwal, S., Zhu, J., and Zhu, J. K. (2006). Methods and concepts in quantifying resistance to drought, salt and freezing, abiotic stresses that affect plant water status. *Plant J.* 45, 523–539. doi: 10.1111/j.1365-313X.2005.02593.x

Véry, A. A., Robinson, M. F., Mansfield, T. A., and Sanders, D. (1998). Guard cell cation channels are involved in Na^+-induced stomatal closure in a halophyte. *Plant J.* 14, 509–521. doi: 10.1046/j.1365-313X.1998.00147.x

Volaire, F., Thomas, H., and Lelievre, F. (1998). Survival and recovery of perennial forage grasses under prolonged Mediterranean drought: I. Growth, death, water relations and solute content in herbage and stubble. *New Phytol.* 140, 439–449. doi: 10.1046/j.1469-8137.1998.00288.x

von Willert, D. J., Eller, B. M., Werger, M. J. A., Brinckmann, E., and Ihlenfeldt, H. D. (1992). *Life Strategies of Succulents in Deserts: with Special Reference to the Namib Desert*. Cambridge: Cambridge University Press.

Wadleigh, C. H., Gauch, H. G., and Magistad, O. C. (1946). *Growth and Rubber Accumulation in Guayule as Conditioned by Soil Salinity and Irrigation Regime*. Washington, DC: United States Department of Agriculture.

Wang, S. M., Wan, C., Wang, Y., Chen, H., Zhou, Z., Fu, H., et al. (2004). The characteristics of Na^+, K^+ and free proline distribution in several drought-resistant plants of the Alxa Desert, China. *J. Arid. Environ.* 56, 525–539. doi: 10.1016/S0140-1963(03)00063-6

Wang, S. M., Zhang, J. L., and Flowers, T. J. (2007). Low-affinity Na^+ uptake in the halophyte *Suaeda maritima*. *Plant Physiol.* 145, 559–571. doi: 10.1104/pp.107.104315

Wang, X., Wang, H., Liu, S., Ferjani, A., Li, J., Yan, J., et al. (2016). Genetic variation in ZmVPP1 contributes to drought tolerance in maize seedlings. *Nat. Genet.* 48, 1233–1241. doi: 10.1038/ng.3636

Wu, B., and Su, X. (2016). Identification of drought response genes in *Zygophyllum xanthoxylum* by suppression subtractive hybridization. *J. Plant Biol.* 59, 377–385. doi: 10.1007/s12374-015-0580-0

Wu, G. Q., Xi, J. J., Wang, Q., Bao, A. K., Ma, Q., Zhang, J. L., et al. (2011). The *ZxNHX* gene encoding tonoplast Na^+/H^+ antiporter from the xerophyte *Zygophyllum xanthoxylum* plays important roles in response to salt and drought. *J. Plant Physiol.* 168, 758–767. doi: 10.1016/j.jplph.2010.10.015

Xie, H., Yang, D.-H., Yao, H., Bai, G., Zhang, Y.-H., and Xiao, B.-G. (2016). iTRAQ-based quantitative proteomic analysis reveals proteomic changes in leaves of cultivated tobacco (*Nicotiana tabacum*) in response to drought stress. *Biochem. Bioph. Res. Commun.* 469, 768–775. doi: 10.1016/j.bbrc.2015.11.133

Yeo, A., and Flowers, T. (1980). Salt tolerance in the halophyte *Suaeda maritima* L. Dum.: evaluation of the effect of salinity upon growth. *J. Exp. Bot.* 31, 1171–1183. doi: 10.1007/BF00392237

Yoshimura, K., Masuda, A., Kuwano, M., Yokota, A., and Akashi, K. (2008). Programmed proteome response for drought avoidance/tolerance in the root of a C_3 xerophyte (wild watermelon) under water deficits. *Plant Cell Physiol.* 49, 226–241. doi: 10.1093/pcp/pcm180

Yuan, H. J., Ma, Q., Wu, G. Q., Wang, P., Hu, J., and Wang, S. M. (2015). *ZxNHX* controls Na^+ and K^+ homeostasis at the whole-plant level in *Zygophyllum xanthoxylum* through feedback regulation of the expression of genes involved in their transport. *Ann. Bot. London* 115, 495–507. doi: 10.1093/aob/mcu177

Yue, L. J., Li, S. X., Ma, Q., Zhou, X. R., Wu, G. Q., Bao, A. K., et al. (2012). NaCl stimulates growth and alleviates water stress in the xerophyte *Zygophyllum xanthoxylum*. *J. Arid. Environ.* 87, 153–160. doi: 10.1016/j.jaridenv.2012.06.002

Zeiger, E. (1983). The biology of stomatal guard cells. *Annu. Rev. Plant Biol.* 34, 441–474. doi: 10.1146/annurev.pp.34.060183.002301

Zhao, M., and Running, S. W. (2010). Drought-induced reduction in global terrestrial net primary production from 2000 through 2009. *Science* 329, 940–943. doi: 10.1126/science.1192666

Zhou, X., Zhou, Z., and Wu, C. (2006). The research of the breeding characters of *Zygophyllum xanthoxylum*. *Pratacult. Sci.* 23, 38–41.

Conflict of Interest Statement: R-JC was employed by company Noble Research Institute LLC.

The remaining authors declare that the research was conducted in the absence of any commercial or financial relationships that could be construed as a potential conflict of interest.

frontiers in Plant Science

ORIGINAL RESEARCH
published: 07 September 2018
doi: 10.3389/fpls.2018.01306

Genome-Wide Analysis of *Glycine soja* Response Regulator *GsRR* Genes Under Alkali and Salt Stresses

Chao Chen[1†], Ailin Liu[1†], Hao Ren[1], Yang Yu[1], Huizi Duanmu[1], Xiangbo Duan[1], Xiaoli Sun[2], Beidong Liu[3] and Yanming Zhu[1*]*

[1] Key Laboratory of Agricultural Biological Functional Genes, Northeast Agricultural University, Harbin, China, [2] Crop Stress Molecular Biology Laboratory, Agronomy College, Heilongjiang Bayi Agricultural University, Daqing, China, [3] Department of Chemistry and Molecular Biology, University of Gothenburg, Gothenburg, Sweden

Soil salt-alkalization is a dramatic challenging factor for plant growth. Wild soybean (*Glycine soja*) exhibits a favorable trait of superior tolerance to salt-alkali stress, and recent discoveries show that response regulator family genes are involved in diverse abiotic stresses. Genomic and transcriptomic analyses of all response regulator genes in wild soybean will provide insight into their function in plant stress response. In this study, we identified and characterized a total of 56 *Glycine soja* response regulator (*GsRR*) genes. Phylogenetic analysis suggested that *GsRR* genes could be classified into five subclasses (A1, A2, B1, B2, and C). We further investigated the chromosome locations, gene duplications and conserved domains of the *GsRRs*. Furthermore, the clustering analysis of *GsRR* transcript profiles revealed five different expression patterns under alkali stress. The A1 and A2 subclasses display significantly higher transcriptional levels than the B subclass. In addition, quantitative real-time PCR results verified that the *GsRR* genes were also significantly influenced by salt stress. Notably, *GsRR2a* in the A1 subclass showed opposite expression patterns under salt stress comparing with alkali stress. Moreover, overexpression of *GsRR2a* in *Arabidopsis* significantly improved the tolerance to alkali stress, but not salt stress. These results suggest the important roles of *GsRR* genes in response to salt and alkaline stresses, and also provide valuable clues for further functional characterization of *GsRR* family genes.

Keywords: ***Glycine soja*, alkali stress, salt stress, response regulator, *GsRR2a***

OPEN ACCESS

Edited by:
Nicholas Provart,
University of Toronto, Canada

Reviewed by:
Ping Lan,
Institute of Soil Science (CAS), China
Shaojun Dai,
Northeast Forestry University, China

***Correspondence:**
Xiaoli Sun
csmbl2016@126.com
Yanming Zhu
ymzhu2001@neau.edu.cn

† These authors have contributed equally to this work

Specialty section:
This article was submitted to Plant Abiotic Stress, a section of the journal Frontiers in Plant Science

Received: *07 February 2018*
Accepted: *17 August 2018*
Published: *07 September 2018*

Citation:
Chen C, Liu A, Ren H, Yu Y, Duanmu H, Duan X, Sun X, Liu B and Zhu Y (2018) Genome-Wide Analysis of Glycine soja Response Regulator GsRR Genes Under Alkali and Salt Stresses. Front. Plant Sci. 9:1306. doi: 10.3389/fpls.2018.01306

INTRODUCTION

Saline-alkali soil is a major factor limiting crop growth, development, and yields. Salt stress in the soil generally causes osmotic stress and ion injury (Zhu, 2003). Alkali stress in the soil is usually characterized by low availability of nutrients, high concentrations of HCO_3^- (bicarbonate) and CO_3^{2-} (carbonate), and high pH (Yang C.W. et al., 2008; An et al., 2016; Song T. et al., 2017). Owing to hydrolyzation of HCO_3^- and CO_3^{2-}, plants growing on such soils suffer not only sodium toxicity, but also the precipitation Ca^{2+}, Mg^{2+}, and $H_2PO_4^-$ (Islam et al., 2011), inhibition of ion uptake (Yang et al., 2007) and disruption of cytoplasmic ion homeostasis (An et al., 2016). Some studies have demonstrated that alkali stress imposes much severer effects than salt stress on plants (Sadras et al., 2003; Shi and Sheng, 2005; Yang et al., 2007), and recent researches also point out a

great difference in the physiological adaptive mechanisms of plants responding to alkali stress and salt stress (Borsani et al., 2005; Miller et al., 2010; Rouphael et al., 2017).

With the recent advances in high-throughput sequencing technologies, genes associated with high salinity and alkaline tolerance have been identified on a large scale at a genome-wide level (Jin et al., 2008; Sun et al., 2013; Zhang et al., 2016). The current knowledge of salt-alkali stress transcriptome mainly focuses on salt stress, whereas only limited information concerning alkali stress is available. Wild soybean (*Glycine soja*) exhibits very high adaptability in extreme environments. Our previous studies showed that the wild soybean (G07256) could germinate and set seed even in sodic soil of pH 9.02, and displayed much superior tolerance to 50 mM $NaHCO_3$ treatment (Ge et al., 2010), demonstrating that it has developed molecular and physiological mechanisms to adapt itself to this severe condition. Additional, we have identified 3,380 alkaline-responsive genes using RNA sequencing, and also characterized some functional genes under alkaline stress, such as *GsCHX19.3* (Jia et al., 2017), *GsJ11* (Song X. et al., 2017), and *GsTIFY10* (Zhu et al., 2011). Therefore, it is a suitable model organism for studying the molecular mechanisms of plant stress tolerance and a valuable source for characterizing alkali stress responsive genes.

Cytokinins (CKs) are regulators of plant growth and development, and have been shown to control plant responses to salt stress (Tran et al., 2007; Wang et al., 2015). The early response to CKs in *Arabidopsis* involves a multi-step signaling network, in which ARRs (Arabidopsis Response Regulators) play central roles (Jeon and Kim, 2013). The ARRs are divided into three types (type A, B, and C). The type-A ARRs (ARR3-9, ARR15-17, and ARR23) are small proteins with a short receiver domain which contains the phosphorylatable aspartate residue. CK-inducible type-A ARRs act mainly as redundant negative regulators in CK signaling (To et al., 2007). The type-B ARRs (ARR1, ARR2, ARR10-14, and ARR18-21) contain a receiver domain and a large C-terminal region harboring a Myb-like DNA-binding domain for transcriptional activation (Yokoyama et al., 2007). The type-B ARRs are not inducible by CKs, but activate transcription factors that induce transcription of type-A ARRs under CK treatment. Type-C ARRs (ARR22 and ARR24) resemble type-A ARRs, but their expression does not depend on CKs (Horak et al., 2008).

In *Arabidopsis*, the function of *ARRs* has been well suggested to be involved in plant development and signal transduction. *ARR2* is a downstream genes of *ETR1* in ethylene signal transduction (Hass et al., 2004). *ARR3* and *ARR4* play important roles in the circadian control through the CK-independent pathway (Salome et al., 2006). *ARR4* also modulates red light signaling by interacting with phytochrome B (Sweere et al., 2001). Furthermore, studies have demonstrated that *ARRs* play regulatory roles in abiotic stresses. The type-A, -B, and -C *ARRs* are reported to differentially respond to salt stress (Nishiyama et al., 2012). *ARR1* and *ARR12* regulate sodium accumulation in the shoots by controlling the expression of *HKT1* in *Arabidopsis* (Mason et al., 2010). Overexpression of *ARR5*, *ARR7*, and *ARR15* promoted freezing tolerance (Shi et al., 2012). The CK-deficient *Arabidopsis* mutants displayed enhanced drought and salt tolerance, as well as increased ABA sensitivity (Nishiyama et al., 2011). In addition, type-A *ARRs* can act as negative regulators in cold stress signaling through the inhibition of the ABA-dependent pathway (Jeon et al., 2010). However, until now, little is known about the *RR* family genes in response to salt and alkali stresses.

In this study, we identified 56 genes encoding RR proteins in *G. soja* genome. By using phylogenetics to characterize the variations within the *GsRR* family, we found expression of *GsRR* family genes were differentially affected by alkali and salt stresses. We further suggested that one of them, *GsRR2a* played a positive role in response to alkali stress.

MATERIALS AND METHODS

Identification and Characteristics of Response Regulator Family Genes in the *G. soja* Genome

To identify all putative RR family genes in wild soybean, we obtained the *G. soja* genome and proteome sequences, respectively (Jeon et al., 2010; Qi et al., 2014). Because of the limited sequence information for *G. soja*, *G. max* database is used to identify the predicted genes and secondary structure (Zeng et al., 2012). Local BLAST search against *G. soja* proteome was carried out by using the HMM profile (build 2.3.2) of the response regulator domain as query. The HMM profile of receiver domain (ID PF00072) was downloaded from the Pfam database (Punta et al., 2012). The molecular weight and isoelectric point of GsRR proteins were predicted using online software Compute pI/Mw[1].

Phylogenetic Tree Construction and Sequence Analysis

To investigate the phylogenetic relationships among GsRR proteins in plants, Clustal X program (Larkin et al., 2007) was used to perform the multiple sequence alignments of all 56 GsRRs from wild soybean and 24 ARRs from *Arabidopsis*. The phylogenetic trees were generated and displayed by using software MEGA 5.0 with the NJ (neighbor-joining) method (Kumar et al., 2008). The MEME[2] was used to discover conserved motifs of GsRR family proteins. Gene structure maps were generated using GSDS (Gene Structure Display Server)[3] (Hu et al., 2015). We defined the gene duplication according to the reported standards (Yang S. et al., 2008).

Plant Materials, Growth Conditions, and Stress Treatments

Seedlings of wild soybean (G07256) were grown in a culture room with the following settings: 60–80% relative humidity, 24–28°C and a light regime of 16 h light/8 h dark. Before sowing, seeds were treated with 98% sulfuric acid for 10–15 min and washed three times with sterile water. Nineteen days after sowing, seedlings were transferred into 1/4 strength Hoagland's

[1]http://au.expasy.org/tools/pi_tool.html

[2]http://meme-suite.org/

[3]http://gsds.cbi.pku.edu.cn/

solution with 50 mM $NaHCO_3$ or 200 mM NaCl for alkali or salt stress. Equal amounts of leaves and roots were sampled as three biological replicates at 0, 1, 3, 6 h time points after treatments.

Transcript Level Analysis

In order to analyze the expression profiles of *GsRR* family genes under alkali stress, hierarchical clustering tree based on the transcript data of *GsRR* genes was created with TM4: MeV 4.9 software (Saeed et al., 2003). The transcript data of *GsRRs* in *G. soja* roots subjected to alkali stress was previously obtained in 1 KP project by using transcriptome sequencing, and the data has been deposited in 1KP project[4].

The expression profiles of *GsRRs* under salt stress were performed by using qRT-PCR (quantitative real-time PCR). The *GAPDH* in *G. soja* was used to normalize all values. Primer sequences of *GsRRs* and *GADPH* are listed in **Supplementary Table S1**. To enable statistical analysis, three fully independent biological replicates were obtained and subjected to qRT-PCR runs in triplicate. Expression levels for all candidate genes were calculated using the $2^{-\Delta\Delta CT}$ method (Livak and Schmittgen, 2001).

Transformation of *Arabidopsis*

The CDS region of *GsRR2a* was cloned into the pCAM230035S vector under the control of CaMV35S promoter (primer pairs: 5′-CGGGATCCATGGACACGGACA GCT TCG-3′ and 5′-GCGTCGACTCAATCGGTGCTGGTCA-3′). The pCAM230035S:GsRR2a construct was introduced into *Agrobacterium tumefactions* strain LBA4404 for transformation through floral-dip method (Clough and Bent, 1998). The transformed seeds were selected on 1/2MS medium containing 50 mg L^{-1} kanamycin, and the T_3 generation overexpression lines were randomly chosen for further studies.

Phenotypic Analysis Under Alkali and Salt Stresses

The *Arabidopsis* seeds were sterilized as described (Sun et al., 2014). During the early seedling growth stage, the WT and overexpression seeds were sown on 1/2 agar medium supplemented with 0, 7, or 8 mM $NaHCO_3$, respectively. The numbers of seedlings with opening and greening leaves were recorded after 12 days. At the adult stage, the 20-day-old WT and overexpression plants grown in nursery pots were irrigated with water or 100 mM $NaHCO_3$ every 3 days. Photos were taken after 21 days. The chlorophyll content was detected using the 80% (v/v) acetone extract (Lewinsohn and Gressel, 1983). The malondialdehyde (MDA) content was determined by using a thiobarbituric acid method (Peever and Higgins, 1989). For salt treatment, the WT and overexpression seeds were sown on 1/2 agar medium supplemented with 0 or 150 mM NaCl, respectively. The germination rates were recorded and photos were taken after 6 days.

All experiments were repeated at least three times and the data was subjected to statistical analyses using the SPSS software by Student's *t*-test.

[4]http://www.onekp.com/samples/list.php

RESULTS

Identification of Response Regulator Genes in *G. soja*

In order to identify GsRR family genes, we used the amino acid sequences of the RR receiver domains (Pfam: PF00072) as queries for BLASTP searches. Sixty-two putative *GsRR* genes were acquired. Then we performed a proteome-wide screen for all putative GsRR by using the Pfam database, four genes were discarded due to the incomplete RR receiver domains and two genes were discarded because of redundancy. Consequently, 56 non-redundant *GsRR* genes were identified, including 19 type-A, 30 type-B, and 7 type-C *GsRRs*. The characteristics of the *GsRR* family genes, including the full CDS length, protein length, molecular weight and pI values are presented in **Table 1**.

Phylogenetic Analysis of GsRR Proteins

To investigate the evolutionary relationship of GsRRs and homologous ARR proteins, we constructed a NJ tree using MEGA 5.0 (**Supplementary Figure S1**). Based on the topology and clade robust bootstrap values, the GsRR proteins were classified into three major classes: type-A, type-B, and type-C. Nineteen GsRRs (GsRR1a to GsRR19a), thirty (GsRR1b to GsRR30b) and seven (GsRR1c to GsRR7c) were clustered into type-A, type-B, and type-C, respectively (**Table 1**). Furthermore, as shown in **Figure 1**, type-A was further divided into two subclasses, designated as A1and as A2. In addition, type-B was also divided into two subclasses (B1 and B2). Most of type-B GsRR proteins belonged to the B1 subclass, only GsRR3b, GsRR8b, GsRR16b, and GsRR18b were clustered into the B2 subclass.

Physical Locations and Gene Duplications of *GsRRs*

The potential mechanisms driving the evolution of the *GsRR* family were elucidated by analyzing the gene duplication events. In this study, 56 *GsRR* genes were distributed among 18 chromosomes, with the exception of chromosome 10 and 20 (**Figure 2**). The number of *GsRR* genes in each chromosome differed considerably. For example, 8 *GsRRs* were located on chromosome 19, which chromosomes 1, 12, 14, and 16 only contain one gene, respectively. Using *G. soja* genome duplication information, thirty duplicated gene pairs were identified among 56 *GsRRs*, including three segmental duplication events between chromosomes.

Conserved Domains and Motifs of *GsRR* Family Genes

The modular structure of ARRs has been studied thoroughly in *Arabidopsis* (D'Agostino et al., 2000), which enables us to analyze domain architecture for GsRRs. We identified three conserved domains: a RR receiver domain (PF06200), a Myb-like DNA-binding domain (PF00249) and a CCT motif (PF06203). The RR receiver domain was variable among three types of *GsRR*s (**Figure 3**). The RR receiver domain of type-B GsRRs contained approximately 120 amino acids with three exclusively

TABLE 1 | Basic information of the *GsRR* family genes of *G. soja*.

Gene name	Full CDS length (bp)	Protein length (aa)	Molecular weight (Da)	pI	Domain	Similarity with *Arabidopsis*	
GsRR1a	735	244	26489.9	5.15	RR	*ARR3*	AT1G59940.1
GsRR2a	723	240	26531	4.99	RR	*ARR3*	AT1G59940.1
GsRR3a	747	248	28265.8	5.61	RR	*ARR9*	AT3G57040.1
GsRR4a	519	172	19577.6	6.44	RR	*ARR9*	AT3G57040.1
GsRR5a	615	204	22219.8	8.49	RR	*ARR6*	AT5G62920.1
GsRR6a	441	146	16118.8	8.35	RR	*ARR17*	AT3G56380.1
GsRR7a	708	235	26476.7	5.32	RR	*ARR9*	AT3G57040.1
GsRR8a	636	211	23187.9	8.23	RR	*ARR5*	AT3G48100.1
GsRR9a	699	232	26149.4	5.2	RR	*ARR9*	AT3G57040.1
GsRR10a	441	146	16003.6	8.34	RR	*ARR17*	AT3G56380.1
GsRR11a	615	204	22139.5	7.63	RR	*ARR6*	AT5G62920.1
GsRR12a	672	223	24610.3	5.27	RR	*ARR3*	AT1G59940.1
GsRR13a	564	187	21226.3	5.62	RR	*ARR9*	AT3G57040.1
GsRR14a	636	211	23722	5.38	RR	*ARR9*	AT3G57040.1
GsRR15a	540	179	20420.5	6.53	RR	*APRR7*	AT5G02810.1
GsRR16a	540	179	20439.5	5.98	RR	*ARR9*	AT3G57040.1
GsRR17a	624	207	22844.7	7.59	RR	*ARR8*	AT2G41310.1
GsRR18a	669	222	24661.3	5.26	RR	*ARR3*	AT1G59940.1
GsRR19a	741	246	27901.5	5.5	RR	*ARR9*	AT3G57040.1
GsRR1b	1902	633	69759.6	6.27	RR/Myb-like	*ARR2*	AT4G16110.1
GsRR2b	1971	656	72493.4	6.36	RR/Myb-like	*ARR12*	AT2G25180.1
GsRR3b	2076	691	76424.3	6.43	RR/CCT motif	*APRR5*	AT5G24470.1
GsRR4b	1908	635	71711.8	5.35	RR/Myb-like	*ARR11*	AT1G67710.1
GsRR5b	1233	411	45938.8	8.14	RR/Myb-like	*ARR1*	AT3G16857.1
GsRR6b	1488	495	55935.2	6.38	RR/Myb-like	*ARR1*	AT3G16857.1
GsRR7b	2091	696	76774.2	6.51	RR/Myb-like	*ARR12*	AT2G25180.1
GsRR8b	2103	700	77092.2	6.67	RR/CCT motif	*APRR5*	AT5G24470.1
GsRR9b	1092	633	69792.6	6.17	RR/Myb-like	*ARR2*	AT4G16110.1
GsRR10b	2040	679	74250.5	5.72	RR/Myb-like	*ARR2*	AT4G16110.1
GsRR11b	1206	401	45439.9	5.63	RR/Myb-like	*ARR14*	AT2G01760.1
GsRR12b	1479	492	54810.5	7.26	RR/Myb-like	*ARR2*	AT4G16110.1
GsRR13b	1782	593	66977.2	5.23	RR/Myb-like	*ARR11*	AT1G67710.1
GsRR14b	2022	673	73845	6.1	RR/Myb-like	*ARR2*	AT4G16110.1
GsRR15b	2097	698	76222	5.57	RR/Myb-like	*ARR12*	AT2G25180.1
GsRR16b	2298	765	83325.3	5.85	RR/CCT motif	*APRR7*	AT5G02810.1
GsRR17b	1815	604	68074.7	5.42	RR/Myb-like	*ARR11*	AT1G67710.1
GsRR18b	1881	626	68442	6.04	RR/CCT motif	*APRR7*	AT5G02810.1
GsRR19b	2043	680	75246.4	5.94	RR/Myb-like	*ARR12*	AT2G25180.1
GsRR20b	1998	665	73548.4	5.84	RR/Myb-like	*ARR12*	AT2G25180.1
GsRR21b	2019	672	73650.7	5.94	RR/Myb-like	*ARR1*	AT3G16857.1
GsRR22b	2094	697	76394.6	5.83	RR/Myb-like	*ARR12*	AT2G25180.1
GsRR23b	2010	669	73975.8	8.08	RR/Myb-like	*ARR2*	AT4G16110.1
GsRR24b	2034	677	73855.1	5.81	RR/Myb-like	*ARR1*	AT3G16857.1
GsRR25b	2046	681	75164.1	5.31	RR/Myb-like	*ARR12*	AT2G25180.1
GsRR26b	2004	667	73691.4	5.9	RR/Myb-like	*ARR12*	AT2G25180.1
GsRR27b	1368	455	51483.7	6.23	RR/Myb-like	*ARR11*	AT1G67710.1
GsRR28b	1008	335	38653.4	7.04	RR/Myb-like	*ARR2*	AT4G16110.1
GsRR29b	1107	369	41812.9	6.95	RR/Myb-like	*ARR2*	AT4G16110.1
GsRR30b	948	315	35909.7	5.39	RR/Myb-like	*ARR2*	AT4G16110.1
GsRR1c	399	132	14767	6.51	RR	*ARR24*	AT5G26594.1
GsRR2c	342	113	12627.8	9.05	RR	*ARR24*	AT5G26594.1
GsRR3c	345	114	12572.2	5.32	RR	*ARR24*	AT5G26594.1

(Continued)

TABLE 1 | Continued

Gene name	Full CDS length (bp)	Protein length (aa)	Molecular weight (Da)	pI	Domain	Similarity with *Arabidopsis*	
GsRR4c	426	141	16341.8	8.7	RR	*ARR24*	AT5G26594.1
GsRR5c	351	116	12977.9	5.31	RR	*ARR24*	AT5G26594.1
GsRR6c	327	108	11984.9	5.08	RR	*ARR24*	AT5G26594.1
GsRR7c	453	150	16958.4	5.56	RR	*ARR24*	AT5G26594.1

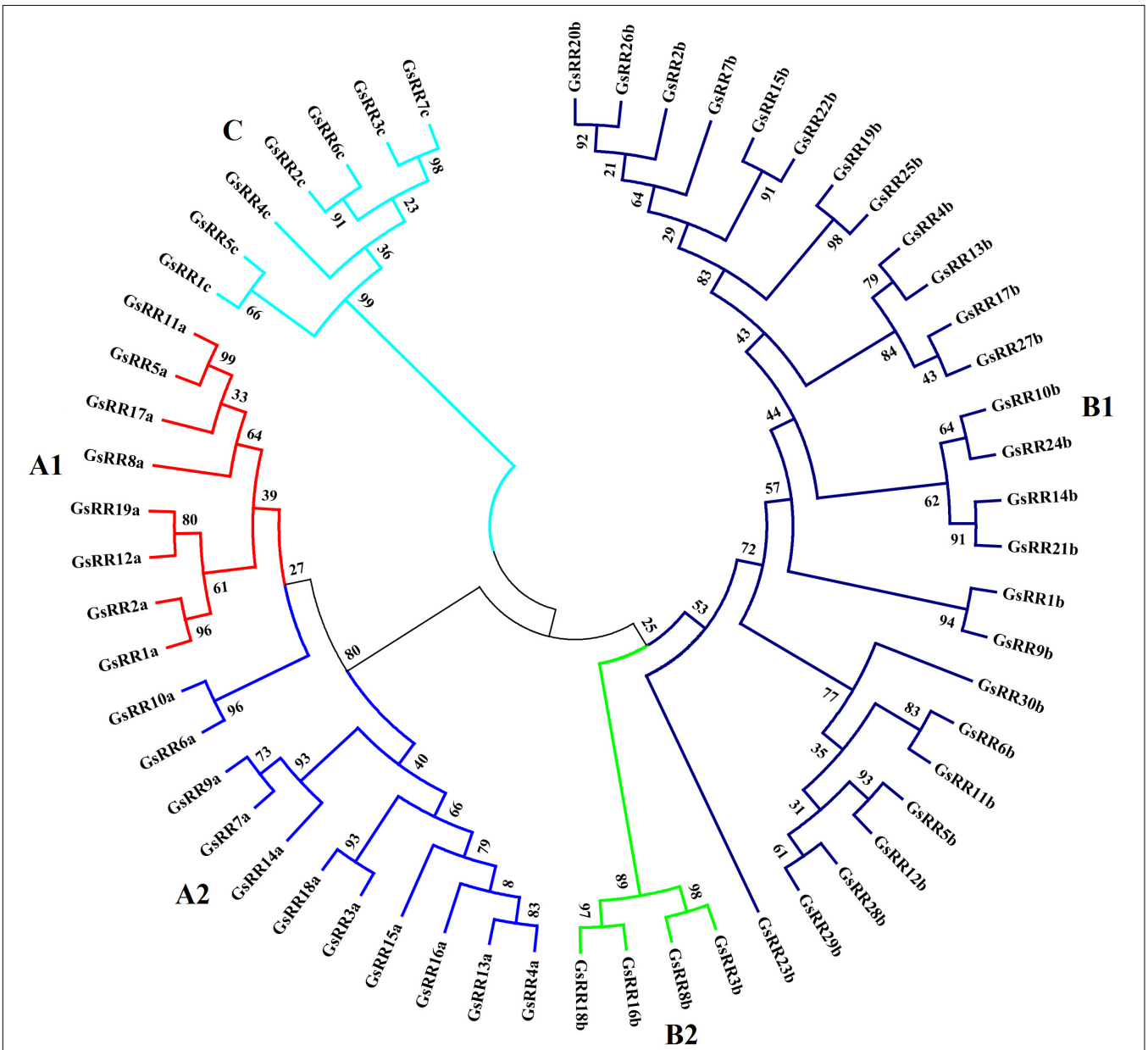

FIGURE 1 | Phylogenetic trees of *GsRR* family genes in *G. soja*. The phylogenetic tree was inferred by MEGA 5.0 with the NJ (neighbor-joining) method after the alignment of protein sequences of the *GsRR* family. The numbers beside the branches represent bootstrap values based on 1,000 replications. *GsRR* family genes were divided into five subclasses and marked by different colors.

conserved phosph-accepting amino acids: an invariant D1 site in the center, a D2 site at the N-terminus and a K site at the C-terminus. Compared with type-B, each type-A GsRR has a variable short insertion in the receiver domain and a short C-terminal extension. Type-C GsRRs lost the conserved D2 site in the N-terminus. Remarkably, besides the RR receiver

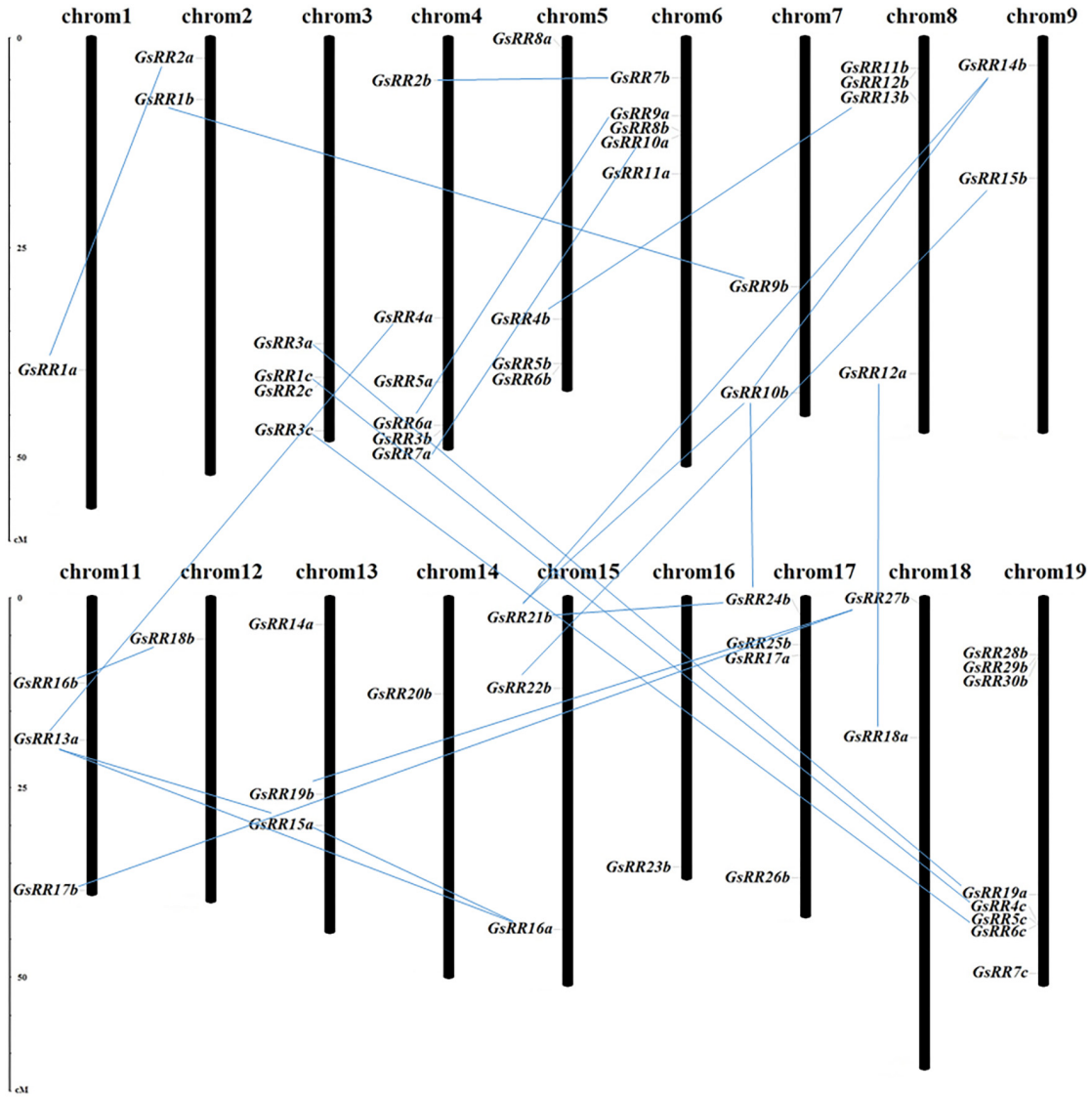

FIGURE 2 | Chromosomal locations and duplications of *GsRR* genes. The scales represent megabases (Mb). The black bars represent the chromosomes. *GsRR* genes distribute on the 18 chromosomes. The paralogous genes are connected by lines.

domain, all type-B1 GsRRs contained a C-terminal conserved domain designated as Myb-likes DNA binding domain, which functions importantly in CK responses. In addition, four type-B2 GsRRs contained a CCT motif in the C-terminus. In general, the classification of GsRRs based on their domain composition well supported the phylogenetic results described above.

To verify the results of domain prediction, the conserved motifs were discovered using MEME on-line tool (Bailey et al., 2009). As shown in **Figure 4** and **Supplementary Figure S2**, when specifying the RR receiver domain, motifs 1, 2, 3, and 4 were found in most type-A and type-B GsRRs. The type-C GsRRs possessed an incomplete RR receiver domain. The Myb-like DNA binding domain, motifs 5 and 6 were distinctively detected in type-B1 members, except GsRR6b, GsRR11b and GsRR28b only included motif 6.

Expression Patterns of *GsRRs* Genes Under Alkali Stress

The RR family genes are known to be involved in abiotic stress response (Jeon et al., 2010; Mason et al., 2010). The wild soybean G07256 exhibits a much greater tolerance to alkali stress than other plants. Therefore, based on our previous transcriptome data of wild soybean roots under alkali stress (Ge et al., 2010; DuanMu et al., 2015), we performed the expression profiles of *GsRR* family genes using Pearson correlation Hierarchical Clustering with TM4: MeV 4.9 software. The results showed that 31 *GsRR*s were responsive to alkali stress, with distinctive induction dynamics (**Figure 5**). In general, five major expression

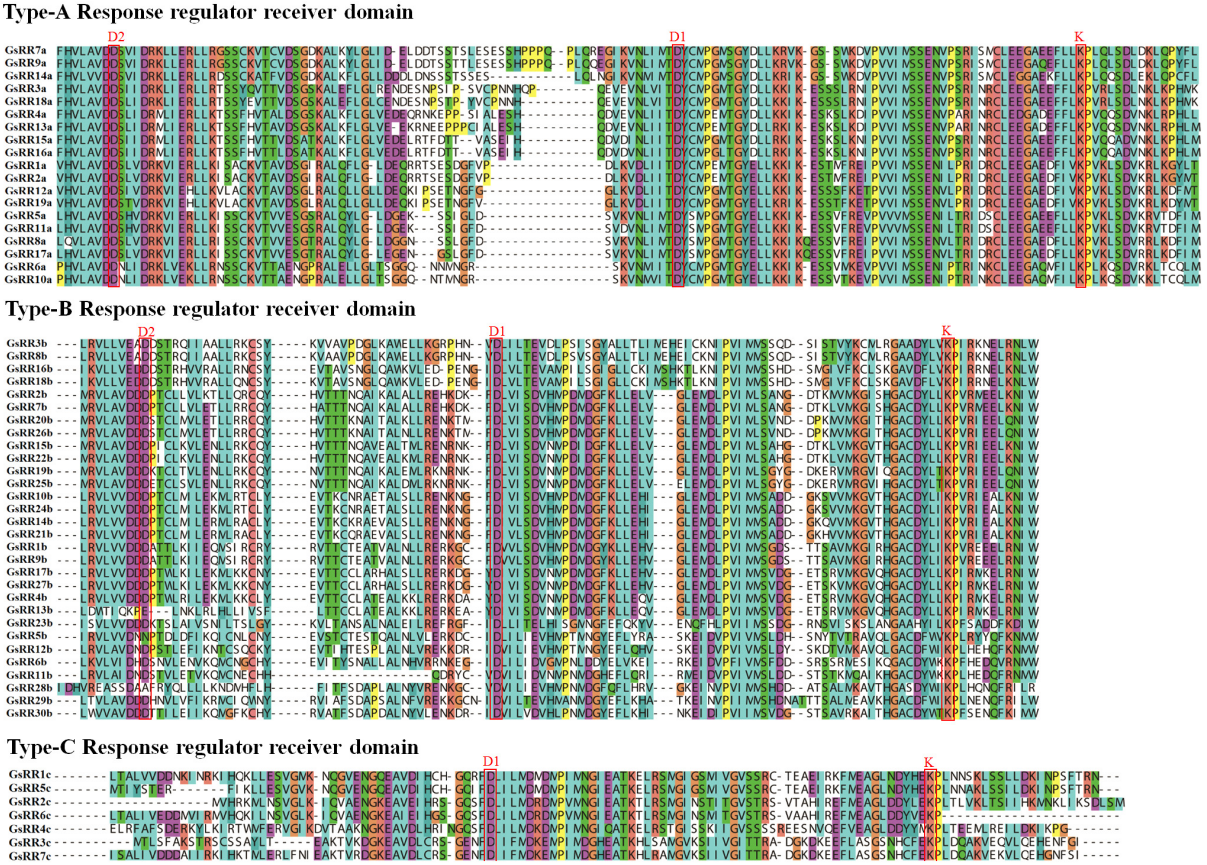

FIGURE 3 | Multiple alignment of *GsRR* family proteins. Multiple sequence alignment shows the RR receiver domains of type-A, -B, and -C. Multiple alignment was performed with Clustal X. The conserved amino acids sites D1, D2, and K are marked.

patterns were unraveled. Five type-A2 *GsRRs* (*15a*, *16a*, *18a*, *13a*, *3a*) and *GsRR19a* formed the first cluster, with significant down-regulation from 1 h to 6 h after alkali stress. Six type-B1 *GsRRs* (*25b*, *10b*, *9b*, *21b*, *7b*, *2b*) and *GsRR8a* showed no obvious change during the treatment. In contrast, type-B GsRRs (*19b*, *20b*, *16b*, *8b* and *3b*) in the third cluster were dramatically up-regulated at 3 h and kept the up-regulated trend in varying degrees until 6 h. The transcript levels of other six *GsRR* genes (*4b*, *14b*, *17b*, *15b*, *22b*, and *26b*) in the fourth cluster were down-regulated and then recovered to the basal levels. It is worth to notice that on the basis of their expression patterns, type-A *GsRRs* were basically separated into two groups, similar with the classification of subclass A1 and A2. The transcript levels of subclass A1 *GsRRs* (*11a*, *2a*, *17a*, and *5a*) were up-regulated at 1 h and then down-regulated at 6 h, which is opposite to subclass A2. These results indicated that *GsRRs* might have different roles in regulating alkali stress response.

Expression Patterns of *GsRRs* Under Salt Treatment

To provide insight into the regulatory mechanisms of *GsRRs* in salt stress, we further analyzed their transcript levels under salt stress using the qRT-PCR analysis. As shown in **Figure 6A**, most type-A *GsRRs* were significantly up-regulated from 1 to 6 h under salt stress. Compared with subclass A2, subclass A1 *GsRRs* responded to salt stress faster and last longer. Unlike alkali stress, among 12 type-A *GsRRs*, only two were down-regulated under salt stress, indicating they responded to salt and alkali stresses in different pathways. For type-B *GsRRs*, three subclass B2 members *GsRR3b*, *GsRR8b*, and *GsRR16b* were down-regulated; eight type-B1 *GsRRs* (*10b*, *13b*, *14b*, *15b*, *20b*, *21b*, and *22b*) were up-regulated from 1 to 6 h, seven type-B1 genes were down-regulated at 1, 3, or 6 h (**Figure 6B**). For type-C *GsRRs*, only *GsRR7c* slightly responded to salt stress (less than twofold) (**Figure 6C**).

QRT-PCR Validation of *GsRR2a* Under Salt and Alkali Stresses

According to the expression analysis under salt and alkali stress, we focused on one of the type-A1 genes *GsRR2a*, whose expression was strongly induced by alkali stresses, but reduced by salt stress. To confirm this finding, we further detected its expression levels in both roots and leaves of *G. soja* seedlings under 200 mM NaCl or 50 mM $NaHCO_3$ by using qRT-PCR analysis. As shown in **Figure 7**, under alkali treatment, *GsRR2a*

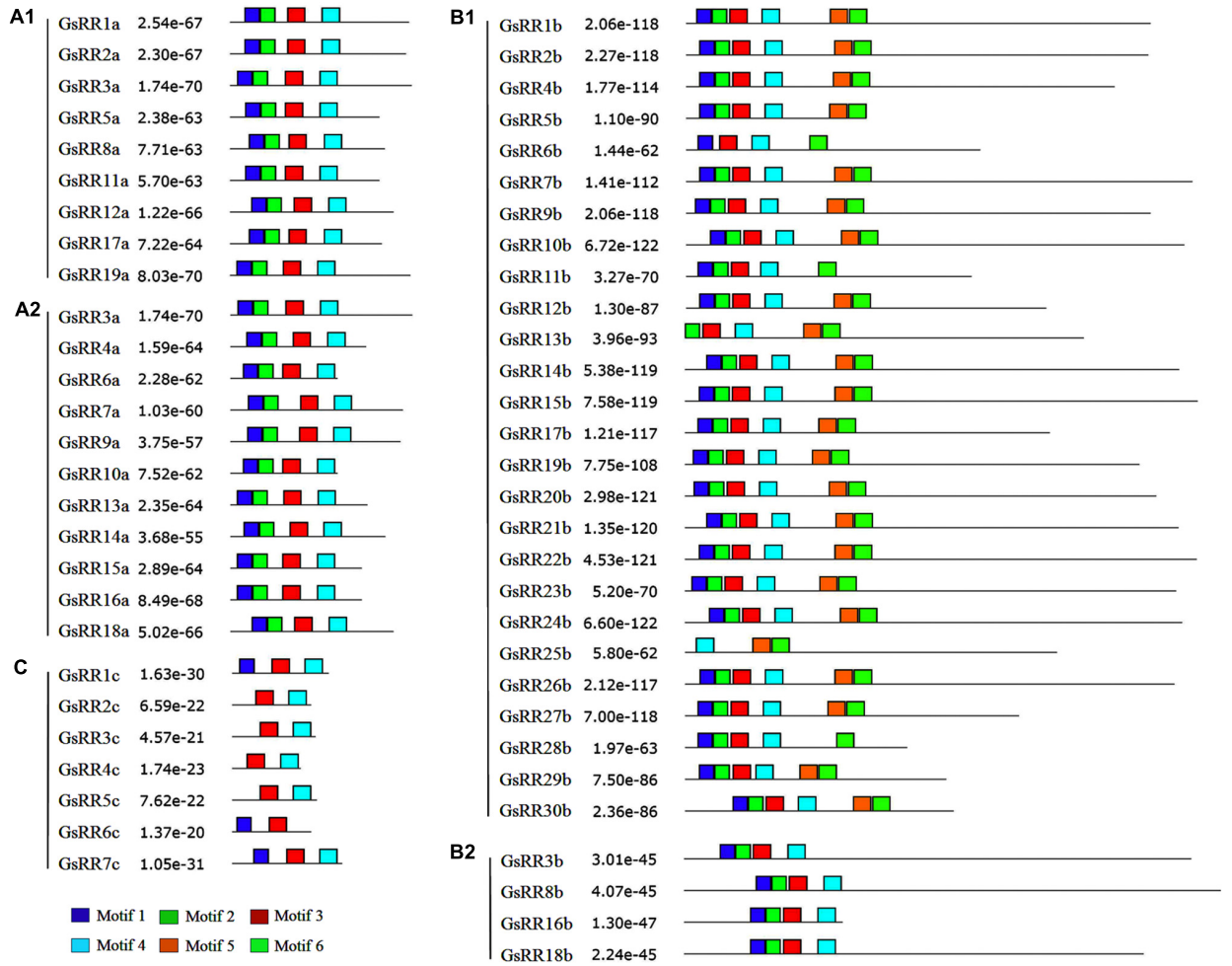

FIGURE 4 | Distribution of conserved motifs in the *GsRR* family members. All motifs were identified by MEME using the full-length amino acid sequences of *GsRR* genes. The *p*-values are showed. Different conserved motifs are indicated by different colors.

showed similar tendencies in leaves and roots. The relative transcript abundance of *GsRR2a* rapidly increased at 1 or 3 h, respectively. Under salt treatment, the transcript abundance of *GsRR2a* was slightly decreased in roots and leaves. These results suggested that *GsRR2a* expression indeed differently responded to alkali and salt stresses.

Overexpression of *GsRR2a* Improved Tolerance to Alkali Stress in *Arabidopsis*

Considering the responsive expression of *GsRR2a* under salt and alkali stresses, we further analyzed the effect of *GsRR2a* overexpression on alkali and salt tolerance. The transgenic lines (#5 and #38) were generated by overexpressing *GsRR2a* in *Arabidopsis*. We firstly performed the early seedling growth assays to determine the tolerance of WT (wide-type) and overexpression lines. Under normal conditions, *GsRR2a* overexpression does not affect plant growth under normal conditions. However, under $NaHCO_3$ stress treatment, *GsRR2a* overexpression lines exhibited more seedlings with open and green leaves than WT (**Figures 8A,B**). Furthermore, to evaluate the alkali tolerance at the adult stage, the WT and *GsRR2a* overexpression lines were irrigated with 150 mM $NaHCO_3$. After 16 days, the overexpression lines appeared much greener and healthier than WT (**Figure 8C**). In addition, statistical analysis revealed that overexpression lines exhibited higher chlorophyll contents but lower MDA contents than WT (**Figures 8D,E**). In contrast with alkali stress, no significant difference was observed between WT and the overexpression lines in the presence of 150 mM NaCl (**Supplementary Figure S3**). These results suggested that overexpression of *GsRR2a* in *Arabidopsis* could significantly improve the tolerance to alkali stress, but not to salt stress.

DISCUSSION

Recent studies have reported that the RR family genes regulate plant environmental stress responses through two-component

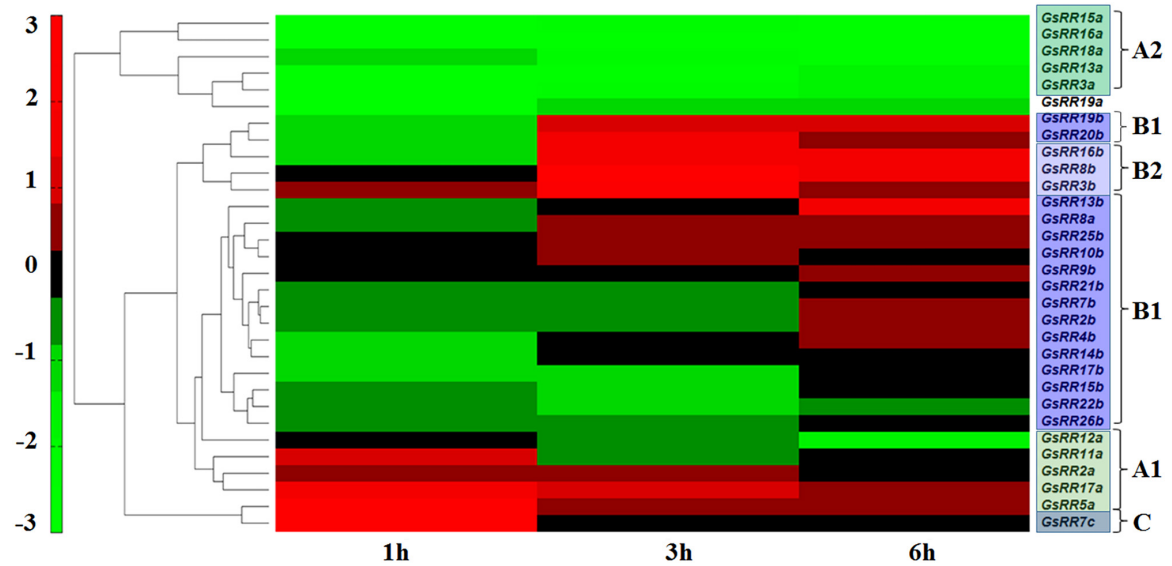

FIGURE 5 | Expression profile of *GsRR* family genes under alkali stress. Expression profiles of *GsRRs* are shown according to the RNA-seq data of wild soybean treated with 50 mM $NaHCO_3$. The expression profiles were conducted using Pearson correlation Hierarchical Clustering with TM4: MeV 4.9 software.

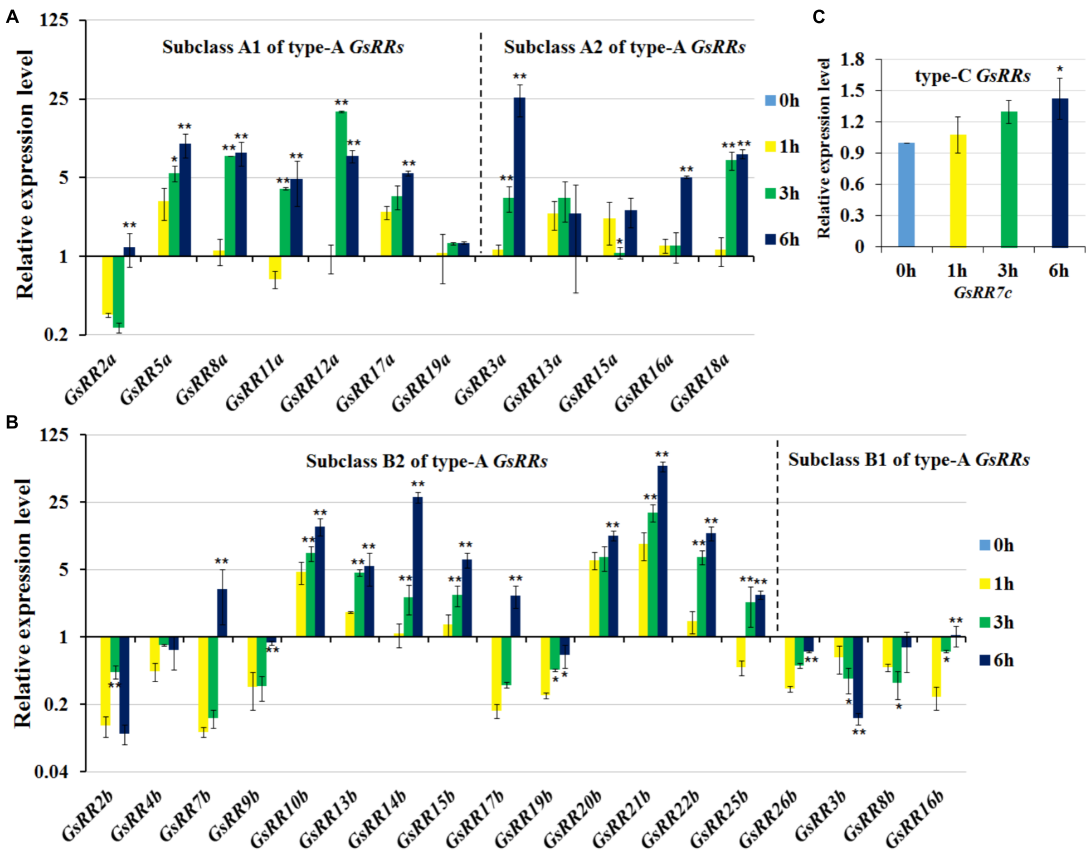

FIGURE 6 | Expression profile of *GsRR* family genes under salt stress. **(A–C)** The expression patterns of *GsRRs* were measured by qRT-PCR analysis with *G. soja* seedlings treated with 200 mM NaCl. Values represent the means of three fully independent biological replicates, and three technology replicates for each. $^{*}P < 0.05$, $^{**}P < 0.01$ by Student's *t*-test.

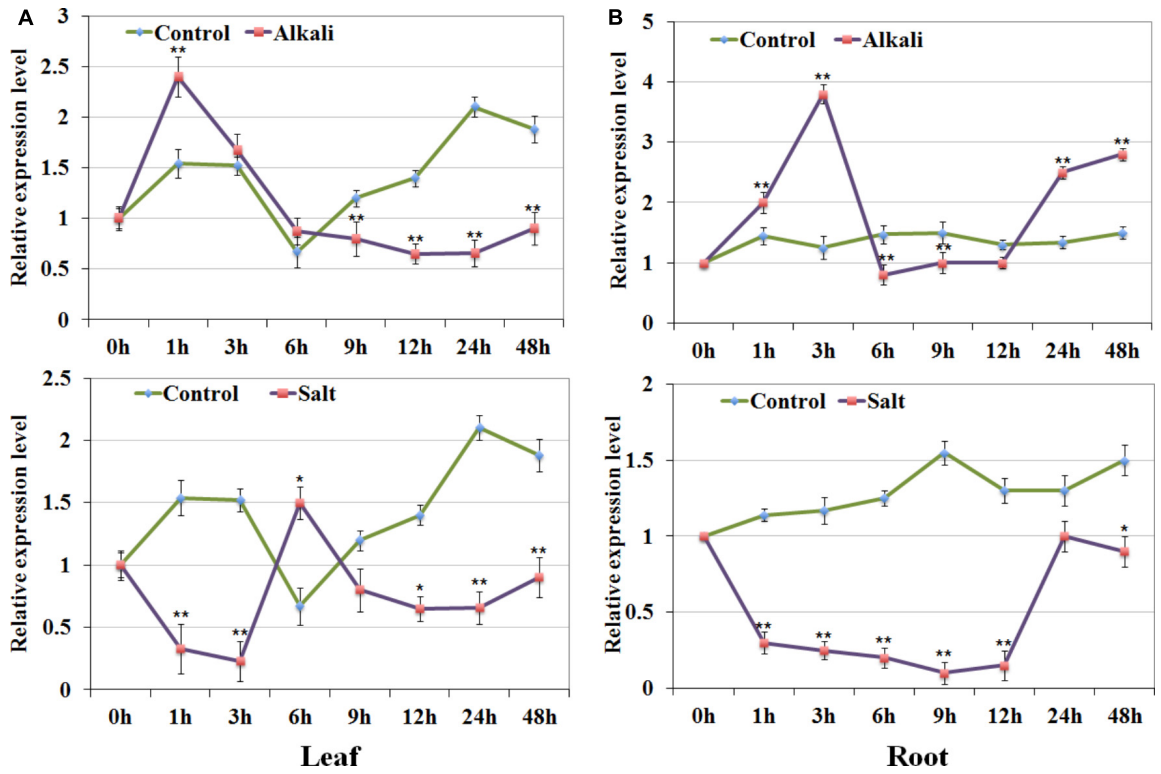

FIGURE 7 | Expression validation of *GsRR2a* in *G. soja*. **(A,B)** Expression levels of *GsRR2a* were detected in root and leaves under salt and alkali stresses using qRT-PCR analysis. Nineteen-day-old of *G. soja* seedlings were submerged into 1/4 Hoagland solution with 50 mM $NaHCO_3$ or 200 mM NaCl, respectively. The untreated plants were used as controls. Values represent the means of three fully independent biological replicates, and three technology replicates for each. $^*P < 0.05$, $^{**}P < 0.01$ by Student's *t*-test.

systems (Tran et al., 2010). However, there is limited information about the functions of RR genes in soybean. This study identified all RR family genes in *G. soja* and systematically analyzed their sequences and their responses to salt and alkali stresses. This information may provide useful clues for functional characterization of GsRRs, especially concerning their role in stress tolerance.

In the current study, a total of 56 *GsRRs* were identified in wild soybean genome. These *GsRRs* were classified into five subclasses according to their phylogeny, which is consistent with previous reports in *Arabidopsis* and rice (D'Agostino et al., 2000; Jain et al., 2006). Interestingly, there were more *GsRRs* containing Myb-like DNA domain in type-B than type-A, which may attribute to gene duplication events. The *Arabidopsis* genome contains almost the same number of type-A and type-B *ARRs*. By contrast, the maize genome contains more type-A *ZmRRs* (Chu et al., 2011). These indicated that type-B RRs containing the Myb-like DNA binding domain might play more important roles in dicots. Different from *Arabidopsis*, type-A *GsRRs* are further divided into two subclasses (8 members in subclass A1 and 11 in subclass A2), which suggests possible divergence of their functions during evolution. Moreover, four type-B *GsRRs* (3b, 8b, 16b, and 18b) were designed as subclass B2. Subclass B2 members are also called the pseudo-response regulators, which are the circadian clock component proteins in *Arabidopsis*. They contain a receiver-like domain lacking the conserved phosphoacceptor aspartic acid residue, and a CCT motif responsible for transcriptional repression (Chu et al., 2011; Wang et al., 2013).

The motif distribution analyzed by MEME was basically consistent with the phylogenetic analysis. *GsRRs* in each individual subclass usually shared subclass-specific motifs. Besides, different types of *GsRRs* contained different numbers of exons (**Supplementary Figure S4**). For example, type-A *GsRRs* contained five exons, whereas type-B GsRRs contained four to nine exons. The different numbers of exons possibly shared evolutionary and structural differences.

Roots are the first point perceiving the underground environment stress. To explore the possible functions of RRs under alkali stress, we investigated the transcript levels of *GsRRs* in wild soybean roots. From their expression profiles, we observed five type-A2 *GsRRs* (*15a*, *16a*, *18a*, *13a*, *3a*) showed the same expression pattern under alkali stress, where they were significantly and continuously down-regulated upon the $NaHCO_3$ treatment. This result suggested these co-expressed type-A2 *GsRRs* might function negatively in alkali stress responses. Interestingly, other five type-A1 genes *GsRR12a*, *GsRR11a*, *GsRR2a*, *GsRR17a*, and *GsRR5a* were also closely clustered and showed co-expression in roots. This further implies the functional redundancy among GsRRs, and functional

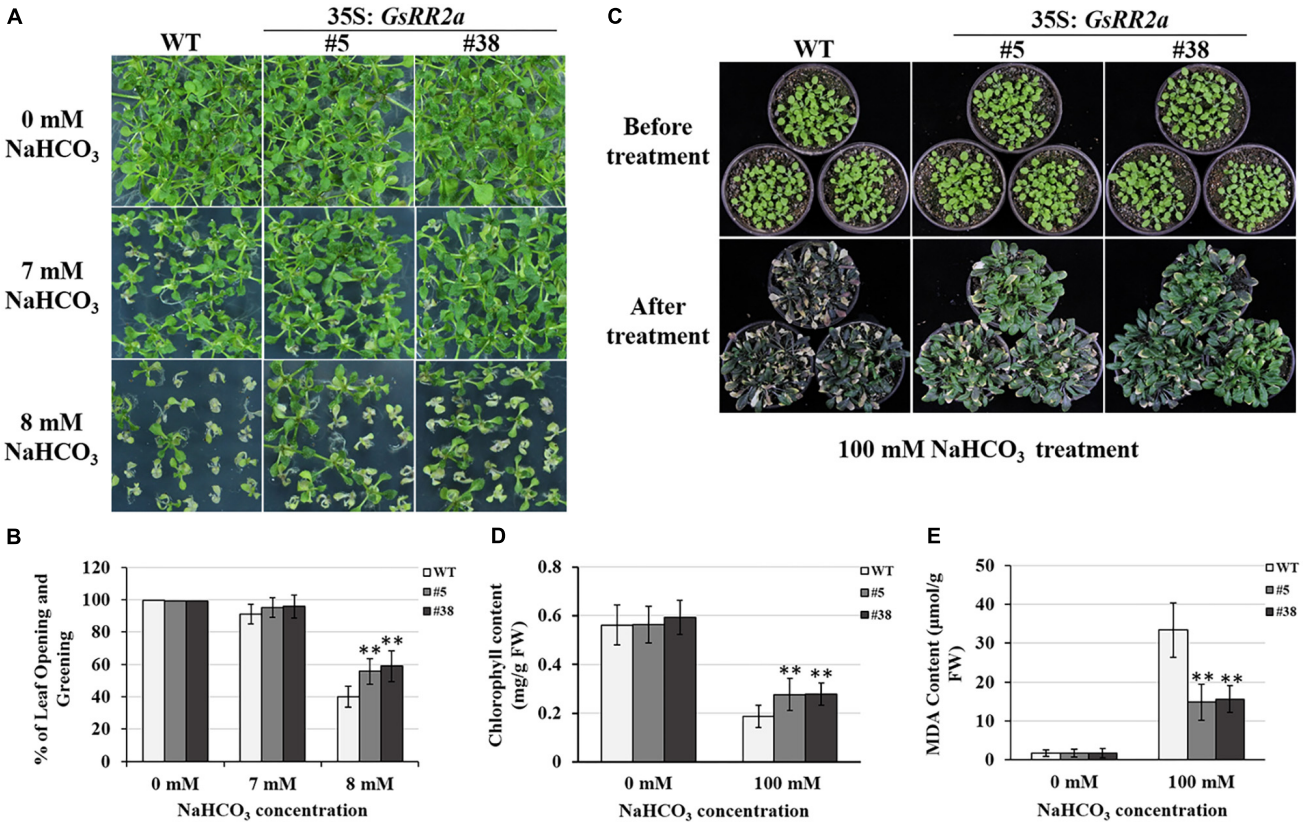

FIGURE 8 | Overexpression of *GsRR2a* in *Arabidopsis* enhances the tolerance to alkali stress. **(A)** The growth performance of WT and overexpression lines on 1/2MS medium containing 0, 7, or 8 mM $NaHCO_3$ at early seeding growth stage. **(B)** The numbers of seedlings with opening and greening leaves of WT and overexpression lines. **(C)** The growth performance of WT and overexpression lines before alkali treatment or treated with 100 mM $NaHCO_3$ for 16 days. **(D)** The chlorophyll content of WT and overexpression lines. **(E)** The malondialdehyde (MDA) content of WT and overexpression lines. $^*P < 0.05$, $^{**}P < 0.01$ by Student's *t*-test.

divergence between type-A1 and type-A2 in plant tolerance to alkali stress. Moreover, *GsRR14b*, *GsRR15b*, *GsRR17b GsRR21b*, *GsRR22b*, and *GsRR26b* in subclass B1 were strongly down-regulated at 1 h or 3 h, while other subclass B1 *GsRRs* were significantly up-regulated at 3 h or 6 h. The difference among subclass B1 members in alkali stress responses may be resulted from different upstream or downstream regulatory elements or factors, which indicated diversified functions within the same subclass.

The great difference in expression patterns of *GsRRs* to alkali and salt stresses bring us to consider there might be other regulatory mechanism and signal pathway in alkali stress. As we know, that salt stress involves osmotic stress and ion injury, and salinity tolerance in plants largely contributed by Na^+ exclusion (Yamaguchi et al., 2013). Actually, it has been pointed out that high HCO_3^- can diminish leaf area and length, decrease shoot biomass, and reduce the photosynthetic rate. However, the molecular mechanism of plant response to alkali stress is rarely known. Considering the important roles of RR proteins in CK signaling, the induction of *GsRRs* expression by salt and alkali stress provides a molecular link between stress and CK signaling. Moreover, *GsRR2a*, the homologous gene of *ARR3*, could enhance plant tolerance to alkali stress, but not to salt stress. One possible reason is that *GsRR2a* was up-regulated under alkali stress which indicated that this gene may be as a positive regulator of plant tolerance to alkali stress. However, *GsRR2a* exhibited the opposite expression pattern to salt and alkali stresses, which implied that *GsRR2a* may participate in different signaling pathways under alkali and salt stresses. In total, these results support the different mechanisms for alkali and salt stresses, and also provide a foundation for future work to elucidate the function of GsRR family genes.

CONCLUSION

In summary, we identified 56 *GsRR* genes, which could be classified into three types (five subclasses). *GsRR* were distributed among 18 chromosomes with gene duplications. Moreover, *GsRR* genes exhibited different expression patterns under alkali and salt stresses. Furthermore, overexpression of *GsRR2a* in *Arabidopsis* significantly improved the tolerance to alkali stress. In total, our results showed that *GsRRs* play crucial roles in plants responses to alkali and salt stresses. These results provided a foundation for further functional characterization of *GsRR* family genes.

AUTHOR CONTRIBUTIONS

CC, AL, HR, YY, HD, and XD performed the experiments and analyzed data. CC and AL wrote the manuscript. BL interpreted data and revised the manuscript. DZ, XS, and YZ provided ideas and designed the research. All authors have read and approved the final manuscript.

FUNDING

This work was supported by the Heilongjiang Provincial Higher School Science and Technology Innovation Team Building Program (2011TD005), Major Special Projects for New Varieties of Genetically Modified Organisms (2018ZX0800912B), BL is supported by the Swedish Cancer Society (CAN 2017/643 and CAN 2015/406), the Swedish Natural Research Council (VR 2015-04984), the National Natural Science Foundation of China (31771692), and National Natural Science Foundation of China (31671596 and 31500204 to XS).

SUPPLEMENTARY MATERIAL

The Supplementary Material for this article can be found online at: https://www.frontiersin.org/articles/10.3389/fpls.2018.01306/full#supplementary-material

FIGURE S1 | Phylogenetic trees of *GsRR* family of *G. soja* and *Arabidopsis*. Neighbor-joining phylogenetic tree of the response regulator members in *G. soja* and *Arabidopsis*. The tree was inferred by MEGA 5.0 with the neighbor-joining method after the alignment of the full-length amino acid sequences of the 56 *G. soja* genes and 24 *Arabidopsis* genes. The numbers beside the branches represent bootstrap values based on 1,000 replications. The scale bar corresponds to 0.1 estimated amino acid substitutions per site.

FIGURE S2 | Distribution of conserved motifs. All motifs were identified by MEME using the complete amino acid sequences of *GsRR* genes.

FIGURE S3 | Overexpression of *GsRR2a* in *Arabidopsis* did not affect the tolerance to salt stress. The WT and overexpression lines are grown on medium containing 0 or 150 mM NaCl. The germination rates were recorded and photos were taken after 6 days.

FIGURE S4 | Structure analysis of *GsRR* genes using GSDS online tools. The UTRs (upstream/downstream sequences), exons and introns are shown with light blue boxes, yellow boxes, and black lines, respectively.

TABLE S1 | Gene-specific primers of *GsRR* family used for q-RT PCR assays.

REFERENCES

An, Y. M., Song, L. L., Liu, Y. R., Shu, Y. J., and Guo, C. H. (2016). De novo transcriptional analysis of alfalfa in response to saline-alkaline stress. *Front. Plant Sci.* 7:931. doi: 10.3389/fpls.2016.00931

Bailey, T. L., Boden, M., Buske, F. A., Frith, M., Grant, C. E., Clementi, L., et al. (2009). MEME Suite: tools for motif discovery and searching. *Nucleic Acids Res.* 37, W202–W208. doi: 10.1093/nar/gkp335

Borsani, O., Zhu, J. H., Verslues, P. E., Sunkar, R., and Zhu, J. K. (2005). Endogenous siRNAs derived from a pair of natural cis-antisense transcripts regulate salt tolerance in *Arabidopsis*. *Cell* 123, 1279–1291. doi: 10.1016/j.cell.2005.11.035

Chu, Z. X., Ma, Q., Lin, Y. X., Tang, X. L., Zhou, Y. Q., Zhu, S. W., et al. (2011). Genome-wide identification, classification, and analysis of two-component signal system genes in maize. *Genet. Mol. Res.* 10, 3316–3330. doi: 10.4238/2011.December.8.3

Clough, S. J., and Bent, A. F. (1998). Floral dip: a simplified method for *Agrobacterium*-mediated transformation of *Arabidopsis thaliana*. *Plant J.* 16, 735–743. doi: 10.1046/j.1365-313x.1998.00343.x

D'Agostino, I. B., Deruere, J., and Kieber, J. J. (2000). Characterization of the response of the *Arabidopsis* response regulator gene family to cytokinin. *Plant Physiol.* 124, 1706–1717. doi: 10.1104/pp.124.4.1706

DuanMu, H., Wang, Y., Bai, X., Cheng, S., Deyholos, M., Wong, G.-S., et al. (2015). Wild soybean roots depend on specific transcription factors and oxidation reduction related genesin response to alkaline stress. *Funct. Integr. Genomics* 15, 651–660. doi: 10.1007/s10142-015-0439-y

Ge, Y., Li, Y., Zhu, Y.-M., Bai, X., Lv, D.-K., Guo, D., et al. (2010). Global transcriptome profiling of wild soybean (*Glycine soja*) roots under NaHCO3 treatment. *BMC Plant Biol.* 10:153. doi: 10.1186/1471-2229-10-153

Hass, C., Lohrmann, J., Albrecht, V., Sweere, U., Hummel, F., Yoo, S. D., et al. (2004). The response regulator 2 mediates ethylene signalling and hormone signal integration in *Arabidopsis*. *EMBO J.* 23, 3290–3302. doi: 10.1038/sj.emboj.7600337

Horak, J., Grefen, C., Berendzen, K. W., Hahn, A., Stierhof, Y. D., Stadelhofer, B., et al. (2008). The *Arabidopsis thaliana* response regulator ARR22 is a putative AHP phospho-histidine phosphatase expressed in the chalaza of developing seeds. *BMC Plant Biol.* 8:77. doi: 10.1186/1471-2229-8-77

Hu, B., Jin, J., Guo, A. Y., Zhang, H., Luo, J., and Gao, G. (2015). GSDS 2.0: an upgraded gene feature visualization server. *Bioinformatics* 31, 1296–1297. doi: 10.1093/bioinformatics/btu817

Islam, M. S., Akhter, M., El Sabagh, A., Liu, L. Y., Nguyen, N. T., Ueda, A., et al. (2011). Comparative studies on growth and physiological responses to saline and alkaline stresses of Foxtail millet (*Setaria italica* L.) and Proso millet (*Panicum miliaceum* L.). *Aust. J. Crop Sci.* 5, 1269–1277.

Jain, M., Tyagi, A. K., and Khurana, J. P. (2006). Molecular characterization and differential expression of cytokinin-responsive type-A response regulators in rice (*Oryza sativa*). *BMC Plant Biol.* 6:1. doi: 10.1186/1471-2229-6-1

Jeon, J., and Kim, J. (2013). *Arabidopsis* response regulator1 and *Arabidopsis* histidine phosphotransfer protein2 (AHP2), AHP3, and AHP5 function in cold signaling. *Plant Physiol.* 161, 408–424. doi: 10.1104/pp.112.207621

Jeon, J., Kim, N. Y., Kim, S., Kang, N. Y., Novak, O., Ku, S.-J., et al. (2010). A subset of cytokinin two-component signaling system plays a role in cold temperature stress response in *Arabidopsis*. *J. Biol. Chem.* 285, 23369–23384. doi: 10.1074/jbc.M109.096644

Jia, B., Sun, M., Duanmu, H., Ding, X., Liu, B., Zhu, Y., et al. (2017). GsCHX19.3, a member of cation/H(+) exchanger superfamily from wild soybean contributes to high salinity and carbonate alkaline tolerance. *Sci. Rep.* 7:9423. doi: 10.1038/s41598-017-09772-3

Jin, H., Kim, H. R., Plaha, P., Liu, S. K., Park, J. Y., Piao, Y. Z., et al. (2008). Expression profiling of the genes induced by Na(2)CO(3) and NaCl stresses in leaves and roots of *Leymus chinensis*. *Plant Sci.* 175, 784–792. doi: 10.1016/j.plantsci.2008.07.016

Kumar, S., Dudley, J., Nei, M., and Tamura, K. (2008). MEGA: a biologist-centric software for evolutionary analysis of DNA and protein sequences. *Brief. Bioinform.* 9, 299–306. doi: 10.1093/bib/bbn017

Larkin, M. A., Blackshields, G., Brown, N. P., Chenna, R., Mcgettigan, P. A., Mcwilliam, H., et al. (2007). Clustal W and clustal X version 2.0. *Bioinformatics* 23, 2947–2948. doi: 10.1093/bioinformatics/btm404

Lewinsohn, E., and Gressel, J. (1983). The determination of chlorophylls a and b together with 14CO2 fixation in the same plant tissue samples. *Anal. Biochem.* 135, 438–442. doi: 10.1016/0003-2697(83)90708-X

Livak, K. J., and Schmittgen, T. D. (2001). Analysis of relative gene expression data using real-time quantitative PCR and the 2(-Delta Delta C(T)) method. *Methods* 25, 402–408. doi: 10.1006/meth.2001.1262

Mason, M. G., Jha, D., Salt, D. E., Tester, M., Hill, K., Kieber, J. J., et al. (2010). Type-B response regulators ARR1 and ARR12 regulate expression of AtHKT1;1

and accumulation of sodium in *Arabidopsis* shoots. *Plant J.* 64, 753–763. doi: 10.1111/j.1365-313X.2010.04366.x

Miller, G., Suzuki, N., Ciftci-Yilmaz, S., and Mittler, R. (2010). Reactive oxygen species homeostasis and signalling during drought and salinity stresses. *Plant Cell Environ.* 33, 453–467. doi: 10.1111/j.1365-3040.2009.02041.x

Nishiyama, R., Le, D. T., Watanabe, Y., Matsui, A., Tanaka, M., Seki, M., et al. (2012). Transcriptome analyses of a salt-tolerant cytokinin-deficient mutant reveal differential regulation of salt stress response by cytokinin deficiency. *PLoS One* 7:e32124. doi: 10.1371/journal.pone.0032124

Nishiyama, R., Watanabe, Y., Fujita, Y., Le, D. T., Kojima, M., Werner, T., et al. (2011). Analysis of cytokinin mutants and regulation of cytokinin metabolic genes reveals important regulatory roles of cytokinins in drought, salt and abscisic acid responses, and abscisic acid biosynthesis. *Plant Cell.* 23, 2169–2183. doi: 10.1105/tpc.111.087395

Peever, T. L., and Higgins, V. J. (1989). Electrolyte leakage, lipoxygenase, and lipid peroxidation induced in tomato leaf tissue by specific and nonspecific elicitors from *Cladosporium fulvum*. *Plant Physiol.* 90, 867–875. doi: 10.1104/pp.90.3.867

Punta, M., Coggill, P. C., Eberhardt, R. Y., Mistry, J., Tate, J., Boursnell, C., et al. (2012). The Pfam protein families database. *Nucleic Acids Res.* 40, D290–D301. doi: 10.1093/nar/gkr1065

Qi, X., Li, M. W., Xie, M., Liu, X., Ni, M., Shao, G., et al. (2014). Identification of a novel salt tolerance gene in wild soybean by whole-genome sequencing. *Nat. Commun.* 5:4340. doi: 10.1038/ncomms5340

Rouphael, Y., Cardarelli, M., Bonini, P., and Colla, G. (2017). Synergistic action of a microbial-based biostimulant and a plant derived-protein hydrolysate enhances lettuce tolerance to alkalinity and salinity. *Front. Plant Sci.* 8:131. doi: 10.3389/fpls.2017.00131

Sadras, V., Baldock, J., Roget, D., and Rodriguez, D. (2003). Measuring and modelling yield and water budget components of wheat crops in coarse-textured soils with chemical constraints. *Field Crops Res.* 84, 241–260. doi: 10.1016/S0378-4290(03)00093-5

Saeed, A., Sharov, V., White, J., Li, J., Liang, W., Bhagabati, N., et al. (2003). TM4: a free, open-source system for microarray data management and analysis. *Biotechniques* 34, 374–378.

Salome, P. A., To, J. P. C., Kieber, J. J., and Mcclung, C. R. (2006). *Arabidopsis* response regulators ARR3 and ARR4 play cytokinin-independent roles in the control of circadian period. *Plant Cell* 18, 55–69. doi: 10.1105/tpc.105.037994

Shi, D. C., and Sheng, Y. M. (2005). Effect of various salt-alkaline mixed stress conditions on sunflower seedlings and analysis of their stress factors. *Environ. Exp. Bot.* 54, 8–21. doi: 10.1016/j.envexpbot.2004.05.003

Shi, Y., Tian, S., Hou, L., Huang, X., Zhang, X., Guo, H., et al. (2012). Ethylene signaling negatively regulates freezing tolerance by repressing expression of CBF and Type-A ARR genes in *Arabidopsis*. *Plant Cell* 24, 2578–2595. doi: 10.1105/tpc.112.098640

Song, T., Xu, H., Sun, N., Jiang, L., Tian, P., Yong, Y., et al. (2017). Metabolomic analysis of alfalfa (*Medicago sativa* L.) root-symbiotic rhizobia responses under alkali stress. *Front. Plant Sci.* 8:1208. doi: 10.3389/fpls.2017.01208

Song, X., Duanmu, H., Yu, Y., Chen, C., Sun, X., Zhu, P., et al. (2017). GsJ11, identified by genome-wide analysis, facilitates alkaline tolerance in transgenic plants. *Plant Cell Tissue Organ Cult.* 129, 411–430. doi: 10.1007/s11240-017-1188-5

Sun, X., Luo, X., Sun, M., Chen, C., Ding, X., Wang, X., et al. (2014). A *Glycine soja* 14-3-3 protein GsGF14o participates in stomatal and root hair development and drought tolerance in *Arabidopsis thaliana*. *Plant Cell Physiol.* 55, 99–118. doi: 10.1093/pcp/pct161

Sun, Y. P., Wang, F. W., Wang, N., Dong, Y. Y., Liu, Q., Zhao, L., et al. (2013). Transcriptome exploration in *Leymus chinensis* under saline-alkaline treatment using 454 pyrosequencing. *PLoS One* 8:e53632. doi: 10.1371/journal.pone.0053632

Sweere, U., Eichenberg, K., Lohrmann, J., Mira-Rodado, V., Baurle, I., Kudla, J., et al. (2001). Interaction of the response regulator ARR4 with phytochrome B in modulating red light signaling. *Science* 294, 1108–1111. doi: 10.1126/science.1065022

To, J. P. C., Deruere, J., Maxwell, B. B., Morris, V. F., Hutchison, C. E., Ferreira, F. J., et al. (2007). Cytokinin regulates type-A *Arabidopsis* response regulator activity and protein stability via two-component phosphorelay. *Plant Cell* 19, 3901–3914. doi: 10.1105/tpc.107.052662

Tran, L.-S. P., Shinozaki, K., and Yamaguchi-Shinozaki, K. (2010). Role of cytokinin responsive two-component system in ABA and osmotic stress signalings. *Plant Signal. Behav.* 5, 148–150. doi: 10.4161/psb.5.2.10411

Tran, L. S. P., Urao, T., Qin, F., Maruyama, K., Kakimoto, T., Shinozaki, K., et al. (2007). Functional analysis of AHK1/ATHK1 and cytokinin receptor histidine kinases in response to abscisic acid, drought, and salt stress in *Arabidopsis*. *Proc. Natl. Acad. Sci. U.S.A.* 104, 20623–20628. doi: 10.1073/pnas.0706547105

Wang, L., Kim, J., and Somers, D. E. (2013). Transcriptional corepressor TOPLESS complexes with pseudoresponse regulator proteins and histone deacetylases to regulate circadian transcription. *Proc. Natl. Acad. Sci. U.S.A.* 110, 761–766. doi: 10.1073/pnas.1215010110

Wang, Y., Shen, W., Chan, Z., and Wu, Y. (2015). Endogenous cytokinin overproduction modulates ROS homeostasis and decreases salt stress resistance in *Arabidopsis thaliana*. *Front. Plant Sci.* 6:1004. doi: 10.3389/fpls.2015.01004

Yamaguchi, T., Hamamoto, S., and Uozumi, N. (2013). Sodium transport system in plant cells. *Front. Plant Sci.* 4:410. doi: 10.3389/fpls.2013.00410

Yang, C., Chong, J., Li, C., Kim, C., Shi, D., and Wang, D. (2007). Osmotic adjustment and ion balance traits of an alkali resistant halophyte *Kochia sieversiana* during adaptation to salt and alkali conditions. *Plant Soil* 294, 263–276. doi: 10.1007/s11104-007-9251-3

Yang, C. W., Shi, D. C., and Wang, D. L. (2008). Comparative effects of salt and alkali stresses on growth, osmotic adjustment and ionic balance of an alkali-resistant halophyte *Suaeda glauca* (Bge.). *Plant Growth Regul.* 56, 179–190. doi: 10.1007/s10725-008-9299-y

Yang, S., Zhang, X., Yue, J.-X., Tian, D., and Chen, J.-Q. (2008). Recent duplications dominate NBS-encoding gene expansion in two woody species. *Mol. Genet. Genomics* 280, 187–198. doi: 10.1007/s00438-008-0355-0

Yokoyama, A., Yamashino, T., Amano, Y. I., Tajima, Y., Imamura, A., Sakakibara, H., et al. (2007). Type-B ARR transcription factors, ARR10 and ARR12, are implicated in cytokinin-mediated regulation of protoxylem differentiation in roots of *Arabidopsis thaliana*. *Plant Cell Physiol.* 48, 84–96. doi: 10.1093/pcp/pcl040

Zeng, Q.-Y., Yang, C.-Y., Ma, Q.-B., Li, X.-P., Dong, W.-W., and Nian, H. (2012). Identification of wild soybean miRNAs and their target genes responsive to aluminum stress. *BMC Plant Biol.* 12:182. doi: 10.1186/1471-2229-12-182

Zhang, J., Wang, J., Jiang, W., Liu, J., Yang, S., Gai, J., et al. (2016). Identification and analysis of NaHCO3 stress responsive genes in wild soybean (*Glycine soja*) roots by RNA-seq. *Front. Plant Sci.* 7:1842. doi: 10.3389/fpls.2016.01842

Zhu, D., Bai, X., Chen, C., Chen, Q., Cai, H., Li, Y., et al. (2011). GsTIFY10, a novel positive regulator of plant tolerance to bicarbonate stress and a repressor of jasmonate signaling. *Plant Mol. Biol.* 77, 285–297. doi: 10.1007/s11103-011-9810-0

Zhu, J. K. (2003). Regulation of ion homeostasis under salt stress. *Curr. Opin. Plant Biol.* 6, 441–445. doi: 10.1016/S1369-5266(03)00085-2

Conflict of Interest Statement: The authors declare that the research was conducted in the absence of any commercial or financial relationships that could be construed as a potential conflict of interest.

frontiers in Plant Science

MINI REVIEW
published: 15 May 2018
doi: 10.3389/fpls.2018.00543

Plant Life in Extreme Environments: How Do You Improve Drought Tolerance?

*Ulrike Bechtold**

School of Biological Sciences, University of Essex, Colchester, United Kingdom

Systems studies of drought stress in resurrection plants and other xerophytes are rapidly identifying a large number of genes, proteins and metabolites that respond to severe drought stress or desiccation. This has provided insight into drought resistance mechanisms, which allow xerophytes to persist under such extreme environmental conditions. Some of the mechanisms that ensure cellular protection during severe dehydration appear to be unique to desert species, while many other stress signaling pathways are in common with well-studied model and crop species. However, despite the identification of many desiccation inducible genes, there are few "gene-to-field" examples that have led to improved drought tolerance and yield stability derived from resurrection plants, and only few examples have emerged from model species. This has led to many critical reviews on the merit of the experimental approaches and the type of plants used to study drought resistance mechanisms. This article discusses the long-standing arguments between the ecophysiology and molecular biology communities, on how to "drought-proof" future crop varieties. It concludes that a more positive and inclusive dialogue between the different disciplines is needed, to allow us to move forward in a much more constructive way.

Keywords: extremophiles, Arabidopsis, drought survival, drought tolerance, drought avoidance

OPEN ACCESS

Edited by:
Nicholas Provart,
University of Toronto, Canada

Reviewed by:
Mauro Guida Santos,
Universidade Federal de Pernambuco, Brazil
Fulai Liu,
University of Copenhagen, Denmark

***Correspondence:**
Ulrike Bechtold
ubech@essex.ac.uk

Specialty section:
This article was submitted to Plant Abiotic Stress, a section of the journal Frontiers in Plant Science

Received: *20 February 2018*
Accepted: *09 April 2018*
Published: *15 May 2018*

Citation:
Bechtold U (2018) Plant Life in Extreme Environments: How Do You Improve Drought Tolerance? Front. Plant Sci. 9:543. doi: 10.3389/fpls.2018.00543

INTRODUCTION

Four hundred and fifty million years of land plant evolution has generated biological complexity, which has allowed plants to adapt to terrestrial environments, ranging from extreme cold environments in the Arctic and Antarctica, high salinity environments to extreme temperature changes and drought conditions in desert environments (von Willert et al., 1990; Alberdi et al., 2002; Amtmann et al., 2005). Plants that inhabit these environments are collectively called extremophiles, which harbor a range of different mechanisms that allow them to withstand these extreme environments.

During the green revolution of late twentieth century, breeding dramatically modified plant architecture, and yield improvements were made by selecting for characteristics such as rapid growth and a reduction of vegetative biomass in favor of fruit and seed production (Pingali, 2012). However, artificial selection for yield inadvertently reduced diversity, resulting in the loss of abiotic stress tolerance, with crop species likely to be more sensitive to abiotic stress compared to their wild ancestors (Mayrose et al., 2011; Koziol et al., 2012). Abiotic stresses dramatically reduce crop yields posing a threat to food security (Boyer, 1982; Cramer et al., 2011), and with the worldwide population growth expected to reach 9.7 billion people by 2050 (United Nations Department of Economic Social Affairs, 2017), the demand for global crop production is expected to double by

2050 (Tilman et al., 2011). This problem is likely to be exacerbated in the future by climate change (Mittler and Blumwald, 2010; Lesk et al., 2016). Furthermore future expansion of agricultural area is likely to occur in drylands and deserts (Millennium Ecosystem Assessment, 2005; Millenium Ecosystem Assessment, 2010), and new solutions to meet the world's future food security by improving crop yields is vital to not only prevent losses where crops are currently grown but also to cultivate them on more marginal land (Foley et al., 2011).

Interestingly, just as the plant stress community is beginning to tackle the molecular mechanisms of combined stress tolerances in models, crops and extremophiles, crop ecophysiologists are reassessing how misconceptions of stress resistance mechanisms may be avoided, advocating the need for clear physiological frameworks to meaningfully integrate the wealth of genetic response data. This article will focus on the efforts being made to understand dehydration resistance mechanisms in extremophile and model plants, and discuss the prospects of unlocking the genetic codes and mechanisms of extremophiles in the battle for stress tolerant crops.

WHY ARE RESURRECTION PLANTS SO SUPERB AT SURVIVING DROUGHT STRESS?

Until recently, our knowledge of the molecular mechanisms of stress tolerance in extremophiles was relatively limited, but with the onset of next generation sequencing technologies, the number genome and transcriptome datasets of extremophiles has steadily increased (Oh et al., 2012; Dinakar and Bartels, 2013). In this context, halophytes have traditionally attracted more attention at the molecular level, partly because they include highly salt tolerant close relatives of *Arabidopsis thaliana*, such as *Thellungiella parvula* and *Eutrema salsugineum* (Dassanayake et al., 2011; Wu et al., 2012), allowing for direct comparisons of stress tolerance mechanisms such as salt, cold, heat, drought, and freezing tolerances already widely studied in Arabidopsis (Lee et al., 2012; Koch and German, 2013). *E. salsugineum* also harbors tolerances to low soil nitrogen (Kant et al., 2008), high boron levels (Lamdan et al., 2012), low phosphate levels (Velasco et al., 2016) and heat stress (Higashi et al., 2013), which is an exciting prospect for translating multiple stress tolerance traits to other plant species, including agronomically relevant *Brassicaceae*.

The interest in vegetative desiccation tolerance is illustrated by the large the number of publications relating to their ecology, physiology and molecular mechanism over the last 20 years, with 700 publications containing a reference to desiccation tolerance in plants, of which 257 were linked to resurrection plants (https://www.ncbi.nlm.nih.gov/pubmed/, search terms: desiccation tolerance, resurrection plants, last searched 3/2/18). With more than 130 known varieties, resurrection plants are mostly found in arid and semi-arid environments, (Gaff, 1971, 1977), and are probably the best studied of the xerophytes. Common to all resurrection plants is a vegetative desiccation tolerance (Oliver et al., 2000), and a small number of different species have been extensively studied with the aim to identify the underlying molecular mechanisms (Farrant, 2000; Bartels and Salamini, 2001; Cooper, 2002; Bartels, 2005; Farrant et al., 2015). Resurrection plants rapidly respond to water deficiency by switching into a "*stress mode*" that leads to a complete inhibition of photosynthesis and an overproduction of reactive oxygen species (ROS) in the chloroplasts due to excess light energy. ROS subsequently oxidize proteins and lipids, damage DNA and RNA, and ultimately lead to programmed cell death (Farrant et al., 2003).

Transcriptome analysis of *Craterostigma plantagineum* and *Haberlea rhodopensis* (Rodriguez et al., 2010; Gechev et al., 2013; Giarola et al., 2017) under early dehydration, desiccation and subsequent rehydration revealed common genetic pathways among desiccation-tolerant species. Resurrection plants undergo different stages during desiccation, which are accompanied by distinct physiological, metabolic, and molecular changes extensively reviewed by Farrant et al. (2015). Essentially, during the early dehydration stage, photosynthesis is shut down, ABA dependent responses to water stress become prominent, there is increased activity of antioxidants and a redirection of metabolism to the increased formation of sucrose and oligosaccharides as osmo-protectants (Rodriguez et al., 2010; Farrant et al., 2015). The late stages of drying are indicated by increased expression of proteins involved in signal transduction, altering sugar metabolism and genes encoding classical stress-associated proteins such as early light-inducible (ELIPs), Heat Shock Proteins (HSPs) and Late Embryogenesis Abundant (LEAs) proteins (Gechev et al., 2013; Farrant et al., 2015; Costa et al., 2017). This reprogramming of metabolism is driven by the induction of known stress responsive transcription factors, such as NACs, NF-Ys, HSFs, and WRKYs (Gechev et al., 2013; Farrant et al., 2015; Costa et al., 2017). It appears that resurrection plants are generally in a constantly "primed state," with high basal levels of protective sugars, antioxidants and defense proteins, allowing a rapid and strong response during desiccation (Rodriguez et al., 2010; Gechev et al., 2013; Costa et al., 2016).

WHAT ARE THE LESSONS LEARNED FROM RESURRECTION PLANTS?

Many of the genes identified in the above transcriptome studies have also been identified in drought responses of Arabidopsis and other plant models (Tripathi et al., 2014; Bechtold et al., 2016), suggesting that common signaling pathways are in operation. The advantages of Arabidopsis as a model for plant molecular biology and the role it played and still plays in investigating abiotic stress response pathways is undisputed (Provart et al., 2016). Many of the stress signaling pathways identified are now known to be general responses that appear to be conserved in many higher plant species (Boscaiu et al., 2012; Provart et al., 2016).

However, there are counterarguments which suggest that too much emphasis is being placed on investigating unsuitable experimental models, such as Arabidopsis (Boscaiu et al., 2012). For example, Arabidopsis and many crop plants die at leaf water potentials of around −3 MPa (van der Weele et al., 2000;

Fitter and Hay, 2002). Consequently, Arabidopsis may not be appropriate to identify dehydration tolerance pathways. Yet most of the biochemical and molecular studies on plant responses to abiotic stress have been carried out using Arabidopsis (Bressan et al., 2009), which has resulted in the identification and isolation of stress-tolerance genes, some of which have been used in modulating crop stress tolerance with varying success (reviewed by Mittler and Blumwald, 2010; Varshney et al., 2011). Especially stress responsive transcription factors (TFs) such as the AP2/EREBP family DREBs, MYB, WRKY, NAC, bHLH, and bZIPs have attracted attention due to their important roles in plant stress responses and improved stress tolerance phenotypes when overexpressed in Arabidopsis and crop plants alike (reviewed by Wang et al., 2016).

From many of these transgenic studies it is evident that TFs have conserved functions across species boundaries including resurrection plants (see above), and many of the Arabidopsis TFs have been shown to confer stress tolerances in unrelated crop species and vice versa (Jiang et al., 2011; Wang et al., 2016). However, the bottom line is that currently few abiotic stress tolerant, high yielding crops are grown in our fields utilizing the genes identified from the many biochemical and molecular analyses carried out on Arabidopsis and/or model crops reviewed by (Mickelbart et al., 2015; Ricroch and Hénard-Damave, 2016).

This has raised several questions with regard to the experimental conditions applied in gene discovery studies, the appropriateness of the stress phenotypes being assessed (Blum and Tuberosa, 2018), or whether common stress signaling pathways are indeed the best targets (Boscaiu et al., 2012). While vegetative desiccation tolerance in resurrection plants is clearly at the extreme end of the stress survival spectrum, it is argued that extremophile species may act as a source of novel genes for the genetic improvement of stress tolerance in crops (Boscaiu et al., 2012). Yet many of the TF families identified in Arabidopsis have also been identified in resurrection plants in response to drought stress (see above; Gechev et al., 2013; Farrant et al., 2015; Costa et al., 2017). It is now generally accepted that many of these common signaling pathways are functional in xerophytes adapted to arid or semi-arid conditions (Farrant et al., 2015; Costa et al., 2016, 2017). Therefore, the argument regarding the suitability of stress sensitive model species vs. xerophytes/resurrection plants in the pursuit to study drought responses is unresolved, and the question remains how studies on resurrection plants are going to lead us to novel genes and stress signaling pathways, when so far, many transcriptome studies have mostly delivered on general stress pathways?

Interestingly, transcriptome studies of resurrection plants not only found a high proportion of unknown transcripts (33% *C. plantagineum* and ∼40% *H. rhodopensis;* Rodriguez et al., 2010; Gechev et al., 2013), but in the case of the *C. plantagineum* transcriptome, also identified many taxonomically restricted genes (TRGs) and non-protein coding RNAs (ncRNAs) (Giarola et al., 2014; Giarola and Bartels, 2015). TRGs are known to code for new traits required for the adaptation of organisms to particular environmental conditions (Johnson and Tsutsui, 2011), and it has been suggested that these may harbor the potential for novel gene discovery linked to desiccation tolerance.

Early attempts to utilize TRGs such as desiccation induced proteins from *C. plantagineum* to improve drought tolerance in tobacco failed (Iturriaga et al., 1992), while recent examples successfully used tonoplast cation/H+ antiporter and H+ pyrophophatases genes from the xerophyte *Zygophyllum xanthoxylum* to enhance stress tolerance in alfalfa and *Lotus corniculatus* (Bao et al., 2014, 2016). These studies suggested that improved "systems wide approaches" of large datasets, together with comparative genomics that aim to identify whole network-based homologies between species could be more successful in discovering novel genes/pathways that underlie differences and similarities across species (Farrant et al., 2015).

THE CONTINUOUS ARGUMENT—ARE WE STUDYING THE RIGHT SYSTEM?

There also appears to be a lack of synergy between different disciplines with physiology, ecophysiology on the one hand, and genetics and molecular biology on the other. Perhaps the problem is not only the type of plant we study, but also how we study stress tolerance mechanisms in general? Crop physiologists rightly argue that molecular mechanisms of plant survival traits are often studied in isolation to physiological responses, whether this is carried out in model species such as Arabidopsis (Blum, 2005), or in extremophiles such as the resurrection plants (Blum and Tuberosa, 2018). This may be confounded by experimental setups that are not fit for purpose or comparable to plant responses under field conditions, for example pot grown vs. field grown plants (Passioura J. B., 2006; Poorter et al., 2012).

Desiccation tolerance in resurrection plants is a survival trait, and survival traits after any given stress have generally been a popular phenotype for gene discovery and gene function in model species (Woo et al., 2008; Skirycz et al., 2011), and drought resistance is often assessed under quite severe conditions in which plant survival is scored after a prolonged period of soil drying. Yet, even with what superficially appears to be simple phenotype (i.e., survival); the mechanisms ensuring drought survival are often no being fully assessed (Blum and Tuberosa, 2018). Plant survival after a period of drought stress, can either be due to dehydration avoidance or dehydration tolerance (Levitt, 1980). Avoidance strategies are observed in plants that maintain high plant water status due to osmotic adjustment during dehydration, while tolerance usually result from a delayed mortality in response to low plant water status (Levitt, 1980). In resurrection plants, the desiccation survival trait is due to delayed mortality and suppression of drought-related senescence pathways (Griffiths et al., 2014). Therefore, when phenotyping for dehydration survival there is a need to distinguish between dehydration avoidance and dehydration tolerance, and how this may affect survival and recovery. Without this distinction, it has been argued that molecular studies performed to identify the genes that underlie this trait might be biased. For example, in gene-expression studies, RNA is sampled after a set period of dehydration, or at a given relative soil water content, and often the assumption is made that all genotypes are therefore subjected to the same level of stress (Des

Marais et al., 2012). Without additional information regarding the physiological- or plant water status this could result in artifacts, where differences in plant water status on the day of sampling are not adequately taken into account. Consequently, an in depth understanding of the physiological basis of the phenotype is essential to avoid misinterpretations (Zhang et al., 2014; Bechtold et al., 2016). While there have clearly been some deficiencies with molecular biology approaches in many molecular/genomic centric studies used to study drought stress, recent critics of the topic fail to mention the progress made by molecular biologists to address some of these early shortcomings in the area. In recent years, much more effort has been placed on linking plant genomic events to the metabolic status and the rate of plant dehydration especially in model species, such as Arabidopsis, *Medicago truncatula* and rice (Harb et al., 2010; Des Marais et al., 2012; Lasky et al., 2014; Zhang et al., 2014; Bechtold et al., 2016; Wilkins et al., 2016), resurrection plants (Farrant et al., 2015) and other extremophiles (Brinker et al., 2010). Often these changes are recorded along a gradient of relative water content, plant water potential, plant physiological or metabolic changes (Brinker et al., 2010; Farrant and Moore, 2011; Zhang et al., 2014; Farrant et al., 2015; Bechtold et al., 2016). For example, a significant relationship between water potential and the number of differentially expressed genes was observed in a progressive drought time-series experiments, allowing the clear distinction between early and late dehydration responses at the transcriptional as well as at the physiological level (Bechtold et al., 2016). More importantly, the switch between early and late dehydration responses coincided with a breakpoint in the soil dehydration profile, and this breakpoint clearly differs between natural accessions of Arabidopsis (Ferguson et al., 2018), suggesting difference in dehydration strategies and potentially drought resistance strategies.

In crop plants drought survival through delayed mortality is unlikely to be a suitable option due to expected growth and yield penalties, and therefore questions regarding the usefulness of survival traits in achieving meaningful improvements still remain (Passioura J. , 2006; Skirycz and Inzé, 2010; Blum, 2011; Skirycz et al., 2011). Resurrection plants, although excellent models to investigate drought tolerance strategies associated with delayed mortality, may therefore not be appropriate to investigate avoidance strategies associated with the maintenance of photosynthesis and growth. Consequently, plant species adapted to arid and semi-arid environments that avoid desiccation may be more useful models to study the phenomena of stress tolerance under extreme environmental conditions. One such species is the C3 desert plant *Rhazya stricta*, which is common in arid zones at elevations of 100–700 m above sea level, and overcomes water restriction through long tap roots to access water in underground river beds (Batanouny and Baeshin, 1983).

THE NEED TO STUDY XEROPHYTES IN THEIR NATIVE ENVIRONMENT

Extensive physiological phenotyping under native growth conditions is essential due to the extreme conditions experienced in their native environments. Furthermore, growth conditions in control environments often do not fully reflect the conditions experienced in desert environments, especially with regards to the prevailing light conditions (**Table 1**), even though light is one of the main contributing factors of chloroplast damage during desiccation (Farrant et al., 2003). Relatively few studies have attempted transcriptome analysis from plants grown in their native environments (**Table 1**), and even fewer have underpinned these studies with extensive physiological characterization of these plants in their native habitats (Yates et al., 2014).

For example, physiological and transcriptome analysis of *R. stricta* in its native desert environment revealed that *R. stricta* maintains growth and high photosynthetic rates at leaf temperatures as high as 43°C, light intensities >1,000 μmol m^{-1} s^{-1} and high vapor pressure deficits (VPDs; Lawson et al., 2014), and is one of the few desert C3 shrubs that achieve such high photosynthetic yields at leaf temperatures above 40°C (Mooney et al., 1978; Tezara et al., 2011; Rivas et al., 2017). Gene expression and gene sequence analysis identified two *RUBISCO ACTIVASE* isoforms, that are likely responsible for the maintenance of high Rubisco activities and photosynthetic rates under these extreme conditions (Lawson et al., 2014). Interestingly, in this very hot and arid environment, *R. strica* is able to maintain an adequate water supply in order to maintain a high and constant photosynthetic activity (Lawson et al., 2014). While strictly speaking *R. stricta* may not suffer from drought stress in those circumstances, it nevertheless gives us an insight into extreme thermo- and high light tolerance in arid environments, which are often part of drought stress conditions experienced in the field. Importantly, by combining detailed physiological analysis with genetic investigations, it was possible to identify some potentially different physiological adaptation mechanisms that go beyond the usual TFs and chaperones mentioned above. Interestingly, a detailed study of the diurnal transcriptome analysis of *R. stricta*, identified considerable overlap with *C. plantagineum* and *P. euphratica* such as cysteine proteases and raffinose synthesis genes, highlighting more general protective mechanisms against high temperature (Yates et al., 2014). Furthermore, gene families specific to *R. stricta*, such as photosynthesis and respiration associated genes, were differentially expressed at midday during a diurnal period responding to VPD, temperature and light levels (Yates et al., 2014). These changes coincided with changes in photosynthetic physiology (Lawson et al., 2014; Yates et al., 2014). Importantly, a number of these unique protein families were found to have diverged from their homologs in other species (Yates et al., 2014). Therefore, C3 species from arid/semi-arid environments that do not undergo a dormant state, could provide novel gene targets responsible for maintaining photosynthesis more commonly associated with dehydration avoidance.

CONCLUSIONS

With unprecedented access to increasing genome information and transcriptome datasets from a variety of plants, coupled with tools to analyse and compare these datasets, we are beginning to identify gene families and gene regulatory networks

TABLE 1 | Comparison of growth conditions in transcriptome, proteome, metabolome, and physiological studies of extremophiles.

	Native habitat conditions	Growth cabinet conditions	Experiment growth conditions	Measurements/ treatments	References
ANASTATICA HIEROCHUNTICA					
	Negev Desert: temperature range−3.6 to 46.8°C, arid	16 h day; 150 μmol m^{-2} s^{-1}; 22°C, RH not specified	Growth cabinet	Metabolic profiling/salt and heat stress (MS agar medium)	Eshel et al., 2017
EUTREMA SALSUGINEUM					
Accession: Yukon	Yukon territory: temperature range 15–24°C, light 1,500 μmol m^{-2} s^{-1}, semi-arid	21 h day, 250 μmol m^{-2} s^{-1}, 22/10°C, RH not specified	Growth cabinet and native habitat	Transcriptome/control vs. native habitat (soil grown)	Champigny et al., 2013
Accession: Shangdon		21 h day, 250 μmol m^{-2} s^{-1}, 22/10°C, RH not specified	Growth cabinet	Transcriptome/ of natural variation (soil grown)	Champigny et al., 2013
Accession: Yukon	Yukon territory: temperature range 15–24°C, light 1,500 μmol m^{-2} s^{-1}, semi-arid	21 h day, 250 μmol m^{-2} s^{-1}, 22/10°C, RH not specified	Growth cabinet and native habitat	Transcriptome and metabolome/ control vs. native habitats (soil grown)	Guevara et al., 2012
RHAZYA STRICTA					
	Bahrah (Saudi Arabia): day temperature 36–43°C, light >1,000 μmol m^{-2} s^{-1}, arid	Not applicable	Native habitat	Diurnal transcriptome	Yates et al., 2014
	Bahrah (Saudi Arabia): day temperature 36–43°C, light >1,000 μmol m^{-2} s^{-1}, arid	Not applicable	Native habitat	Diurnal changes in photosynthesis leaf physiology	Lawson et al., 2014
EUTREMA PARVULUM					
	Salt flats in Tuz (Central Anatolia, Turkey)	12 h day, 22/20°C, 60%RH, light not specified	Growth cabinet	Chloroplast physiology, salt stress (soil mixture)	Uzilday et al., 2015
CRATEROSTIGMA PLANTAGINEUM					
	South Africa (conditions not specified)	16 h day, 4,000 lux, 23/19°C RH not specified	Growth cabinet	Transcriptome/different dehydration levels (artificial clay)	Rodriguez et al., 2010
	South Africa (conditions not specified)	14 h day, 24/20°C, 60,000 lx, 60% RH	Growth cabinet	Expression profile of GRP1/desiccation (clay)	Giarola et al., 2016
	South Africa (conditions not specified)		Growth cabinet	Expression profile of EDR1 and CRP1/dehydration and rehydration (clay)	Giarola et al., 2014
SPOROBOLUS STAPFIANUS					
	Verena, Transvaal, South Africa	16 h day, 28/19°C, light and RH not specified	Growth cabinet	Transcriptome and metabolome/dehydration and rehydration (soil)	Yobi et al., 2017
		16 h day, 28/19°C, light and RH not specified	Growth cabinet	Proteome/dehydration (soil)	Oliver et al., 2011b
SPOROBOLUS PYRAMIDALIS					
		16 h day, 28/19°C, light and RH not specified	Growth cabinet	Metabolome/during dehydration (soil) Comparison with *S. stapfianus*	Oliver et al., 2011a
CYNANCHUM KOMAROVII					
	Yinchuan City, Ningxia, China	16 h day, 28/16°C, natural light (intensity not specified)	Growth cabinet	Transcriptome/drought stress (soil and vermiculite)	Ma et al., 2015
HABERLEA RHODOPENSIS					
	Rhodope Mountains, Bulgaria, light at harvesting side 20 μE m^{-2} s^{-1}	16 h day, 21°C, 20 μE m^{-2} s^{-1}, RH 65%	Growth cabinet	Transcriptome and metabolomics (soil)	Gechev et al., 2013
ZYGOPHYLLUM XANTHOXYLUM					
	Desert areas in China and Mongolia	16 h day, 28/23°C, 800 μmol m^{-2} s^{-1}, RH 65–70%	Growth cabinet	Transcriptome/ salt and osmotic stress (sand)	Ma et al., 2016

(Continued)

TABLE 1 | Continued

	Native habitat conditions	Growth cabinet conditions	Experiment growth conditions	Measurements/treatments	References
POPULUS EUPHRATICA					
	Shapotou Desert Experiment and Research, Ningxia, China	12 h day, 25°C, 70 μmol m^{-2} s^{-1}, RH not specified	Growth cabinet	Transcriptome / salt stress (MS agar medium)	Qiu et al., 2011
CALOTROPIS PROCERA					
	Saudi Arabia, field site near Jeddah: day temperature 36–43°C, light >1,000 μmol m^{-2} s^{-1}, arid	16 h day, 25–28°C, 8,000lx, RH not specified	Growth cabinet	Transcriptome and metabolome/salt and drought stress (growth medium not specified)	Mutwakil et al., 2017
	Vargas State, Venezuela: light 100–1,500 μmol m^{-2} s^{-1}, temperature 25–32°C, RH 65–85%	Not applicable	Native habitat	Photosynthetic physiology	Tezara et al., 2011

RH, relative humidity.

behind complex traits such as dehydration tolerance. It is only by developing a more realistic framework in which to study drought resistance mechanism that we will make progress in understanding how plant productivity can be maximized under water limiting conditions. For this to happen, a more positive and inclusive dialogue between the different disciplines, all primarily concerned with "drought-proofing" future crop varieties, is essential in order to move forward in a much more constructive way.

AUTHOR CONTRIBUTIONS

The author confirms being the sole contributor of this work and approved it for publication.

REFERENCES

Alberdi, M., Bravo, L. A., Gutiérrez, A., Gidekel, M., and Corcuera, L. J. (2002). Ecophysiology of Antarctic vascular plants. *Physiol. Plant* 115, 479–486. doi: 10.1034/j.1399-3054.2002.1150401.x

Amtmann, A., Bohnert, H. J., and Bressan, R. A (2005). Abiotic Stress and plant genome evolution search for new models. *Plant Physiol.* 138, 127–130. doi: 10.1104/pp.105.059972

Bao, A. K., Du, B. Q., Touil, L., Kang, P., Wang, Q. L., and Wang, S. M. (2016). Co-expression of tonoplast Cation/H^+antiporter and H^+-pyrophosphatase from xerophyte *Zygophyllum xanthoxylum* improves alfalfa plant growth under salinity, drought and field conditions. *Plant Biotechnol. J.* 14, 964–975. doi: 10.1111/pbi.12451

Bao, A. K., Wang, Y. W., Xi, J. J., Liu, C., Zhang, J. L., and Wang, S. M. (2014). Co-expression of xerophyte *Zygophyllum xanthoxylum* ZxNHX and ZxVP1-1 enhances salt and drought tolerance in transgenic *Lotus corniculatus* by increasing cations accumulation. *Funct. Plant Biol.* 41, 203–214. doi: 10.1071/FP13106

Bartels, D. (2005). Desiccation tolerance studied in the resurrection plant *Craterostigma plantagineum*. *Integr. Comp. Biol.* 45, 696–701. doi: 10.1093/icb/45.5.696

Bartels, D., and Salamini, F. (2001). Desiccation tolerance in the resurrection plant *Craterostigma plantagineum*. a contribution to the study of drought tolerance at the molecular level. *Plant Physiol.* 127, 1346–1353. doi: 10.1104/pp.010765

Batanouny, K. H., and Baeshin, N. A. (1983). Plant communities along the Medina-Badr road across the Hejaz mountains, Saudi Arabia. *Vegetatio* 53, 33–43. doi: 10.1007/BF00039769

Bechtold, U., Penfold, C. A., Jenkins, D. J., Legaie, R., Moore, J. D., Lawson, T., et al. (2016). Time-series transcriptomics reveals that AGAMOUS-LIKE22 affects primary metabolism and developmental processes in drought-stressed arabidopsis. *Plant Cell* 28, 345–366. doi: 10.1105/tpc.15.00910

Blum, A. (2005). Drought resistance, water-use efficiency, and yield potential—are they compatible, dissonant, or mutually exclusive? *Aust. J. Agric. Res.* 56, 1159–1168. doi: 10.1071/AR05069

Blum, A. (2011). *Plant Breeding for Water-Limited Environments*. (New York, NY: Springer).

Blum, A., and Tuberosa, R. (2018). Dehydration survival of crop plants and its measurement. *J. Exp. Bot.* 69:erx445. doi: 10.1093/jxb/erx445

Boscaiu, M., Donat, P., Llinares, J., and Vicente, O. (2012). Stress-tolerant wild plants: a source of knowledge and biotechnological tools for the genetic improvement of stress tolerance in crop plants. *Not. Bot. Horti Agrobot. Cluj-Napoca* 40, 323–327. doi: 10.15835/nbha4028199

Boyer, J. S. (1982). Plant productivity and environment. *Science* 218, 443–448. doi: 10.1126/science.218.4571.443

Bressan, R., Bohnert, H., and Zhu, J. K. (2009). Abiotic stress tolerance: from gene discovery in model organisms to crop improvement. *Mol. Plant* 2, 1–2. doi: 10.1093/mp/ssn097

Brinker, M., Brosché, M., Vinocur, B., Abo-Ogiala, A., Fayyaz, P., Janz, D., et al. (2010). Linking the salt transcriptome with physiological responses of a salt-resistant populus species as a strategy to identify genes important for stress acclimation. *Plant Physiol.* 154, 1697–1709. doi: 10.1104/pp.110.164152

Champigny, M. J., Sung, W. W., Catana, V., Salwan, R., Summers, P. S., Dudley, S. A., et al. (2013). RNA-Seq effectively monitors gene expression in *Eutrema salsugineum* plants growing in an extreme natural habitat and in controlled growth cabinet conditions. *BMC Genomics* 14:578. doi: 10.1186/1471-2164-14-578

Cooper, K. (2002). Recovery of the resurrection plant *Craterostigma wilmsii* from desiccation: protection versus repair. *J. Exp. Bot.* 53, 1805–1813. doi: 10.1093/jxb/erf028

Costa, M. C. D., Farrant, J. M., Oliver, M. J., Ligterink, W., Buitink, J., and Hilhorst, H. M. W. (2016). Key genes involved in desiccation tolerance and dormancy across life forms. *Plant Sci.* 251, 162–168. doi: 10.1016/j.plantsci.2016.02.001

Costa, M. D., Artur, M. A. S., Maia, J., Jonkheer, E., Derks, M. L., Nijveen, H., et al. (2017). A footprint of desiccation tolerance in the genome of *Xerophyta viscosa*. *Nat. Plants* 3, 17038. doi: 10.1038/nplants.2017.38

Cramer, G. R., Urano, K., Delrot, S., Pezzotti, M., and Shinozaki, K. (2011). Effects of abiotic stress on plants: a systems biology perspective. *BMC Plant Biol.* 11:163. doi: 10.1186/1471-2229-11-163

Dassanayake, M., Oh, D. H., Haas, J. S., Hernandez, A., Hong, H., Ali, S., et al. (2011). The genome of the extremophile crucifer *Thellungiella parvula*. *Nat. Genet.* 43, 913–918. doi: 10.1038/ng.889

Des Marais, D. L., McKay, J. K., Richards, J. H., Sen, S., Wayne, T., and Juenger, T. E. (2012). Physiological genomics of response to soil drying in diverse Arabidopsis accessions. *Plant Cell* 24, 893–914. doi: 10.1105/tpc.112.096180

Dinakar, C., and Bartels, D. (2013). Desiccation tolerance in resurrection plants: new insights from transcriptome, proteome and metabolome analysis. *Front. Plant Sci.* 4:482. doi: 10.3389/fpls.2013.00482

Eshel, G., Shaked, R., Kazachkova, Y., Khan, A., Eppel, A., Cisneros, A., et al. (2017). Anastatica hierochuntica, an Arabidopsis Desert relative, is tolerant to multiple abiotic stresses and exhibits species-specific and common stress tolerance strategies with its halophytic relative, Eutrema (Thellungiella) salsugineum. *Front. Plant Sci.* 7:992. doi: 10.3389/fpls.2016.01992

Farrant, J. M. (2000). A comparison of mechanisms of desiccation tolerance among three angiosperm resurrection plant species. *Plant Ecol.* 151, 29–39. doi: 10.1023/A:1026534305831

Farrant, J. M., and Moore, J. P. (2011). Programming desiccation-tolerance: from plants to seeds to resurrection plants. *Curr. Opin. Plant Biol.* 14, 340–345. doi: 10.1016/j.pbi.2011.03.018

Farrant, J. M., Cooper, K., Hilgart, A., Abdalla, K. O., Bentley, J., Thomson, J. A., et al. (2015). A molecular physiological review of vegetative desiccation tolerance in the resurrection plant *Xerophyta viscosa* (Baker). *Planta* 242, 407–426. doi: 10.1007/s00425-015-2320-6

Farrant, J. M., Vander Willigen, C., Loffell, D. A., Bartsch, S., and Whittaker, A. (2003). An investigation into the role of light during desiccation of three angiosperm resurrection plants. *Plant Cell Environ.* 26, 1275–1286. doi: 10.1046/j.0016-8025.2003.01052.x

Ferguson, J. N., Humphry, M., Lawson, T., Oliver, B., and Bechtold, U. (2018). Natural variation of life-history traits, water use, and drought responses in Arabidopsis. *Plant Direct*. 2:e00035. doi: 10.1002/pld3.35

Fitter, A., and Hay, R. (2002). *4 - Water BT - Environmental Physiology of Plants*, *3rd Edn*. London: Academic Press.

Foley, J. A., Ramankutty, N., Brauman, K. A., Cassidy, E. S., Gerber, J. S., Johnston, M., et al. (2011). Solutions for a cultivated planet. *Nature* 478, 337–342. doi: 10.1038/nature10452

Gaff, D. F. (1971). Desiccation-tolerant flowering plants in southern Africa. *Science* 174, 1033–1034. doi: 10.1126/science.174.4013.1033

Gaff, D. F. (1977). Desiccation tolerant vascular plants of southern Africa. *Oecologia* 31, 95–109. doi: 10.1007/BF00348713

Gechev, T. S., Benina, M., Obata, T., Tohge, T., Sujeeth, N., Minkov, I., et al. (2013). Molecular mechanisms of desiccation tolerance in the resurrection glacial relic *Haberlea rhodopensis*. *Cell. Mol. Life Sci.* 70, 689–709. doi: 10.1007/s00018-012-1155-6

Giarola, V., and Bartels, D. (2015). What can we learn from the transcriptome of the resurrection plant *Craterostigma plantagineum*? *Planta* 242, 427–434. doi: 10.1007/s00425-015-2327-z

Giarola, V., Hou, Q., and Bartels, D. (2017). Angiosperm plant Desiccation tolerance: hints from transcriptomics and genome sequencing. *Trends Plant Sci.* 22, 705–717. doi: 10.1016/j.tplants.2017.05.007

Giarola, V., Krey, S., Frerichs, A., and Bartels, D. (2014). Taxonomically restricted genes of *Craterostigma plantagineum* are modulated in their expression during dehydration and rehydration. *Planta* 241, 193–208. doi: 10.1007/s00425-014-2175-2

Giarola, V., Krey, S., von den Driesch, B., and Bartels, D. (2016). The *Craterostigma plantagineum* glycine-rich protein CpGRP1 interacts with a cell wall-associated protein kinase 1 (CpWAK1) and accumulates in leaf cell walls during dehydration. *New Phytol.* 210, 535–550. doi: 10.1111/nph.13766

Griffiths, C. A., Gaff, D. F., and Neale, A. D. (2014). Drying without senescence in resurrection plants. *Front. Plant Sci.* 5:36. doi: 10.3389/fpls.2014.00036

Guevara, D. R., Champigny, M. J., Tattersall, A., Dedrick, J., Wong, C. E., Li, Y., et al. (2012). Transcriptomic and metabolomic analysis of Yukon Thellungiella plants grown in cabinets and their natural habitat show phenotypic plasticity. *BMC Plant Biol.* 12:175. doi: 10.1186/1471-2229-12-175

Harb, A., Krishnan, A., Ambavaram, M. M., and Pereira, A. (2010). Molecular and physiological analysis of drought stress in Arabidopsis reveals early responses leading to acclimation in plant growth. *Plant Physiol.* 154, 1254–1271. doi: 10.1104/pp.110.161752

Higashi, Y., Ohama, N., Ishikawa, T., Katori, T., Shimura, A., Kusakabe, K., et al. (2013). HsfA1d, a protein identified via FOX hunting using thellungiella salsuginea cDNAs improves heat tolerance by regulating heat-stress-responsive gene expression. *Mol. Plant* 6, 411–422. doi: 10.1093/mp/sst024

Iturriaga, G., Schneider, K., Salamini, F., and Bartels, D. (1992). Expression of desiccation-related proteins from the resurrection plant *Craterostigma plantagineum* in transgenic tobacco. *Plant Mol. Biol.* 20, 555–558. doi: 10.1007/BF00040614

Jiang, F., Wang, F., Wu, Z., Li, Y., Shi, G., Hu, J., et al. (2011). Components of the Arabidopsis CBF cold-response pathway are conserved in non-heading Chinese cabbage. *Plant Mol. Biol. Rep.* 29, 525–532. doi: 10.1007/s11105-010-0256-3

Johnson, B. R., and Tsutsui, N. D. (2011). Taxonomically restricted genes are associated with the evolution of sociality in the honey bee. *BMC Genomics* 12:164. doi: 10.1186/1471-2164-12-164

Kant, S., Bi, Y. M., Weretilnyk, E., Barak, S., and Rothstein, S. J. (2008). The Arabidopsis halophytic relative Thellungiella halophila Tolerates nitrogen-limiting conditions by maintaining growth, nitrogen uptake, and assimilation. *Plant Physiol.* 147, 1168–1180. doi: 10.1104/pp.108.118125

Koch, M. A., and German, D. A. (2013). Taxonomy and systematics are key to biological information: Arabidopsis, Eutrema (Thellungiella), Noccaea and Schrenkiella (*Brassicaceae*) as examples. *Front. Plant Sci.* 4:267. doi: 10.3389/fpls.2013.00267

Koziol, L., Rieseberg, L. H., Kane, N., and Bever, J. D. (2012). Reduced drought tolerance during domestication and the evolution of weediness results from tolerance-growth trade-offs. *Evolution* 66, 3803–3814. doi: 10.1111/j.1558-5646.2012.01718.x

Lamdan, N. L., Attia, Z., Moran, N., and Moshelion, M. (2012). The Arabidopsis-related halophyte Thellungiella halophila: boron tolerance via boron complexation with metabolites? *Plant Cell Environ.* 35, 735–746. doi: 10.1111/j.1365-3040.2011.02447.x

Lasky, J. R., Des Marais, D. L., Lowry, D. B., Povolotskaya, I., McKay, J. K., Richards, J. H., et al. (2014). Natural variation in abiotic stress responsive gene expression and local adaptation to climate in *Arabidopsis thaliana*. *Mol. Biol. Evol.* 31, 2283–2296. doi: 10.1093/molbev/msu170

Lawson, T., Davey, P. A., Yates, S. A., Bechtold, U., Baeshen, M., Baeshen, N., et al. (2014). C3 photosynthesis in the desert plant *Rhazya stricta* is fully functional at high temperatures and light intensities. *New Phytol.* 201, 862–873. doi: 10.1111/nph.12559

Lee, Y. P., Babakov, A., de Boer, B., Zuther, E., and Hincha, D. K. (2012). Comparison of freezing tolerance, compatible solutes and polyamines in geographically diverse collections of *Thellungiella* sp. and *Arabidopsis thaliana* accessions. *BMC Plant Biol.* 12:131. doi: 10.1186/1471-2229-12-131

Lesk, C., Rowhani, P., and Ramankutty, N. (2016). Influence of extreme weather disasters on global crop production. *Nature* 529, 84–87. doi: 10.1038/nature16467

Levitt, J. (1980). "Responses of plants to environmental stresses," in *Water, Radiation, Salt, and Other Stresses, Vol 2,* edn 2 (New York, NY: Academic Press), 607.

Ma, Q., Bao, A. K., Chai, W. W., Wang, W. Y., Zhang, J. L., Li, Y. X., et al. (2016). Transcriptomic analysis of the succulent xerophyte *Zygophyllum xanthoxylum* in response to salt treatment and osmotic stress. *Plant Soil* 402, 1–19. doi: 10.1007/s11104-016-2809-1

Ma, X., Wang, P., Zhou, S., Sun, Y., Liu, N., Li, X., et al. (2015). De novo transcriptome sequencing and comprehensive analysis of the drought-responsive genes in the desert plant *Cynanchum komarovii*. *BMC Genomics* 16, 753. doi: 10.1186/s12864-015-1873-x

Mayrose, M., Kane, N. C., Mayrose, I., Dlugosch, K. M., and Rieseberg, L. H. (2011). Increased growth in sunflower correlates with reduced defences and altered gene expression in response to biotic and abiotic stress. *Mol. Ecol.* 20, 4683–4694. doi: 10.1111/j.1365-294X.2011.05301.x

Mickelbart, M. V., Hasegawa, P. M., and Bailey-Serres, J. (2015). Genetic mechanisms of abiotic stress tolerance that translate to crop yield stability. *Nat. Rev. Genet.* 16, 237–251. doi: 10.1038/nrg3901

Millenium Ecosystem Assessment (2010). *Ecosystems and Human Well-Being: Biodiversity Synthesis.*

Millennium Ecosystem Assessment (2005). *Ecosystems and Human Well-Being: Desertification Synthesis*.

Mittler, R., and Blumwald, E. (2010). Genetic engineering for modern agriculture: challenges and perspectives. *Annu. Rev. Plant Biol.* 61, 443–462. doi: 10.1146/annurev-arplant-042809-112116

Mooney, H., Björkman, O., and Collatz, G. (1978). Photosynthetic acclimation to temperature in the desert shrub, Larrea divaricata. I. carbon dioxide exchange characteristics of intact leaves. *Plant Physiol.* 61, 406–410. doi: 10.1104/pp.61.3.406

Mutwakil, M. Z., Hajrah, N. H., Atef, A., Edris, S., Sabir, M. J., Al-Ghamdi, A. K., et al. (2017). Transcriptomic and metabolic responses of *Calotropis procera* to salt and drought stress. *BMC Plant Biol.* 17, 231. doi: 10.1186/s12870-017-1155-7

Oh, D. H., Dassanayake, M., Bohnert, H. J., and Cheeseman, J. M. (2012). Life at the extreme: Lessons from the genome. *Genome Biol.* 13:241. doi: 10.1186/gb-2012-13-3-241

Oliver, M. J., Guo, L., Alexander, D. C., Ryals, J. A., Wone, B. W., and Cushman, J. C. (2011a). A sister group contrast using untargeted global metabolomic analysis delineates the biochemical regulation underlying desiccation tolerance in *Sporobolus stapfianus*. *Plant Cell* 23, 1231–1248. doi: 10.1105/tpc.110.082800

Oliver, M. J., Jain, R., Balbuena, T. S., Agrawal, G., Gasulla, F., and Thelen, J. J. (2011b). Proteome analysis of leaves of the desiccation-tolerant grass, *Sporobolus stapfianus*, in response to dehydration. *Phytochemistry* 72, 1273–1284. doi: 10.1016/j.phytochem.2010.10.020

Oliver, M. J., Tuba, Z., and Mishler, B. D. (2000). The evolution of vegetative desiccation tolerance in land plants. *Plant Ecol.* 151, 85–100. doi: 10.1023/A:1026550808557

Passioura, J. (2006). Increasing crop productivity when water is scarce - from breeding to field management. *Agric. Water Manag.* 176–196. doi: 10.1016/j.agwat.2005.07.012

Passioura, J. B. (2006). Viewpoint: the perils of pot experiments. *Funct. Plant Biol.* 33, 1075–1079. doi: 10.1071/FP06223

Pingali, P. (2012). Green revolution:impacts, limits, and the path ahead. *Proc. Natl. Acad. Sci. U.S.A.* 109, 12302–12308. doi: 10.1073/pnas.0912953109

Poorter, H., Bühler, J., Van Dusschoten, D., Climent, J., and Postma, J. A. (2012). Pot size matters: a meta-analysis of the effects of rooting volume on plant growth. *Funct. Plant Biol.* 39, 839–850. doi: 10.1071/FP12049

Provart, N. J., Alonso, J., Assmann, S. M., Bergmann, D., Brady, S. M., Brkljacic, J., et al. (2016). 50 years of Arabidopsis research: highlights and future directions. *New Phytol.* 209, 921–944. doi: 10.1111/nph.13687

Qiu, Q., Ma, T., Hu, Q., Liu, B., Wu, Y., Zhou, H., et al. (2011). Genome-scale transcriptome analysis of the desert poplar, *Populus euphratica*. *Tree Physiol.* 31, 452–461. doi: 10.1093/treephys/tpr015

Ricroch, A. E., and Hénard-Damave, M. C. (2016). Next biotech plants: new traits, crops, developers and technologies for addressing global challenges. *Crit. Rev. Biotechnol.* 36, 675–690. doi: 10.3109/07388551.2015.1004521

Rivas, R., Frosi, G., Ramos, D. G., Pereira, S., Benko-Iseppon, A. M., and Santos, M. G. (2017). Photosynthetic limitation and mechanisms of photoprotection under drought and recovery of *Calotropis procera*, an evergreen C3from arid regions. *Plant Physiol. Biochem.* 118, 589–599. doi: 10.1016/j.plaphy.2017.07.026

Rodriguez, M. C., Edsgärd, D., Hussain, S. S., Alquezar, D., Rasmussen, M., Gilbert, T., et al. (2010). Transcriptomes of the desiccation-tolerant resurrection plant *Craterostigma plantagineum*. *Plant J.* 63, 212–228. doi: 10.1111/j.1365-313X.2010.04243.x

Skirycz, A., and Inzé, D. (2010). More from less: plant growth under limited water. *Curr. Opin. Biotechnol.* 21, 197–203. doi: 10.1016/j.copbio.2010.03.002

Skirycz, A., Vandenbroucke, K., Clauw, P., Maleux, K., De Meyer, B., Dhondt, S., et al. (2011). Survival and growth of Arabidopsis plants given limited water are not equal. *Nat. Biotechnol.* 29, 212–214. doi: 10.1038/nbt.1800

Tezara, W., Colombo, R., Coronel, I., and Marín, O. (2011). Water relations and photosynthetic capacity of two species of Calotropis in a tropical semi-arid ecosystem. *Ann. Bot.* 107, 397–405. doi: 10.1093/aob/mcq245

Tilman, D., Balzer, C., Hill, J., and Befort, B. L. (2011). Global food demand and the sustainable intensification of agriculture. *Proc. Natl. Acad. Sci. U.S.A.* 108, 20260–20264. doi: 10.1073/pnas.1116437108

Tripathi, P., Rabara, R. C., and Rushton, P. J. (2014). A systems biology perspective on the role of WRKY transcription factors in drought responses in plants. *Planta* 239, 255–266. doi: 10.1007/s00425-013-1985-y

United Nations Department of Economic and Social Affairs, P. D. (2017). World population prospects the 2017 revision key findings and advance tables. *World Popul. Prospect.* 2017, 1–46. doi: 10.1017/CBO9781107415324.004

Uzilday, B., Ozgur, R., Sekmen, A. H., Yildiztugay, E., and Turkan, I. (2015). Changes in the alternative electron sinks and antioxidant defence in chloroplasts of the extreme halophyte Eutrema parvulum (*Thellungiella parvula*) under salinity. *Ann. Bot.* 115, 449–463. doi: 10.1093/aob/mcu184

van der Weele, C. M., Spollen, W. G., Sharp, R. E., and Baskin, T. I. (2000). Growth of *Arabidopsis thaliana* seedlings under water deficit studied by control of water potential in nutrient-agar media. *J. Exp. Bot.* 51, 1555–1562. doi: 10.1093/jexbot/51.350.1555

Varshney, R. K., Bansal, K. C., Aggarwal, P. K., Datta, S. K., and Craufurd, P. Q. (2011). Agricultural biotechnology for crop improvement in a variable climate: hope or hype? *Trends Plant Sci.* 16, 363–371. doi: 10.1016/j.tplants.2011.03.004

Velasco, V. M., Mansbridge, J., Bremner, S., Carruthers, K., Summers, P. S., Sung, W. W., et al. (2016). Acclimation of the crucifer *Eutrema salsugineum* to phosphate limitation is associated with constitutively high expression of phosphate-starvation genes. *Plant Cell Environ.* 39, 1818–1834. doi: 10.1111/pce.12750

von Willert, D. J., Eller, B. M., Werger, M. J. A., and Brinckmann, E. (1990). Desert succulents and their life strategies. *Vegetatio* 90, 133–143. doi: 10.1007/BF00033023

Wang, H., Wang, H., Shao, H., and Tang, X. (2016). Recent advances in utilizing transcription factors to improve plant abiotic stress tolerance by transgenic technology. *Front. Plant Sci.* 7:67. doi: 10.3389/fpls.2016.00067

Wilkins, O., Hafemeister, C., Plessis, A., Holloway-Phillips, M. M., Pham, G. M., Nicotra, A. B., et al. (2016). EGRINs (Environmental Gene Regulatory Influence Networks) in rice that function in the response to water deficit, high temperature, and agricultural environments. *Plant Cell.* 28, 365–2384. doi: 10.1105/tpc.16.00158

Woo, N. S., Badger, M. R., and Pogson, B. J. (2008). A rapid, non-invasive procedure for quantitative assessment of drought survival using chlorophyll fluorescence. *Plant Methods* 4:27. doi: 10.1186/1746-4811-4-27

Wu, H. J., Zhang, Z., Wang, J. Y., Oh, D. H., Dassanayake, M., Liu, B., et al. (2012). Insights into salt tolerance from the genome of *Thellungiella salsuginea*. *Proc. Natl. Acad. Sci. U.S.A.* 109, 12219–12224. doi: 10.1073/pnas.1209954109

Yates, S. A., Chernukhin, I., Alvarez-Fernandez, R., Bechtold, U., Baeshen, M., Baeshen, N., et al. (2014). The temporal foliar transcriptome of the perennial C3 desert plant *Rhazya stricta* in its natural environment. *BMC Plant Biol.* 14:2. doi: 10.1186/1471-2229-14-2

Yobi, A., Schlauch, K. A., Tillett, R. L., Yim, W. C., Espinoza, C., Wone, B. W., et al. (2017). *Sporobolus stapfianus*: insights into desiccation tolerance in the resurrection grasses from linking transcriptomics to metabolomics. *BMC Plant Biol.* 17:67. doi: 10.1186/s12870-017-1013-7

Zhang, J. Y., Cruz de Carvalho, M. H., Torres-Jerez, I., Kang, Y., Allen, S. N., Huhman, D. V., et al. (2014). Global reprogramming of transcription and metabolism in *Medicago truncatula* during progressive drought and after rewatering. *Plant. Cell Environ.* 37, 2553–2576. doi: 10.1111/pce.12328

Conflict of Interest Statement: The author declares that the research was conducted in the absence of any commercial or financial relationships that could be construed as a potential conflict of interest.

frontiers in Plant Science

ORIGINAL RESEARCH
published: 23 April 2018
doi: 10.3389/fpls.2018.00417

Newly Identified Wild Rice Accessions Conferring High Salt Tolerance Might Use a Tissue Tolerance Mechanism in Leaf

*Manas R. Prusty[1], Sung-Ryul Kim[1], Ricky Vinarao[1], Frederickson Entila[1], James Egdane[1], Maria G. Q. Diaz[2] and Kshirod K. Jena[1]**

[1] Strategic Innovation Platform, International Rice Research Institute, Manila, Philippines, [2] Institute of Biological Sciences, University of the Philippines Los Baños, Los Baños, Philippines

Cultivated rice (*Oryza sativa* L.) is very sensitive to salt stress. So far a few rice landraces have been identified as a source of salt tolerance and utilized in rice improvement. These tolerant lines primarily use Na^+ exclusion mechanism in root which removes Na^+ from the xylem stream by membrane Na^+ and K^+ transporters, and resulted in low Na^+ accumulation in shoot. Identification of a new donor source conferring high salt tolerance is imperative. Wild relatives of rice having wide genetic diversity are regarded as a potential source for crop improvement. However, they have been less exploited against salt stress. Here, we simultaneously evaluated all 22 wild *Oryza* species along with the cultivated tolerant lines including Pokkali, Nona Bokra, and FL478, and sensitive check varieties under high salinity (240 mM NaCl). Based on the visual salt injury score, three species (*O. alta*, *O. latifolia*, and *O. coarctata*) and four species (*O. rhizomatis*, *O. eichingeri*, *O. minuta*, and *O. grandiglumis*) showed higher and similar level of tolerance compared to the tolerant checks, respectively. All three CCDD genome species exhibited salt tolerance, suggesting that the CCDD genome might possess the common genetic factors for salt tolerance. Physiological and biochemical experiments were conducted using the newly isolated tolerant species together with checks under 180 mM NaCl. Interestingly, all wild species showed high Na^+ concentration in shoot and low concentration in root unlike the tolerant checks. In addition, the wild-tolerant accessions showed a tendency of a high tissue tolerance in leaf, low malondialdehyde level in shoot, and high retention of chlorophyll in the young leaves. These results suggest that the wild species employ tissue tolerance mechanism to manage salt stress. Gene expression analyses of the key salt tolerance-related genes suggested that high Na^+ in leaf of wild species might be affected by *OsHKT1;4*-mediated Na^+ exclusion in leaf and the following Na^+ sequestration in leaf might be occurring independent of tonoplast-localized OsNHX1. The newly isolated wild rice accessions will be valuable materials for both rice improvement to salinity stress and the study of salt tolerance mechanism in plants.

Keywords: wild rice, *Oryza sativa*, salt tolerance, Na^+ exclusion, tissue tolerance

OPEN ACCESS

Edited by:
Ruth Grene,
Virginia Tech, United States

Reviewed by:
Lingaraj Sahoo,
Indian Institute of Technology Guwahati, India
Narendra Singh Yadav,
Ben-Gurion University of the Negev, Israel

***Correspondence:**
Kshirod K. Jena
k.jena@irri.org

Specialty section:
This article was submitted to Plant Abiotic Stress, a section of the journal Frontiers in Plant Science

Received: *28 October 2017*
Accepted: *15 March 2018*
Published: *23 April 2018*

Citation:
Prusty MR, Kim S-R, Vinarao R, Entila F, Egdane J, Diaz MGQ and Jena KK (2018) Newly Identified Wild Rice Accessions Conferring High Salt Tolerance Might Use a Tissue Tolerance Mechanism in Leaf. Front. Plant Sci. 9:417. doi: 10.3389/fpls.2018.00417

INTRODUCTION

The increasing trend of Na^+ in the agricultural land is a global threat and a major concern for food security (Yamaguchi and Blumwald, 2005; Shahbaz and Ashraf, 2013). Worldwide, approximately 830 million hectares (ha) of the land is affected from soil salinization and bears an annual loss of US$ 12–27.3 billion due to reductions in crop productivity (Qadir et al., 2014). Further the continued practice of poor irrigation system with improper drainage in the agricultural land and due to changing climate events, 50% of all arable land is expected to be impacted by salinity by 2050 (Wang et al., 2003; Rengasamy, 2010; Assaha et al., 2017). Salinity is measured in terms of electrical conductivity and is defined as saline when the value exceeds a threshold of 4 dSm^{-1} (Munns and Tester, 2008). The effect of salinity stress is brought to the plant in two phases over the time scale, the osmotic stress which is immediately felt by the plants soon after exposure to salt solution and the later ionic stress (Al-Tamimi et al., 2016). In the osmotic stress, plant experience a limited supply of water and solute as a result of NaCl-induced reduction in solute potential in soil. The ionic stress phase is initiated once the Na^+ from the soil enters the plant. Na is a nonessential element for plant (except in some C_4 plants) (Nieves-Cordones et al., 2010; Kronzucker et al., 2013) and its elevated level within plant tissues interfere with K^+ function. K^+ participates in a series of enzymatic reaction linked to vital metabolic pathways and the high external Na^+ competes for K^+ and inhibits its activity and disturbs the cellular homeostasis. Hence, maintenance of a low Na^+/K^+ in a plant cell is considered to be a key salt-tolerant trait (Shabala and Pottosin, 2014; Munns et al., 2016). To keep the cytosolic Na^+ at low level and to maintain osmotic balance, plants employ several mechanisms controlled by the regulation of different physiological, biochemical, and molecular processes at various level of plant structural organization (Flowers, 2004).

Rice (*Oryza sativa*), the dietary staple food for more than half of the world population is a salt sensitive crop (Munns and Tester, 2008). Particularly, the seedling and reproductive stages of rice growth are critically affected by salinity. Rice yield starts to decline beyond a threshold EC of 3 dSm^{-1} with 12% reduction in yield per unit rise in EC (Chinnusamy et al., 2005; Reddy et al., 2014). Therefore, most of the modern high yielding varieties experience up to 50% yield reduction under salt stress of 6 dSm^{-1} and they become totally unproductive beyond 12 dSm^{-1} (Linh et al., 2012). Hence, there is an urgent need to develop salt-tolerant rice cultivar either by breeding or biotechnology approach to sustain rice production. Rice plants mainly employ three mechanisms, ion exclusion, osmotic tolerance, and tissue tolerance to adapt in salt stress (Munns and Tester, 2008; Roy et al., 2014). These mechanisms are brought in to play during the various stages of Na^+ uptake from soil and its translocation to shoot. The solutes and water from the soil can reach xylem via a symplastic or apoplastic route. In species-like rice, a significant amount (50% of the total Na^+ uptake) of Na^+ transport is mediated through apoplastic route, i.e., the movement occurs mainly through intracellular spaces which are also called as "bypass flow" (Horie et al., 2012). Plant salt tolerance at this level can be contributed by casparian strips and suberin layers present in the root endodermal and exodemal layers which act as barriers to this bypass flow (Chen et al., 2011). In the root tip and in the initiation site of lateral roots, these structures are partially effective and hence are the suitable sites for Na^+ entry into the stele. On the other hand in the symplastic route, Na^+ is transported radially into the stellar region, loaded in to xylem and finally reaches the shoot by the transpiration stream. In this case the plant salt tolerance can be achieved by the regulation of the transporters localized in the cells of cortex, pericycle, and xylem parenchyama bordering xylem. *SOS1* is a plasma membrane anti-porter present in the root epidermis provides the resistance to Na^+ uptake by excluding Na^+ to external environment (Shi et al., 2000). However, the function of *SOS1* depends on the severity of the salt stress. The *SOS1* gene in the Arabidosis (*AtSOS1*) may function both in Na^+ loading (low or moderate level of salinity) and unloading (high salinity) (Olías et al., 2009; Yadav et al., 2012). The over-expression of rice transporter *OsSOS1* in Arabidopsis has been shown to increase salt tolerance (Martínez-Atienza et al., 2007). It is also known that lower expression of *OsSOS1* in rice old leaves may decrease frequency of retrieving Na^+ from old leaf cells (Wang et al., 2012). Rice HKT family transporter, *OsHK2;1* present in the plasma membrane of epidermis mediates Na^+ transport to the root; however, in the cortical region it prevents the radial flow of Na^+ and restricts its movement to the xylem (Horie et al., 2007). Similarly, *OsHKT1;5* localized in the xylem parenchyma retrieves Na^+ from xylem sap to xylem parenchyma (Ren et al., 2005). Transporters like *OsHKT2;1*, *OsHKT1;5*, and *OsSOS1* are the control points in the root soil boundary and their regulation decides the fate of Na^+ entry in to the xylem (Zhang et al., 2017). Once Na^+ is loaded to xylem it is transported via transpiration pull to the shoot. In monocot species like rice *OsHKT1;4* transporter, located in the leaf sheath region can further retrieve the Na^+ from the xylem to xylem parenchyma lowering their delivery to the leaf blade (Suzuki et al., 2016). Most of the metabolic process of the plant is carried in the leaf blade and hence it is needed to be kept away from reaching a toxic concentration of Na^+. Re-circulation of Na^+ from the leaf/shoot to the root via phloem is a possible mechanism for salt tolerance and which occurs in plants like Arabidopsis and reeds but in rice it is not a well-established mechanism (Berthomieu et al., 2003; Horie et al., 2005). However, *OsHKT2;1* localized to the shoot vascular bundle is believed to recirculate Na^+ to the root via phloem (Golldack et al., 2002; Laurie et al., 2002). There are certain salt-tolerant glycophytes and halophytes that are able to grow in high salt concentration (>200 mM NaCL) and their tissues can also tolerate equivalent concentration of Na^+ (Flowers and Colmer, 2008; Katschnig et al., 2015). The Na^+ in their tissue acts like an osmoticum to adjust the osmotic pressure and they are not completely dependent on the synthesis of organic solute which is energetically expensive. The capacity of the tissue to function while containing a high internal concentration of Na^+

Abbreviations: DMRT, Duncan's multiple range test; DSS, days of seedling survival; IRRI, International Rice Research Institute; MDA, malondialdehyde; QTL, quantitative trait loci; ROS, reactive oxygen species; SES, standard evaluation system; VI, vigor score; VSI, visual salt injury; XPC, xylem perenchyma cells.

is known as tissue tolerance. Intracellular compartmentalization of Na^+ in to the vacuole by tonoplast Na^+/H^+ exchanger, *NHX* is a key mechanism of tissue tolerance for which the Na^+ concentration remains relatively low in the cytoplasm. However, other factors like synthesis of compatible solutes, synthesis of enzymes for catalyzing detoxification of ROS, and maintenance of cell volume and turgor also contribute to tissue tolerance (Munns et al., 2016).

Salt tolerance in rice primarily depends on Na^+ exclusion principle. Most of the salt-tolerant accessions of cultivated rice maintain a low Na^+ concentration in the actively growing plant parts. *OsHKT1;5* in rice is a major determinant for salt tolerance. The activity of *OsHKT1;5* is more robust in salt-tolerant rice cultivars and was originally detected from a salt-tolerant land race Nona Bokra (Bonilla et al., 2002; Ren et al., 2005). It is also believed to be the causal gene in *Saltol* QTL region which accounts important aspect of seedling salt tolerance (Bonilla et al., 2002; Lin et al., 2004). Cultivated rice has a narrow genetic diversity for salt tolerance with a less number of donor source, limited to traditional rice land races only. Due to this limitation, the rice breeding program has no alternative choice rather using these donors repeatedly for improving salt tolerance in rice varieties. (Thomson et al., 2010; Platten et al., 2013; Reddy et al., 2014). Identification of diverse germplasm with high salt tolerance is an imperative and important strategy to adapt to a high salinity projected from the current climate change. The wild relatives of rice offer an untapped genetic resource of novel genes with diverse sets of adaptive mechanisms for development of climate resilient rice cultivar (Brar and Khush, 1997). These germplasm has to be exploited in depth to find suitable tolerance source and to further use it in rice breeding. There are 22 wild species in the rice genus along with two cultivated rice (Marathi et al., 2014). Around 4,370 accessions of wild species are available at the gene bank of IRRI and are grouped into 11 different genome types (AA, BB, CC, BBCC, CCDD, EE, FF, GG, HHJJ, HHKK, and KKLL) (Jena, 2010; Sanchez et al., 2013). So far salt tolerance is of concern, and a few wild germplasm are known to be salt tolerant with unknown salt tolerance mechanism. This study attempts to evaluate the wild rice accessions from all genomes of wild rice species to isolate promising salt-tolerant sources and to understand the salt tolerance mechanism of different genomes.

MATERIALS AND METHODS

Plant Materials and Preparation of Seedlings

A total of 22 different wild *Oryza* species (one accession per species) with salt-tolerant checks (Pokkali, Nona Bokra, and FL478) and salt-sensitive checks (IR29 and IR75862-206-2-8-3) were used in this study. Seeds of these materials were obtained from the International Rice Genebank of IRRI. Seeds were kept in a convection oven at 50°C for 5 days for dormancy breaking and were dehusked. The seeds were sterilized by treatment of 70% ethanol for 1 min and 1.5% sodium hypochlorite solution for 30 min. After which, the seeds were washed with sterilized water for 5 times. Seeds were transferred into culture tubes with one quarter-strength of Murashige and Skoog media and kept in the dark room for 48 h to obtain uniform germination. Once the seeds started sprouting, the culture tubes were kept under light condition for 5 days and the plantlets were transferred to seedling floats in a tray containing Yoshida nutrient solution (Yoshida et al., 1976). For curing of any plant damage during seedling transfer, the trays were kept for 3 days in Yoshida solution at the phytotron plant growth facility of IRRI. Seeds of *O. coarctata*, *O. schlechteri,* and *O. meyeriana* were hard to germinate, hence the seedlings were established in nutrient solution by cutting internodes.

Plant Growth and Salt Stress Treatment

For salinization, initially 60 mM NaCl (EC6) in Yoshida solution was applied to the seedling plants after curing and an increment of 60 mM NaCl was carried at an interval of 2 days until 180 mM NaCl for physiological and biochemical analyses and 240 mM NaCl for the determination of days of seedling survival (DSS). Nutrient solutions containing salt (NaCl) were replaced every 5 days and the solution was maintained with a pH of 5.0 daily. As a control condition, an identical set of seedlings were continuously kept in a normal Yoshida solution.

Determination of Days of Seedling Survival

The DSS was determined by counting the number of days the seedling survived under 240 mM NaCl condition. When the plants were completely wilted, it was regarded as dead. The mean values of DSS were obtained from the two independent experiments (eight plants per entry in each experiment).

Visual Salt Injury (VSI)

The VSI score for different entries were determined after 16 days of salinization in 180 mM NaCl. VSI scores were given following the standard evaluation system (SES) of IRRI (Gregorio et al., 1997). Briefly, the scores of 1, 3, 5, 7, and 9 were assigned for highly tolerant, tolerant, moderately tolerant, sensitive, and highly sensitive, respectively to salt stress. Mean values were calculated from the two replications. In each experiment, eight plants per entry were scored.

Plant Vigor

To test the vigor (VI) of growth, all entries were grown in normal Yoshida solution for 20 days. Then, shoots of each plant were harvested for the measurement of fresh biomass and shoot length. Mean values were obtained from the five plants per entry. The difference obtained between the maximum and minimum mean value of the entries were divided by 5 and all entries were assigned into five groups with scores from 1, 3, 5, 7 to 9 (from high to low VI score).

Plant Growth Reduction by Salt Stress

Shoot length and biomass were compared between the control and salt stress condition (180 mM NaCl) and plant growth reduction by salt stress was represented in percentage. The mean

values were obtained from five plants per entry in the normal and salt stress conditions, respectively.

Quantification of Malondialdehyde

To assess the damage incurred from the stress, malondialdehyde (MDA) levels were measured from leaf tissues following Hodges et al. (1999) with minor modifications. Briefly, leaf tissues were harvested from the plants after 10 days of salt treatment (180 mM NaCl) and homogenized in liquid N_2. 0.5 g of the homogenized leaf was mixed with 0.1% (w/v) trichloroacetic acid solution and the homogenate was centrifuged at 4,000 × *g* for 15 min at 4°C. Aliquots of 1 mL of the supernatant were placed in two tubes, one with thiobarbituric acid (TBA) reagent and another without TBA reagent. The mixture was incubated at 90°C for 25 min and the reaction was stopped by placing the tubes in an ice bath. Absorbance of the supernatant was obtained at 440, 532, and 600 nm and MDA estimates were computed and expressed in fresh weight basis. The MDA values were obtained from the average of three plants per entry.

Chlorophyll Quantification in Young Emerging Leaf

To quantify chlorotic symptoms due to salinity stress, chlorophyll content was determined following Lichtenthaler and Buschmann (2001) with slight modifications. Young emerging leaves (L6) were collected 10 days after salinization with 180 mM NaCl and were temporarily stored at −80°C until assay. Ten milligrams of the homogenized leaf samples were placed into 10 ml of 95% ethanol and were incubated at 80°C for 10 min, cooled at room temperature thereafter, and then reconstituted to the original volume by adding 95% ethanol. Absorbance values were obtained at 470, 649, and 664 nm using spectrophotometer. The chlorophyll concentrations were determined by following the equation of Lichtenthaler and Buschmann (2001). Total chlorophyll content was measured from five plants per accession in the control and 180 mM NaCl conditions.

Measurement of Ion Content in Leaf and Root

Shoot and root were harvested at 16 days after salt treatment (180 mM) and were dried in an oven (65°C) for 48 h. Approximately 10 mg was weighed, placed in 50 ml conical tubes and digested by 10 ml of 0.1 N acetic acid (Sigma-Aldrich, United States) at 90°C for 2 h. The extracts were cooled at room temperature, left overnight, and then filtered using Whatman filter paper. Finally, Na^+ and K^+ ions were measured using a PerkinElmer AAnalyst 200 atomic absorption spectrophotometer (PerkinElmer, United States), operating in emission mode. Mean values of Na^+ and K^+ contents in both root and leaf were obtained from five plants per entry.

Tissue Tolerance Assay

Tissue tolerance assay is an indirect way of estimating the process of Na^+ sequestration (Yeo et al., 1990). It was conducted for the specific wild salt-tolerant species and the check lines. The same sets of genotypes were treated to a series of salt concentrations (0, 60, 120, 180, and 240 mM NaCl). Initially, 60 mM NaCl was given to all plants in the setup and an increment of 60 mM NaCl was applied at an interval of 2 days to reach higher salt concentrations. The phenotype of each material under different salt concentrations was monitored through the observation of VSI scores based on the IRRI SES (Gregorio et al., 1997). Once a genotype reached an SES score of 7 at the highest salinity level (240 mM), the youngest fully expanded leaf (6th Leaf, L6) was harvested from each salt concentration. The experiment was continued until all the genotypes were harvested and the harvested samples were analyzed for Na^+ content and chlorophyll content. The tissue tolerance score was estimated from the LC_{50} score which represents the Na^+ content at which 50% reduction of the chlorophyll content occurs. Mean value obtained from two replications (four plants per entry in each replication) were used for determining the LC_{50} scores.

Measurement of Na^+ Content of Leaf Surface

Two to three leaves were detached from a similar position in each plant after 10 days at 180 mM NaCl and were carefully put in a tube containing 10 ml of double distilled water. The tubes were shaken vigorously for 2 min to wash the leaf surface properly. After washing, the solution was used for Na^+ quantification and the leaf tissues were scanned to measure the total leaf surface area. Na^+ content per unit leaf area was calculated from five plants per accession.

Leaf Anatomy

Leaf tissues were detached from all wild tolerant genotypes and were fixed in glacial acetic acid–ethanol (1:3) solution for 24–48 h. Transverse sections of the leaf samples were made using a razor blade and stained with 1% toluidine blue solution. The specimen was observed under a light microscope (Olympus BX53).

Gene Expression Analysis of the Known Salt Tolerance Genes

A floating tray containing 20-day-old seedling plants in Yoshida solution was transferred to the salt-added Yoshida solution with the following concentrations: 80 mM NaCl for 8 h, 160 mM NaCl for 16 h, and 240 mM NaCl for 24 h. Leaf and root tissues were then collected from the normal and the salt-treated conditions, respectively. Each sample tube contained the tissues derived from 2 to 4 seedling plants and three tubes per experiment were prepared. Total RNA was extracted and cDNA was synthesized using an ImProm-II Reverse Transcription system (Promega, United States). The expression of salt-tolerant genes including *OsNHXl, OsHKTl;4, OsHKTl;5,* and *OsSOSl* were performed using SYBR select master mix and ABI7500 machine (Applied Biosystems, United States). The primer sequences for the target genes are listed in Supplementary Table S1 (Additional File 1). The *OsActl* gene was used as an internal control and the relative expression level was calculated based on the $\Delta\Delta Ct$ method. Each data point represents the mean value of three biological replications.

TABLE 1 | Salt stress phenotypes as determined by VSI score and days of seeding survival (DSS).

Species	Accessions (IRGC No.)/variety	Genome	VSI score ($M \pm SE$)	VSI group^{+}	DSS	VS score^{++}
O. brachyantha	Acc.101232	FF	9.0^{a}	HS	2.8 ± 0.09^{q}	9^{a}
O. granulata	Acc.102118	GG	9.0^{a}	HS	2.8 ± 0.18^{q}	9^{a}
O. longiglumis	Acc.105148	HHJJ	9.0^{a}	HS	2.8 ± 0.09^{q}	8^{b}
O. schlecteri	Acc.82047	HHKK	9.0^{a}	HS	3.3 ± 0.12^{pq}	9^{a}
O. sativa	Acc.IR75862-206-2-8-3	AA	9.0^{a}	HS	3.0 ± 0.17^{pq}	7.2^{c}
O. sativa	IR29	AA	8.1 ± 0.24^{b}	HS	4.6 ± 0.12^{l}	7^{cd}
O. nivara	Acc.80455	AA	9.0^{a}	HS	4 ± 0.15^{mn}	5.4g
O. rufipogon	Acc.80671	AA	8.2 ± 0.24^{b}	HS	3.5 ± 0.19^{nop}	6.2^{ef}
O. ridleyi	Acc.100821	HHJJ	7.8 ± 0.24^{bc}	S	4.9 ± 0.27^{i}	9^{a}
O. meridionalis	Acc.105301	AA	7.8 ± 0.24^{bc}	S	4.6 ± 0.19^{l}	7^{cd}
O. glumaepatula	Acc.105692	AA	7.8 ± 0.24^{bc}	S	4.4 ± 0.12^{lm}	7^{cd}
O. australiensis	Acc.100882	EE	7.8 ± 0.24^{bc}	S	3.7 ± 0.10^{no}	8^{b}
O. meyeriana	Acc.89241	GG	7.3 ± 0.19^{c}	S	5.6 ± 0.12^{K}	9^{a}
O. longistaminata	Acc.110404	AA	6.2 ± 0.24^{de}	MT	6.6 ± 0.27^{j}	3^{i}
O. punctata	Acc.105690	BB	5.0^{gh}	MT	8.6 ± 0.12^{h}	6^{f}
O. sativa	IR64	AA	5.8 ± 0.24^{ef}	MT	$7.5 \pm .0.21^{i}$	5.2^{g}
O. barthii	Acc.100936	AA	6.6 ± 0.19^{d}	MT	5.6 ± 0.19^{k}	7.2^{c}
O. glaberrima	Acc.96717	AA	6.6 ± 0.19^{d}	MT	5.6 ± 0.19^{k}	6^{f}
O. officinalis	Acc.100896	CC	5.3 ± 0.19^{fg}	MT	7.4 ± 0.24^{i}	8^{b}
O. rhizomatis	Acc.105432	CC	4.6 ± 0.19^{hi}	T	10.3 ± 0.24^{g}	8^{b}
O. eichingeri	Acc.101424	CC	4.3 ± 0.23^{i}	T	11.5 ± 0.26^{f}	6.8^{cd}
O. grandiglumis	Acc.101405	CCDD	3.7 ± 0.24^{jk}	T	15.8 ± 0.18^{c}	6.6^{de}
O. minuta	Acc.101141	BBCC	4.1 ± 0.24^{ij}	T	15.8 ± 0.22^{c}	9^{a}
O. sativa	FL478	AA	4.3 ± 0.23^{i}	T	11.8 ± 0.28^{f}	4.4^{h}
O. sativa	Pokkali	AA	4.2 ± 0.24^{ij}	T	13.1 ± 0.09^{e}	1^{j}
O. sativa	Nona Bokra	AA	4.1 ± 0.24^{ij}	T	14.8 ± 0.20^{d}	4.2^{h}
O. latifolia	Acc.105133	CCDD	2.8 ± 0.21^{k}	HT	26.1 ± 0.24^{b}	7.2^{c}
O. alta	Acc.105143	CCDD	1.3 ± 0.19^{l}	HT	33 ± 0.21^{a}	7^{cd}
O. coarctata	Acc.104502	KKLL	1.0^{l}	HT	*	9^{a}

$^{+}$HS, highly sensitive; S, sensitive; MT, moderately tolerant; T, tolerant; HT, highly tolerant. VSI is determined following IRRI SES and was obtained after 10 days of growth at 180 mM NaCl. VSI score of 8.0–9.0 = HS; 7.0–7.9 = S; 5.0–6.9 = MT; 3.0–4.9 = T; and <2.9 = HT. The DSS was obtained at 240 mM NaCl. $^{++}$VS of different genotypes is determined from their growth rate in nonsaline nutrient solution. Mean value with different letteres statistically different at $p < (0.05)$ based on DMRT.

RESULTS

Wild Rice Species Possesses Higher Tolerance to Salinity

To isolate new salt-tolerant germplasm, representative from 24 *Oryza* species together with tolerant and sensitive checks were exposed to salt stress. The wild rice accessions showed various degrees of tolerance to salt stress at both 180 and 240 mM of NaCl (**Table 1** and **Figure 1**) compared to control condition (Additional File 2: Supplementary Figure S1). Based on the plant phenotype under salt stress as rated by the VSI score, five wild *Oryza* species (*O. nivara*, *O. brachyantha*, *O. granulata*, *O. longiglumis*, *O. rufipogon*, and *O. schlechteri*) were classified as highly salt sensitive like the susceptible check cultivars (IR29 and IR75862-206-2-8-3) and these species survived only for <5 days at 240 mM NaCl (DSS score 2.8–4.6). Seven wild species accessions (*O. meridionalis*, *O. glumaepatula*, *O. australiensis*, *O. ridleyi*, and *O. meyeriana*) were classified as the sensitive group and they survived for 5–7 days. The five wild species accessions (*O. punctata*, *O. barthii*, *O. officinalis*, *O. longistaminata*, and *O. glaberrima*) and one rice cultivar (IR64) showed moderate level of salt tolerance (VSI score 5.0–6.6) and their DSS was in the range of 5.6–8.6 days. Four wild species accessions (*O. rhizomatis*, *O. eichingeri*, *O. minuta*, and *O. grandiglumis*) along with the three tolerant check cultivars (FL478, Pokkali, and Nona Bokra) belonged to the tolerant group and they survived upto 16 days at 240 mM NaCl (DSS score 10.3–15.8). The wild species, *O. latifolia*, *O. alta*, and *O. coarctata* showed high salt tolerance. *O. coarctata* was the most tolerant wild species as it survived during the seedling stage without any detrimental effect and grew up to reproductive stage. The species, *O. alta* which was found to be the second most highly tolerant species had a DSS of 33 days in 240 mM NaCl. The DSS of *O. latifolia*, *O. alta*, and *O. coarctata* was significantly higher ($p < 0.001$) than the tolerant check cultivars FL478, Pokkali, and Nona Bokra. Visual difference in tolerance between the wild-tolerant species (*O. alta*, *O. latifolia*, and *O. coarctata*) and the conventional tolerant checks is presented in **Figure 2**. On the basis of DSS, salt tolerance of all tolerant genotypes was ranked in the following order: *O. coarctata*, *O. alta*, *O.*

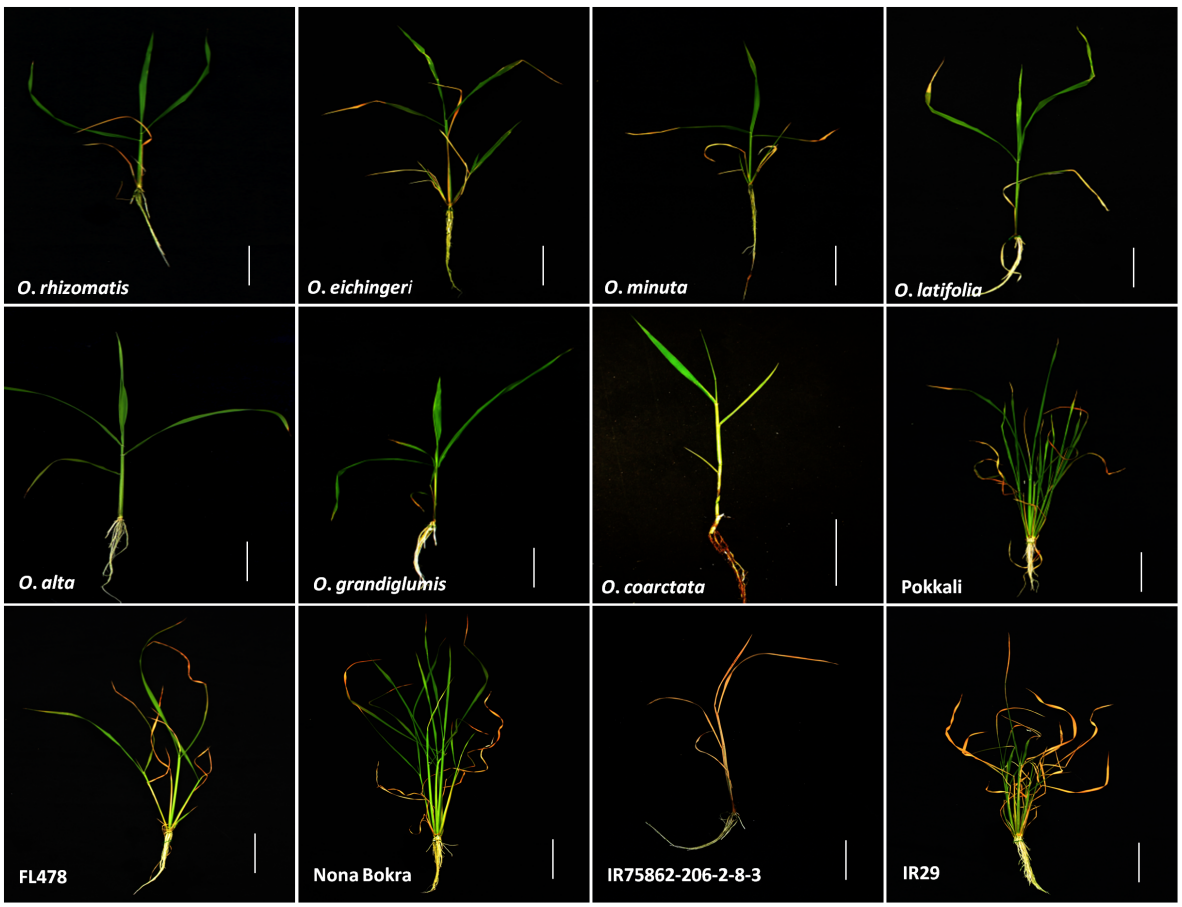

FIGURE 1 | Seedling phenotype of tolerant wild species with cultivated checks after 10 days of 180 mM NaCl treatment. Scale bar = 5 cm.

latifolia, *O. grandiglumis*, *O. minuta*, Nona Bokra, Pokkali, FL478, *O. eichingeri*, and *O. rhizomatis*.

Plant vigor is positively associated with salt tolerance in rice species. To check the plant vigor in this study, we measured shoot biomass and shoot length of all the test material after 20 days of their growth in normal condition (non-saline nutrient solution). The cultivated checks especially Pokkali and Nona Bokra grew faster than the wild accessions and showed vigorous growth (VS score 1.0 and 4.2, respectively) (**Table 1**). The wild species-tolerant lines grew slower than the cultivated check during the same 20 days of observational period. The vigor score of the wild species-tolerant lines differed significantly ($p < 0.001$) from that of cultivated tolerant lines. The correlation of vigor score with salt tolerance was high ($r^2 = 0.90$) for cultivated rice lines whereas it was low for wild species ($r^2 = 0.026$).

Shoot part is mostly affected in salt stress than the root. To observe the effect of salinity on shoot growth, shoot length and shoot biomass were measured from the newly identified tolerant species along with the check lines (**Table 2**). Except for *O. coarctata*, a significant reduction in shoot length and shoot biomass was observed in all the wild and cultivated check lines. Among the tolerant lines, Nona Bokra experienced least reduction in shoot length (16.28%) and *O. alta* encountered least reduction (30.60%) in shoot biomass. While the highest reductions of both shoot length (34.02%) and biomass (53.24%) occurred in *O. rhizomatis*. The susceptible checks (IR75862-206-2-8-3 and IR29) showed dramatic growth inhibition by salt stress (54.89 and 45.73% in shoot length and 85.10 and 66.0% in biomass, respectively). *O. coarctata* did not encounter any reduction in growth parameter under salt concentration rather its shoot length and shoot biomass increased as 10.45 and 11.6%, respectively, in saline condition.

Wild-Tolerant Species Sustained Minimal Cell Injury Under Salinity Stress

Oxidative damage is regarded as the manifestation of stress susceptibility and one of its causes is extensive membrane lipid peroxidation. MDA level is widely used as an indicator of the extent of oxidation damage under salt stress. MDA content of shoot was measured from the tolerant wild species and the check lines which were stressed by 180 mM NaCl. The sensitive checks IR29 and IR75862-206-2-8-3 showed high MDA content in the shoot, indicating a higher degree of lipid peroxidation and cell membrane damage while both cultivated and wild-tolerant species contained low level of MDA (**Figure 3**). Among the

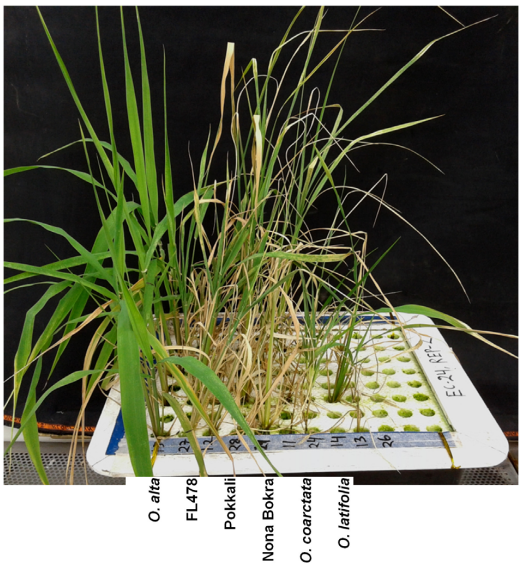

FIGURE 2 | Seedlings phenotype of the three highly tolerant wild species with the tolerant check lines after 10 days of 240 mM NaCl treatment. Scale bar = 5 cm.

tolerant lines, MDA content was significantly lower (0.4- to 1.5-fold) in all wild-tolerant lines than tolerant cultivars which indicates the wild-tolerant lines have a better stress amelioration. The lowest MDA level was obtained for *O. coarctata*.

Tolerant Wild Species Accessions Showed High Chlorophyll Content in the Young Emerging Leaves Under Salt Stress Condition

Retention of chlorophyll level in the leaves under salt stress is used as an index for salt tolerance. Total chlorophyll content was measured from the young emerging leaves in both normal and salt conditions (**Table 3**). Difference of chlorophyll content between normal and salt conditions was very high (39.16–69.57%) in the sensitive and tolerant checks. In contrast, the salt-tolerant wild species showed relatively low chlorophyll reduction with wide variations (4.59–39.80%). Chlorophyll reduction was very less in *O. eichingeri*, *O. minuta*, and *O. coarctata* (4.50–13.10%).

Tolerant Wild Species Lines Showed High Na^+ Content in Leaves and Low Accumulated Na^+ Content in Roots

Na^+ exclusion at root xylem epithelial region is considered to be the primary mechanism of salt tolerance in conventional tolerant lines like FL478, Nona Bokra, and Pokkali. Low Na^+ in the shoot is used as selection criteria to breed salt-tolerant cultivar in wheat, barley, and rice. However, in our study, we observed an opposite trend in shoot Na^+ and Na^+/K^+ pattern between the tolerant wild species (except *O. coarctata*) and tolerant cultivars (**Figures 4A,B**). The cultivated tolerant checks and *O. coarctata* showed low Na^+ and low Na^+/K^+ in the leaves. Oppositely, Na^+ and Na^+/K^+ ratio in the newly isolated wild-tolerant lines was significantly high even higher than sensitive check lines IR29 and IR75862-206-2-8-3. Similarly to the leaf, a contrasting root ion profile was also observed between the newly identified tolerant wild species and the cultivated tolerant checks. The root Na^+ content and Na^+/K^+ were found to be high in cultivated salt-tolerant checks while it was low in wild-tolerant species and in the sensitive checks (**Figures 4C,D**).

Gene Conservation and Expression Analyses of the Salt Transporter Genes in the Wild-Tolerant Accessions

Several salt tolerance-involved genes including *OsNHX1*, *OsHKT1;4*, *OsHKT1;5*, and *OsSOS1* have been identified and studied in rice. We conducted PCR amplifications of the above genes in tolerant wild species because the species of *Oryza* genus

TABLE 2 | Reduction in the shoot biomass and shoot length of the salt-tolerant wild accessions and check lines at 180 mM NaCl.

Genotypes	Shoot length (cm)			Shoot biomass (g)		
	Control	180 mM NaCl	% Reduction from control	Control	180 mM NaCl	% Reduction from control
O. rhizomatis	31.6 ± 0.96	20.34 ± 0.31	34.02^{bc}	0.74 ± 0.05	0.34 ± 0.02	53.24^{c}
O. eichingeri	55.1 ± 0.13	36.55 ± 1.10	34.35^{bc}	2.73 ± 0.06	1.32 ± 0.05	52.57^{c}
O. minuta	21.8 ± 1.15	17.17 ± 0.55	20.32^{de}	0.87 ± 0.04	0.66 ± 0.02	26.9^{e}
O. latifolia	48 ± 1.81	36.22 ± 1.42	24.79^{cde}	2.53 ± 0.10	1.52 ± 0.02	47^{cd}
O. alta	51.2 ± 0.91	39.57 ± 0.95	23.06^{cde}	2.22 ± 0.08	1.75 ± 0.05	30.6^{e}
O. grandiglumis	59.7 ± 1.19	41.17 ± 1.19	30.23^{cd}	3.13 ± 0.44	1.75 ± 0.04	49.7^{c}
O. coarctata	13.4 ± 0.83	14.65 ± 0.40	-10.45^{f}	0.28 ± 0.01	0.39 ± 0.08	-11.6^{f}
IR75862-206-2-8-3	47 ± 1.52	21.13 ± 0.33	54.89^{a}	3.08 ± 0.06	0.39 ± 0.08	85.10^{a}
IR29	50.2 ± 1.11	27.67 ± 0.69	45.73^{ab}	2.92 ± 0.07	0.96 ± 0.02	66^{b}
FL478	64.1 ± 0.98	44.80 ± 0.54	24.49^{cde}	8.24 ± 0.48	4.91 ± 0.25	37.2^{de}
Pokkali	89.5 ± 0.89	66.50 ± 0.69	19.26^{de}	17.42 ± 0.45	10.5 ± 0.28	37.6^{de}
Nona Bokra	75.8 ± 1.58	57.17 ± 0.93	16.28^{e}	8.38 ± 0.45	5.40 ± 0.26	36.9^{de}

The data represented are mean values (n = 5) with standard errors. Different letters in the % reduction coulmn are statistically different as inferred from DMRT at p < (0.05).

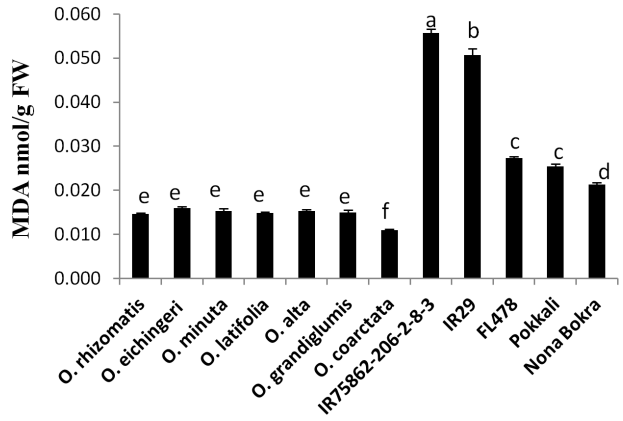

FIGURE 3 | Leaf MDA content of tolerant wild species and the cultivated checks. Leaf tissues were collected after 10 days from a 180 mM NaCl-treated experimental set up and mean value of MDA (n = 3) was calculated in nmol per gram FW of the leaf. Vertical bar indicates ± standard error. Different letters in error bars are statistically different as inferred from DMRT at $p < 0.05$.

TABLE 3 | Reduction in chlorophyll content in the young leaves (L6) of the salt-tolerant wild accessions and check lines at 180 mM NaCl.

Genotypes	Chlorophyll content		% of reduction*
	Control	180 mM NaCl	
O. rhizomatis	2.46 ± 0.15	1.48 ± 0.21	39.80^{de}
O. eichingeri	2.78 ± 0.18	2.42 ± 0.19	13.10^{g}
O. minuta	2.85 ± 0.18	2.63 ± 0.19	8.10^{h}
O. latifolia	2.86 ± 0.21	2.08 ± 0.31	37.16^{e}
O. alta	1.82 ± 0.13	1.38 ± 0.18	23.22^{f}
O. coarctata	2.09 ± 0.18	2.00 ± 0.18	4.50^{h}
O. grandiglumis	1.82 ± 0.18	1.20 ± 0.18	36.26^{e}
IR75862-206-2-8-3	2.95 ± 0.20	0.86 ± 0.18	69.57^{a}
IR29	2.95 ± 0.22	1.90 ± 0.18	39.16^{de}
FL478	3.19 ± 0.24	1.88 ± 0.19	50.90^{b}
Pokkali	2.79 ± 0.16	1.55 ± 0.15	43.65^{cd}
Nona Bokra	2.20 ± 0.15	1.18 ± 0.14	45.81^{bc}

**The data represented are mean values (n = 5) with standard errors. Different letters in the % reduction coulmn are statistically different as inferred from DMRT at p < (0.05).*

diversified in the ancient time. Three primer sets for *OsNHX1*, two primer sets for *OsHKT1;4*, six primer sets for *OsHKT1*;*5*, and four primer sets for *OsSOS1* were designed (Additional File 1: Supplementary Table S1) and applied for the PCRs with genomic DNA of the wild-tolerant accessions. All four genes tested in this study were amplified in all wild-tolerant species and the checks, except for few sets of primer (Additional File 3: Supplementary Figure S2). This result supports that these four salt-related genes existed in the origin of the *Oryza* genus before diversification of species. In the case of *OsHKT1;4* gene, OsH4F1 primer set showed different PCR band size between wild species and cultivated rice (*O. sativa*) (Additional File 3: Supplementary Figure S2B), suggesting that the *O. sativa* allele might be separated during species differentiation or domestication. In the case of *OsHKT1*;*5* gene, four primer sets locating intron or 5'-untranslated region (UTR) of the gene showed no PCR bands in wild species (Additional File 3: Supplementary Figure S2C), indicating that the sequences of intron or 5'-UTR are highly variable between wild species and *O. sativa*. For *OsSOS1* gene, one primer set (SOS1F2) which has binding site two the exonic regions amplified in case of cultivated rice but did not amplified for wild species (Additional File 3: Supplementary Figure S2D).

After confirmation of presence of four genes in the wild species, we conducted gene expression analyses in root and leaf tissues of seedling plants grown under normal and salt-added nutrient solution, respectively. One salt-sensitive check IR29, two conventional tolerant lines Pokkali and FL478, and three CCDD genome species (*O. alta*, *O. latifolia*, and *O. grandiglumis*) were tested. Transcription of *OsNHX1* increased in root tissue and decreased in leaf tissue in all three cultivated rice under salt stress (**Figure 5A**). In contrast, the *OsNHX1* transcripts were almost non-detectable in all samples of the three CCDD genome species (**Figure 5A**). The expression level of *OsHKT1;4* was relatively high in leaf tissues of all wild species compared to checks in which the gene weakly expressed in root (**Figure 5B**). In the cases of *OsHKT1;5* and *OsSOS1* genes, transcription of both genes was dramatically increased by salt stress in root tissue in all tested materials including salt-sensitive IR29 (**Figures 5C,D**), indicating that these two genes are functioning in root to exclude Na^+ from xylem in response to salt stress.

Tolerant Wild Species Lines Showed High Tissue Tolerance in Leaf

Tissue tolerance of a genotype is defined as the capacity of the tissue to function while containing a high concentration of Na^+. This component of salt tolerance emphasizes the process of Na^+ sequestration in the vacuole as a result of which metabolic activities in a cell are less affected. Tissue tolerance score (LC_{50}) from our experiment for different genotypes was determined from the Na^+ concentration at which a 50% of the chlorophyll reduction occurs. Low LC_{50} value was obtained for the Na^+ excluding tolerant cultivars Pokkali (LC_{50} = 0.6 mg/g), Nona Bokra (LC_{50} = 0.9 mg/g), and FL478 (LC_{50} = 1.2 mg/g) (**Figure 6A**), implying that they can undergo rapid chlorophyll loss even at low Na^+ concentration. The salt-sensitive check IR29 has higher tissue tolerance score (LC_{50} = 1.57 mg/g) than the cultivated salt-tolerant checks. Interestingly, all the tolerant wild species exhibited high tissue tolerance score than that of the cultivated tolerant checks as well as the sensitive check IR29. The wild species, *O. rhizomatis* had the highest tissue tolerance score (LC_{50} = 4.5 mg/g) among all wild-tolerant lines and is followed by *O. eichingeri* (LC_{50} = 3.4 mg/g) (**Figure 6B**).

Na^+ Content from Leaf Washing Solution

The sodium ions concentration released through leaf washing was calculated per mm^2 of the leaf from the wild-tolerant species and the check lines. The Na^+ content was very low in leaf-washed solution from all wild-tolerant materials, except for *O. coarctata* (Additional File 4: Supplementary Figure S3). The Na^+ content

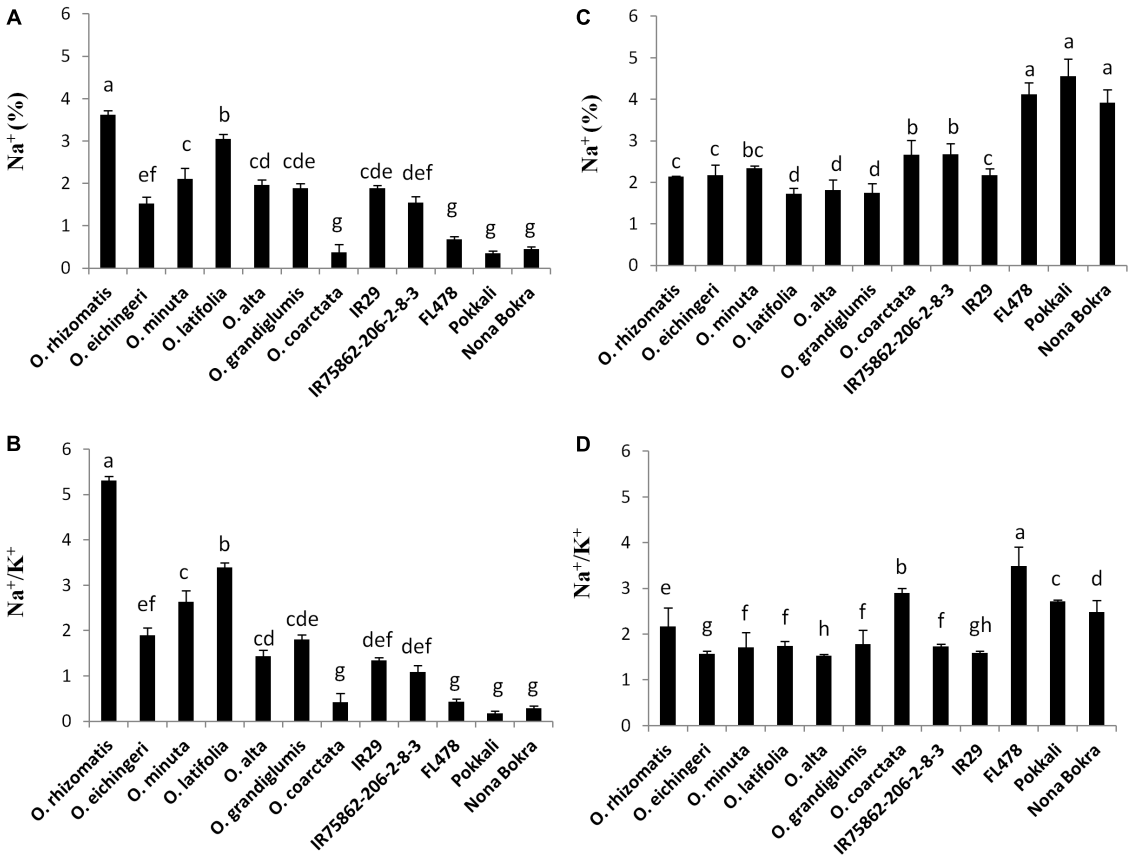

FIGURE 4 | Na^+ content (%) and Na^+/K^+ ratio in shoot **(A,B)** and root **(C,D)**, respectively, in the tolerant wild species and the cultivated checks after 10 days of 180 mM NaCl treatment. Mean values were obtained from five plants. Vertical bars indicates ±SE. Different letters in error bars are statistically different as inferred from DMRT at $p < 0.05$.

released from *O. coarctata* was 0.50% which was dramatically higher ($p < 0.001$) than the remaining genotypes and suggested Na^+ ion extrusion from leaf surface. To observe the leaf surface of the wild-tolerant species, leaf anatomy was conducted. The salt exuding gland was observed only in the leaves of *O. coarctata* (Additional File 5: Supplementary Figure S4).

DISCUSSION

Currently limited salt-tolerant genotypes are available in the cultivated species of *O. sativa* and *O. glabberrima*, and those genotypes have been extensively used in rice breeding. The salt-tolerant cultivar, Pokkali is one such example which has been used as a potential donor in several rice breeding programs (Waziri et al., 2016). The narrow genetic diversity of the cultivated rice with a handful source of salt-tolerant donors is a major limitation for further augmentation of salt tolerance trait in the elite rice varieties. Apart from the two cultivated rice species, *O. sativa* and *O. glaberrima*, the rice germplasm has 22 different wild species. Compared to the cultivated rice, the wild species of rice has a wide genetic diversity. Today's cultivated rice is the result of a long-term domestication process of the wild ancestor and during which many of the valuable genes are thought to have been lost. It is estimated that only 10–20% of the wild species diversity is present in cultivated rice (Zhu et al., 2007; Palmgren et al., 2014). To develop a climate resilient agriculture for sustainable rice production, time has come to go back to the wild progenitors to capture the untapped traits and improve rice breeding with exotic genes. While the wild rice germplasm has been identified with carrying different resistance/tolerance factor for various stress, a very limited knowledge has been acquired for salt tolerance. To identify salt-tolerant lines in the wild AA genome, Akbar et al. (1987) carried out salinity screening in seven wild rice species along with two cultivated species in a hydroponic experiment system but none of the wild species accessions tested was found to be as tolerant as the cultivated landrace Nona Bokra. The salt tolerance of *O. coarctata* (KKLL genome) is well documented from several previous studies (Bal and Dutt, 1986; Jena, 1994; Sengupta and Majumder, 2010; Menguer et al., 2017). Salt tolerance in other wild species like *O. punctata*, *O. officinalis*, and *O. rufipogon* was also reported (Farooq et al., 1992; Tian et al., 2011; Mishra et al., 2016; Zhou et al., 2016). In this study, we simultaneously tested all 22 wild species together with the cultivated checks at a high NaCl concentration (240 mM NaCl) compared to the earlier screening conditions to identify

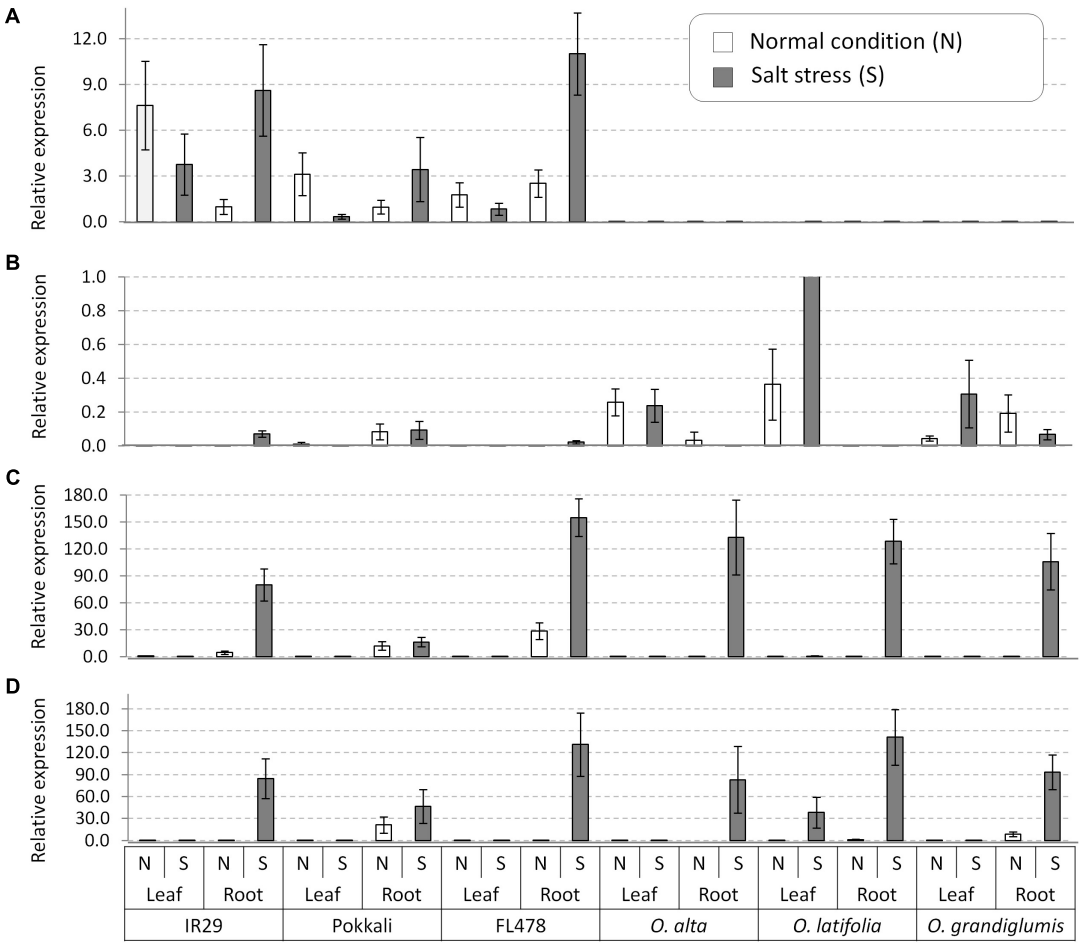

FIGURE 5 | Gene expression analyses of the salt tolerance genes in leaf and root tissues collected from the salt tolerant wild species having the CCDD genomes and the checks varieties. **(A)** *OsNHX1*, **(B)** *OsHKT1;4*, **(C)** *OsHKT1;5*, and **(D)** *OsSOS1*. *OsActil1* was used as an internal control of qRT-PCR. N, normal nutrition solution (white bar); S, salt stress (gray bar). Error bar means SD (n = 3).

salt-tolerant species and to understand their salt tolerance mechanism through physiological, biochemical, and molecular studies. Except for *O. coarctata*, six wild rice species were newly identified in this study (**Table 1**). But the previously isolated tolerant species did not show salt tolerance in this study probably due to use of different accessions of the species or a different screening conditions. Around 4,370 accessions of wild species are available in the IRRI gene bank. Hence, future research can include more accessions for salinity screening and it can get more salt-tolerant sources for further improvement of rice cultivars.

One of the interesting result came out from the analysis of ionic content was the occurrence of high Na^+ and high Na^+/K^+ ratio in the young leaves of novel salt-tolerant germplasm, an opposite ionic paradigm in tolerant cultivars. Salt tolerance trait in rice cultivars is likely to be dependent on their ability to maintain low Na^+ concentration in young leaves through Na^+ exclusion (Lin et al., 2004; Thomson et al., 2010; Platten et al., 2013). Consistent to earlier research, this study also found low Na^+ in shoot and high in root in the cultivated salt-tolerant lines implying that Na^+ has been actively excluded through the root. In contrast, the novel salt-tolerant wild species accessions accumulated high Na^+ and showed high Na^+/K^+ ratio in shoot. For the wild species-tolerant lines, the high Na^+ and Na^+/K^+ ratio per unit dry mass in the shoot than root implies a poor Na^+ exclusion process unlike tolerant cultivars. Wild accessions of *O. eichingeri* and *O. minuta* had low shoot/root Na^+ but it was not low as cultivated salt-tolerant lines. The high ionic content in wild-tolerant species suggested us to check for the presence of the three key Na^+ excluding genes *OsSOS1*, *OsHKT1;5*, *OsHKT1;4*, and one Na^+ sequestration gene *OsNHX1* in wild-tolerant species and to observe their expression pattern under salt stress. From PCR amplifications with genomic DNA, it was found that the primers binding to the intronic regions did not generate the PCR products (e.g., OsHF1, OsHF2, OsHF3, and OsHF4 primer sets for *OsHKT1;5* and SOS1F2 for *OsSOS1*). In contrast, most of the primers binding to the exonic regions produced expected PCR amplicon in the wild species like in the checks, except for the OsH4F1 primer set for *OsHKT1;4* (Additional File 3: Supplementary Figure S2B). These PCR results indicate that the nucleotide variations are very high in intronic

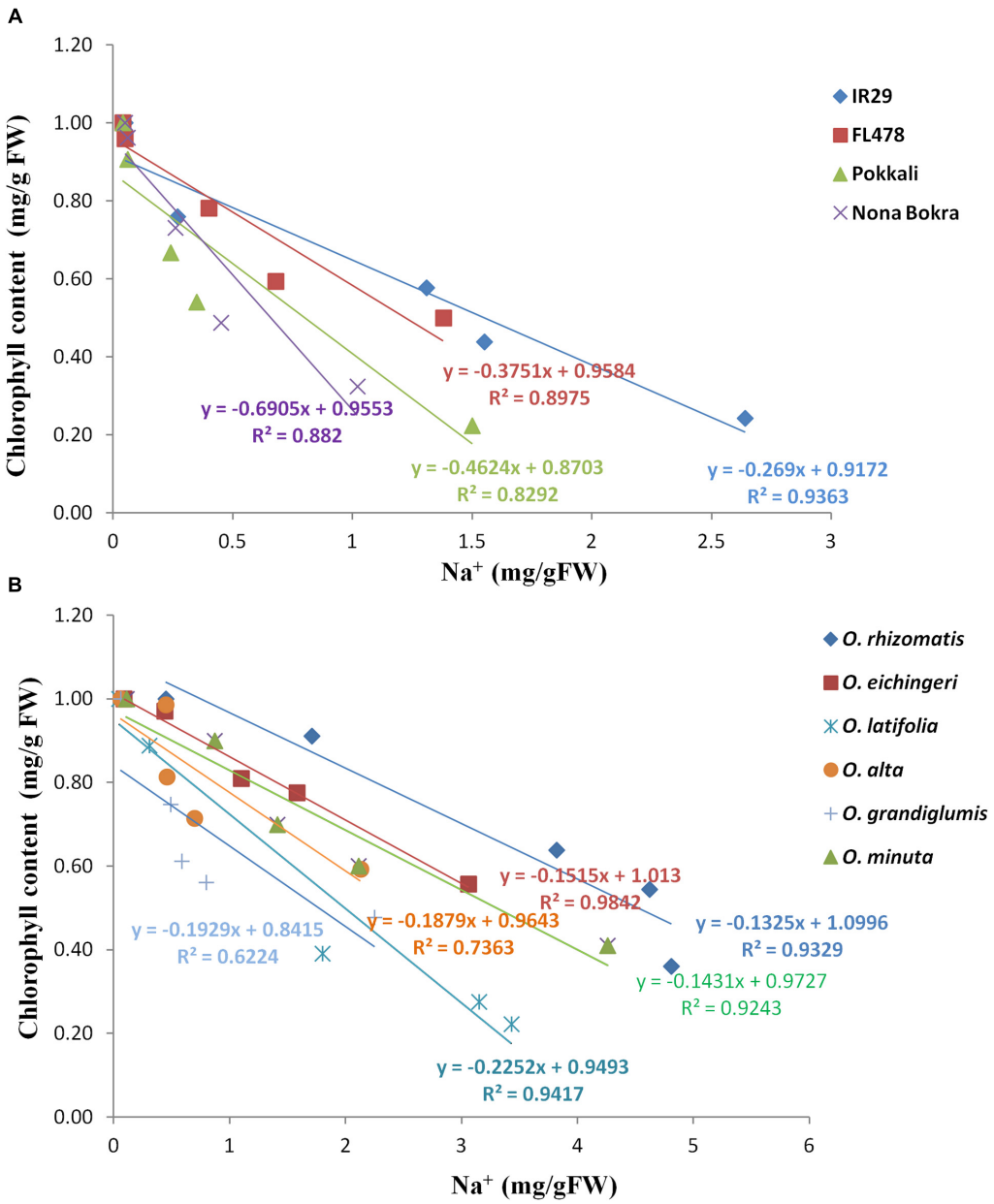

FIGURE 6 | Tissue tolerance score of tolerant wild species and cultivated checks as determined from the LC_{50} value. Check lines **(A)** and wild salt-tolerant lines **(B)**.

regions compared to exonic regions between the cultivated and wild rice species. Characterization of the gene sequences and comparisons between the sensitive and tolerant accessions will be required to understand the functional nucleotides for salt tolerance in the future.

For further gene expression analysis, all three CCDD genome species with the checks were used. Unexpectedly, *OsHKT1;5* and *OsSOS1* were strongly transcribed by salt stress in both cultivated and wild salt-tolerant accessions. And also similar expression pattern of these two genes were observed in the salt-sensitive cultivar IR29. However, Na^+ accumulation pattern was different among the samples tested, although all samples showed same expression patterns of the Na^+ excluding genes in root under salt stress condition. Platten et al. (2013) reported 10 allele types of *OsHKT1;5* from the diverse cultivated accessions through PCR-Sanger sequencing method and showed the different level of Na^+ exclusion among the different allele types in root. Similarly, the sequence difference in coding regions of the *OsHKT1;5* and *OsSOS1* genes among accessions in this study might cause different protein sequence, resulting in differential Na^+ accumulation patterns. For *OsHKT1;4*, we detected a high expression in the leaf of all CCDD wild species at the seedling growth stage both in normal and stress conditions while *OsHKT1;4* expression was very low in the cultivated checks.

Moreover, *OsHKT1;4* expression level increased for *O. latifolia* (**Figure 5B**) under salt stress. One of the distinctive features of *OsHKT1;4* is its steady-state expression in the leaf sheaths in Nipponbare throughout the whole growth stage. In salt-stressed Nipponbare, *OsHKT1;4*-mediated transport contributes for Na^+ homeostasis for the reproductive growth phase rather than vegetative growth (Suzuki et al., 2016). We assume that the *OsHKT1;4* expression in the leaf tissue of wild species may contribute to Na^+ exclusion from the leaf and its further sequestration in the vacuole or to the apoplast space. The *OsNHX1* gene is known to play a key role in the vacuolar compartmentalization (Yamaguchi et al., 2013). It has been shown in many plant species that over expression of *OsNHX1* gene confers salt tolerance (Apse et al., 1999; Zhang et al., 2001; Agarwal et al., 2013). In the study, *OsNHX1* expression was increased at the root under salt stress in case of cultivated checks implying Na^+ sequestration in the root vacuole. This may be one of the reasons for getting a high Na^+ content in the roots of tolerant cultivated checks. *OsNHX1* did not express in any of the CCDD genome species both at normal and stress (**Figure 5A**). This result suggests that excess Na^+ in these species might be sequestrated in vacuole without assistance of *OsNHX1* gene. It has been also reported that the Na^+ uptake to vacuole can also be possible through pinocytosis, which is an energy efficient way without requiring Na^+/H^+ exchange activity in halophytes (Shabala and Mackay, 2011). In this process, the invagination of tonoplast can engulf the apoplastic Na^+ and move it to vacuole. Further study is required to elucidate the sequestration mechanism in leaf for tissue tolerance.

Tissue tolerance is also an important mechanism for salinity tolerance in crop plant. Tissue tolerance is defined as the ability of cell or tissues to tolerate internal Na^+ and Cl^-. A number of factor can contribute to maintain tissue tolerance such as compartmentalization of excess Na^+ in the vacuole keeping its cytosolic concentration at much low level, adequate translocation of K^+, adjustment of osmotic pressure, and regulation of ROS (Munns et al., 2016). Osmotic adjustment is essential for plant to maintain the turgor pressure and prevent water loss during salinity stress. Since at the elevated Na^+ and Na^+/K^+ ratio, the newly identified tolerant wild species showed a better morphology and we hypothesize that these high Na^+ would have benefited in the adjustment of osmotic pressure. A large portion of the osmotic adjustment is carried by the synthesis of organic solutes which is an energy requiring process (Munns and Gilliham, 2015). Alternatively, the high accumulation of Na^+ in the cellular organelle like vacuole may function like osmoticum to maintain osmotic balance (Maathuis et al., 2014; Shabala and Pottosin, 2014). This energy-efficient strategies are used by halophytes (Flowers and Colmer, 2008) and salt-tolerant non-halophyte plant like barley. The indication of the probable involvement of tissue tolerance also came from MDA assay. The level of lipid peroxidation has been widely used as an indicator of ROS-mediated damage to cell membranes under stressful conditions (Borsani et al., 2001; Apel and Hirt, 2004). Increase in lipid peroxidation under salinity stress associates with increased production of ROS. MDA is one of the final products of peroxidation of unsaturated fatty acids in phospholipids and is responsible for cell membrane damage. Plants with low accumulation of MDA under stress condition are more adaptable to the stress than high MDA. Especially, the wild-tolerant species had the lowest level of MDA, suggesting the proper regulation of ROS through various scavenging mechanisms. Another indication of the tissue tolerance came from the observation that wild salt-tolerant species accumulated more Na^+ in their leaves with the less chlorophyll loss. Loss of chlorophyll pigment can lead to photosynthesis decline. Retention of high chlorophyll in the leaves under salinity is an indication of tissue tolerance (Yeo and Flowers, 1986; Munns et al., 2016). In our study, we exclusively estimated the chlorophyll level in the young emerging leaves (L6) under the salt stress and its reduction from the control condition. In the cultivated tolerant checks, the chlorophyll reduction was very high even higher than the sensitive check IR29. However, chlorophyll level in wild-tolerant lines undergoes less reduction under salinity. Salinity toxic symptoms such as chlorosis, leaf rolling, and meristem dehydration were more apparent in salinity-tolerant cultivars than the wild relatives. The third evidence for tissue tolerance came from Na^+ tissue tolerance assay. All the wild species were found to have a high Na^+ tissue tolerance which means a 50% of chlorophyll degradation occurs at a higher concentration of Na^+ which is an opposite phenomenon in cultivated tolerant lines. In the case of cultivated tolerant lines, the 50% reduction of chlorophyll occurred in spite of having a low Na^+ concentration in their leaves. The increased Na^+ ions in shoot without apparent loss of photosynthetic function and sustained cellular integrity resulting to unhampered growth suggest tissue tolerance as the primary means under saline perturbation.

To observe other possible component of salt tolerance we investigated the role of plant vigor and salt excretion from leave surface. Vigorous growth with larger biomass provides salt dilution and maintains low tissue Na^+ concentration that helps the plant to survive under salt stress (Yeo et al., 1990). Breeding more vigorous plant for saline-affected soil was suggested to get more yields (Richards, 1992). In rice, most of the traditional salt-tolerant landraces are vigorous in growth (Yeo et al., 1990). Similarly, in our study a strong positive correlation was observed between vigor score and salt tolerance in the cultivated tolerant lines. However, on the contrary vigor score was not correlated with salt tolerance in the tolerant wild species. Na^+ exudation from the leaf through pore-like structures such as hydathode and salt glands lowers the cytosolic Na^+ and prevents chlorophyll loss (Bal and Dutt, 1986; Flowers et al., 1990; Negrão et al., 2011). To know whether any other wild species use this component of salinity tolerance mechanism, we measured ion content from leaf-washed solution from all genotypes. None of the genotypes, except for *O. coarcctata*, accumulate Na^+ outside the leaves and salt glands were not observed in their leaves suggesting this mechanism of salt tolerance is absent in other tolerant wild accessions.

The phloem recirculation may also be a mechanism of salt tolerance where Na^+ in the leaf can be redistributed to root via phloem. This phloem recirculation is not a well-established mechanism in rice although *OsHK2;1* located in shoot vascular

bundle is believed to have a role. The result from using positron-emitting tracer imaging system which can trace the direction of Na^+ transport, it was found that the Na^+ accumulates in shoot only (Fujimaki et al., 2015). In our study, a low Na^+ content was detected in wild-tolerant species roots which suggest no noticeable role of Na^+ recirculation via phloem.

Our study revealed availability of new salt tolerance sources in the wild germplasm which will be certainly helpful for the future rice breeding and biotechnology research. In addition to the mechanism study of salt tolerance using the newly isolated wild rice species, utilization of the trait is also crucial to improve salt tolerance of the cultivated rice varieties. For this, development of introgression lines (ILs) having the wild rice chromosome segments, screening of the ILs against salt stress, and identifications of QTL/gene using the ILs are required in the future. The QTLs/gene(s) can be easily transferred to the rice varieties through the marker-assisted breeding (MAB). And also the additive effects between the conventional salt tolerance genes and the newly identified genes derived from wild species need to be tested. Alternatively, the advanced genomics tools can be employed for rapid validation of the genes. Sequence comparisons of the major salt tolerance genes between salt sensitive and tolerant species are one of priorities to find a commonality like functional nucleotide polymorphisms (FNPs) causing the trait. Finally, this can be confirmed by direct-transferring of the target genes from wild rice species to rice varieties using transgenic method. This work will be valuable to isolate superior alleles of the known genes.

AUTHOR CONTRIBUTIONS

KJ, MP, MD, and S-RK conceived the idea and designed the research. MP, RV, JE, and FE conducted the experiment. KJ, MP, and S-RK wrote the manuscript. All authors contributed to the conceptualization of the study, read, and approved the final version of the manuscript.

FUNDING

The funding was provided by the International Rice Research Institute (IRRI). We are grateful to Rural Development Administration (RDA), South Korea for providing partial funding support through the Cooperative Research Program between IRRI and RDA (DRPC No. 2013-45 and Project No. PJ013494012018) and Lee Foundation Program (DRPC No. A-2012-208/BR-00-11173) of IRRI for financial support to carry out this study.

ACKNOWLEDGMENTS

We thank Ms. Janice Sapin, research technician for seeds preparation and germination, Mr. Norberto Quilloy and Mr. Marlon Camalate, research technicians for helping in the salinity screening; and Ms. Mariane Ilagan for the preparation of nutrient solution and maintenance of pH, and Mr. James Egdane for assisting in the Na^+ and K^+ quantification analysis. We also thank to Dr. R. K. Singh, Dr. G. D. Prahalada, and Dr. Ajay Kohli for critical review of the manuscript. We thank IRRI communication team for carefully editing the manuscript.

SUPPLEMENTARY MATERIAL

The Supplementary Material for this article can be found online at: https://www.frontiersin.org/articles/10.3389/fpls.2018.00417/full#supplementary-material

REFERENCES

Agarwal, P. K., Shukla, P. S., Gupta, K., and Jha, B. (2013). Bioengineering for salinity tolerance in plants: state of art. *Mol. Biotechnol.* 54, 102–123. doi: 10.1007/s12033-012-9538-3

Akbar, M., Jena, K. K., and Seshu, D. V. (1987). Salt tolerance in wild rices. *Int. Rice Res. Instit. News Lett.* 12:15.

Al-Tamimi, N., Brien, C., Oakey, H., Berger, B., Saade, S., Ho, Y. S., et al. (2016). Salinity tolerance loci revealed in rice using high-throughput non-invasive phenotyping. *Nat. Commun.* 7:13342. doi: 10.1038/ncomms13342

Apel, K., and Hirt, H. (2004). Reactive oxygen species metabolism oxidative stress, and signals transduction. *Annu. Rev. Plant Biol.* 55, 373–399. doi: 10.1146/annurev.arplant.55.031903.141701

Apse, M. P., Aharon, G. S., Snedden, W. A., and Blumwald, E. (1999). Salt tolerance conferred by overexpression of a vacuolar Na+/H+ antiport in Arabidopsis. *Science* 285, 1256–1258. doi: 10.1126/science.285.5431.1256

Assaha, D. V. M., Ueda, A., Saneoka, H., Al-Yahyai, R., and Yaish, M. W. (2017). The role of Na+ and K+ transporters in salt stress adaptation in glycophytes. *Front. Physiol.* 8:509. doi: 10.3389/fphys.2017.00509

Bal, A. R., and Dutt, S. K. (1986). Mechanisms of salt tolerance in wild rice (*Oryza coarctata* Roxb). *Plant Soil* 92, 399–404. doi: 10.1007/BF02372487

Berthomieu, P., Conéjéro, G., Nublat, A., Brackenbury, W. J., Lambert, C., Savio, C., et al. (2003). Functional analysis of AtHKT1 in Arabidopsis shows that Na+ recirculation by the phloem is crucial for salt tolerance. *EMBO J.* 22, 2004–2014. doi: 10.1093/emboj/cdg207

Bonilla, P., Dvorak, J., Mackill, D., Deal, K., and Gregorio, G. (2002). RFLP and SSLP mapping of salinity tolerance genes in chromosome 1 of rice (*Oryza sativa L.*) using recombinant inbred lines. *Philipp. Agric. Sci.* 85, 68–76.

Borsani, O., Valpuesta, V., and Botella, M. A. (2001). Evidence for a role of salicylic acid in the oxidative damage generated by NaCl and osmotic stress in Arabidopsis seedling. *Plant Physiol.* 126, 1024–1030. doi: 10.1104/pp.126.3.1024

Brar, D. S., and Khush, G. S. (1997). Alien introgression in rice. *Plant Mol. Biol.* 35, 35–47. doi: 10.1023/A:1005825519998

Chen, T., Cai, X., Wu, X., Karahara, I., Schreiber, L., and Lin, J. (2011). Casparian strip development and its potential function in salt tolerance. *Plant Signal. Behav.* 6, 1499–1502. doi: 10.4161/psb.6.10.17054

Chinnusamy, V., Jagendorf, A., and Zhu, J. K. (2005). Understanding and proving salt tolerance in plants. *Crop Sci.* 45, 437–448. doi: 10.2135/cropsci2005.0437

Farooq, S., Asghar, M., Iqbal, N., and Shah, T. M. (1992). Variability in salt tolerance of accessions of wild rice species *Oryza punctata* and *O. officinalis*. *Int. Rice Res. Inst. News Lett.* 17:16.

Flowers, T. J. (2004). Improving crop salt tolerance. *J. Exp. Bot.* 55, 307–319. doi: 10.1093/jxb/erh003

Flowers, T. J., and Colmer, T. D. (2008). Salinity tolerance in halophytes. *New Phytol.* 179, 945–963. doi: 10.1111/j.1469-8137.2008.02531.x

Flowers, T. J., Flowers, S. A., Hajibagheri, M. A., and Yeo, A. R. (1990). Salt tolerance in the halophytic wild rice, *Porteresia coarctata* T. *New Phytol.* 114, 675–684. doi: 10.1111/j.1469-8137.1990.tb00439.x

Fujimaki, S., Maruyama, T., Suzui, N., Kawachi, N., Miwa, E., and Higuchi, K. (2015). Base to tip and long-distance transport of sodium in the root of common reed (*Phragmites australis* Cav.) Trin. ex Steud.] at steady state under constant high-salt conditions. *Plant Cell Physiol.* 56, 943–950. doi: 10.1093/pcp/pcv021

Golldack, D., Su, H., Quigley, F., Kamasani, U. R., Muñoz-Garay, C., Balderas, E., et al. (2002). Characterization of a HKT-type transporter in rice as a general alkali cation transporter. *Plant J.* 31, 529–542. doi: 10.1046/j.1365-313X.2002.01374.x

Gregorio, G. B., Senadhira, D., and Mendoza, R. D. (1997). *Screening Rice for Salinity Tolerance*. Laguna: International Rice Research Institute.

Hodges, D. M., DeLong, J. M., Forney, C. F., and Prange, R. K. (1999). Improving the thiobarbituric acid-reactive substances assay for estimating lipid peroxidation in plant tissues containing anthocyanin and other interfering compounds. *Planta* 207, 604–611. doi: 10.1007/s004250050524

Horie, T., Costa, A., Kim, T. H., Han, M. J., Horie, R., Leung, H. Y., et al. (2007). Rice OsHKT2; 1 transporter mediates large Na+ influx component into K+-starved roots for growth. *EMBO J.* 26, 3003–3014. doi: 10.1038/sj.emboj.7601732

Horie, T., Karahara, I., and Katsuhara, M. (2012). Salinity tolerance mechanisms in glycophytes: an overview with the central focus on rice plants. *Rice* 5:11. doi: 10.1186/1939-8433-5-11

Horie, T., Motoda, J., Kubo, M., Yang, H., Yoda, K., Horie, R., et al. (2005). Enhanced salt tolerance mediated by AtHKT1 transporter-induced Na+ unloading from xylem vessels to xylem parenchyma cells. *Plant J.* 44, 928–938. doi: 10.1111/j.1365-313X.2005.02595.x

Jena, K. K. (1994). Production of intergenic hybrid between rice and *Porteresia coarctata* T. *Curr. Sci.* 67, 744–746.

Jena, K. K. (2010). The species of the genus *Oryza* and transfer of useful gene from wild species in to cultivated rice, *O. sativa*. *Breed. Sci.* 60, 518–523. doi: 10.1270/jsbbs.60.518

Katschnig, D., Bliek, T., Rozema, J., and Schat, H. (2015). Constitutive high-level *SOS1* expression and absence of HKT1; 1 expression in the salt-accumulating halophyte Salicornia dolichostachya. *Plant Sci.* 234, 144–154. doi: 10.1016/j.plantsci.2015.02.011

Kronzucker, H. J., Coskun, D., Schulze, L. M., Wong, J. R., and Britto, D. T. (2013). Sodium as nutrient and toxicant. *Plant Soil* 369, 1–23. doi: 10.1007/s11104-013-1801-2

Laurie, S., Feeney, K. A., Maathuis, F. J., Heard, P. J., Brown, S. J., and Leigh, R. A. (2002). A role for HKT1 in sodium uptake by wheat roots. *Plant J.* 32, 139–149. doi: 10.1046/j.1365-313X.2002.01410.x

Lichtenthaler, H. K., and Buschmann, C. (2001). "Chlorophylls and carotenoids: measurement and characterization by UV-VIS spectroscopy," in *Current Protocols in Food Analytical Chemistry*, eds R. E. Wrolstad, T. E. Acree, H. An, E. A. Decker, M. H. Penner, D. S. Reid, et al. (New York, NY: John Wiley & Sons, Inc), 1–4.

Lin, H. X., Zhu, M. Z., Yano, M., Gao, J. P., Liang, Z. W., Su, W. A., et al. (2004). QTLs for Na+ and K+ uptake of the shoots and roots controlling rice salt tolerance. *Theor. Appl. Genet.* 108, 253–260. doi: 10.1007/s00122-003-1421-y

Linh, L. H., Linh, T. H., Xuan, T. D., Ham, L. H., Ismail, A. M., and Khanh, T. D. (2012). Molecular breeding to improve salt tolerance of rice (*Oryza sativa* L.) in the Red River Delta of Vietnam. *Int. J. Plant Genom.* 2012:949038. doi: 10.1155/2012/949038

Maathuis, F. J. M., Ahmad, I., and Patishtan, J. (2014). Regulation of Na+ fluxes in plants. *Front. Plant Sci.* 5:467. doi: 10.3389/fpls.2014.00467

Marathi, B., Ramos, J., Hechanova, S. L., Oane, R. H., and Jena, K. K. (2014). SNP genotyping and characterization of pistil traits revealing a distinct phylogenetic relationship among the species of Oryza. *Euphytica* 201, 131–148. doi: 10.1007/s10681-014-1213-2

Martínez-Atienza, J., Jiang, X., Garciadeblas, B., Mendoza, I., Zhu, J. K., Pardo, J. M., et al. (2007). Conservation of the salt overly sensitive pathway in rice. *Plant Physiol.* 143, 1001–1012. doi: 10.1104/pp.106.092635

Menguer, P. K., Sperotto, R. A., and Ricachenevsky, F. K. (2017). A walk on the wild side: *Oryza* species as source for rice abiotic stress tolerance. *Genet. Mol. Biol.* 40(1 Suppl. 1), 238–252. doi: 10.1590/1678-4685-GMB-2016-0093

Mishra, S., Sing, B., Panda, K., Sing, B. P., Singh, N., Mishra, P., et al. (2016). Association of SNP haplotypes of HKT family genes with salt tolerance in Indian wild rice germplasm. *Rice* 9:15. doi: 10.1186/s12284-016-0083-8

Munns, R., and Gilliham, M. (2015). Salinity tolerance of crops – what is the cost? *New Phytol.* 208, 668–673. doi: 10.1111/nph.13519

Munns, R., James, R. A., Gilliham, M., Flowers, T. J., and Colmer, T. D. (2016). Tissue tolerance: an essential but elusive trait for salt-tolerant crops. *Funct. Plant Biol.* 43, 1103–1113. doi: 10.1071/FP16187

Munns, R., and Tester, M. (2008). Mechanisms of salinity tolerance. *Annu. Rev. Plant Biol.* 59, 651–681. doi: 10.1146/annurev.arplant.59.032607.092911

Negrão, S., Courtois, B., Ahmadi, N., Abreu, I., Saibo, N., and Oliveira, M. M. (2011). Recent updates on salinity stress in rice: from physiological to molecular responses. *Crit. Rev. Plant Sci.* 30, 329–377. doi: 10.1080/07352689.2011.587725

Nieves-Cordones, M., Alemán, F., Martínez, V., and Rubio, F. (2010). The *Arabidopsis thaliana* HAK5 K+ transporter is required for plant growth and K+ acquisition from low K+ solutions under saline conditions. *Mol. Plant* 3, 326–333. doi: 10.1093/mp/ssp102

Olías, R., Eljakaoui, Z., Li, J., De Morales, P. A., Marín-Manzano, M. C., Pardo, J. M., et al. (2009). The plasma membrane Na+/H+ antiporter SOS1 is essential for salt tolerance in tomato and affects the partitioning of Na+ between plant organs. *Plant Cell Environ.* 32, 904–916. doi: 10.1111/j.1365-3040.2009.01971.x

Palmgren, M. G., Edenbrandt, A. K., Vedel, S. E., Andersen, M. M., Landes, X., Østerberg, J. T., et al. (2014). Are we ready for back-to-nature crop breeding? *Trends Plant Sci.* 20, 155–164. doi: 10.1016/j.tplants.2014.11.003

Platten, J. D., Egdane, J. A., and Ismail, A. M. (2013). Salinity tolerance, Na+ exclusion and allele mining of *HKT1;5* in *Oryza sativa* and *O. glaberrima*: many sources, many genes, one mechanism? *BMC Plant Biol.* 13:32. doi: 10.1186/1471-2229-13-32

Qadir, M., Quillérou, E., Nangia, V., Murtaza, G., Singh, M., Thomas, R. J., et al. (2014). Economics of salt-induced land degradation and restoration. *Nat. Resour. Forum* 38, 282–295. doi: 10.1111/1477-8947.12054

Reddy, A. M., Francies, R. M., Rasool, S. N., and Reddy, V. R. P. (2014). Breeding for tolerance stress triggered by salinity in rice. *Int. J. Appl. Biol. Pharm. Technol.* 5, 167–176.

Ren, Z. H., Gao, J. P., Li, L. G., Cai, X. L., Huang, W., Chao, D. Y., et al. (2005). A rice quantitative trait locus for salt tolerance encodes a sodium transporter. *Nat. Genet.* 37, 1141–1146. doi: 10.1038/ng1643

Rengasamy, P. (2010). Soil processes affecting crop production in salt-affected soils. *Aust. J. Soil Res.* 37, 613–620. doi: 10.1071/FP09249

Richards, R. A. (1992). Increasing salinity tolerance of grain crops: is it worthwhile? *Plant and Soil.* 146, 89–98. doi: 10.1007/BF00012000

Roy, S. J., Negrao, S., and Tester, M. (2014). Salt resistant crop plants. *Curr. Opin. Biotechnol.* 26, 115–124. doi: 10.1016/j.copbio.2013.12.004

Sanchez, P. L., Wing, R. A., and Brar, D. S. (2013). "The wild relative of rice: genomes and genomics," in *Genetics and Genomics of Rice, Plant Genetics and Genomics: Crops and Models* 5, eds Q. Zhang and R. A. Wing (New York, NY: Springer Science), 9–25. doi: 10.1007/978-1-4614-7903-1_2

Sengupta, S., and Majumder, A. L. (2010). Porteresia coarctata (Roxb.) Tateoka, a wild rice: a potential model for studying salt-stress biology in rice. *Plant Cell Environ.* 33, 526–542. doi: 10.1111/j.1365-3040.2009.02054.x

Shabala, S., and Mackay, A. (2011). Ion transport in halophytes. *Adv. Bot. Res.* 57, 151–187. doi: 10.1016/B978-0-12-387692-8.00005-9

Shabala, S., and Pottosin, I. (2014). Regulation of potassium transport in plants under hostile conditions: implications for abiotic and biotic stress tolerance. *Physiol. Plant.* 151, 257–279. doi: 10.1111/ppl.12165

Shahbaz, M., and Ashraf, M. (2013). Improving salinity tolerance in cereals. *Crit. Rev. Plant Sci.* 32, 237–249. doi: 10.1080/07352689.2013.758544

Shi, H., Ishitani, M., Kim, C., and Zhu, J.-K. (2000). The *Arabidopsis thaliana* salt tolerance gene SOS1 encodes a putative Na+/H+ antiporter. *Proc. Natl. Acad. Sci. U.S.A.* 97, 6896–6901. doi: 10.1073/pnas.120170197

Suzuki, K., Costa, A., Nakayama, H., Katsuhara, M., Shinmyo, A., and Horie, T. (2016). OsHKT2; 2/1-mediated Na+ influx over K+ uptake in roots potentially increases toxic Na+accumulation in a salt-tolerant landrace of rice Nona Bokra upon salinity stress. *J. Plant Res.* 129, 67–77. doi: 10.1007/s10265-015-0764-1

Thomson, M. J., de Ocampo, M., Egdane, J., Rahman, M. A., Sajise, A. G., Adorada, D. L., et al. (2010). Characterizing the Saltol quantitative trait locus for salinity tolerance in rice. *Rice* 3, 148–160. doi: 10.1007/s12284-010-9053-8

Tian, L., Tan, L., Liu, F., Cai, H., and Sun, C. (2011). Identification of quantitative trait loci associated with salt tolerance at seedling stage from *Oryza rufipogon*. *J. Genet. Genomics* 38, 593–601. doi: 10.1016/j.jgg.2011.11.005

Wang, H., Zhang, M., Guo, R., Shi, D., Liu, B., Lin, X., et al. (2012). Effects of salt stress on ion balance and nitrogen metabolism of old and young leaves in rice (*Oryza sativa* L.). *BMC Plant Biol.* 12:194. doi: 10.1186/1471-2229-12-194

Wang, W., Vinocur, B., and Altman, A. (2003). Plant responses to drought, salinity and extreme temperatures: towards genetic engineering for stress tolerance. *Planta* 218, 1–14. doi: 10.1007/s00425-003-1105-5

Waziri, A., Kumar, P., and Purty, R. S. (2016). Saltol QTL and their role in salinity tolerance in rice. *Austin J. Biotechnol. Bioeng.* 3, 1067–1072.

Yadav, N. S., Shukla, P. S., Jha, A., Agarwal, P. K., and Jha, B. (2012). The SbSOS1 gene from the extreme halophyte *Salicornia brachiata* enhances Na+ loading in xylem and confers salt tolerance in transgenic tobacco. *BMC Plant Biol.* 12:188. doi: 10.1186/1471-2229-12-188

Yamaguchi, T., and Blumwald, E. (2005). Developing salt-tolerant crop plants: challenges and opportunities. *Trends Plant Sci.* 10, 615–620. doi: 10.1016/j.tplants.2005.10.002

Yamaguchi, T., Hamamoto, S., and Uozumi, N. (2013). Sodium transport system in plant cells. *Front. Plant Sci.* 4:410. doi: 10.3389/fpls.2013.00410

Yeo, A. R., and Flowers, T. J. (1986). Salinity resistance in rice (*Oryza sativa* L.) and a pyramiding approach to breeding varieties for saline soils. *Funct. Plant Biol.* 13, 161–173. doi: 10.1071/PP9860161

Yeo, A. R., Yeo, M. E., Flowers, S. A., and Flowers, T. J. (1990). Screening of rice (*Oryza sativa* L.) genotypes for physiological characters contributing to salinity resistance, and their relationship to overall performance. *Theor. Appl. Genet.* 79, 377–384. doi: 10.1007/BF01186082

Yoshida, S., Forno, D. A., Cock, J. H., and Gomez, K. A. (1976). *Laboratory Manual for Physiological Studies of Rice*. Laguna: International Rice Research Institute, 83.

Zhang, H. H., Hodson, J. N., Williams, J. P., and Blumwald, E. (2001). Engineering salt-tolerant *Brassica* plants: characterization of yield and seed oil quality in transgenic plants with increased vacuolar sodium accumulation. *Proc. Natl. Acad. Sci. U.S.A.* 98, 12832–12836. doi: 10.1073/pnas.231476498

Zhang, W.-D., Wang, P., Bao, Z., Ma, Q., Duan, L.-J., Bao, A.-K., et al. (2017). SOS1, HKT1;5, and *NHX1* synergistically modulate Na+ homeostasis in the halophytic grass *Puccinellia tenuiflora*. *Front. Plant Sci.* 8:576. doi: 10.3389/fpls.2017.00576

Zhou, Y., Yang, P., Cui, F., Zhang, F., Luo, X., and Xie, J. (2016). Transcriptome analysis of salt stress responsiveness in the seedlings of Dongxiang wild rice (*Oryza rufipogon* Griff.). *PLoS One* 11:e0146242. doi: 10.1371/journal.pone.0146242

Zhu, Q., Zheng, X., Luo, J., Gaut, B. S., and Ge, S. (2007). Multilocus analysis of nucleotide variation of *Oryza sativa* and its wild relatives: Severe bottleneck during domestication of rice. *Mol. Biol. Evol.* 24, 875–888. doi: 10.1093/molbev/msm005

Conflict of Interest Statement: The authors declare that the research was conducted in the absence of any commercial or financial relationships that could be construed as a potential conflict of interest.

frontiers in Plant Science

ORIGINAL RESEARCH
published: 02 March 2018
doi: 10.3389/fpls.2018.00269

Expression Patterns and Identified Protein-Protein Interactions Suggest That Cassava CBL-CIPK Signal Networks Function in Responses to Abiotic Stresses

Chunyan Mo†, Shumin Wan†, Youquan Xia†, Ning Ren, Yang Zhou and Xingyu Jiang**

Hainan Key Laboratory for Sustainable Utilization of Tropical Bioresources, Institute of Tropical Agriculture and Forestry, Hainan University, Haikou, China

Cassava is an energy crop that is tolerant of multiple abiotic stresses. It has been reported that the interaction between Calcineurin B-like (CBL) protein and CBL-interacting protein kinase (CIPK) is implicated in plant development and responses to various stresses. However, little is known about their functions in cassava. Herein, 8 *CBL* (*MeCBL*) and 26 *CIPK* (*MeCIPK*) genes were isolated from cassava by genome searching and cloning of cDNA sequences of *Arabidopsis CBL*s and *CIPK*s. Reverse-transcriptase polymerase chain reaction (RT-PCR) analysis showed that the expression levels of *MeCBL* and *MeCIPK* genes were different in different tissues throughout the life cycle. The expression patterns of 7 *CBL* and 26 *CIPK* genes in response to NaCl, PEG, heat and cold stresses were analyzed by quantitative real-time PCR (qRT-PCR), and it was found that the expression of each was induced by multiple stimuli. Furthermore, we found that many pairs of CBLs and CIPKs could interact with each other via investigating the interactions between 8 CBL and 25 CIPK proteins using a yeast two-hybrid system. Yeast cells co-transformed with cassava *MeCIPK24*, *MeCBL10*, and Na^+/H^+ antiporter *MeSOS1* genes exhibited higher salt tolerance compared to those with one or two genes. These results suggest that the cassava CBL-CIPK signal network might play key roles in response to abiotic stresses.

Keywords: calcineurin B-like protein, CBL-interacting protein kinase, abiotic stress, signal pathway, cassava

OPEN ACCESS

Edited by:
Nicholas Provart, University of Toronto, Canada

Reviewed by:
Fouad Lemtiri-Chlieh, King Abdullah University of Science and Technology, Saudi Arabia
David M. Rhoads, California State University, San Bernardino, United States

***Correspondence:**
Yang Zhou
zhoy2013@163.com
Xingyu Jiang
jiangxingyuhu@163.com

†These authors have contributed equally to this work.

Specialty section:
This article was submitted to Plant Abiotic Stress, a section of the journal Frontiers in Plant Science

Received: *07 November 2017*
Accepted: *14 February 2018*
Published: *02 March 2018*

Citation:
Mo C, Wan S, Xia Y, Ren N, Zhou Y and Jiang X (2018) Expression Patterns and Identified Protein-Protein Interactions Suggest That Cassava CBL-CIPK Signal Networks Function in Responses to Abiotic Stresses. Front. Plant Sci. 9:269. doi: 10.3389/fpls.2018.00269

INTRODUCTION

Calcium is used by most cells to convert external signals into cytosolic information, which can drive processes that are required for full responses to a particular stimulus (Zhai et al., 2013). Therefore, calcium ions play a crucial role as second messengers in mediating various adaptive responses in plants under environmental stresses. Elevation of the cytosolic calcium concentration is a primary event in the responses to many environmental stresses, such as high salinity, drought and cold (Ma et al., 2010). Transient Ca^{2+} change may be sensed by several Ca^{2+}-binding proteins including calmodulin (CaM), Ca^{2+}-dependent protein kinases (CDPKs) and calcineurin B-like proteins (CBL) (Luan et al., 2002). Such calcium-binding proteins likely function as sensors that recognize changes in calcium parameters and relay these signals into downstream responses, such as phosphorylation cascades and regulation of gene expression (Sanders et al., 2002; Luan et al., 2009).

CBL proteins are important components of three major classes of Ca^{2+} sensors that have been characterized in plants. These proteins are most similar to both the regulatory B subunit of calcineurin (CNB) and neuronal calcium sensors (NCS) in animals. CBL proteins contain an important structural component consisting of four EF-hand domains as calcium-binding sites to capture Ca^{2+} ions (Nagae et al., 2003; Sanchez-Barrena et al., 2005) but do not have enzymatic activity. However, upon Ca^{2+} binding, these proteins interact with their respective target proteins and modulate their activity. The target proteins interacting with CBLs are a family of protein kinases referred to as CBL-interaction protein kinases (CIPKs), which are most similar to the sucrose nonfermenting (SNF) protein kinase from yeast and AMP-dependent kinase (AMPK) from animals in the kinase domain (Batistic and Kudla, 2009; Luan, 2009). Plant SNF1 related kinase (SnRK) have been grouped into three subfamilies: SnRK1, SnRK2, and SnRK3 (Hrabak et al., 1996). SnRK1 plays a role in regulation of carbon and nitrogen metabolism, and SnRK2 and SnRK3 have roles in stress signaling (Shukla and Mattoo, 2008). The CIPK protein, also known as SnRK3, had a conserved NAF/FISL motif in the C-terminal regulatory domain which is required and sufficient for interacting with CBL-type calcium sensors (Albrecht et al., 2001; Guo et al., 2001). Bioinformatics analyses of *Arabidopsis* genome sequences showed a complex signaling network comprised 10 CBLs and 26 CIPKs (Drerup et al., 2013). The first CBL-CIPK pathway was identified during screening for the salt overly sensitive (SOS) phenotype in *Arabidopsis*. In this pathway, a protein kinase complex consisting of AtCBL4 (SOS3) and AtCIPK24 (SOS2) was activated by a salt-stress elicited calcium signal, and then the AtCBL4-AtCIPK24 complex regulated Na^+/H^+ exchange activity of SOS1 via phosphorylating a serine residue at its C-terminus in *Arabidopsis* plants under salinity stress (Zhu, 2003; Quintero et al., 2011). AtCBL1 regulated positively the response to salt and drought stresses (Albrecht et al., 2003). In contrast, AtCBL9-AtCIPK3 complex negatively regulated the ABA response during seed germination (Pandey et al., 2008). AtCBL2 interacts with AtCIPK11 and negatively regulates a plasmalemma H^+-ATPase AHA2 (Fuglsang et al., 2007). AtCBL10 interacts with SOS2 and recruits SOS2 to the plasma membrane to activate a plasma membrane Na^+/H^+ antiporter (SOS1) in *Arabidopsis* shoots, which is similar to the function of SOS3 in roots (Quan et al., 2007). Ren et al. reported that AtCBL10 could regulate K^+ homeostasis by directly interacting with AKT1 in *Arabidopsis* (Ren et al., 2013). AtCBL1/CIPK23 or AtCBL9/CIPK23 complexes could activate the K^+ channel AKT1 in the plasma membrane and increased *Arabidopsis* ability to uptake K^+ under low K^+ conditions (Xu et al., 2006). AtCBL3 interacts with AtCIPK9 to regulate K^+ homeostasis (Liu et al., 2013). AtCIPK24 regulates vacuolar Na^+/H^+ and Ca^{2+}/H^+ exchange activities in *Arabidopsis thaliana* to promote salt tolerance (Cheng et al., 2004; Qiu et al., 2004). AtCBL1-AtCIPK7 kinase complex had an important role in the plant cold tolerance (Huang et al., 2011). The over-expression of AtCBL5 conferred salt and osmotic tolerances to transgenic *Arabidopsis* plants (Cheong et al., 2010). A multivalent interacting network comprised of CBL2/3 and CIPK/26 complexes could protect plants from Mg^{2+} toxicity by sequestrating magnesium (Mg^{2+}) into the vacuolar (Tang et al., 2015). AtCIPK8 might regulate nitrate transport activity of AtNRT1.1 at the low-affinity phase (Hu et al., 2009). Therefore, CBL-CIPK calcium signal pathways play vital roles in plant responses to abiotic stresses. Recently, CBL and CIPK families have been identified in other species, including a total of 10 CBLs and 30 CIPKs in rice (Kolukisaoglu et al., 2004), 7 CBLs and 23 CIPKs in canola (Zhang et al., 2014), and 7 CBLs and 29 CIPKs in wheat (Sun et al., 2015). However, except for *Arabidopsis*, the studies on the functions of CBL and CIPK proteins from other plants are still quite limited.

Cassava (*Manihot esculenta*) is one of the most important crop plants. As a food security crop, it provides nourishment for 800 million people around the tropical and sub-tropical world (Oliveira et al., 2014). Cassava is tolerant to environmental stresses such as drought and heat (Zeng et al., 2014). However, the reports about cassava response to abiotic stresses are rare. Therefore, to understand the mechanisms of cassava responses to abiotic stresses, we cloned the *CBL* (*MeCBL*) and *CIPK* (*MeCIPK*) family genes from cassava and analyzed their expression patterns under different abiotic stresses. Furthermore, we systematically studied the interactions between MeCBLs and MeCIPKs. Through this work, we are attempting to establish the CBL-CIPK network in cassava responses to abiotic stress.

MATERIALS AND METHODS

Identification of *CBL* and *CIPK* Family Genes in Cassava

The protein sequences of 10 CBLs and 26 CIPKs from *Arabidopsis* (Kolukisaoglu et al., 2004; Drerup et al., 2013) were used as queries to search against the cassava genomic DNA database (http://www.phytozome.net/cassava) using BLASTP with *E*-value less than 1E-5. The putative cassava CBL and CIPK proteins were further compared with the CBLs and CIPKs from *Arabidopsis* and rice by constructing a phylogenetic tree using the Neighbor-Joining (NJ) method. *MeCBLs* and *MeCIPKs* were then named and classified via referring to their orthologous genes from *Arabidopsis* and rice using bootstrap replicates of the Maximum Likelihood phylogenetic tree with values higher than 70 as previously described (Yu et al., 2007).

Plant Growth and Gene Cloning

Cassava cultivar SC8 (*Manihot esculent* Crantz cv. SC8) plants were grown in the field under natural conditions. The roots, stems, young leaves, old leaves, flowers and storage roots from mature plants were collected and immediately stored at −80°C for the RNA extractions. Meanwhile, the explants were cut from the mother plants, and cultivated on the Murashige and Skoog (MS) medium to induce seedlings in a greenhouse with a 16 h/35°C day and 8 h/20°C night, and a relative humidity of 70%. Forty-day-old seedlings in MS medium were treated with 200 mM NaCl or 20% PEG (polyethylene glycol 6000) at normal temperature. For temperature treatment, the seedlings were cultured under 42° and 4°C conditions. The roots and leaves were harvested at different time intervals (0, 3 and 9 h) and stored at in −80°C immediately for the RNA extraction.

Total RNA was extracted from the *M. esculent* plants using an RNA extraction kit (Tiangen, China). Complementary DNA (cDNA) was synthesized with total RNA as template using the PrimeScript RT reagent kit (TaKaRa, Japan). The gene specific primers of *MeCBL* and *MeCIPK* genes were designed using Primer Premier 5 software. Primers used in this study are shown in **Table S1**. *MeCBLs* and *MeCIPKs* were amplified by polymerase chain reaction (PCR) from cDNA mixtures. The PCR amplification conditions were initiated at 94°C for 5 min, followed by 35 cycles of 94°C for 30 s, 50°–60°C (depends on the TM value of gene-specific primers) for 30 s, 72°C for 1 min per kilo-base pair (kb), then a final extension at 72°C for 10 min. The PCR products were then examined by electrophoresis and sequenced.

Bioinformation Analysis

The isoelectric point (pI) and molecular weight (MW) of each MeCBL and MeCIPK protein were predicted using the ExPASy tool (http://web.expasy.org/protparam/). The palmitoylation sites and myristoylation sites were predicted by CSS-Palm 3.0 (http://csspalm.biocuckoo.org/). Predictions of motifs were generated using MEME (Multiple Em for Motif Elicitation) program (http://meme-suite.org/tools/meme). Gene structures of MeCBLs and MeCIPKs were analyzed using the Gene Structure Display Server (GSDS 2.0, http://gsds.cbi.pku.edu.cn/). Sequence alignments were predicted by the DNAMAN software. The classification and naming of MeCBL and MeCIPK proteins were performed as described in the above section "Identification of *CBL* and *CIPK* Family Genes in Cassava." The *cis*-acting elements in the 2,000 bp upstream sequences of coding region of cassava *MeCBL* and *MeCIPK* genes (http://www.phytozome.net/cassava) were analyzed using the PlantCARE software (http://bioinformatics.psb.ugent.be/webtools/plantcare/html/) as previously reported (Xi et al., 2017).

Gene Expression Analysis

To analyze the tissue specificity of *MeCBL* and *MeCIPK*, the expression levels in different tissues were examined by semi-quantitative RT-PCR. The housekeeping gene *Actin* was used as an internal control. The primers are shown in **Table S1**. The PCR conditions were as follows: 95°C for 5 min; 95°C for 45 s, 56°C for 30 s, 72°C for 45 s for 28 cycles; and a final extension of 72°C for 5 min. The PCR products were examined on 2% agarose gel and photographed under UV light.

Forty-day-old seedlings were treated with different stresses as described above. Then, the roots and leaves were collected. Quantitative real-time PCR (qRT-PCR) was performed using an ABI 7900HT system (TaKaRa, Japan). The qRT-PCR amplification conditions were as follows: 95°C for 1 min, followed by 45 cycles at 95°C for 5 s and 60°C for 30 s. A dissociation curve from 60° to 95°C was generated to verify the primer specificity. The relative expression levels were calculated by the $2^{-\Delta\Delta CT}$ method. Three replicate biological experiments were conducted. Primers used in this study are shown in **Table S1**.

Yeast Two-Hybrid Assays

The MatchMaker yeast two-hybrid system (Clontech, USA) was used to examine protein interactions. Firstly, the *MeCBL* genes were inserted into the pGBKT7 vector and the *MeCIPK* genes were cloned into the pGADT7 vector. Primers used in this study are shown in **Table S1**. Then, the plasmids were transformed into the yeast strain Y2HGold according to the Yeast Protocols Handbook (Clontech). After screening on SD medium lacking leucine and tryptophan (SD-L-T, DDO), the positive clones were examined using PCR. Subsequently, the positive clones were incubated in DDO medium at 28°C for 1 day. Aliquots (10 μL) were spotted onto non-selective medium (DDO) and selective medium (lacking leucine, tryptophan, histidine and adenine, SD-L-T-H-A, QDO) supplemented with 40 μg/mL X-α-Gal and 125 ng/mL aureobasidin A and incubated for 5 days before being photographed.

Yeast Complementation Test

The coding sequence of cassava Na^+/H^+ antiporter gene *MeSOS1* was obtained from the cassava genomic DNA database (http://www.phytozome.net/cassava) using *AtSOS1* sequence as a query (Quan et al., 2007; Quintero et al., 2011), And then the *MeSOS1* gene was inserted into the yeast expression vector pYPGE15. The full length coding regions of genes *MeCIPK24* and *MeCBL10* were cloned by PCR using the primers shown in **Table S1** and then inserted into the yeast expression vector p414, respectively. The three plasmids (p414-*MeCIPK24*, p414-*MeCBL10* and pYPGE15-*MeSOS1*) were co-transformed into the yeast strain AXT3K (*ena1*:: *HIS3*:: *ena4*, *nha1*::*LEU2*, and *nhx1*::*KanMX4*) lacking the endogenous NHX1 protein, the plasma membrane Na^+ efflux transporters NHA1 and the sodium pumps ENA1-4 according to the previous report (Zhou et al., 2015). The positive clones were screened on YNB medium (0.17% yeast nitrogen base without amino acids, 0.5% ammonium sulfate, 2% glucose) and yeast complementation tests were analyzed on AP medium (0.174% arginine, 2% glucose, 8 mM H_3PO_4, 2 mM $MgSO_4$, 0.2 mM $CaCl_2$, 1 mM KCl, 1 × trace elements and 1 × vitamins) with different NaCl concentrations (Zhou et al., 2015). After incubation for 5 days at 28°C, the growth was imaged and analyzed.

Statistics Analysis

The real-time PCR data were determined with the SDS plate utility software version 2.4. Data were analyzed using Microsoft Excel and Statistical Package for the Social Sciences (Chicago, IL, USA). The means were separated using Student's *t*-test at the 5% level of significance.

RESULTS

Identification of *CBL* and *CIPK* Family Genes in Cassava

In order to identify the *CBL* and *CIPK* genes from cassava, 10 CBL and 26 CIPK protein sequences from *Arabidopsis* were used as queries to run BLAST searches using the cassava genomic DNA database (http://www.phytozome.net/cassava). As a result, 8 CBLs (MeCBL1 to MeCBL10, except for MeCBL3

and MeCBL7) and 26 CIPKs were identified and named based on the similarities to *Arabidopsis* orthologs with *Me* standing for *Manihot esculent* (**Table 1**). The detailed information, including protein length, isoelectric point (pI), molecular weight (MW), palmitoylation sites and myristoylation sites, of the identified MeCBLs and MeCIPKs is listed in **Table 1**. The MW of the predicted MeCBL proteins ranged from 24.50 to 28.74 kD and of the MeCIPK proteins ranged from 40.94 to 56.05 kD.

Furthermore, sequence alignments of the multiple amino acids between MeCBLs and AtCBLs are shown in **Figure 1**. The results indicate that the sequences of MeCBLs are highly conserved: all the MeCBLs containing four EF hand motifs, which are similar to the AtCBLs EF-hand motifs. The MeCBL proteins also have conserved linkers between each EF motif. There are 22 amino acids between EF1 and EF2 domains, 25 amino acids between EF2 and EF3 domains, and 32 amino acids between EF3 and EF4 domains (**Figure 1**). However, there are 32 amino acids between EF2 and EF3 domains in the MeCBL5 protein (**Figure 1**). In addition, seven CBLs have palmitoylation sites, but MeCBL6 does not; five CBLs have a myristoylation site in the N-terminal domain, but MeCBL4, MeCBL6 and MeCBL10 do not (**Figure 1**, **Table 1**).

Similarly, the alignment results showed that all the MeCIPKs contain an N-terminal catalytic kinase domain and a C-terminal regulatory domain, which are jointed by a variable domain. The NAF/FISL motif is conserved in all the MeCIPKs (**Figure 2**). This motif has been reported to be necessary for mediating interactions between CIPK and CBL proteins (Albrecht et al., 2001; Guo et al., 2001). Sequence analysis also showed that a protein-phosphatase interaction (PPI) motif is conserved in the C-terminus of the kinases (**Figure 2**). In addition, eight CIPKs, including MeCIPK4, 6, 10, 11, 18, 21, 23, and 24, have palmitoylation sites. Nine CIPKs, including MeCIPK2, 13, 15, 16, 17, 18, 20, 21, and 23, have a myristoylation site in the N-terminal domain. MeCIPK1, 6 and 8 have two myristoylation sites in the N-terminal domain (**Table 1**).

Phylogenetic Analysis of Cassava CBL and CIPK Proteins

To investigate the evolutionary history between cassava CBL and CIPK proteins and other species, a Neighbor-Joining phylogenetic tree was constructed using CBL and CIPK protein sequences from cassava, *Arabidopsis* and rice. The CBL and CIPK family proteins were clustered into four (**Figure S1**) and five (**Figure S2**) groups, respectively. The results showed that MeCBL6 and MeCBL10 are clustered in group I and were identified as orthologous with AtCBL10 and OsCBL10. MeCBL2 is homologous to AtCBL2 in group II. In group III, MeCBL1 and MeCBL9 are close to AtCBL1 and AtCBL9. MeCBL4 and MeCBL5 are similar in sequence and homologous to AtCBL4, and MeCBL8 is close to AtCBL8. MeCBL4 and MeCBL5 formed in Group IV. A phylogenetic tree showed that the CIPK family contains five groups (**Figure S2**). Group A includes MeCIPK1, 3, 8, 9, 17, 21, 22, 23, 24, and 26. Group B contains MeCIPK4, 6, 7 and 18. Group C contains MeCIPK2, 5, 10, 13, 15, 16, 20, and 25. Group D contains MeCIPK11 and MeCIPK14. Group E contains MeCIPK12 and MeCIPK19.

In addition, closely-related orthologous pairs of CBLs and CIPKs were identified between cassava and *Arabidopsis*, with bootstrap values higher than 80, such as for MeCBL8 and AtCBL8 (**Figure S1**), MeCIPK8 and AtCIPK8, MeCIPK21 and AtCIPK21, MeCIPK24, and AtCIPK24 (**Figure S2**). These results suggest that an ancestral set of *CBL* and *CIPK* genes existed prior to the divergence of cassava and *Arabidopsis*.

Gene Structure and Conserved Motifs of Cassava MeCBLs and MeCIPKs

In order to investigate the structural features of cassava CBL and CIPK genes and proteins, intron/exon organization and conserved motifs were investigated by GSDS and MEME software, respectively. As shown in **Figure 3A** and **Figure S3A**, there are twelve motifs in MeCBL proteins. All MeCBL proteins contain motif 1 to motif 4, which were annotated as the four EF-hand domains (**Figure 1**, **Figure S3A**). Motif 10 is only found in group I, including MeCBL6 and MeCBL10, and the motif 11 is only present in MeCBL4 and MeCBL5 belonging to Group IV, which suggests that these motifs play specific roles in the corresponding groups. Furthermore, the intron/exon structural analyses revealed that all the *MeCBL* genes contain seven introns, except that genes in group I have eight introns (**Figure 3B**).

Eighteen motifs were identified in MeCIPK proteins (**Figure 4A**, **Figure S3B**). Of them, motif 9 is the NAF/FISL domain and it is widely distributed in all MeCIPKs. Motif 8, which is annotated as a PPI domain for phosphatase interaction, is also widely distributed in MeCIPK proteins except for MeCIPK3, MeCIPK4 and MeCIPK7 (**Figure 4A**). Furthermore, the GSDS software predicted that the intron-rich *MeCIPK* genes cluster in group A, but the number of introns varied from nine to thirteen. Genes in the other four groups (B, C, D and E) have no introns except that *MeCIPK7* has one intron (**Figure 4B**).

Promoter Analysis of *MeCBL* and *MeCIPK* Genes

To analyze the possible regulatory mechanisms of transcription of *MeCBL* and *MeCIPK* genes, the *cis*-acting elements in 2,000 bp of the immediate upstream sequences of the coding regions of *MeCBL* and *MeCIPK* genes were searched using the PlantCARE software. Besides the common CAAT-box and TATA-box elements, sixty-nine potential *cis*-acting elements were detected and divided into four types according to their biological functions (**Table S2**). The first type is light response-related elements such as the CT1-motif, the GT1-motif, the ATC-motif, the GATT-motif and the CG-motif. The Box 4 element was detected in all the 8 *CBL* genes with the most being detected in the *MeCBL6* gene (6 of the Box 4 type), *MeCBL10* gene (5 of the Box 4 type) and *MeCBL9* gene (5 of the Box 4 type). Similarly, the Box 4 element was detected in most *CIPK* genes except for *MeCIPK8* and *MeCIPK26*, which had the most numbers in *MeCIPK12* gene (16 of the Box 4 type) and *MeCIPK20* gene (11 of the Box 4 type). The second type is hormone-responsive elements such as the ABRE element involved in the abscisic acid response,

TABLE 1 | Features of *CBL* and *CIPK* genes in cassava.

Gene name	Locus name	Arabidopsis ortholog/AGI No.	Protein length	pI	MW (kD)	Palmitoylation sites Amino acid (location)	Myristoylation sites Amino acid (location)
MeCBL1	cassava4.1_016071m.g	AtCBL1/At4g17615	213	4.62	24.56	C (3)	G (2)
MeCBL2	cassava4.1_023888m.g	AtCBL2/At5g55990	223	4.77	25.84	C (4)	G (7)
MeCBL4	cassava4.1_015878m.g	AtCBL4/At5g24270	218	5.20	25.36	C (8), C (10)	–
MeCBL5	cassava4.1_022392m.g	AtCBL5/At4g01420	225	4.60	25.94	C (8), C (10)	G (7)
MeCBL6	cassava4.1_014733m.g	AtCBL6/At4g16350	248	4.70	28.56	–	–
MeCBL8	cassava4.1_023193m.g	AtCBL8/At1g64480	214	4.78	24.51	C (7)	G (6)
MeCBL9	cassava4.1_016083m.g	AtCBL9/At5g47100	213	4.76	24.50	C (3)	G (2)
MeCBL10	cassava4.1_014701m.g	AtCBL10/At4g33000	249	4.70	28.74	C (20)	–
MeCIPK1	cassava4.1_008050m.g	AtCIPK1/At3g17510	431	7.15	48.47	–	G (4), G (9)
MeCIPK2	cassava4.1_007534m.g	AtCIPK2/At5g07070	449	8.37	51.35	–	G (5)
MeCIPK3	cassava4.1_010345m.g	AtCIPK3/At2g26980	362	5.85	40.94	–	–
MeCIPK4	cassava4.1_008191m.g	AtCIPK4/At4g14580	427	9.12	47.53	C (218)	–
MeCIPK5	cassava4.1_029811m.g	AtCIPK5/At5g10930	448	8.69	50.74	–	–
MeCIPK6	cassava4.1_031025m.g	AtCIPK6/At4g30960	438	9.19	49.43	C (236)	G (2), G (8)
MeCIPK7	cassava4.1_008412m.g	AtCIPK7/At3g23000	420	9.07	47.08	–	–
MeCIPK8	cassava4.1_007600m.g	AtCIPK8/At4g24400	446	7.63	50.53	–	G (7)
MeCIPK9	cassava4.1_007907m.g	AtCIPK9/At1g01140	437	8.94	49.29	–	–
MeCIPK10	cassava4.1_007266m.g	AtCIPK10/At5g58380	459	8.30	51.94	C (231)	–
MeCIPK11	cassava4.1_034294m.g	AtCIPK11/At2g30360	433	9.10	49.13	C (179)	–
MeCIPK12	cassava4.1_006117m.g	AtCIPK12/At4g18700	499	6.63	56.05	–	–
MeCIPK13	cassava4.1_024110m.g	AtCIPK13/At2g34180	450	9.12	50.94	–	G (5)
MeCIPK14	cassava4.1_008116m.g	AtCIPK14/At5g01820	429	7.08	48.24	–	–
MeCIPK15	cassava4.1_006767m.g	AtCIPK15/At5g01810	476	8.92	53.95	–	G (5)
MeCIPK16	cassava4.1_028375m.g	AtCIPK16/At2g25090	453	8.66	50.87	–	G (5)
MeCIPK17	cassava4.1_007161m.g	AtCIPK17/At1g48260	463	8.79	51.89	–	G (5), G (10)
MeCIPK18	cassava4.1_007849m.g	AtCIPK18/At1g29230	438	9.05	49.11	C (236)	G (8)
MeCIPK19	cassava4.1_006740m.g	AtCIPK19/At5g45810	477	8.08	53.63	–	–
MeCIPK20	cassava4.1_025576m.g	AtCIPK20/At5g45820	454	9.20	51.32	–	G (7)
MeCIPK21	cassava4.1_006970m.g	AtCIPK21/At5g57630	469	6.08	52.97	C (379), C (383)	G (2)
MeCIPK22	cassava4.1_030445m.g	AtCIPK22/At2g38490	398	9.02	44.72	–	–
MeCIPK23	cassava4.1_007136m.g	AtCIPK23/At1g30270	463	8.95	51.77	C (302)	G (5)
MeCIPK24	cassava4.1_007604m.g	AtCIPK24/At5g35410	447	8.29	50.17	C (441)	–
MeCIPK25	cassava4.1_007324m.g	AtCIPK25/At5g25110	457	8.79	51.76	–	–
MeCIPK26	cassava4.1_007827m.g	AtCIPK26/At5g21326	439	6.88	50.26	–	–

The nomenclature of MeCBL and MeCIPK followed that of Arabidopsis CBL and CIPK proteins through a comparison using MEGA 5.0 software. The protein length, isoelectric point (pI) and molecular weight (MW) of the encoded proteins were predicted by ExPASy tool (http://web.expasy.org/protparam/). The palmitoylation sites and myristoylation sites were predicted by CSS-Palm 3.0 (http://csspalm.biocuckoo.org/), G represent the glycine residue, and C represent the cysteine residue.

the CGTCA-motif involved in the MeJA-response, the ethylene-responsive element ERE and the gibberellin-responsive element GARE-motif. The *cis*-acting element CE1 type involved in ABA responsiveness was only detected in *MeCIPK6* and *MeCIPK18*. The third type is plant development-related elements such as the GCN4-motif involved in endosperm expression, the RY-element involved in seed-specific regulation, the CCGTCC-box related to meristem specific activation and HD-Zip 1, which is involved in differentiation of the palisade mesophyll cells. The Skn-1 motif, *cis*-acting regulatory element required for endosperm expression, was detected in all the 8 *CBL* genes with the most being detected in the *MeCBL2* gene (4 of the Skn-1 motif) and *MeCBL5* gene (4 of the Skn-1 motif). The MBSI element involved in flavonoid biosynthetic genes regulation was only detected in *MeCBL9* gene. The last type is abiotic stress related elements. The HSE element involved in the heat stress response was detected in *MeCBL6*, *8*, *9*, and *10*, and all *MeCIPKs* except *MeCIPK1*, *2*, *3*, *4*, *11* and *24*. The LTR element involved in low-temperature response was detected in *MeCBL5*, *8* and *9* and *MeCIPK1*, *3*, *9*, *10*. The MBS element containing the MYB binding site involved in the drought response was detected in *MeCBL1*, *4*, *5,* and *8* and all *MeCIPKs* except *MeCIPK5*, *6*, *7*, *10*, *12*, *17*, *20*, *21*, *24,* and *25*. The TC-rich repeats involved in defense and some stress responses was detected in all the *MeCBLs* and *MeCIPKs* except *MeCIPK2*, *8*, *12*, *13,* and *17* (**Table S2**).

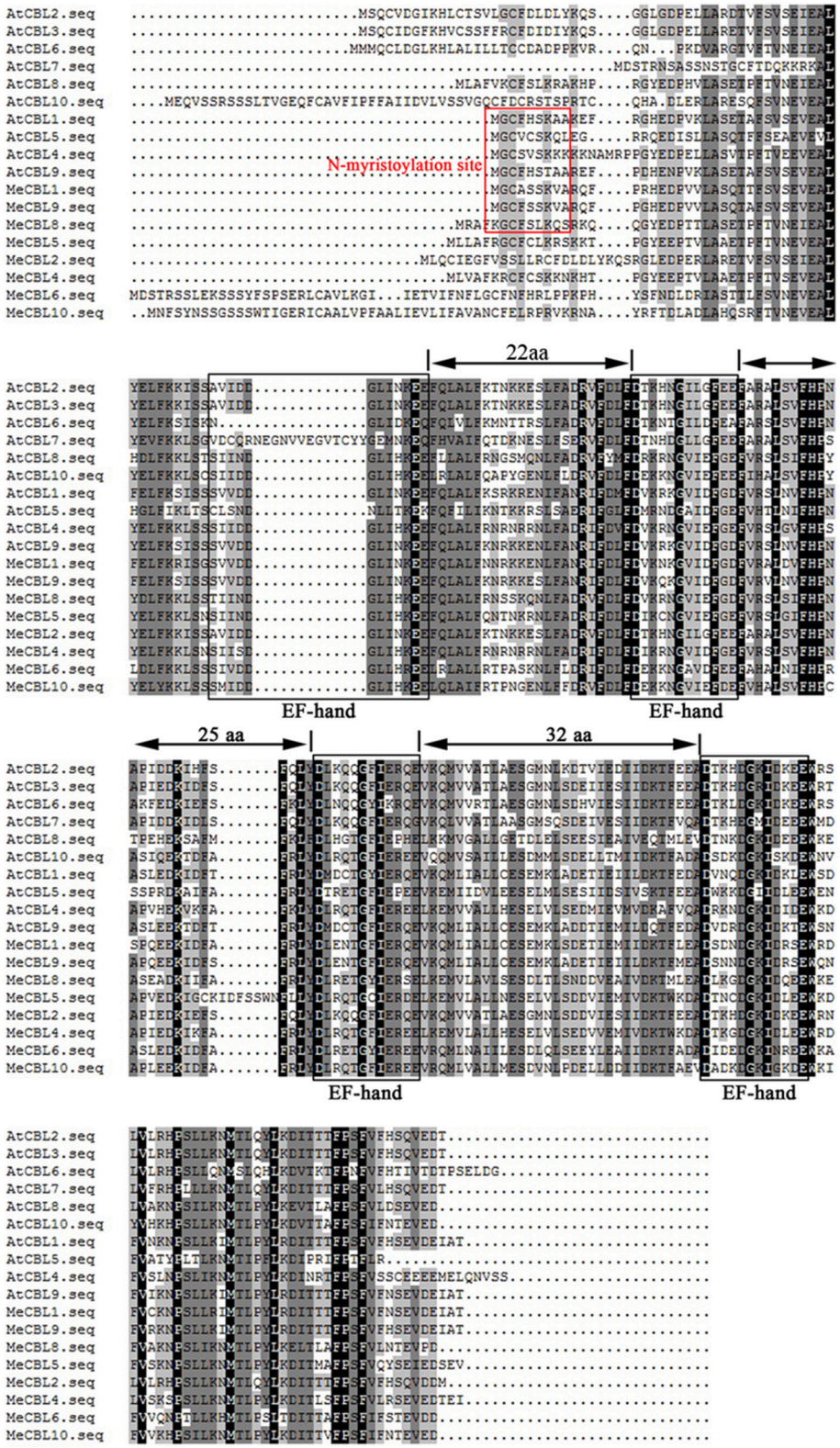

FIGURE 1 | Multiple sequence alignment between cassava and *Arabidopsis* CBL proteins. Sequence alignment was performed using DNAMAN 5.0 software. Identical amino acids are shaded in black, and similar amino acids are shaded in gray. The four EF hand motifs are indicated by black boxes. The myristoylation sites are in the red box.

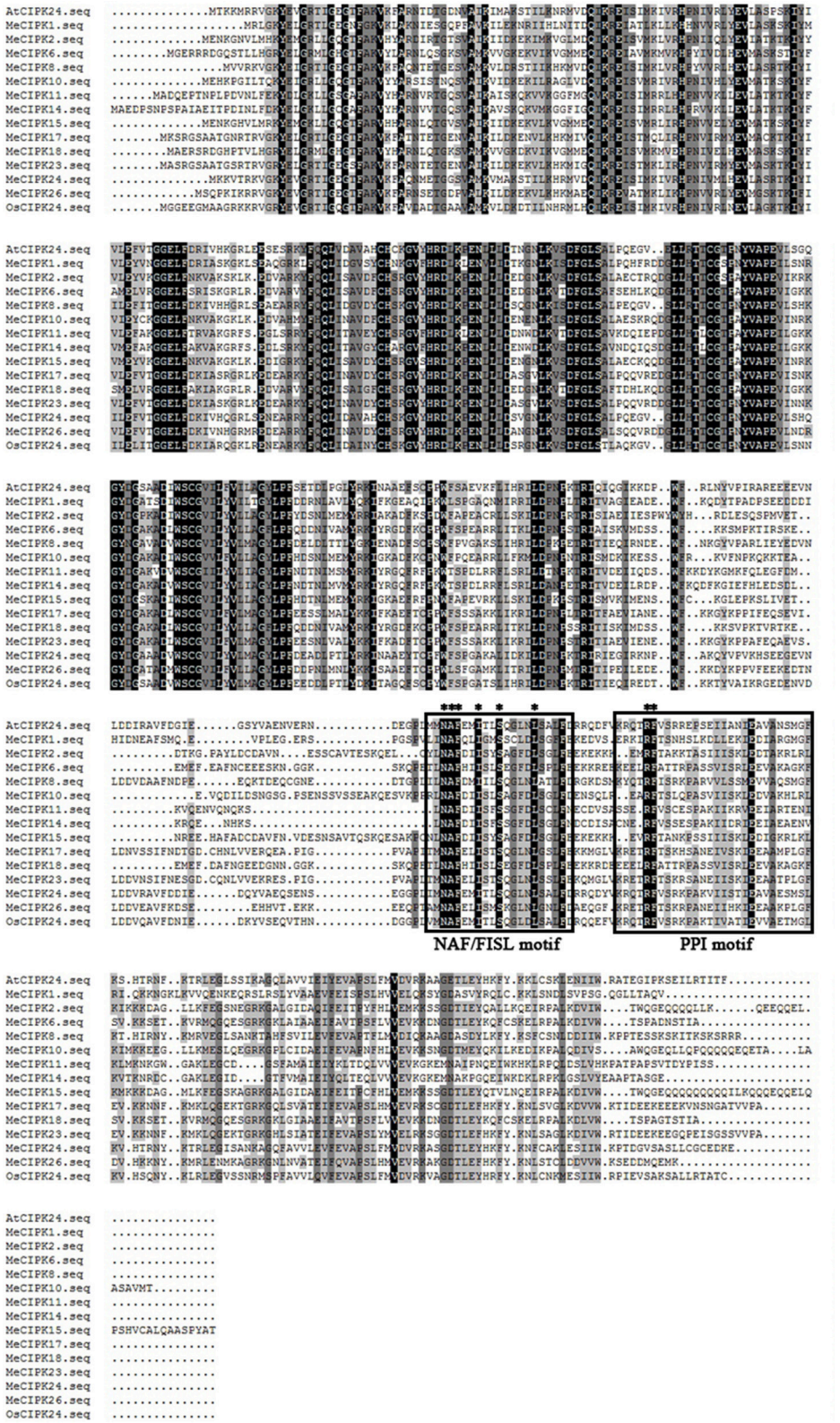

FIGURE 2 | Multiple sequence alignment between cassava and *Arabidopsis* CIPK proteins. Sequence alignment was performed using DNAMAN 5.0 software. Identical amino acids are shaded in black, and similar amino acids are shaded in gray. The NAF/FISL and PPI motifs are indicated by black boxes. The conserved amino acids in the motifs are indicated by asterisk.

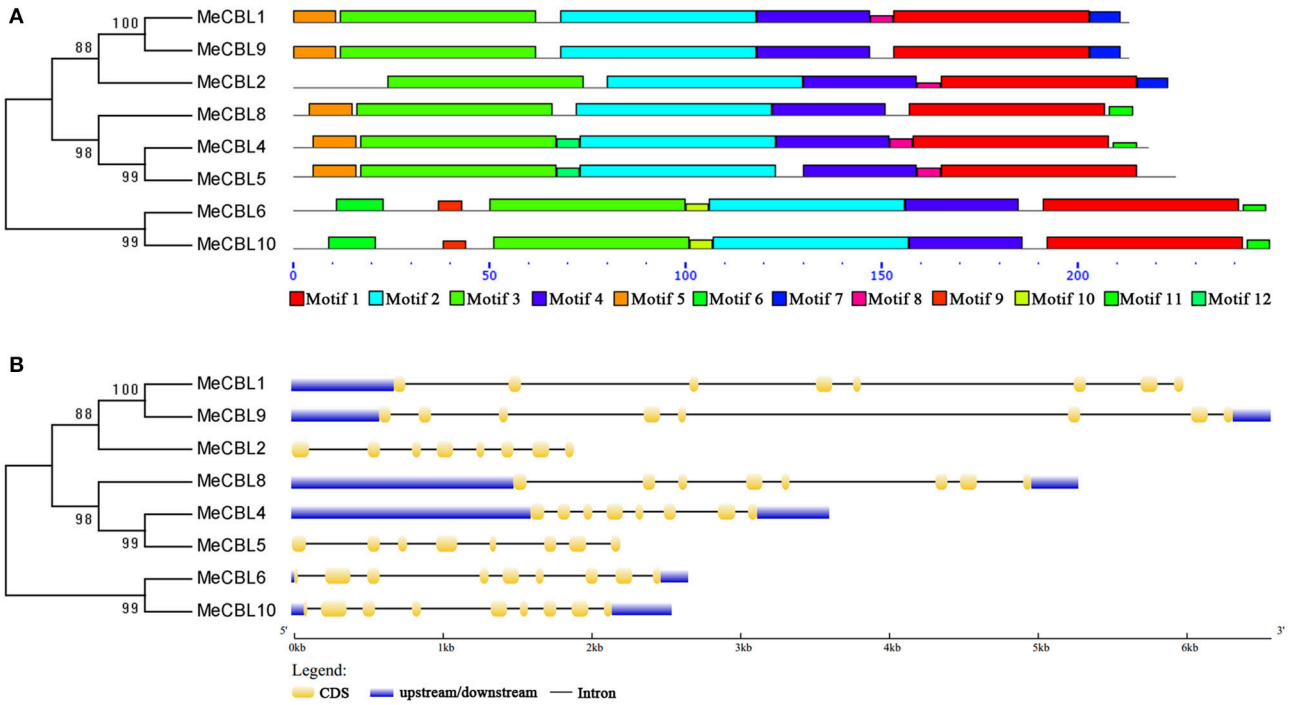

FIGURE 3 | Conserved motifs **(A)** and gene structures **(B)** of cassava CBL proteins and genes, respectively. **(A)** The conserved motifs were identified using the MEME program and are arranged according to the phylogenetic tree. Different motifs are highlighted with different color boxes. The length of boxes corresponds to motif length. **(B)** The gene structures were drawn using the GSDS program and arranged according to the phylogenetic tree. The yellow boxes represent exons, the blue boxes represent upstream and downstream UTRs and the lines represent introns.

Expression Analyses of *MeCBL* and *MeCIPK* Family Genes

To investigate the spatial expression patterns of *MeCBLs* and *MeCIPKs* in cassava, transcript levels were studied using RT-PCR in different tissues of seedlings and mature plants, including root (seedling and mature stage), stem (seedling and mature stage), leaf (seedling stage, and mature stage: young leaves and old leaves), flower and storage root (**Figure 5**). The results show that the expression levels of most of *MeCBLs* and *MeCIPKs* are different in all tissues tested. However, some genes such as *MeCBL2*, *MeCIPK5*, *6*, *9,* and *10* were constitutively expressed in all tissues and at all developmental stages. Some genes were mainly expressed in specific organs. For example, *MeCIPK16* and *MeCIPK20* were mainly expressed in flower, indicating that these genes might have specific roles in this organ. Other genes, like *MeCBL5*, *MeCIPK16*, *19,* and *20* had very low transcript levels in the tested organs. Moreover, the gene expression levels in seedlings are different from mature plants, for example, *MeCBL1*, *MeCBL9,* and *MeCIPK23* have higher transcriptional levels in the mature stage than that in the seedling stage (stems and leaves).

It has been reported that the *CBL* and *CIPK* genes play significant roles in response to abiotic stresses (Chen et al., 2011; Yu et al., 2014; Zhang et al., 2014; Sun et al., 2015; Xi et al., 2017). Therefore, forty-day-old cassava seedlings were subjected to stresses including salt (200 mM NaCl), drought (20% PEG6000), cold (4°C) and heat (42°C) treatment and the expression profiles of *MeCBL* and *MeCIPK* genes were investigated using qRT-PCR. The levels of all the MeCBLs and MeCIPKs were altered under stress treatments, and the transcript levels of 7 *MeCBLs* and 26 *MeCIPKs* in roots and leaves are shown in **Figures 6–8**. Under 200 mM NaCl treatment, *MeCBL6* and *MeCBL8* in roots were up-regulated at both 3 h and 9 h time-points. *MeCBL4* and *MeCBL5* transcript levels showed up-regulation at the 9 h time-point, but these genes were down-regulated at 3 h after salt treatment of roots (**Figure 6A**). *MeCBL10* was the only up-regulated gene in leaves upon salt stress (**Figure 6B**). In PEG-treated cassava seedlings, *MeCBL4* and *MeCBL10* were up-regulated in leaves at 9 h after treatment, but the other genes did not significantly change at any time point tested in roots (**Figure 6A**) or leaves (**Figure 6B**). In addition, *MeCBL2*, *4*, *5*, *9,* and *10* were all induced by high temperature or cold stress in roots (**Figure 6A**). *MeCBL4* and *MeCBL5* in leaves were up-regulated at both 3 and 9 h time-points when treated with high temperature stress (**Figure 6B**).

As for the *MeCIPK* genes assayed, *MeCIPK4*, *5*, *11*, *16*, *20*, *22,* and *24* in roots and *MeCIPK14* and *20* in leaves were up-regulated at the 3 h time-point by salt stress (**Figures 7**, **8**). In 9 h PEG-treated cassava roots, *MeCIPK11*, *17*, *19,* and *25* were up-regulated and expression of the *MeCIPK7*, *14*, *21*, *22,* and *24* were down-regulated (**Figure 7**). However, only *MeCIPK11* was induced in leaves after PEG treatment (**Figure 8**).

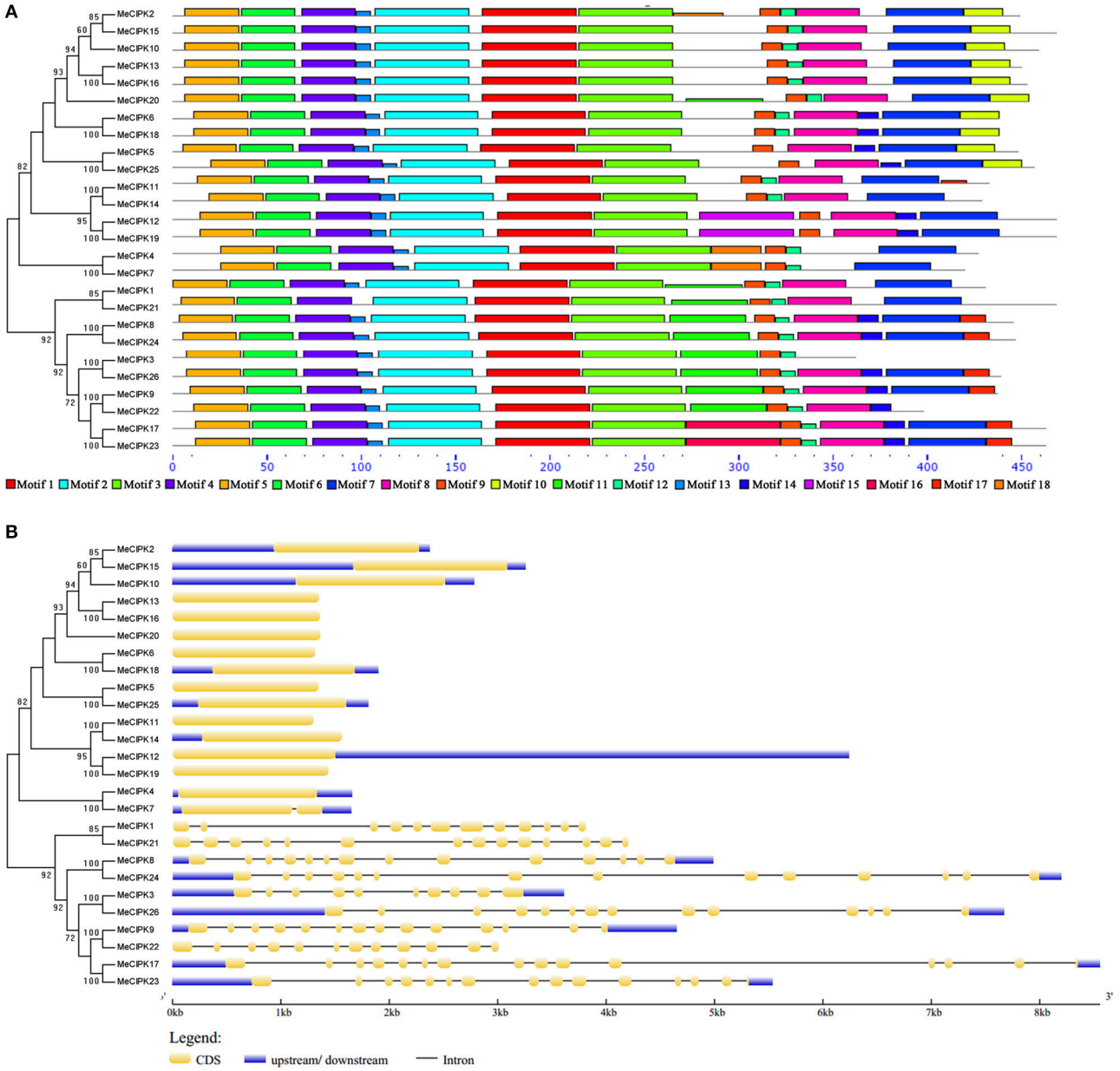

FIGURE 4 | Conserved motifs **(A)** and gene structures **(B)** of cassava CIPK genes. **(A)** The conserved motifs were using the MEME program and arranged corresponding to the phylogenetic tree. Different motifs are highlighted with different color boxes. The length of boxes corresponded to motif length. **(B)** The gene structures were drawn using the GSDS program and arranged corresponding to the phylogenetic tree. The yellow boxes represent exons, the blue boxes represent upstream and downstream UTRs and the lines represent introns.

MeCIPK7 was significantly induced in roots by cold treatment. *MeCIPK10* and *13* in roots (**Figure 7**) and *MeCIPK12* and *16* in leaves (**Figure 8**) were also affected after cold treatment. The expression of *MeCIPK19* in roots (**Figure 7**) and *MeCIPK2*, *4*, *17*, and *25* in leaves (**Figure 8**) was induced by heat treatment at both time-points. Some genes like *MeCIPK8*, *9*, *15*, *18*, and *26* were not affected significantly by NaCl, PEG, cold and heat stresses, but might be induced by other abiotic stresses. It is worth noting that *MeCIPK24*, the ortholog of *AtCIPK24* (*AtSOS2*) which regulates salt tolerance via activating Na^+/H^+ exchange activity of AtSOS1 in *Arabidopsis* (Quintero et al., 2011), was only up-regulated in roots exposed to salt stress. So the gene was chosen for further salt tolerant assays.

The expression profiles of *MeCBLs* and *MeCIPKs* in cassava exposed to various stress conditions suggests that different CBLs and CIPKs may participate in the same signaling process and play roles in abiotic stresses.

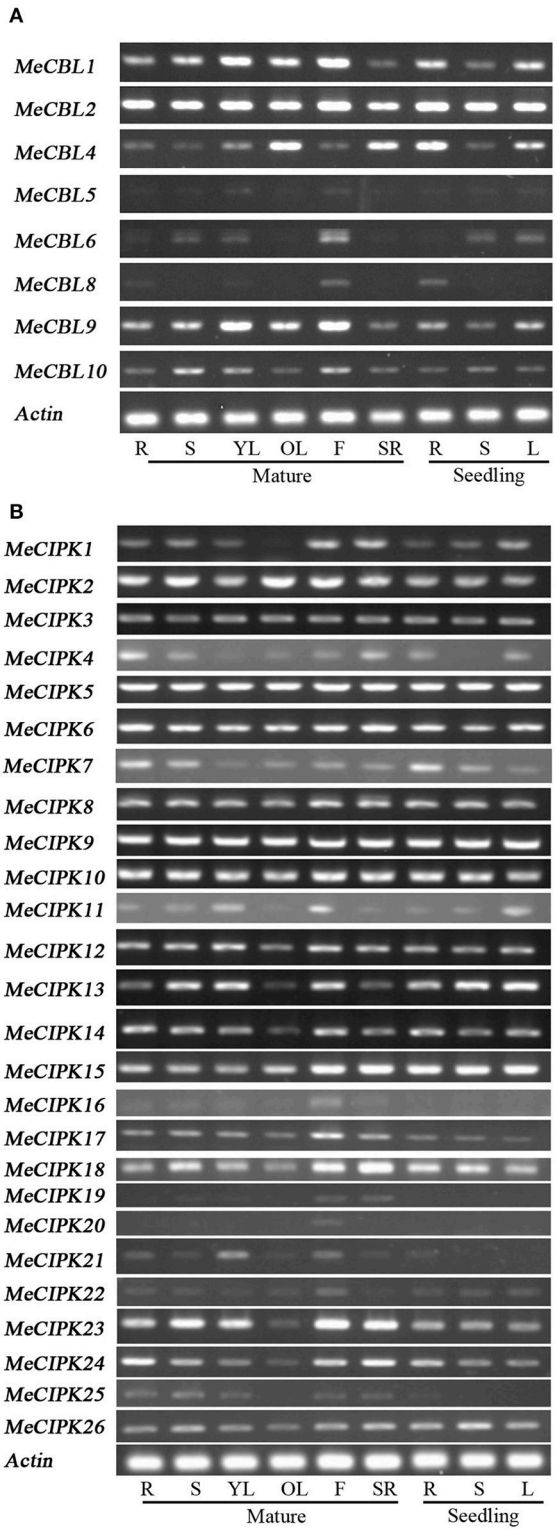

FIGURE 5 | Expression profile analyses of *MeCBL* **(A)** and *MeCIPK* **(B)** genes in cassava tissues using the RT-PCR method. "R" represents roots from mature plants or seedlings, "S" represents stems from mature plants or seedlings, "YL" and "OL" represent young leaves and old leaves of mature plants, respectively, "F" represents flowers, "SR" represents storage roots, and "L" represents the seedlings leaves.

Interaction Analyses of MeCBL and MeCIPK Proteins

Many reports have demonstrated that some CIPK proteins interact with specific CBL proteins in response to environment stresses (Xu et al., 2006; Ho et al., 2009; Tang et al., 2015; Wang et al., 2016). To investigate the interaction preferences of MeCBL and MeCIPK proteins, the yeast two-hybrid system was used. Eight *MeCBL*s and 25 *MeCIPK*s were cloned and inserted into the pGBKT7 and pGADT7 vectors, respectively, and then transformed into the yeast strain Y2HGold. The interaction relationships between MeCBL and MeCIPK proteins were detected by yeast growth on non-selective medium (DDO) and selective medium (QDO+X+). As shown in **Table 2** and **Figure S4**, MeCBL4 could interact with eight CIPKs (MeCIPK2, 7, 10, 14, 16, 18, 19, and 22), and MeCBL5 could interact with seven CIPKs (MeCIPK3, 4, 8, 10, 14, 17, and 19), the two CBL proteins have been identified as orthologs of AtCBL4 (**Figure S1**). MeCBL10, orthologous with AtCBL10 and OsCBL10 (**Figure S1**), showed strong interaction with eight CIPKs (MeCIPK1, 5, 8, 18, 19, 22, 23, and 24). In contrast, MeCIPK6 and MeCIPK11 could not interact with any of the eight MeCBL proteins in this study, suggesting that they might participate in other signaling pathways with other unidentified MeCBL proteins in cassava. MeCIPK12 only interacted with MeCBL2, MeCIPK20 only interacted with MeCBL6 and MeCIPK25 only interacted with MeCBL9, which suggests that some CIPK proteins interact only with a specific CBL protein. As for MeCIPK24, an ortholog of *Arabidopsis* AtCIPK24 (AtSOS2), it could strongly interact with MeCBL2, 6, and 10, which suggests that MeCIPK24-MeCBL2, MeCIPK24-MeCBL6, and MeCIPK24-MeCBL10 might take part in regulating salt tolerance in cassava.

Co-Expression *CBL10* and *CIPK24* Improves Salt Tolerance in Transgenic Yeast

CBL10 is a calcium sensor and CIPK24/SOS2 is a protein kinase that, together with SOS1, are the three key components comprising the salt tolerance signaling pathway identified in *Arabidopsis*. The CBL10-CIPK24 complex activates the Na^+/H^+ exchange activity of SOS1 to extrude Na^+ out of cells during salt stress (Quan et al., 2007). The SOS signaling pathway has been demonstrated to be conserved in *Arabidopsis*, rice and poplar plants, and SOS-like proteins from these three distantly related plants could form inter-species protein complexes and regulate salt tolerance of transgenic yeast cells (Martinez-Atienza et al., 2007; Tang et al., 2010). As seen from **Figure 9**, *MeCBL10* and *MeCIPK24* are orthologs of *AtCBL10* and *AtCIPK24* in *Arabidopsis* and were up-regulated by salt stress in cassava (**Figures 6**, **7**). Also, the yeast two-hybrid assay showed that MeCBL10 could interact with MeCIPK24 (**Table 2**, **Figure S4**), so theoretically the MeCBL10-MeCIPK24 complex could be involved in cassava salt tolerance by regulating the Na^+/H^+ antiport activity of SOS1. To test the hypothesis, *MeCBL10, MeCIPK24,* and *MeSOS1* were co-transformed into a yeast mutant strain AXT3K. Functional analyses indicated

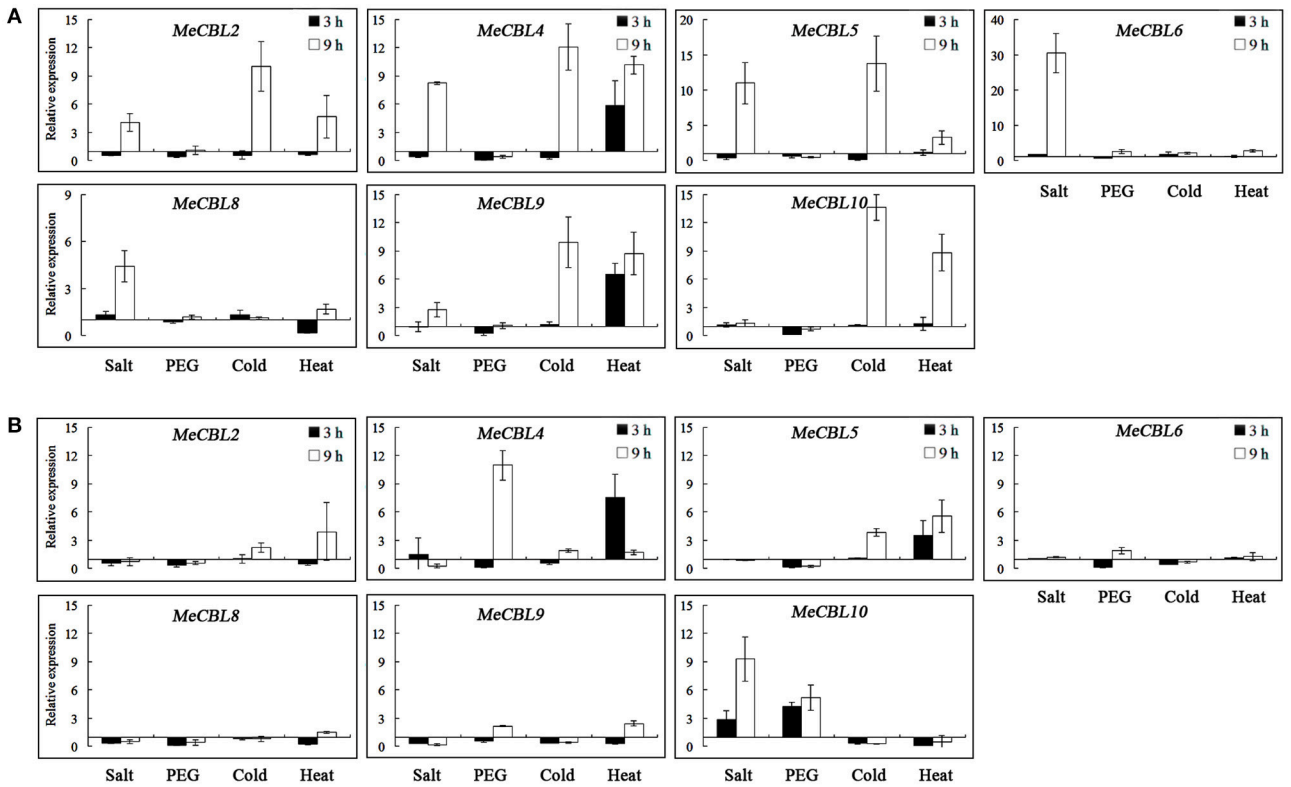

FIGURE 6 | Expression analyses of *MeCBL* genes in roots **(A)** and leaves **(B)** responding to abiotic stresses, including salt (200 mM NaCl), drought (20% PEG6000), cold (4°C) and heat (42°C) treatments. Data are the means of three biological replicates ± SE at 3 h and 9 h time points standardized at 0 h.

that the co-expression of three genes conferred stronger salt tolerance to transgenic yeast cells than *MeCIPK24-MeSOS1* co-transgenic or single *MeSOS1* transgenic cells. These results suggest that the SOS pathway, comprised of MeCBL10, MeCIPK24 and MeSOS1, is conserved, and that a MeCBL10-MeCIPK24 signal pathway regulates cassava salt tolerance together with the plasma membrane Na^+/H^+ antiporter SOS1.

DISCUSSION

Calcium participates in the signal transduction response to various environmental stimuli. As a calcium sensor, CBL protein, often work with it target kinase, CIPK protein, to regulate plant response to abiotic stresses (Kudla et al., 2010). CBL-CIPK signaling networks have been studied in many plants, such as *Arabidopsis*, canola, grapevine, poplar, rice, wheat, and other plants (Kolukisaoglu et al., 2004; Xiang et al., 2007; Zhang et al., 2008, 2014; Sun et al., 2015; Xi et al., 2017). But there are few studies in cassava at present.

Multiple alignments showed that all the CBL proteins contained four EF hand motifs, which are necessary for CBL proteins to bind Ca^{2+} (Nagae et al., 2003; Sanchez-Barrena et al., 2005). The EF-hand domains are less conserved and may contribute functional diversity, while the linkers between each EF motif are absolutely conserved in CBL proteins (Zhang et al., 2008). In this study, 8 *CBL* and 26 *CIPK* genes were identified from the cassava genome. The EF-hand motifs are organized in fixed spaces that are often 22, 25, and 32 amino acids between EF1 and EF2, EF2 and EF3, EF and EF4 domains, respectively, except for MeCBL5, in which there were 32 amino acids between EF2 and EF3 domains (**Figure 1**). However, phylogenetic analysis of MeCBL5 did indicate that it has high homology with *Arabidopsis* AtCBL4 protein (**Figure S1**).Therefore, MeCBL5 might have a specific function, but this needs to be investigated further. Furthermore, five MeCBLs, including MeCBL1, 2, 5, 8, and 9, were determined to have a myristoylation site in the N-terminus, which is a Ca^{2+}-binding domain (Du et al., 2011). The CIPK proteins have been demonstrated to contain two domains: the N-terminal kinase catalytic domain and the C-terminal regulatory domain harboring the NAF/FISL motif and PPI motif. The NAF/FISL motif is necessary for interaction between CIPK and CBL proteins (Guo et al., 2001). In the present study, all the MeCIPKs possess a NAF domain in the C-terminal region except for MeCIPK4, which seems to lack this domain. Because of homology to AtCIPK4 and OsCIPK4 (**Figure S2**), MeCIPK4 is still considered to be a valid MeCIPK. The PPI motif in AtCIPK24 (AtSOS2) is necessary for interaction with ABI2 (abscisic acid-insensitive 2), a protein phosphatase 2C (Ohta et al., 2003). In the PPI motif in AtCIPK24, the Arg-340 and Phe-341 are important

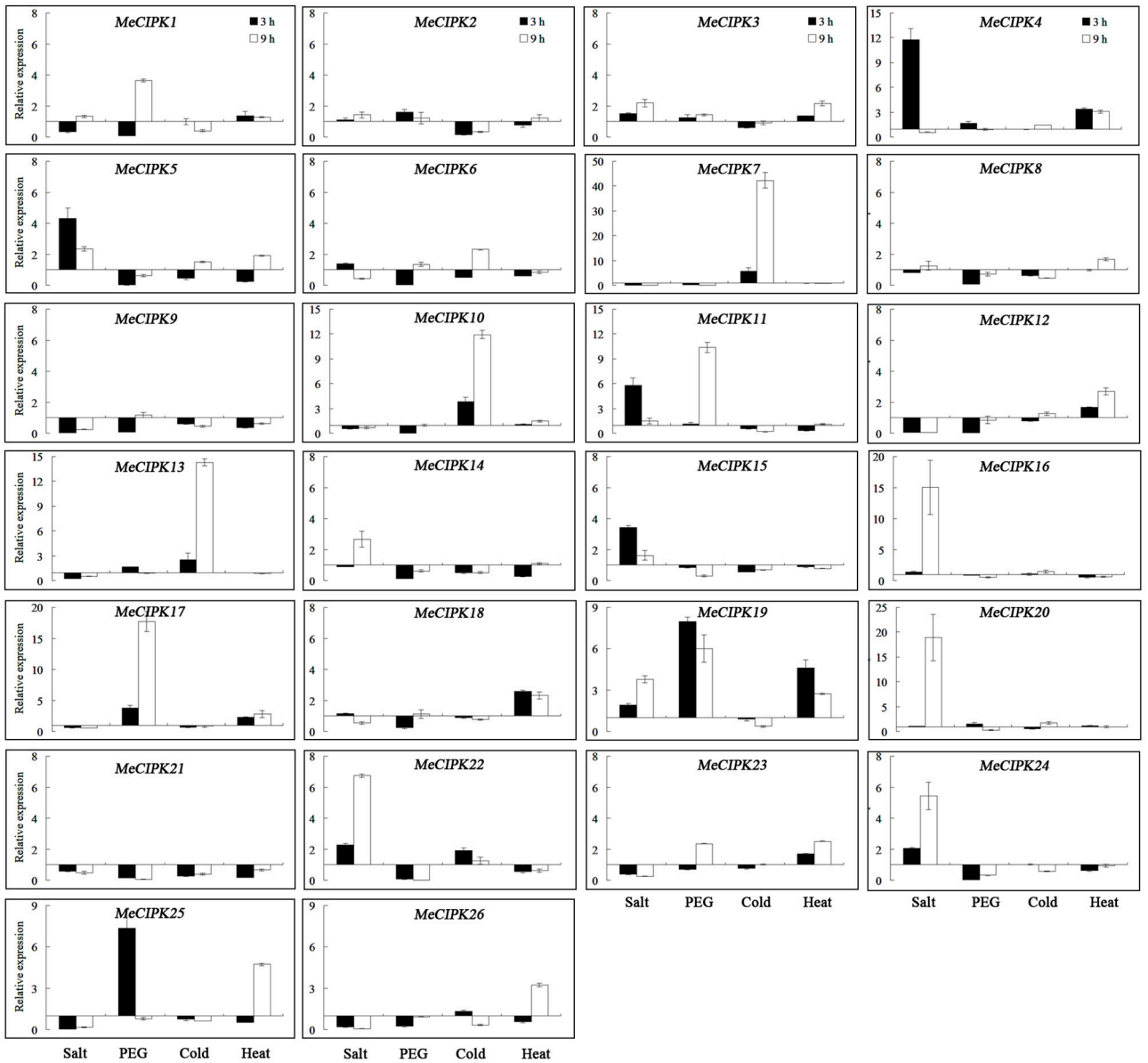

FIGURE 7 | Expression analyses of *MeCIPK* genes in roots responding to abiotic stresses, including salt (200 mM NaCl), drought (20% PEG6000), cold (4°C) and heat (42°C) treatments. Data are the means of three biological replicates ± SE at 3 and 9 h time-point standardized at 0 h.

for the kinases to interact with protein phosphatases. When the amino acids were substituted with alanine, the interaction was abolished (Ohta et al., 2003). Sequence alignments showed that arginine and phenylalanine are highly conserved in MeCIPK proteins (**Figure 2**).

Intron/exon organizations often reflect the evolution of some gene families (Wang et al., 2013; Liu et al., 2014). Most *MeCBL* genes have seven introns, while *MeCBL6* and *MeCBL10* have eight introns (**Figure 3B**). The phylogenetic tree analysis showed that MeCBL6 and MeCBL10 belong to group I (**Figure S1**). These suggest that the functions of CBL proteins might be different. As shown in **Figure S2**, *MeCIPK* genes were divided into five groups. Most interestingly, the members from groups B, C, D and E have fewer introns (and some have no introns) compared to genes from group A, which each contain at least nine introns (**Figure 4B**). This feature of *CIPK* gene structures was also found in *Arabidopsis*, rice, maize and soybean (Kolukisaoglu et al., 2004; Chen et al., 2011; Zhu et al., 2016), which suggests that intron gain or loss have played important roles in CIPK evolution.

Many researches have demonstrated that CBL and CIPK function in response to environment stress. Loss of *AtCBL1* rendered plants drought sensitive and over-expression of *AtCBL1* reduced transpirational water loss (Albrecht et al., 2003).

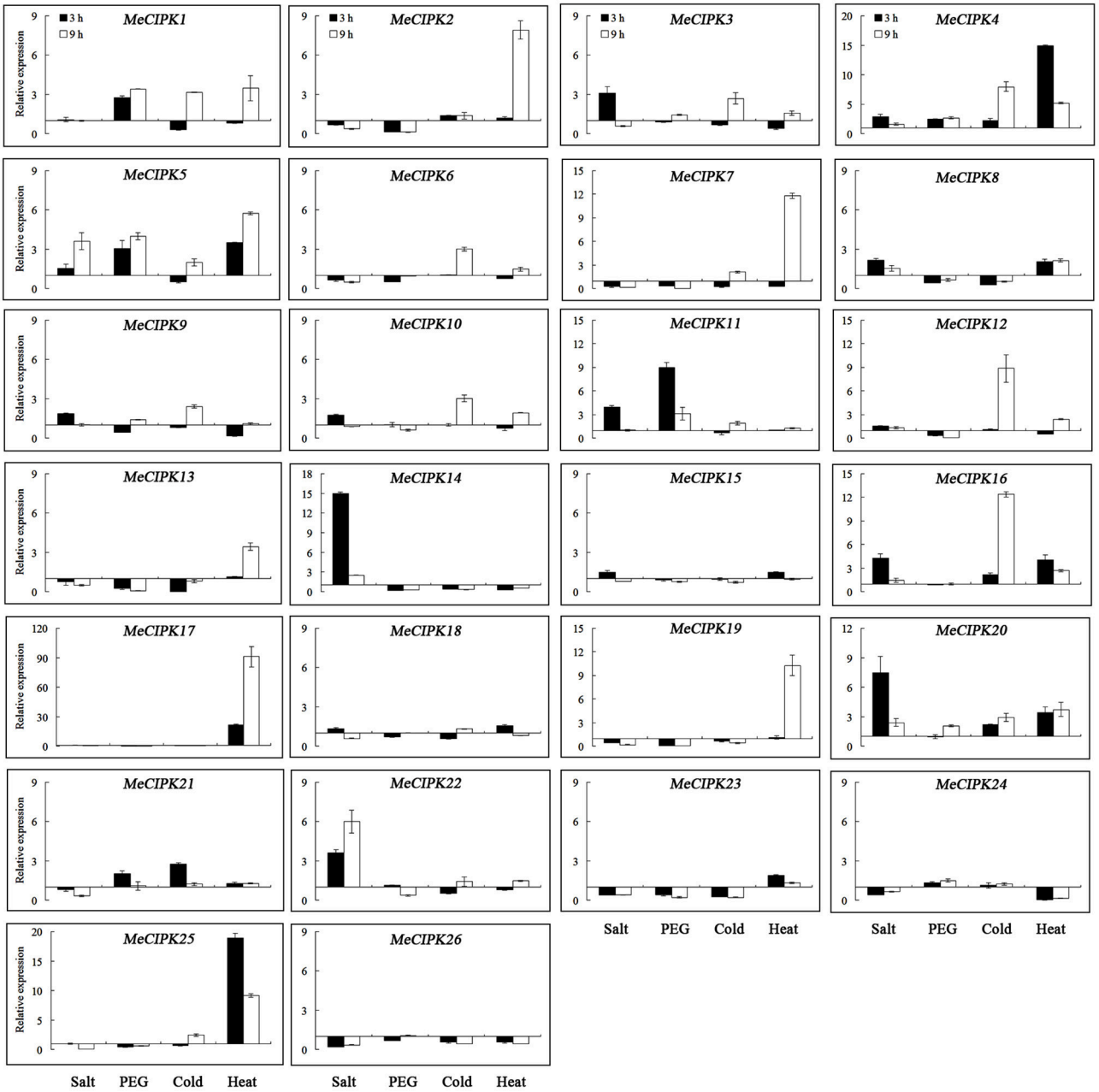

FIGURE 8 | Expression analyses of *MeCIPK* genes in leaves responding to abiotic stresses, including salt (200 mM NaCl), drought (20% PEG6000), cold (4°C) and heat (42°C) treatments. Data are the means of three biological replicates ± SE at 3 h and 9 h time-point standardized at 0 h.

Over-expression of *AtCBL5* increased salt or osmotic tolerance of transgenic plants (Cheong et al., 2010). *MeCBL5* was up-regulated by salt stress and cold stress in roots. Drought related element MYB and low-temperature response element LTR were also found in the promoter region of *MeCBL5* (**Figure 6**, **Table S2**). Transgenic rice over-expressing barley *HsCBL8* showed enhanced salt tolerance (Guo et al., 2016). The orthologous gene *MeCBL8* was up-regulated by salt stress and stress response element TC-rich repeats was found in the *MeCBL8* promoter region (**Figure 6**, **Table S2**). *AtCIPK3* was responsive to ABA and cold stress conditions, and, therefore AtCIPK3 might participate in abscisic acid and cold signal transduction in *Arabidopsis* (Kim et al., 2003). The orthologous gene *MeCIPK3* was induced by salt stress and cold in leaves and low-temperature responses element LTR was found in the *MeCIPK3* promoter region (**Figure 8**, **Table S2**). AtCIPK8 participates in regulating the low-affinity phase of the primary nitrate response (Hu et al., 2009). However, MeCIPK8 was

not significantly affected by the four treatments applied in this study (**Figure 7**, **8**). Additionally, heat treatment induced the expression of *MeCIPK19* in roots (**Figure 7**) and *MeCIPK7*, *17* and *25* in leaves (**Figure 8**), and the heat stress response element HSE was found in the promoter region of each of these genes (**Table S2**).

TABLE 2 | Interaction of MeCBLs and MeCIPKs in yeast two-hybrid assay.

	MeCBL1	MeCBL2	MeCBL4	MeCBL5	MeCBL6	MeCBL8	MeCBL9	MeCBL10
MeCIPK1	−	−	−	−	+	+	+	+
MeCIPK2	+	+	+	-	+	−	−	−
MeCIPK3	−	−	−	+	+	−	−	−
MeCIPK4	−	−	−	+	+	−	−	−
MeCIPK5	−	−	−	−	+	−	−	+
MeCIPK6	−	−	−	−	−	−	−	−
MeCIPK7	−	+	+	−	+	−	−	−
MeCIPK8	+	−	−	+	+	−	+	+
MeCIPK9	−	−	−	−	+	−	+	−
MeCIPK10	+	+	+	+	+	+	+	−
MeCIPK11	−	−	−	−	−	−	−	−
MeCIPK12	−	+	−	−	−	−	−	−
MeCIPK13	−	+	−	−	+	−	−	−
MeCIPK14	+	−	+	+	+	+	+	−
MeCIPK15	+	+	−	−	+	+	−	−
MeCIPK16	+	+	+	−	+	+	+	−
MeCIPK17	+	−	−	+	−	−	−	−
MeCIPK18	+	−	+	−	+	+	+	+
MeCIPK19	+	−	+	+	+	+	+	+
MeCIPK20	−	−	−	−	+	−	−	−
MeCIPK22	−	−	+	−	+	−	−	+
MeCIPK23	+	+	−	−	+	−	+	+
MeCIPK24	−	+	−	−	+	−	−	+
MeCIPK25	−	−	−	−	−	−	+	−
MeCIPK26	+	−	−	−	+	+	+	−

The interaction analyses of MeCBL and MeCIPK proteins were performed using yeast two-hybrid system. Eight MeCBLs and 25 MeCIPKs was cloned and inserted into the pGADT7 and pGBKT7 plasmid, respectively. The plasmids were transformed into the yeast strain Y2HGold through lithium acetate method, and the interacting relationships were detected by the yeast growth on non-selective medium (DDO: SD-T-L) and selective medium (QDO+X+AbA: SD-T-L-H-A+40 μg/mL X-α-Gal + 125 ng/mL Aureobasidin A). + represents growth (interaction), − represents no growth (no interaction).

Furthermore, the CBL-CIPK complex also has been shown to regulate plant growth in response to abiotic stresses. The CBL1-CIPK6 component plays an important role in the plant response to high salinity, phosphorous deficiency and ABA signaling in *Brassica napus* (Chen et al., 2012). Both PtCBL10A and PtCBL10B could regulate poplar salt tolerance via interacting with PtSOS2 (Tang et al., 2013). AtCBL2 and AtCBL3 could recruit AtCIPK21 to the tonoplast and regulate *Arabidopsis* response to osmotic or salt stress (Pandey et al., 2015). The activity of AKT1 was also regulated by CIPK6 or CIPK16 in a CBL1-dependent manner (Lee et al., 2007). AtCIPK24 interaction with AtCBL4 or AtCBL10 regulates the activity of AtSOS1 to enhance *Arabidopsis* salt tolerance (Quan et al., 2007; Quintero et al., 2011). *MeCBL4* and *MeCBL10*, homologous with *AtCBL4* and *AtCBL10*, were induced by salt stress in roots and leaves, respectively (**Figure 6**), *MeCIPK24*, orthologous with *AtCIPK24*, was up-regulated in roots under salt treatment (**Figure 7**). The yeast two-hybrid test showed that MeCIPK24 could interact with MeCBL10 (**Table 2**, **Figure S4**). Yeast cells co-expressing *MeCBL10*, *MeCIPK24,* and *MeSOS1* showed enhanced salt tolerance compared with cells that have just expression of *MeSOS1* or co-expression of *MeCIPK24* and *MeSOS1* (**Figure 9**), which suggests that MeCIPK24 interaction with MeCBL10 could regulate the activity of MeSOS1 in yeast cells. MeCIPK24 interacted with MeCBL2 and MeCBL6 in addition to MeCBL10 (**Table 2**, **Figure S4**). *MeCBL6* was mainly induced by salt stress in roots (**Figure 6**), and demonstrated similar expression patterns with *MeCIPK24* (**Figure 7**), which suggests that the MeCIPK24-MeCBL6 complex might play a role in regulating salt tolerance in cassava. Upon cold stress, the expression level of MeCIPK7 showed the biggest change (**Figure 7**), and MeCIPK7 interacted with MeCBL2, MeCBL4 and MeCBL6 (**Table 2**, **Figure S4**). *MeCBL2* was mainly induced by cold stress and showed a similar expression profile to *MeCIPK7*, which suggests that the MeCIPK7-MeCBL2 complex might be involved in cold signal transduction. Under the treatment of heat, the expression level of *MeCIPK17* had the biggest change, the expression level reached a peak of 91-fold

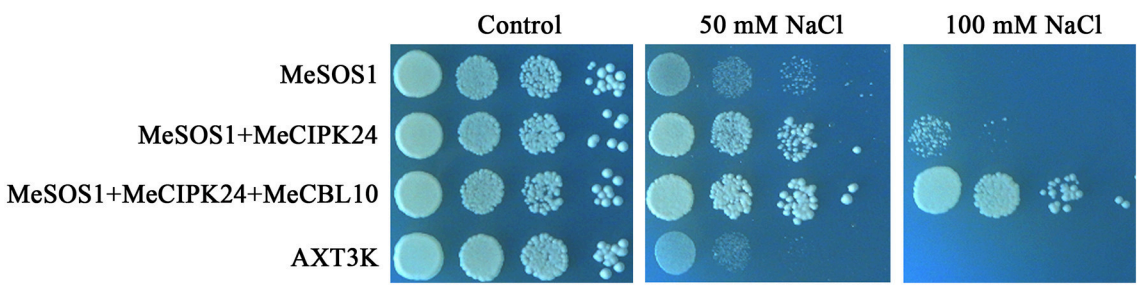

FIGURE 9 | The effect of salinity stress on yeast growth. Transgenic and untransformed yeast cells were pre-cultured to saturation, and serial 10-fold dilutions of yeast cells were spotted on AP plates without or with NaCl as described. After 5 days, the growth of yeast cells on plates was recorded. MeSOS1, AXT3K strain transformed with the Na^+/H^+ antiporter gene *MeSOS1*; MeSOS1+MeCIPK24, AXT3K strain transformed with *MeSOS1* and *MeCIPK24* genes; MeSOS1+MeCIPK24+MeCBL10, AXT3K strain transformed with *MeSOS1*, *MeCIPK24* and *MeCBL10* genes; AXT3K, untransformed AXT3K strain.

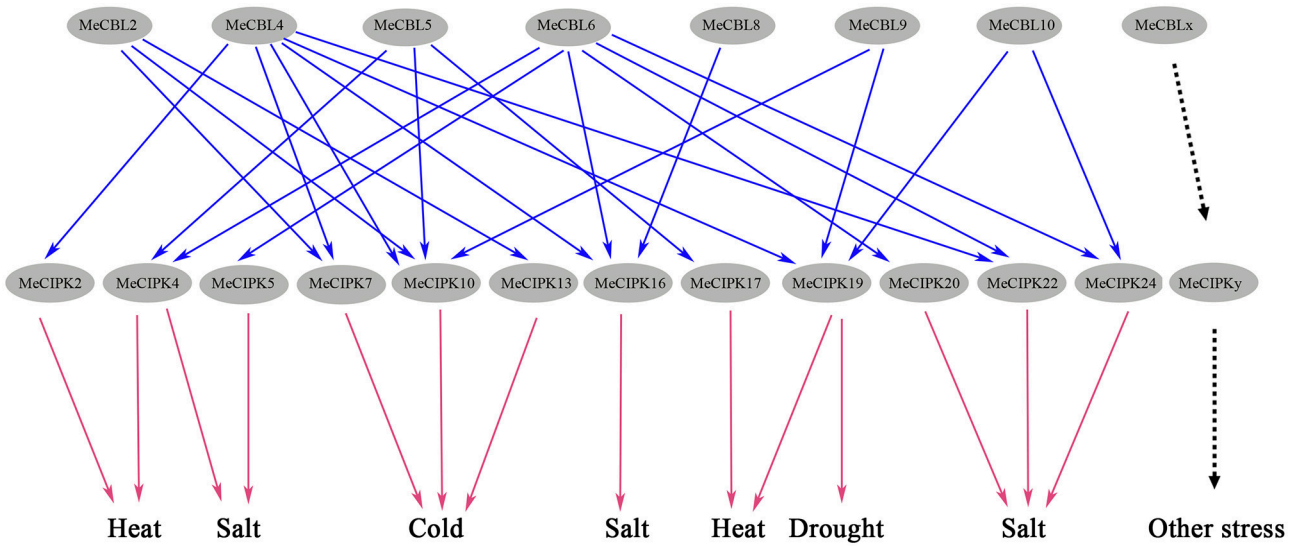

FIGURE 10 | Potential CBL-CIPK signaling networks in cassava response to abiotic stresses. Blue arrows represent the interaction relationships between MeCBL and MeCIPK proteins, as indicated by protein-protein interaction data and red arrows represent observed gene expression responses to abiotic stresses.

after 9 h of treatment (**Figure 8**), and MeCIPK17 interacted with MeCBL5 (**Table 2**, **Figure S4**), which suggests that the MeCIPK17-MeCBL5 complex might be involved in the plant response to heat stress. As shown in **Figures 6**, **7**, *MeCBL4*, *MeCBL10,* and *MeCIPK19* were induced by PEG, which suggests that MeCIPK19 might regulate drought tolerance through interaction with MeCBL4 or MeCBL10.

In summary, the expression of *MeCBLs* and *MeCIPKs* in response to salt stress, drought, high and low temperature stress and tissue development was very diverse, but induction was observed in each stress treatment. Different MeCBLs could interact with one or more MeCIPKs (**Table 2**, **Figure S4**), indicating that various MeCBLs and MeCIPKs may participate in the signal transduction response to these stresses (**Figure 10**).

AUTHOR CONTRIBUTIONS

XJ and YZ conceived and designed the experiments; CM, SW, YX, and NR performed the experiments; YZ, CM, and SW analyzed the data; XJ contributed reagents, materials, analysis tools; YZ and XJ wrote the paper.

ACKNOWLEDGMENTS

We thank the reviewer for English language editing. This work was supported by the Natural Science Foundation of China (31660253, 31260218), the Scientific and Technological Foundation of Hainan Province (HNGDhs201502) and the National Key Technology Support Program (2015BAD 01B02).

SUPPLEMENTARY MATERIAL

The Supplementary Material for this article can be found online at: https://www.frontiersin.org/articles/10.3389/fpls.2018.00269/full#supplementary-material

Figure S1 | Phylogenetic relationships of cassava CBL proteins were compared with *Arabidopsis* and rice CBL family proteins. The Neighbor-Joining phylogenetic tree was constructed using MEGA 5.0 software with bootstrap value 1000 based on the amino acid sequences of CBL proteins from representative species. The cassava CBL proteins (MeCBL) are marked by triangle. The *Arabidopsis* CBL proteins (AtCBL) are marked by dots. The rice CBL proteins (OsCBL) are marked by square.

Figure S2 | Phylogenetic relationships of cassava CIPK proteins were compared with *Arabidopsis* and rice CIPK family proteins. The Neighbor-Joining phylogenetic tree was constructed using MEGA 5.0 software with bootstrap value 1,000 based on the amino acid sequences of CIPK proteins from representative species. The cassava CIPK proteins (MeCIPK) are marked by triangles. The *Arabidopsis* CIPK proteins (AtCIPK) are marked by dots. The rice CIPK proteins (OsCIPK) are marked by square.

Figure S3 | The amino acid sequences of each motif identified in CBL **(A)** and CIPK **(B)** proteins. The conserved motifs were identified using the MEME program. Width represents the number of each motif.

Figure S4 | The interaction analysis of cassava MeCBL and MeCIPK proteins were performed using the Y2H method. The *MeCBL* genes were inserted into the pGBKT7 vector and the *MeCIPK* genes were cloned into the the pGADT7 vector. Yeast cells co-transformed with *MeCBL* and *MeCIPK* were grown on non-selective (lacking Leu and Trp, DDO) or selective media containing 40 μg/mL X-α-gal and 125 ng/mL Aureobasidin A (lacking Leu, Trp, His and Ade, QDO/X/A).

Table S1 | Primers used in this study.

Table S2 | Promoter analysis of *MeCBL* and *MeCIPK* genes. Types of potential *cis*-acting elements along with their functions (left) were identified in the 2,000 bp up-stream regions of 8 CBL genes and 26 CIPK genes (top).

REFERENCES

Albrecht, V., Ritz, O., Linder, S., Harter, K., and Kudla, J. (2001). The NAF domain defines a novel protein-protein interaction module conserved in Ca^{2+}-regulated kinases. *EMBO J.* 20, 1051–1063. doi: 10.1093/emboj/20.5.1051

Albrecht, V., Weinl, S., Blazevic, D., D'Angelo, C., Batistic, O., Kolukisaoglu, U., et al. (2003). The calcium sensor CBL1 integrates plant responses to abiotic stresses. *Plant J.* 36, 457–470. doi: 10.1046/j.1365-313X.2003.01892.x

Batistic, O., and Kudla, J. (2009). Plant calcineurin B-like proteins and their interacting protein kinases. *Biochim. Biophy. Acta* 1793, 985–992. doi: 10.1016/j.bbamcr.2008.10.006

Chen, L., Ren, F., Zhou, L., Wang, Q. Q., Zhong, H., and Li, X. B. (2012). The *Brassica napus* calcineurin B-like 1/CBL-interacting protein kinase 6 (CBL1/CIPK6) component is involved in the plant response to abiotic stress and ABA signaling. *J. Exp. Bot.* 63, 6211–6222. doi: 10.1093/jxb/ers273

Chen, X. F., Gu, Z. M., Xin, D. D., Hao, L. A., Liu, C. J., Huang, J., et al. (2011). Identification and characterization of putative *CIPK* genes in maize. *J. Genet. Genomics* 38, 77–87. doi: 10.1016/j.jcg.2011.01.005

Cheng, N. H., Pittman, J. K., Zhu, J. K., and Hirschi, K. D. (2004). The protein kinase SOS2 activates the *Arabidopsis* $H^+/Ca2^+$ antiporter CAX1 to integrate calcium transport and salt tolerance. *J. Biol. Chem.* 279, 2922–2926. doi: 10.1074/jbc.M309084200

Cheong, Y. H., Sung, S. J., Kim, B. G., Pandey, G. K., Cho, J. S., Kim, K. N., et al. (2010). Constitutive overexpression of the calcium sensor CBL5 confers osmotic or drought stress tolerance in *Arabidopsis*. *Mol. Cells* 29, 159–165. doi: 10.1007/s10059-010-0025-z

Drerup, M. M., Schlucking, K., Hashimoto, K., Manishankar, P., Steinhorst, L., Kuchitsu, K., et al. (2013). The calcineurin B-like calcium sensors CBL1 and CBL9 together with their interacting protein kinase CIPK26 regulate the *Arabidopsis* NADPH oxidase RBOHF. *Mol. Plant* 6, 559–569. doi: 10.1093/mp/sst009

Du, W. M., Lin, H. X., Chen, S., Wu, Y. S., Zhang, J., Fuglsang, A. T., et al. (2011). Phosphorylation of SOS3-like calcium-binding proteins by their interacting SOS2-like protein kinases is a common regulatory mechanism in *Arabidopsis*. *Plant Physiol.* 156, 2235–2243. doi: 10.1104/pp.111.173377

Fuglsang, A. T., Guo, Y., Cuin, T. A., Qiu, Q., Song, C., Kristiansen, K. A., et al. (2007). *Arabidopsis* protein kinase PKS5 inhibits the plasma membrane H^+-ATPase by preventing interaction with protein. *Plant Cell* 19, 1617–1634. doi: 10.1105/tpc.105.035626

Guo, W., Chen, T., Hussain, N., Zhang, G., and Jiang, L. (2016). Characterization of salinity tolerance of transgenic rice lines harboring *HsCBL8* of wild barley (*Hordeum spontanum*) line from Qinghai-Tibet plateau. *Front. Plant Sci.* 7:1678. doi: 10.3389/fpls.2016.01678

Guo, Y., Halfter, U., Ishitani, M., and Zhu, J. K. (2001). Molecular characterization of functional domains in the protein kinase SOS2 that is required for plant salt tolerance. *Plant Cell* 13, 1383–1400. doi: 10.1105/tpc.13.6.1383

Ho, C., Lin, S., Hu, H., and Tsay, Y. (2009). CHL1 functions as a nitrate sensor in plants. *Cell* 138, 1184–1194. doi: 10.1016/j.cell.2009.07.004

Hrabak, E. M., Chan, C. W. M., Gribskov, M., Harper, J. M., Choi, J. H., Halford, N. G., et al. (1996). Characterization of eight new members of the calmodulin-like domain protein kinase gene family from *Arabidopsis thaliana*. *Plant Mol. Biol.* 31, 405–412. doi: 10.1007/BF00021802

Hu, H. C., Wang, Y. Y., and Tsay, Y. F. (2009). AtCIPK8, a CBL-interacting protein kinase, regulates the low-affinity phase of the primary nitrate response. *Plant J.* 57, 264–278. doi: 10.1111/j.1365-313X.2008.03685.x

Huang, C., Ding, S., Zhang, H., Du, H., and An, L. (2011). CIPK7 is involved in cold response by interacting with CBL1 in *Arabidopsis thaliana*. *Plant Sci.* 181, 57–64. doi: 10.1016/j.plantsci.2011.03.011

Kim, K. N., Cheong, Y. H., Grant, J. J., Pandey, G. K., and Luan, S. (2003). CIPK3, a calcium ensorassociated protein kinase that regulates abscisic acid and cold signal transduction in *Arabidopsis*. *Plant Cell* 15, 411–423. doi: 10.1105/tpc.006858

Kolukisaoglu, U., Weinl, S., Blazevic, D., Batistic, O., and Kudal, J. (2004). Calcium sensors and their interacting protein kinases: genomics of the *Arabidopsis* and rice CBL-CIPK signaling networks. *Plant Physiol.* 134, 43–58. doi: 10.1104/pp.103.033068

Kudla, J., Batistic, O., and Hashimoto, K. (2010). Calcium signals: the lead currency of plant information processing. *Plant Cell* 22, 541–563. doi: 10.1105/tpc.109.072686

Lee, S. C., Lan, W. Z., Kim, B. G., Li, L., Cheong, Y. H., Pandey, G. K., et al. (2007). A protein phosphorylation/dephosphorylation network regulates a plant potassium channel. *Proc. Natl. Acad. Sci. U.S.A.* 104, 15959–15964. doi: 10.1073/pnas.0707912104

Liu, J. Y., Chen, N. N., Chen, F., Cai, B., Dal Santo, S., Tornielli, G. B., et al. (2014). Genome-wide analysis and expression profile of the bZIP transcription factor gene family in grapevine (*Vitis vinifera*). *BMC Genomics* 15:281. doi: 10.1186/1471-2164-15-281

Liu, L. L., Ren, H. M., Chen, L. Q., Wang, Y., and Wu, W. H. (2013). A protein kinase, calcineurin B-like protein-interacting protein kinase 9, interacts with calcium sensor calcineurin B-like protein 3 and regulates potassium homeostasis under low-potassium stress in *Arabidopsis*. *Plant Physiol.* 161, 266–277. doi: 10.1104/pp.112.206896

Luan, S. (2009). The CBL-CIPK network in plant calcium signaling. *Trenes Plant Sci.* 14, 37–42. doi: 10.1016/j.tplants.2008.10.005

Luan, S., Kudla, J., Rodriguez-Concepcion, M., Yalovsky, S., and Gruissem, W. (2002). Calmodulins and calcineurin B-like proteins: calcium sensors for specific signal response coupling in plants. *Plant Cell* 14, S389–S400. doi: 10.1105/tpc.001115

Luan, S., Lan, W. Z., and Lee, S. C. (2009). Potassium nutrition, sodium toxicity, and calcium signaling: connections through the CBL-CIPK network. *Curr. Opin. Plant Biol.* 12, 339–346. doi: 10.1016/j.pbi.2009.05.003

Ma, B. J., Gu, Z. M., Tang, H. J., Chen, X. F., Liu, F., and Zhang, H. S. (2010). Preliminary study on function of calcineurin B-like protein gene *OsCBL8* in Rice. *Rice Sci.* 17, 10–18. doi: 10.1016/S1672-6308(08)60099-2

Martinez-Atienza, J., Jiang, X. Y., Garciadeblas, B., Mendoza, I., Zhu, J. K., Pardo, J. M., et al. (2007). Conservation of the salt overly sensitive pathway in rice. *Plant Physiol.* 143, 1001–1012. doi: 10.1104/pp.106.092635

Nagae, M., Nozawa, A., Koizumi, N., Sano, H., Hashimoto, H., Sato, M., et al. (2003). The crystal structure of the novel calcium-binding protein AtCBL2 from *Arabidopsis thaliana*. *J. Biol. Chem.* 278, 42240–42246. doi: 10.1074/jbc.M303630200

Ohta, M., Guo, Y., Halfter, U., and Zhu, J. K. (2003). A novel domain in the protein kinase SOS2 mediates interaction with the protein phosphatase 2C ABI2. *Proc. Natl. Acad. Sci. U.S.A.* 100, 11771–11776. doi: 10.1073/pnas.2034853100

Oliveira, E. J., Santana, F. A., Oliveira, L. A., and Santos, V. S. (2014). Genetic parameters and prediction of genotypic values for root quality traits in cassava using REML/BLUP. *Genet. Mol. Res.* 13, 6683–6700. doi: 10.4238/2014.August.28.13

Pandey, G. K., Grant, J. J., Cheong, Y. H., Kim, B. G., Li, L. G., and Luan, S. (2008). Calcineurin-B-like protein CBL9 interacts with target kinase CIPK3 in the regulation of ABA response in seed germination. *Mol. Plant* 1, 238–248. doi: 10.1093/mp/ssn003

Pandey, G. K., Kanwar, P., Singh, A., Steinhorst, L., Pandey, A., Yadav, A. K., et al. (2015). CBL-interacting protein kinase, CIPK21, regulates osmotic and salt stress responses in *Arabidopsis*. *Plant Physiol.* 169, 780–792. doi: 10.1104/pp.15.00623

Qiu, Q. S., Guo, Y., Quintero, F. J., Pardo, J. M., Schumaker, K. S., and Zhu, J. K. (2004). Regulation of vacuolar Na^+/H^+ exchange in *Arabidopsis thaliana* by the salt-overly-sensitive (SOS) pathway. *J. Biol. Chem.* 279, 207–215. doi: 10.1074/jbc.M307982200

Quan, R., Lin, H. X., Mendoza, I., Zhang, Y. G., Cao, W. H., Yang, Y. Q., et al. (2007). SCABP8/CBL10, a putative calcium sensor, interacts with the protein kinase SOS2 to protect *Arabidopsis* shoots from salt stress. *Plant Cell* 19, 1415–1431. doi: 10.1105/tpc.106.042291

Quintero, F. J., Martinez-Atienza, J., Villalta, I., Jiang, X. Y., Kim, W. Y., Ali, Z., et al. (2011). Activation of the plasma membrane Na/H antiporter SOS1 by phosphorylation of an auto-inhibitory C-terminal domain. *Proc. Natl. Acad. Sci. U.S.A.* 108, 2611–2616. doi: 10.1073/pnas.1018921108

Ren, X. L., Qi, G. N., Feng, H. Q., Zhao, S., Zhao, S. S., Wang, Y., et al. (2013). Calcineurin B-like protein CBL10 directly interacts with AKT1 and modulates K^+ homeostasis in *Arabidopsis*. *Plant J.* 74, 258–266. doi: 10.1111/tpj.12123

Sanchez-Barrena, M. J., Martinez-Ripoll, M., Zhu, J. K., and Albert, A. (2005). The structure of the *Arabidopsis thaliana* SOS3: molecular mechanism of

sensing calcium for salt stress response. *J. Mol. Biol.* 345, 1253–1264. doi: 10.1016/j.jmb.2004.11.025

Sanders, D., Pelloux, J., Brownlee, C., and Harper, J. F. (2002). Calcium at the crossroads of signaling. *Plant Cell* 14, S401–S417. doi: 10.1105/tpc.002899

Shukla, V., and Mattoo, A. K. (2008). Sucrose non-fermenting 1-related protein kinase 2 (SnRK2): a family of protein kinases involved in hyperosmotic stress signaling. *Physiol. Mol. Biol. Plants* 14, 91–100. doi: 10.1007/s12298-008-0008-0

Sun, T., Wang, Y., Wang, M., Li, T. T., Zhou, Y., Wang, X. T., et al. (2015). Identification and comprehensive analyses of the *CBL* and *CIPK* gene families in wheat (*Triticum aestivem* L.). *BMC Plant Biol.* 15:269. doi: 10.1186/s12870-015-0657-4

Tang, R. J., Liu, H., Bao, Y., Lv, Q. D., Yang, L., and Zhang, H. X. (2010). The woody plant poplar has a functionally conserved salt overly sensitive pathway in response to salinity stress. *Plant Mol. Biol.* 74, 367–380. doi: 10.1007/s11103-010-9680-x

Tang, R. J., Yang, Y., Yang, L., Liu, H., Wang, C. T., Yu, M. M., et al. (2013). Poplar calcineurin B-like proteins PtCBL10A and PtCBL10B regulate shoot salt tolerance through interaction with PtSOS2 in the vacuolar membrane. *Plant Cell Environ.* 37, 573–588. doi: 10.1111/pce.12178

Tang, R. J., Zhao, F. G., Garcia, V. J., Kleist, T. J., Yang, L., Zhang, H. X., et al. (2015). Tonoplast CBL-CIPK calcium signaling network regulates magnesium homeostasis in *Arabidopsis*. *Proc. Natl. Acad. Sci. U.S.A.* 112, 3134–3139. doi: 10.1073/pnas.1420944112

Wang, N., Zheng, Y., Xin, H. P., Fang, L. C., and Li, S. H. (2013). Comprehensive analysis of NAC domain transcription factor gene family in *Vitis vinifera*. *Plant Cell Rep*. 32, 61–75. doi: 10.1007/s00299-012-1340-y

Wang, X. P., Chen, L. M., Liu, W. X., Shen, L. K., Wang, F. L., Zhou, Y., et al. (2016). AtKC1 and CIPK12 synergistically modulate AKT1-mediated low-potassium stress responses in *Arabidopsis*. *Plant Physiol.* 170, 2264–2277. doi: 10.1104/pp.15.01493

Xi, Y., Liu, J., Dong, C., and Cheng, Z. M. (2017). The, C. B. L., and CIPK gene family in grapevine (Vitis vinifera): genome-wide analysis and expression profiles in response to various abiotic stresses. *Front. Plant Sci.* 8:978. doi: 10.3389/fpls.2017.00978

Xiang, Y., Huang, Y., and Xiong, L. A. (2007). Characterization of stress responsive *CIPK* genes in rice for stress tolerance improvement. *Plant Physiol.* 144, 1416–1428. doi: 10.1104/pp.107.101295

Xu, J., Li, H. D., Chen, L. Q., Wang, Y., Liu, L. L., He, L., et al. (2006). A protein kinase, interacting with two calcineurin B-like proteins, regulates K^+ transporter AKT1 in *Arabidopsis*. *Cell* 125, 1347–1360. doi: 10.1016/j.cell.2006.06.011

Yu, Q., An, L., and Li, W. (2014). The CBL-CIPK network mediates different signaling pathways in plants. *Plant Cell Rep*. 33, 203–214. doi: 10.1007/s00299-013-1507-1

Yu, Y. H., Xia, X. L., Yin, W. L., and Zhang, H. X. (2007). Comparative genomic analysis of *CIPK* gene family in *Arabidopsis* and *Populus*. *Plant Growth Regul.* 52, 101–110. doi: 10.1007/s10725-007-9165-3

Zeng, C., Chen, Z., Xia, J., Zhang, K., Chen, X., Zhou, Y., et al. (2014). Chilling acclimation provides immunity to stress by altering regulatory networks and inducing genes with protective functions in cassava. *BMC Plant Biol*. 14:207. doi: 10.1186/s12870-014-0207-5

Zhai, J. L., Xu, H. X., Cong, X. L., Deng, Y. C., Xia, Z. H., Huang, X., et al. (2013). Ca^{2+}/H^+ exchange in the plasma membrane of *Arabidospsis thaliana* leaves. *Acta Physiol. Plant* 35, 161–173. doi: 10.1007/s11738-012-1059-y

Zhang, H. C., Yin, W. L., and Xia, X. L. (2008). Calcineurin B-like family in Populus: comparative genome analysis and expression pattern under cold, drought and salt stress treatment. *Plant Growth Regul.* 56, 129–140. doi: 10.1007/s10725-008-9293-4

Zhang, H. F., Yang, B., Liu, W. Z., Li, H. W., Wang, L., Wang, B. Y., et al. (2014). Identification and characterization of *CBL* and *CIPK* gene families in canola (*Brassica napus* L.). *BMC Plant Biol*. 14:8. doi: 10.1186/1471-2229-14-8

Zhou, Y., Yin, X. C., Duan, R. J., Hao, G. P., Guo, J. C., and Jiang, X. Y. (2015). SpAHA1 and SpSOS1 coordinate in transgenic yeast to improve salt tolerance. *PLoS ONE* 10:e0137447. doi: 10.1371/journal.pone.0137447

Zhu, J. K. (2003). Regulation of ion homeostasis under salt stress. *Curr. Opin. Plant Biol.* 6, 441–445. doi: 10.1016/S1369-5266(03)00085-2

Zhu, K., Chen, F., Liu, J., Chen, X., Hewezi, T., and Cheng, Z. M. (2016). Evolution of an intron-poor cluster of the *CIPK* gene family and expression in response to drought stress in soybean. *Sci. Rep*. 6:28225. doi: 10.1038/srep28225

Conflict of Interest Statement: The authors declare that the research was conducted in the absence of any commercial or financial relationships that could be construed as a potential conflict of interest.

frontiers in Plant Science

ORIGINAL RESEARCH
published: 21 February 2018
doi: 10.3389/fpls.2018.00128

Genotyping by Sequencing and Genome–Environment Associations in Wild Common Bean Predict Widespread Divergent Adaptation to Drought

Andrés J. Cortés[1]† and Matthew W. Blair[2]*

[1] Department of Biological and Environmental Sciences, University of Gothenburg, Gothenburg, Sweden, [2] Department of Agricultural and Environmental Science, Tennessee State University, Nashville, TN, United States

Drought will reduce global crop production by >10% in 2050 substantially worsening global malnutrition. Breeding for resistance to drought will require accessing crop genetic diversity found in the wild accessions from the driest high stress ecosystems. Genome–environment associations (GEA) in crop wild relatives reveal natural adaptation, and therefore can be used to identify adaptive variation. We explored this approach in the food crop *Phaseolus vulgaris* L., characterizing 86 geo-referenced wild accessions using genotyping by sequencing (GBS) to discover single nucleotide polymorphisms (SNPs). The wild beans represented Mesoamerica, Guatemala, Colombia, Ecuador/Northern Peru and Andean groupings. We found high polymorphism with a total of 22,845 SNPs across the 86 accessions that confirmed genetic relationships for the groups. As a second objective, we quantified allelic associations with a bioclimatic-based drought index using 10 different statistical models that accounted for population structure. Based on the optimum model, 115 SNPs in 90 regions, widespread in all 11 common bean chromosomes, were associated with the bioclimatic-based drought index. A gene coding for an ankyrin repeat-containing protein and a phototropic-responsive NPH3 gene were identified as potential candidates. Genomic windows of 1 Mb containing associated SNPs had more positive Tajima's D scores than windows without associated markers. This indicates that adaptation to drought, as estimated by bioclimatic variables, has been under natural divergent selection, suggesting that drought tolerance may be favorable under dry conditions but harmful in humid conditions. Our work exemplifies that genomic signatures of adaptation are useful for germplasm characterization, potentially enhancing future marker-assisted selection and crop improvement.

Keywords: drought tolerance, adaptation, genomic signatures of selection, divergent selection, SNP markers, Tajima's D

OPEN ACCESS

Edited by:
Nicholas Provart, University of Toronto, Canada

Reviewed by:
Frédéric Marsolais, Agriculture and Agri-Food Canada, Canada
Umesh K. Reddy, West Virginia State University, United States

***Correspondence:**
Andrés J. Cortés
acortes@corpoica.org.co

***Present address:**
Andrés J. Cortés, Centro de Investigación La Selva, Corporación Colombiana de Investigación Agropecuaria, Vereda Llano Grande, Colombia

Specialty section:
This article was submitted to Plant Abiotic Stress, a section of the journal Frontiers in Plant Science

Received: *06 November 2017*
Accepted: *23 January 2018*
Published: *21 February 2018*

Citation:
Cortés AJ and Blair MW (2018) Genotyping by Sequencing and Genome–Environment Associations in Wild Common Bean Predict Widespread Divergent Adaptation to Drought. Front. Plant Sci. 9:128. doi: 10.3389/fpls.2018.00128

INTRODUCTION

Understanding the genomic signatures associated with environmental variation is of great interest as it provides insights into how organisms adapt to their environment (Stinchcombe and Hoekstra, 2008; Hoffmann and Sgro, 2011; Savolainen et al., 2013). Recent genomic studies in wild plant populations have demonstrated that genome–environment associations (GEA)

can be used to identify adaptive loci and predict phenotypic variation. Generally, the studies have associated single nucleotide polymorphism (SNP) alleles and parameters from the accessions' environment of origin, to determine the potential for abiotic stress adaptation. For instance, Turner et al. (2010) predicted genetic adaptive variation to serpentine soils in *Arabidopsis lyrata*, Hancock et al. (2011) identified climate-adaptive genetic loci among a set of geographically diverse *Arabidopsis thaliana*, Fischer et al. (2013) predicted adaptive variation to topo-climatic factors in *Arabidopsis halleri*, Pluess et al. (2016) predicted genetic local adaptation to climate at a regional scale in *Fagus sylvatica*, and Yeaman et al. (2016) detected convergent local adaptation in two distantly related species of conifers.

The GEA approach has been also been explored in some crop accessions as a prospection strategy for discovering wild germplasm or landraces for breeding as an alternative to traditional phenotyping. For example, Lasky et al. (2012) and Des Marais et al. (2014) looked at natural variation in *Arabidopsis* for drought resistance and water use efficiency, Yoder et al. (2014) was able to capture adaptive variation to thermal tolerance, drought tolerance, and resistance to pathogens in *Medicago truncatula*, Lasky et al. (2015) predicted genotype × environment interactions to drought stress and aluminum toxicity in *Sorghum bicolor*, and Berthouly-Salazar et al. (2016) uncovered genomic regions involved in adaptation to abiotic and biotic stress on two climate gradients in *Cenchrus americanus*. Our group has focused on exploring the marker × environment association approach with wild relatives of the food crop common bean (*Phaseolus vulgaris* L.) and we have shown candidate genes such as DREB, ASR, and ERECTA to have haplotypes associated with drought tolerance (Cortés et al., 2012a,b; Blair et al., 2016). In this study, we couple genome–environment association with estimates of genome-wide diversity in wild accessions by using a whole-genome marker method with thousands of SNPs combined with climatic indices.

Among the most comprehensive marker systems for common bean SNP detection is the method called genotyping by sequencing (GBS). This technique has the flexibility of being adaptable to wild relatives with no previous sequence information needed although a reference genome for the species is useful (Elshire et al., 2011). To date, the GBS method has mostly been conducted for cultivars of common bean but rarely for wild accessions, which was one of the purposes of our research. A critical step for GBS assays is the preparation of restriction enzyme digested reduced representation libraries of genomic DNA that is barcoded for evaluation on a high throughput sequencer. As an initial example of the method for genetic mapping in common bean, Hart and Griffiths (2015) compared *Pst*I as a methylation sensitive enzyme to the non-methylation sensitive *Ape*K1 proposed for most small-genome species by Elshire et al. (2011) and evaluated a population of 84 lines and 12 parental checks. Bhakta et al. (2015) used the *PstI* GBS method to perform high resolution mapping on a population of 188 RILs from the cross of Jamapa × Calima, cultivated beans from opposite genepools and discovered nearly 2,000 usable SNP loci for genetic mapping. In parental surveys, Zou et al. (2013) used *Hae*III digestion and library construction in 36 Canadian small seeded breeding lines to discover nearly 25,000 physically tagged SNPs. Subsequently, Ariani et al. (2016) used another new enzyme, the four base pair cutter *Cvi*AII, to evaluate a broader range of 18 common beans (one ancestral wild, four Andean domesticates, four wild Mesoamericans and nine cultivated Mesoamerican) finding 3,200–21,000 SNPs/genotype. Schroder et al. (2016), in contrast, used a combination of *Mse*I and *Taq*I enzymes along with size selections to compare the feasibility of double digestion and small fragment size generation with four bp cutters, to the *Ape*K1 method for 25 Mesoamerican beans, finding up to 12.5 times more usable SNPs with an 8X coverage. More recently, Ariani et al. (2017) used the same protocol than Ariani et al. (2016) to reveal the spatial and temporal scales of range expansion in wild common bean. In all cases size selection, sequencing depth and a reference genome from Schmutz et al. (2014) were critical for calling SNPs and avoiding missing data or false positives due to poor sequence coverage. DARTseq, a modification of the GBS method, has been used on 188 cultivated Brazilian genotypes for diversity assessment finding its value in population structure analysis (Valdisser et al., 2017). With these results in the literature, we were confident that the GBS method would be practical for generating many SNPs in wild accessions of common bean and could be used for both diversity evaluation and association analysis.

Wild bean are thought to have diverged from its sister species in the tropical Andes (Rendón-Anaya et al., 2017) to later diversified in South and Central America from an original range in Central America, after which domestication in the southern and northern ends of each region gave origin to Andean and Mesoamerican domesticates, respectively (Gepts and Debouck, 1991; Kwak and Gepts, 2009; Schmutz et al., 2014). Studies of wild beans, show that despite the bimodality in domestication, they are loosely structured across the full range of environments from Northern Mexico to Northern Argentina, with identifiable sub-populations of wild types centered in Argentina/Southern Bolivia, Ecuador/Northern Peru, Colombia, Guatemala, Highland Mexico, and Lowland Mexico (Blair et al., 2012; Cortés, 2013; Cortés et al., 2013). The southernmost sub-population is typical of the Andean genepool while the two northern most sub-populations parallel the races found in Mesoamerican common bean with the centrally located sub-populations being intermediate. Among the wild beans many accessions survive and reproduce well in drought-affected regions of the New World, but have not been used for breeding the important seed types of the region.

Further wild germplasm characterization is important as common bean is a key source of nutrients and dietary protein for over 500 million people in Latin America and Africa and more than 4.5 out of 23 million hectares are grown in zones where drought is severe, such as in northeastern Brazil, coastal Peru, the central and northern highlands of Mexico, and in Eastern and Southern Africa (Broughton et al., 2003). This situation may become worst as increased drought due to climate change will reduce global crop production in >10% by 2050 with a potential to substantially worsen global malnutrition (Tai et al., 2014). Meanwhile wild beans are adapted as herbaceous species to dry forests and semi-arid regions of the Americas. Therefore,

increasing drought tolerance in common bean commercial varieties is highly desirable and one potential source of resistance is from the wild accessions of the species. Given this, our milestones for this study were to: (1) implement GBS technology in wild accessions of common bean, (2) characterize geo-referenced climate information about the geographic origins of the wild accessions, and (3) find marker × environment associations at the whole genome level using the SNP loci discovered in the germplasm set. Specifically, we quantified SNP allelic associations with a bioclimatic-based drought index in order to identify adaptive variation suitable to breed drought tolerant varieties.

MATERIALS AND METHODS

Plant Material and Compilation of the Bioclimatic-Based Drought Index

A total of 86 DNAs from *Phaseolus vulgaris* were used in this study, extracted from 86 geo-referenced wild common bean accessions (**Supplementary Table S1**). All the genotypes were provided by the Genetic Resources Unit at the International Center for Tropical Agriculture and are preserved under the treaty for genetic resources from the Food and Agriculture Organization hereafter abbreviated as the FAO collection. These accessions were selected to be a representative of a core collection for wild beans (Tohme et al., 1996) and all five subpopulations and genepools were uncovered by single-sequence repeat (SSR) markers by Blair et al. (2012). Geographic information provided for each accession by the Genetic Resource Unit[1] was also used as described in Cortés et al. (2013) to estimate drought stress at each collection site based on the precipitation regimes coupled with potential evapotranspiration (PET) models (Thornthwaite and Mather, 1957; Hamon, 1961) accounting for the effects of historical temperature and radiation (Hijmans et al., 2005).

More concretely, monthly mean air temperature and monthly precipitation averaged for the years 1970–2000 were downloaded from WorldClim[2] for each accession coordinate. The Thornthwaite method was then used to calculate PET (Cortés et al., 2013 for the detailed equations) considering the effects of both temperature and radiation (Thornthwaite and Mather, 1957). PET and the precipitation data were then combined in a monthly drought index that was averaged and normalized across all 12 months (Cortés et al., 2013 for the detailed equations). This normalized annual mean drought index (**Supplementary Figure S1**, Shapiro–Wilk normality test P-value = 0.106), fed by monthly environmental data averaged for the years 1970–2000, is hereafter referred as bioclimatic-based drought index. Two properties of this index must be noted. First, it assumes that plant distribution is in equilibrium with niche requirements and ecological forces, so that the errant presence of poorly adapted genotypes can be discarded (Forester et al., 2016). Second, this index is stable across years as it is based on climate data averaged across three decades. The ecological optimum, the stability and the normality of this index make it ideal for GEA analyses, in contrast with crude environmental measures.

Sample Collection, DNA Extraction, and Genotyping-by-Sequencing

Leaf tissue weighing approximately 20 mg was harvested at 40 days after plant germination and was immediately dried in Silica Gel (Sigma–Aldrich, Germany). Genomic DNA was extracted using the QIAGEN DNeasy Plant Mini Kit (QIAGEN, Germany), following the manufacturer's instructions, and quantified using a Qubit® dsDNA HS Fluorometer (Life Technologies, Stockholm, Sweden). One 96-plex GBS assay was made according to Elshire et al. (2011) for the 86 accessions, with library preparation performed with *ApeKI* digestions at the Biotechnology Resource Center of the Institute for Genomic Diversity (Cornell University, United States). Genotyping and SNP calling were done with TASSEL software v. 3.0 (Glaubitz et al., 2014) based on the reference genome v. 2.0 for *P. vulgaris* deposited at the Phytozome website[3]. Sequence tags were aligned to the *P. vulgaris* reference genome (Schmutz et al., 2014), using the BWA method (Li and Durbin, 2007). A customized physical map was calculated and drawn using R v.3.3.1 (R Core Team) to place each new GBS locus.

Identification of Loci Associated with the Bioclimatic-Based Drought Index

In order to account for possible demographic effects we examined subpopulation structure in the 86 geo-referenced wild common bean accessions using principal coordinates analysis (PCoA) implemented in the software Trait Analysis by aSSociation, Evolution and Linkage, Tassel v.5 (Bradbury et al., 2007). The same dataset and software were used to perform association analyses between the SNP markers and the bioclimatic-based drought index from Cortés et al. (2013). A total of ten generalized (GLM) and mixed (MLM) linear models were compared. Within each model family, five models were built as follows: (1) model with the genepool identity and the first two PCoA axes scores as covariates; (2) models with the within-genepool subpopulation identity, according to Blair et al. (2012), and the first two PCoA axes scores as covariates; (3) model with the first two PCoA axes scores as covariates; (4) model with the within-genepool subpopulation identity, according to Blair et al. (2012), as covariate; and (5) model with the genepool identity as covariate. Despite that GLMs usually exhibit a higher rate of false positives (Rosenberg et al., 2010), they were still considered in the present study for comparative purposes. All five MLMs used a centered IBS kinship matrix as a random effect to control for genomic background implementing the EMMA and P3D algorithms to reduce computing time (Zhang et al., 2010). QQ-plots of the P-values were inspected to assess whether excessive numbers of false positives were generated and choose in this way the optimum model. Significant associations were determined using a strict Bonferroni correction of P-values at alpha = 0.001, leading to a significance threshold of 4.4×10^{-8} (0.001 divided by the

[1] genebank.ciat.cgiar.org

[2] http://www.worldclim.org

[3] https://phytozome.jgi.doe.gov/pz/portal.html

number of markers, 22,845) or $-\log_{10}(4.4 \times 10^{-8}) = 7.36$. The construction of customized PCoA and Manhattan diagrams was carried out with the software R v.3.3.1 (R Core Team).

Potential candidate genes were identified within the 1,000 bp sections flanking each SNP marker that was associated with the bioclimatic-based drought index by using the common bean reference genome (Schmutz et al., 2014) and the PhytoMine and BioMart tools in Phytozome v.12[3].

Sliding Window Analysis

We used a sliding window approach (window size = 1×10^6 bps, step size = 200 kb) to describe patterns of variation and overall divergence across the genome. We computed per-window averages of SNP density, nucleotide diversity as measured by π (Nei, 1987), Watterson's theta (θ) estimator (Watterson, 1975), and Tajima's D (Tajima, 1989) using the software Tassel v.5 (Bradbury et al., 2007) and customized R scripts. Results of all windowed analyses were plotted against window midpoints in millions of base pairs (Mb) also using the software R v.3.3.1 (R Core Team).

Bootstrap-based means and 95% confidence intervals around the mean were calculated for these four summary statistics (SNP density, π, θ and Tajima's D) when computed in sliding windows that contained or did not contain at least one marker that was associated with the bioclimatic-based drought index. Each summary statistic of windows containing and not containing associated SNPs was randomly resampled with replacement (bootstrapping) across windows within grouping factor (associated vs. no associated), and the overall mean was stored for each grouping factor. This step was iterated 1,000 times using customized R scripts. Bootstrapping was performed independently for each summary statistic in order to eliminate correlations among these.

RESULTS

GBS Results

The raw Illumina DNA sequence data (180,540,321 high-quality barcoded reads per lane) were processed through the GBS analysis pipeline as implemented in TASSEL-GBS v3.0. The GBS analysis generated 1,625,330 unique sequence clusters (tags, Elshire et al., 2011; Glaubitz et al., 2014). Of the total number of tags, 71.2% aligned uniquely to the *P. vulgaris* reference genome, 10.1% had multiple matches and 18.7% were unaligned. A total of 197,314 putative SNP markers where identified in the aligned tags. Of these, 47% with more than 20% missing data, a default threshold used for GBS studies (Glaubitz et al., 2014), and further 18% with minimum allele frequencies (MAF) below 0.05 were excluded from the dataset. The high number of missing data/unaligned sequences and low MAF value SNPs can be explained by the naturally high levels of sequence diversity in wild accessions (Glaubitz et al., 2014). Still the GBS project yielded 22,845 SNP markers of high quality with an average read depth of 13.6X gene coverage. The locations of these GBS-derived SNP loci for the wild accessions were identified by sequence similarity and drawn to scale based on their physical map distribution in the common bean genome (**Figure 1**). The centromeres according to Schmutz et al. (2014) were marked with the extent of the centromeric repeats in comparison with the GBS derived markers.

There Were 115 Associated SNPs Widespread in 90 Regions in All 11 Chromosomes

The GBS-derived SNP markers recovered the well-described Andean and Mesoamerican genepool structure and five within-genepool subpopulations, as depicted by the principal components analysis (**Figure 2**, compare to Blair et al., 2012). QQ-plots from the association analyses between the 22,845 SNP markers and the bioclimatic-based drought index from Cortés et al. (2013) indicated that GLM analyses likely had excessive rates of false positives (**Supplementary Figure S2**) whereas MLM models controlling for population structure and using a kinship matrix more effectively reduced the false positive rate (**Supplementary Figure S3**). The MLM model with the first two PCoA axes scores used as covariates, was the best at controlling for false positives because it exhibited the smoothest transition toward significant outliers.

This last model yielded a total of 115 SNP markers associated with the bioclimatic-based drought index at the Bonferroni-corrected significance threshold of 7.36 $-\log_{10}$ (*P*-value) (**Figure 3**). This group of SNPs had an average R^2 of 51.3% $\pm$ 0.4, fairly stable across markers (**Supplementary Table S2**). The 115 SNPs were clustered in 90 different regions, defined here as overlapping 1,000 bp sections that flanked associated markers. Associated SNPs and regions were widespread in all 11 common bean chromosomes (**Table 1**).

Chromosomes Pv3 and Pv8 had the highest number of associated SNPs with 21 and 32 SNPs clustered in 16 and 21 different regions, respectively. Chromosomes Pv1, Pv2, Pv4, Pv5, Pv6, and Pv9 contained an intermediate number of associated SNPs with 11, 6, 11, 7, 12, and 9 SNPs clustered in 11, 6, 8, 6, 8, and 9 different regions, respectively. Chromosomes Pv7, Pv10 and Pv11 had the fewest number of associated SNPs with 3, 2, and 1 SNPs clustered in 3, 1, and 1 different regions, respectively. Chromosome Pv8 had more regions with at least two associated SNPs than any other chromosome, and these regions had more associated SNPs that in any other chromosome for a total of five regions with an average number of 3.2 associated SNPs in each region. The single region that contained the most associated SNPs was also situated on chromosome Pv8 with 6 SNPs and an average R^2 of 51.1% $\pm$ 0.3. After this chromosome, Pv3 was also notable for having four regions with an average number of 2.5 associated SNPs per region.

A total of 75 regions, comprising 99 SNP markers associated with the bioclimatic-based drought index, contained at least one gene, for a total of 77 genes identified as potential candidates for drought tolerance from the wild accession analysis (**Supplementary Table S3**). Most genes were from chromosomes Pv1, Pv3, and Pv8 with 11, 14, and 16 genes. Only two regions, at chromosomes Pv1 and Pv8 and containing a total of seven different SNPs, spanned two or more genes. The one in Pv8 was

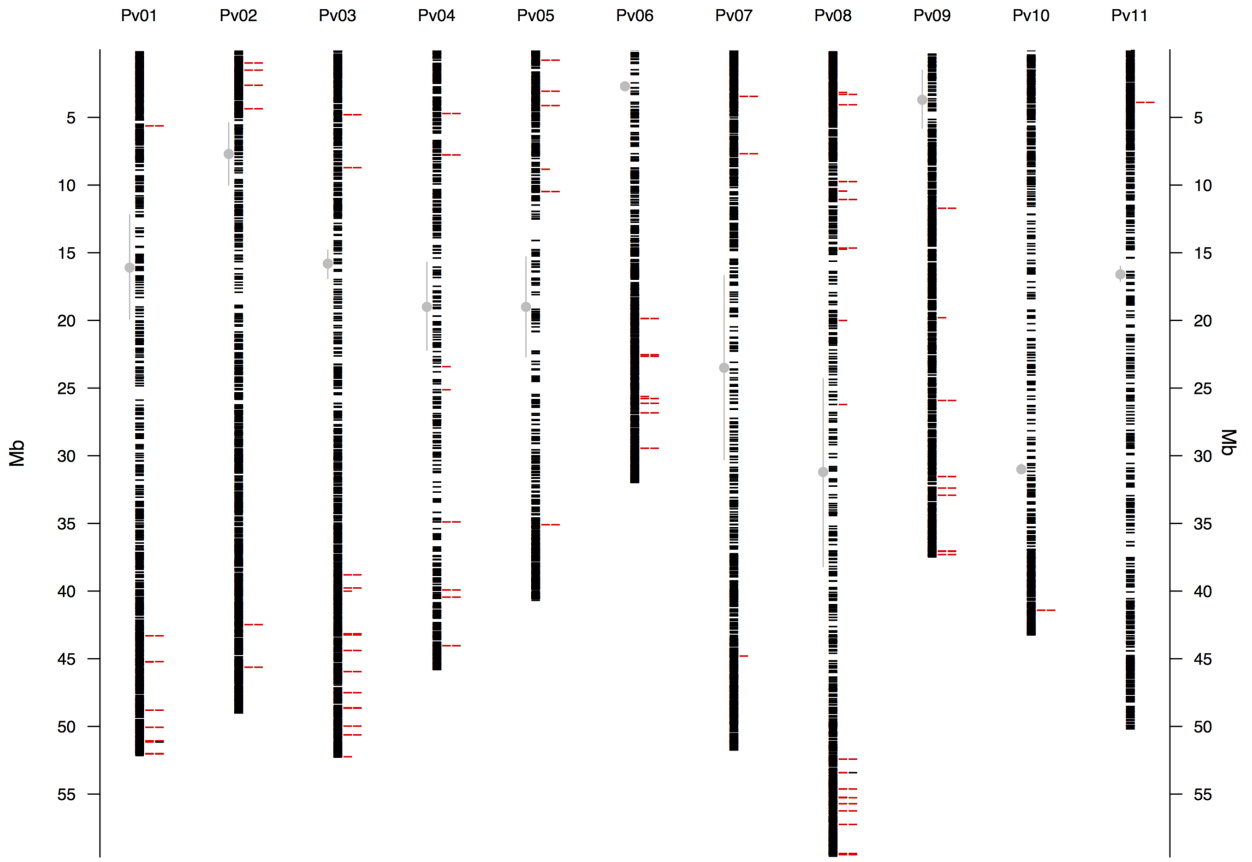

FIGURE 1 | Physical map of the 22,845 GBS-derived SNP markers for all 11 common bean (Pv) chromosomes. Physical position is shown in millions of base pairs (Mb). Each black hyphen corresponds to a SNP marker and the first column of red hyphens indicate markers associated with the bioclimatic-based drought index (**Figure 3**), as calculated by Cortés et al. (2013). The second column of red hyphens marks the 75 associated regions that contained one gene (**Supplementary Table S3**). The two black hyphens in this column at chromosomes Pv1 and Pv8 indicate associated regions that had two genes. Regions are defined here as overlapping 1,000 bp sections that flanked associated markers. Vertical gray lines with a central filled gray dot mark the centromeres according to Schmutz et al. (2014).

the region with more associated SNPs. One of the two genes in this region encoded an ankyrin repeat-containing protein, which was associated with osmotic regulation via the assembly of cation channels in the membranes (Voronin and Kiseleva, 2008). Among other identified potential candidate genes there was a phototropic-responsive NPH3 gene (Pedmale and Liscum, 2007) in Pv3. The associated SNPs flanking these genes had an average R^2 of 49% ± 0.2.

Associated Genomic Windows Were Enriched for SNP Density and Positive Tajima's D Scores

A sliding window analysis (window size = 1×10^6 bp, step size = 200 kb) was used to explore the patterns of genome-wide diversity. Marker density decayed drastically toward the centromeres. Average marker density was 44 SNPs per million base pairs (95% CI, 4–143, **Figure 4A**). Average nucleotide diversity as measured by π was 0.3 per million base pairs (95% CI, 0.2–0.4, **Figure 4B**). Average Watterson's theta (θ) was 0.20 per million base pairs (95% CI, 0.19–0.21, **Figure 4C**). Average Tajima's D was 0.68 per million base pairs (95% CI, 0.05–1.22, **Figure 4D**).

These statistics were compared between 1 Mb sliding windows that contained (associated windows) or did not contain at least one marker that was associated with the bioclimatic-based drought index (non-associated windows). Genomic windows containing at least one associated SNP had overall higher SNP density (79 ± 6 vs. 39 ± 2, **Figure 5A**), lower scores for Watterson's theta (θ) scores (0.2016 ± 0.0001 vs. 0.2026 ± 0001, **Figure 5C**) and more positive Tajima's D scores (0.71 ± 0.02 vs. 0.678 ± 0.009, **Figure 5D**) than windows without associated markers. Nucleotide diversity, as measured by π, was slightly elevated in associated windows when compared with no associated windows (0.322 ± 0.006 vs. 0.317 ± 0.003, **Figure 5B**).

DISCUSSION

This research indicates that adaptation to drought in common bean, as estimated by bioclimatic variables, is widespread across all 11 common bean chromosomes and has been under natural

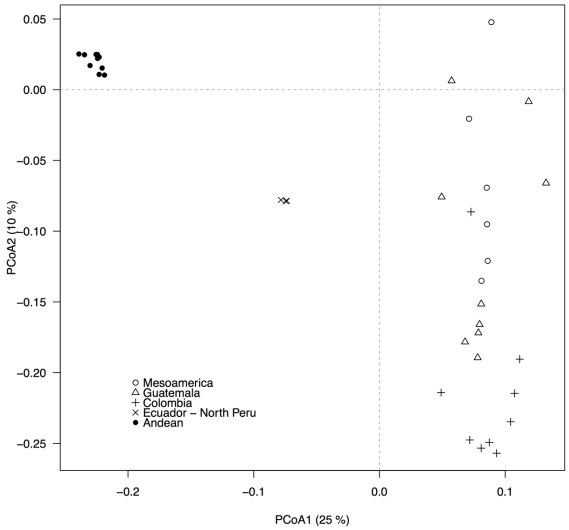

FIGURE 2 | Population structure, as revealed by a principal coordinates analysis (PCoA), based on 22,845 GBS-derived SNP markers. Filled and empty symbols correspond to accessions from the Andean and the Mesoamerican genepool, respectively. Five within-genepool subpopulations, according to Blair et al. (2012), are indicated by different symbols. The percentage of explained variation by each axis is shown within parenthesis in the label of the correspond axis.

divergent selection (inflated Tajima's D values). Both of these results imply that the genetic sources for drought tolerance are abundant in wild common bean and that natural drought tolerance may be favorable under dry conditions but harmful in more humid conditions. The awareness about this trade-off, upon which natural divergent selection has been acting for thousands of years, may aid the breeding of new drought tolerant varieties specifically adapted to unique micro-environments and local regions rather than varieties, eventually obsolete, originally intended for a wider range of environments. Below we first discuss the evidence that support the main conclusion of widespread divergent adaptation to drought. Later, we follow up by discussing the implications of this finding.

Wild Common Bean Exhibit Widespread Divergent Adaptation to Drought

It is well known that selective processes, such as purifying selection and local adaptation (divergent selection), differentially imprint regions within the same genome, causing a heterogeneous departure of genetic variation from the neutral expectations and from the background trend (Ellegren and Galtier, 2016). Specifically, habitat-mediated purifying selection is associated with localized low values of nucleotide diversity (π) (Nei, 1987) and Tajima's D (Tajima, 1989) and high scores of the Watterson's theta (θ) estimator (Watterson, 1975) because only low-frequency polymorphisms can avoid being eliminated by widespread directional selection. Although recent population bottlenecks tend to achieve the same reduction in nucleotide variation, this pattern is expected at a more genome-wide level. Similarly, local adaptation tends to homogenize haplotypes within the same niche and fix polymorphisms in different populations. Consequently, few haplotypes with high frequency are retained, corresponding to high values of nucleotide diversity (π) and Tajima's D, and low scores of the Watterson's theta (θ) estimator (Wakeley, 2008). While independent domestication events, extensive population structure, and population expansions after bottlenecks can produce the same patterns (Nei, 2010), these demographic processes are expected to be observed at a more genome-wide level.

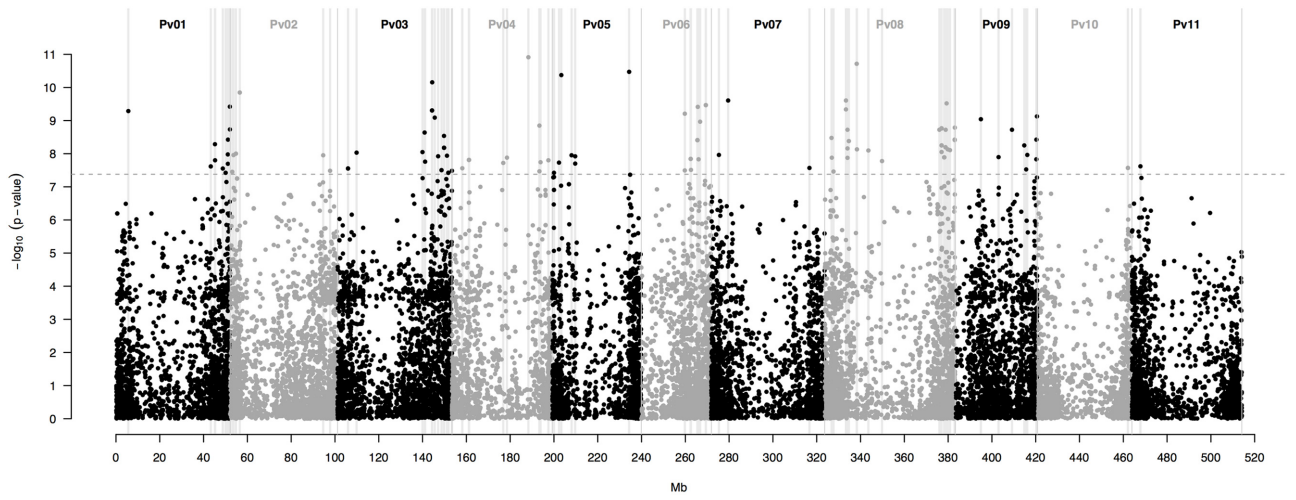

FIGURE 3 | Manhattan plot of the optimum genome-environment association (GEA) analysis for drought tolerance in 86 common bean accessions based on 22,845 GBS-derived SNP markers. The bioclimatic-based drought index follows Cortés et al. (2013). The Manhattan plot despites per-marker $-\log_{10}$ (*P*-value) according to a mixed linear model with a centered IBS kinship matrix as a random effect, and the first two PCoA axes scores **(Figure 2)** as covariates. The gray dashed horizontal line marks the *P*-value threshold after Bonferroni-correction for multiple comparisons. Black and gray colors highlight different common bean (Pv) chromosomes. Gray vertical boxes indicate the 1,000 bp flanking region of each marker that was associated with the bioclimatic-based drought index.

TABLE 1 | Per-chromosome (Pv) summary statistics for the 115 SNP markers associated with the bioclimatic-based drought index (Cortés et al., 2013) in 86 common bean accessions based on the optimum association analysis (**Figure 3**).

Pv	Number of associated SNPs	Average – $\log_{10}$ (*P*-value)	Average R^2 (%)	Number of associated regions	Number of regions with more than one associated SNP	Average number of associated SNPs in regions with more than one associated SNP	Number of associated regions containing genes	Number of genes
Pv1	11	8 ± 2	51 ± 1	11	0	NA	10	11
Pv2	6	8 ± 3	50 ± 2	6	0	NA	6	6
Pv3	21	8 ± 2	51 ± 1	16	4	2.25	14	14
Pv4	11	8 ± 2	50 ± 1	8	2	2.50	6	6
Pv5	7	8 ± 3	52 ± 2	6	1	2.00	5	5
Pv6	12	8 ± 2	52 ± 1	8	4	2.00	7	7
Pv7	3	8 ± 5	50 ± 2	3	0	NA	2	2
Pv8	32	8 ± 1	52 ± 1	21	5	3.20	15	16
Pv9	9	8 ± 3	51 ± 1	9	0	NA	8	8
Pv10	2	7.6	47.8	1	1	2.00	1	1
Pv11	1	7.6	47.1	1	0	NA	1	1
Total	115	8 ± 1	51.3 ± 0.4	90	17	2.47	75	77

*Given are results of a mixed linear model with a centered IBS kinship matrix as a random effect, and the first two PCoA axes scores (**Figure 2**) as covariates. Regions are defined here as overlapping 1,000 bp sections that flanked associated markers. Potential candidate genes were identified within the 1,000 bp section flanking each associated marker.*

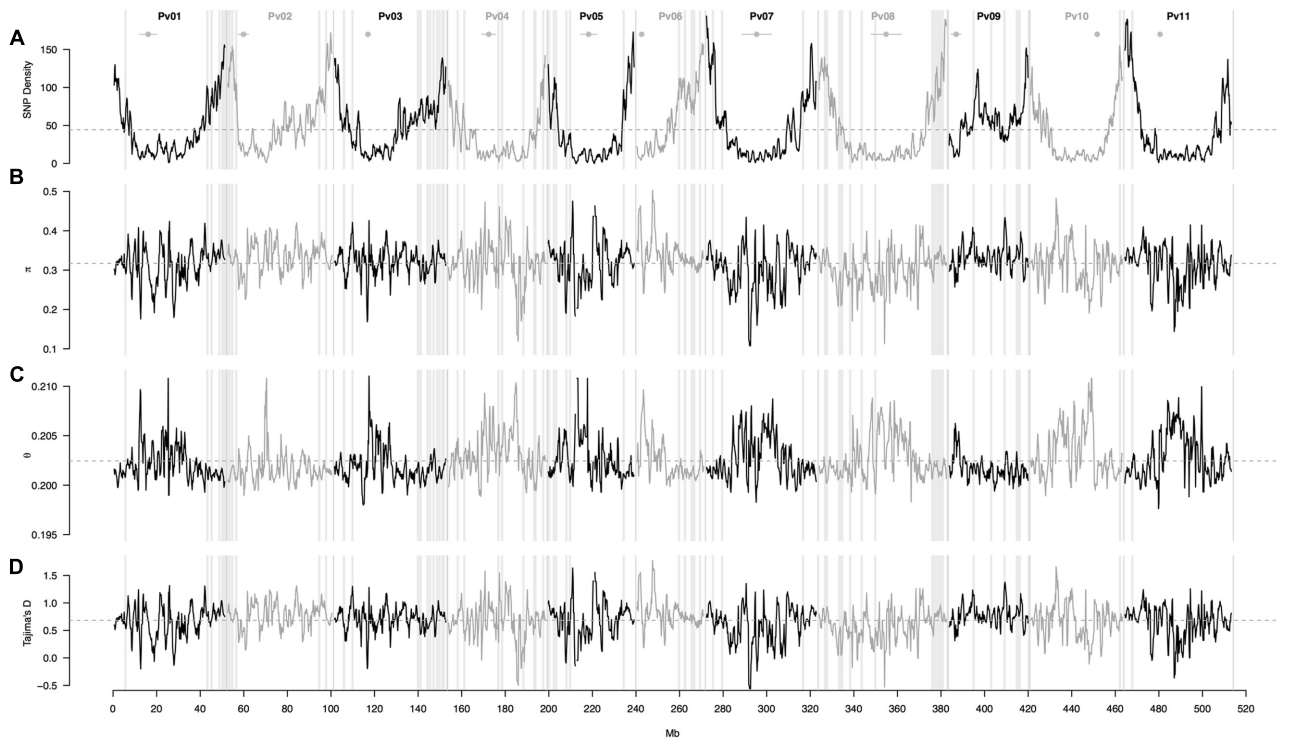

FIGURE 4 | Patterns of genome-wide diversity in 86 common bean accessions based on 22,845 GBS-derived SNP markers. A sliding window analysis (window size = 1 × 10^6 bp, step size = 200 kb) was used to compute **(A)** SNP density, **(B)** nucleotide diversity as measured by π, **(C)** Watterson's theta estimator (θ), and **(D)** Tajima's D. Results of all windowed analyses are plotted against window midpoints in millions of base pairs (Mb). Black and gray colors highlight different common bean (Pv) chromosomes. Gray dashed horizontal lines indicate genome-wide averages. Gray vertical boxes indicate the 1,000 bp flanking region of each marker that was associated with the bioclimatic-based drought index **(Figure 3)**. Horizontal gray lines with a central filled gray dot at the top of the figure mark the centromeres according to Schmutz et al. (2014).

Since divergent selection tends to homogenize haplotypes within the same niche and fix polymorphisms in different populations, few haplotypes with high frequency are retained, matching high values of nucleotide diversity and Tajima's D, and low values of the Watterson's theta (θ) estimator (Wakeley, 2008). In this study we have found that the genomic regions associated with the bioclimatic-based drought index, widespread in all 11 common bean chromosomes, displayed these very same signatures: inflated Tajima's D values and lowered Watterson's theta (θ) estimator. In other words, few haplotypes with high frequency are being differentially fixed in populations coming from contrasting environments. This result speaks for divergent selection acting on the genetic variants that are associated with drought tolerance, as compared to the opposite signal of directional selection, in which few dominant haplotypes are expected.

Yet, genomic signatures associated with habitat heterogeneity can still result from causes other than adaptation and selection (Nei, 2010), for example random genetic drift and population structure, and are also influenced by differences in ancestral variation and recombination in the genome (Strasburg et al., 2011; Cortés, 2015; Cortés et al., 2015a; Ellegren and Galtier, 2016; Wolf and Ellegren, 2016). Moreover, the origin of habitat-associated variants from novel or standing genetic variation leads to distinctively different patterns of genomic divergence (Hermisson and Pennings, 2005; Barrett and Schluter, 2008; Pritchard et al., 2010). A way to distinguish these underlying causes of divergence is comparing summary statistics (i.e., Tajima's D) from different genomic sections, as we did here, because demographic processes usually leave genome-wide signatures while selection tends to imprint more localized regions (Wakeley, 2008). With this in mind, the signatures of divergent selection displayed in the genomic regions that in this study were associated with the bioclimatic-based drought index are unlikely due to confounding demographic processes such as independent domestication events, extensive population structure and population expansions after bottlenecks because the mixed linear model that we chose to identify the GEA accounted for population structure and demographic processes usually leave genome-wide signatures that should have imprinted the no associated windows as well. Therefore, the signatures displayed on the genetic variants that are associated with drought tolerance seem to reflect true divergent selection rather that confounding demographic processes like independent domestication events, extensive population structure, or population expansions after bottlenecks.

One potential caveat may concern the fact that we used GBS with the *ApeK1* restriction enzyme for the first time in wild accessions of common bean, possibly leading to problems like missing data due to sequence divergence compared to the cultivated reference genome. Nonetheless, wild-cultivated divergent regions with a high proportion of missing data seem to be rare because the U-shaped pattern of SNP density is just as expected when using a non-methylation sensitive enzyme. This decay in diversity proportional to the decay in the rate of recombination (toward the centromeres) was first described in *D. melanogaster* and has been confirmed in many organisms since then (Ellegren and Galtier, 2016). The pattern was understood as an effect of genetic hitchhiking, but background selection may also be a contributing factor, perhaps even the dominating one.

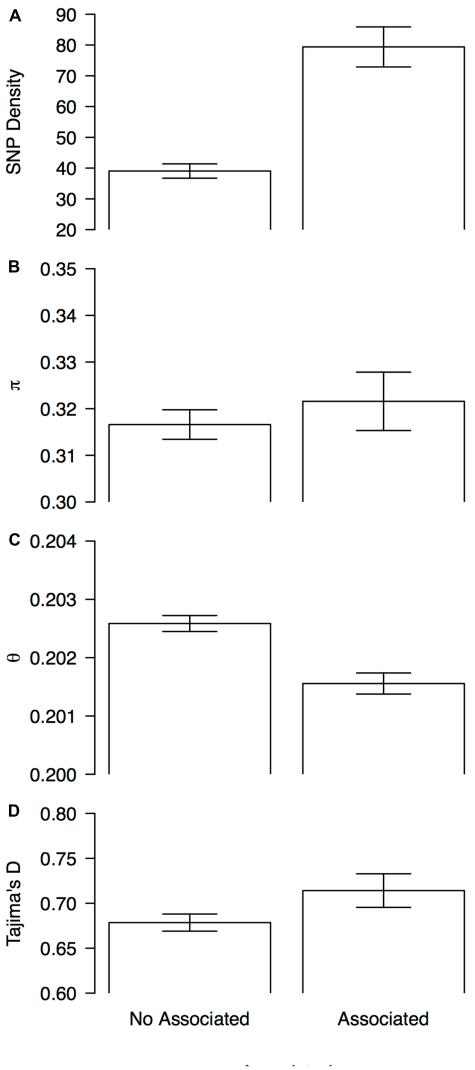

FIGURE 5 | Patterns of genome-wide diversity in genomic windows associated and no associated with drought tolerance. Means and 95% permutation-based confidence intervals are shown for **(A)** SNP density, **(B)** nucleotide diversity as measured by π, **(C)** Watterson's theta estimator (θ), and **(D)** Tajima's D, when computed in sliding windows (window size = 1×10^6 bp, step size = 200 kb) that contained (associated) or did not contained (no associated) at least one marker that was associated with the bioclimatic-based drought index (**Figure 4**).

It is also appropriate to clarify that the power to detect marker-trait associations in this study was not limited by the number of markers. Every three SNPs are redundant and replaceable given a criterion of linkage disequilibrium, or LD (Carlson et al., 2004), which is higher in selfing plants (Slatkin, 2008; Rossi et al., 2009), like common bean (Broughton et al., 2003; Rossi et al., 2009; Blair et al., 2018). At least in humans, a 0.8 R^2 threshold is used to identify maximally informative SNPs for association analyses by

reducing the redundancy due to LD (Carlson et al., 2004), and this could apply to other species as well (Slate et al., 2009). Here, average marker density was 44 SNPs per million base pairs, or average distance between any two SNP markers in the reference genome was 23 thousand base pairs. Since LD in wild common bean, measured as marker correlation R^2, was reported to decay to 0.8 per every 81 thousand base pairs (Rossi et al., 2009; Blair et al., 2018), on average every 3, physically linked, GBS-derived SNP markers are in sufficient LD to be considered redundant by the association analysis.

Finally, despite that the modest sample size used in the association analysis may overlook the majority of associations with low effect sizes and large-effect genes that segregate at low frequency (Maher, 2008), genes with major effects that segregate at moderate frequencies are still identifiable. In fact, this may be the case of a gene coding for an ankyrin repeat-containing protein, associated with osmotic regulation (Voronin and Kiseleva, 2008), and a phototropic-responsive NPH3 gene (Pedmale and Liscum, 2007), found in regions in chromosomes Pv8 and Pv3 flanking associated SNPs with an average R^2 of 49%.

Wild Accessions May Be Useful to Breed Drought Tolerant Varieties in Common Bean

Previous research from Tiranti and Negri (2007) and Ariani et al. (2017) demonstrated that selective micro-environmental effects play a role in shaping genetic diversity and structure in common bean wild accessions. In this study, we have confirmed that ecological gradients related with drought stress are associated with divergent selection in wild common beans, after accounting for genepool and subpopulation structure. This divergent selective pressure might be a consequence of local level rainfall patterns. Specifically, in tropical environments near the equator with bimodal rainfall a mid-season dry period occurs that can last 2–4 weeks. In contrast in the sub-tropics, a dry period of three or more months can occur. In response to this mid-cycle drought of the sub-tropics, *P. vulgaris* enters a survival mode of slow growth and reduced physiological activity until rainfall resumes and flowering occurs (Beebe et al., 2008). Beans growing in wetter conditions on the other hand are less frequently subjected to these environmental pressures and have a fitness advantage to mature in a shorter length of time. Given these ecological differences, the reaction typically associated with drought tolerance although favorable under dry conditions seems detrimental under more humid conditions, which is consistent with the genomic signature of divergent selection observed in this study. This trade-off must be accounted for when breeding for drought tolerance, reinforcing the need of varieties locally adapted to unique micro-environments and narrow regions instead of varieties intended for a wider range of environments (Cortés and Blair, 2018a,b).

Furthermore, wild accessions of common bean occupy more geographical regions with extensive drought stress than cultivated accessions (Cortés et al., 2013). Those regions include the arid areas of Peru, Bolivia, and Argentina, and the valleys of northwest Mexico. Hence, a broad habitat distribution for wild common bean has exposed these genotypes to both dry and wetter conditions, while cultivated common bean has a narrower distribution and is traditionally considered susceptible to drought. These differences in the ecologies of wild and cultivated common bean have been associated with higher genetic diversity in the former group when surveying candidate genes for drought tolerance such as the ASR (Cortés et al., 2012a), DREB (Cortés et al., 2012b), and ERECTA (Blair et al., 2016) gene families, once population structure (Blair et al., 2012) and the background distribution of genetic diversity have been accounted for.

Although not all associated markers may be causal, but rather linked with causal elements, in this study we were able to identify a wide genetic source for drought tolerance, including new potential candidates like a gene coding for an ankyrin repeat-containing protein (Voronin and Kiseleva, 2008) and a phototropic-responsive NPH3 gene (Pedmale and Liscum, 2007). We were also able to identify some further differences between the adaptations of wild accessions found in arid and more humid environments, which may be valuable for plant breeding. Therefore, we reinforce, as was envisioned by Acosta et al. (2007), that wild accessions and landraces of common bean be taken into account to exploit naturally available divergent variation for drought tolerance.

PERSPECTIVES

The potential candidate genes identified in this study should be validated as candidates for drought tolerance through re-sequencing and controlled drought stress treatments under green house and field conditions, ideally in a diverse panel of common bean accessions and closely related species, such as Tepary bean (*P. acutifolius*) that is known for growing in desert and semi-arid environments. Our group is currently running this initiative as part of a larger project spanning several other candidate genes, such as DREB, ASR, and ERECTA (Cortés et al., 2012a,b; Blair et al., 2016).

The work presented here ultimately illustrates that genomic signatures of adaptation are useful for germplasm characterization, potentially enhancing future marker-assisted selection and crop improvement. We envision that GEA studies coupled with estimates of genome-wide diversity will become more common in the oncoming years. They both might allow assessing the naturally available genetic variability for adaptation to various types of stress that, like drought, are expected to worsen with climate change. For instance, frost (Wheeler et al., 2014, 2016), nutrient limitation (Sedlacek et al., 2014; Little et al., 2016), altered snowmelt (Cortés et al., 2015b; Cortés, 2016, 2017a), distorted biotic interactions (Wheeler et al., 2015), and altered growing (Sedlacek et al., 2015, 2016) and flowering (Cortés et al., 2014) seasons, can easily be modeled and associated with allelic variants using a genome-wide diversity background. GEA studies coupled with estimates of genome-wide diversity could also be expandable to heterogeneous collections that include a mix of commercial

accessions, landraces, wild populations and wild relatives, and that span a variety of ecologically diverse managed and natural ecosystems (Madriñán et al., 2013; Cortés and Wheeler, 2018) screened with a wide range of genotyping techniques (Cortés et al., 2011; Galeano et al., 2012; Kelleher et al., 2012; Blair et al., 2013). Genomic selection models, which are becoming increasingly popular (Desta and Ortiz, 2014), in conjunction with a wide-spectrum of stochastic models (Cortés, 2017b, 2018), could even incorporate at some point environmental variables and estimates of genome-wide diversity in order to improve the prediction of phenotypic variance and the estimation of the genotype × environment interactions.

DATA ACCESSIBILITY

The pipeline configuration file and SNP dataset are archived at the Dryad Digital Repository under doi: 10.5061/dryad.j2c24.

AUTHOR CONTRIBUTIONS

AC designed the study with insights from MB. AC collected and analyzed the data. AC wrote the manuscript with contributions from MB.

FUNDING

This research was supported by the Lundell and Tullberg grants to AC as PI. The Geneco mobility fund from Lund University is acknowledged for making possible the synergistic kickoff meeting between AC and MB in the spring of 2015 at Nashville, TN, United States. Writing time by the first author was possible thanks to the grants CTS14:55 from the Carl Trygger Foundation to S. Berlin, and 4.1-2016-00418 from Vetenskapsrådet (VR) and BS2017-0036 from Kungliga Vetenskapsakademien (KVA) to AC, and by MB thanks to the Evans Allen fund from the United States Department of Agriculture. The publication fund of the Colombian Corporation for Agricultural Research is very much appreciated for supporting the publication of this work.

ACKNOWLEDGMENTS

We are grateful to Daniel G. Debouck and the Genetic Resources Unit at the International Center for Tropical Agriculture for donating the seeds and sharing the geographic coordinates of the plant material that was used in this study. Reassurance from J. M. Osorio toward this work is very much appreciated.

SUPPLEMENTARY MATERIAL

The Supplementary Material for this article can be found online at: https://www.frontiersin.org/articles/10.3389/fpls.2018.00128/full#supplementary-material

FIGURE S1 | Boxplot and histogram of the bioclimatic-based drought index (DI), according to Cortés et al. (2013), for the 86 common bean accessions used in this study.

FIGURE S2 | Genome–environment association (GEA) analyses for drought tolerance according to five different general linear models (GLMs) in 86 common bean accessions based on 22,845 GBS-derived SNP markers. Given are Manhattan plots **(A**,**C**,**E**,**G**,**I)** and QQ-plots **(B**,**D**,**F**,**H**,**J)** of $-\log_{10}$ (*P*-value) for the following models: **(A**,**B)** GLM with the genepool identity and the first two PCoA axes scores **(Figure 2)** as covariates; **(C**,**D)** GLM with the within-genepool subpopulation identity, according to Blair et al. (2012), and the first two PCoA axes scores **(Figure 2)** as covariates; **(E**,**F)** GLM with the first two PCoA axes scores **(Figure 2)** as covariates; **(G**,**H)** GLM with the within-genepool subpopulation identity, according to Blair et al. (2012), as covariate; and **(I**,**J)** GLM with the genepool identity as covariate. The bioclimatic-based drought index follows Cortés et al. (2013). The gray dashed horizontal line marks the *P*-value threshold after Bonferroni-correction for multiple comparisons. Black and gray colors highlight different common bean (Pv) chromosomes.

FIGURE S3 | Genome–environment association (GEA) analyses for drought tolerance according to five different mixed linear models (MLMs) in 86 common bean accessions based on 22,845 GBS-derived SNP markers. Given are Manhattan plots **(A**,**C**,**E**,**G**,**I)** and QQ-plots **(B**,**D**,**F**,**H**,**J)** of $-\log_{10}$ (*P*-value) for the following models: **(A**,**B)** MLM with the genepool identity and the first two PCoA axes scores **(Figure 2)** as covariates; **(C**,**D)** MLM with the within-genepool subpopulation identity, according to Blair et al. (2012), and the first two PCoA axes scores **(Figure 2)** as covariates; **(E**,**F)** MLM with the first two PCoA axes scores **(Figure 2)** as covariates (model shown in **Figure 3**); **(G**,**H)** MLM with the within-genepool subpopulation identity, according to Blair et al. (2012), as covariate; and **(I**,**J)** MLM with the genepool identity as covariate. All models used a centered IBS kinship matrix as a random effect. The bioclimatic-based drought index follows Cortés et al. (2013). The gray dashed horizontal line marks the *P*-value threshold after Bonferroni-correction for multiple comparisons. Black and gray colors highlight different common bean (Pv) chromosomes.

TABLE S1 | Identity of the 86 common bean accessions used in this study. The G identification number (from the Genetic Resources Unit at the International Center for Tropical Agriculture) and the country of origin are shown according to the following convention: ARG for Argentina, BOL for Bolivia, COL for Colombia, ECU for Ecuador, GTM for Guatemala, HND for Honduras, MEX for Mexico and PER for Peru. The bioclimatic-based drought index (DI) according to Cortés et al. (2013) is also shown (and in **Supplementary Figure S1**). It appears in red if the accession was found in a dry environment (high drought index, above zero) or in blue if it was found in a very wet habitat (low drought index, below zero).

TABLE S2 | Statistics from the optimum association analysis for the 115 SNP markers associated with the bioclimatic-based drought index in 86 common bean accessions based on 22,845 GBS-derived SNP markers. Given are results of a mixed linear model (depicted in **Figure 3**) with a centered IBS kinship matrix as a random effect, and the first two PCoA axes scores (**Figure 2**) as covariates. Among other statistics, the *F*-value, the $-\log_{10}$ (*P*-value) and the variation explained (R^2) by each marker, are shown. Marker names are given as chromosome and position on the common bean reference genome from Schmutz et al. (2014). Unique regions containing one or more SNPs are named with a consecutive number per chromosome under the column called "region." Gray cells in this column mark regions with two or more associated SNPs. Regions are defined here as overlapping 1,000 bp sections that flanked associated markers.

TABLE S3 | List of 77 genes in the 75 associated regions that contained at least one gene. The position of each gene and its functional description are shown together with other identifiers and descriptors. The list of associated SNP markers surrounding each gene is also depicted, for a total of 99 SNPs. Genes co-occurring in the same region are marked with gray cell under the column "associated SNPs." Regions are defined here as overlapping 1,000 bp sections that flanked associated markers.

REFERENCES

Acosta, J. A., Kelly, J. D., and Gepts, P. (2007). Prebreeding in common bean and use of genetic diversity from wild germplasm. *Crop Sci.* 47, S44–S59. doi: 10.2135/cropsci2007.04.0008IPBS

Ariani, A., Berny, J. C., and Gepts, P. (2016). Genome-wide identification of SNPs and copy number variation in common bean (*Phaseolus vulgaris* L.) Using Genotyping-by-Sequencing (Gbs). *Mol. Breed.* 36:87. doi: 10.1007/s11032-016-0512-9

Ariani, A., Berny Mier, Y. T. J., and Gepts, P. (2017). Spatial and temporal scales of range expansion in wild *Phaseolus vulgaris*. *Mol. Biol. Evol.* 35, 119–131. doi: 10.1093/molbev/msx273

Barrett, R. D., and Schluter, D. (2008). Adaptation from standing genetic variation. *Trends Ecol. Evol.* 23, 38–44. doi: 10.1016/j.tree.2007.09.008

Beebe, S., Rao, I. M., Cajiao, C., and Grajales, M. (2008). Selection for drought resistance in common bean also improves yield in phosphorus limited and favorable environments. *Crop Sci.* 48, 582–592. doi: 10.2135/cropsci2007.07.0404

Berthouly-Salazar, C., Thuillet, A. C., Rhone, B., Mariac, C., Ousseini, I. S., Couderc, M., et al. (2016). Genome scan reveals selection acting on genes linked to stress response in wild pearl millet. *Mol. Ecol.* 25, 5500–5512. doi: 10.1111/mec.13859

Bhakta, M. S., Jones, V. A., and Vallejos, C. E. (2015). Punctuated distribution of recombination hotspots and demarcation of pericentromeric regions in *Phaseolus vulgaris* L. *PLoS One* 10:e0116822. doi: 10.1371/journal.pone.0116822

Blair, M. W., Cortés, A. J., Farmer, A. R., Wei, H., Ambachew, D., Penmetsa, V., et al., (2018). Uneven recombination rate and linkage disequilibrium across a reference SNP map for common bean (*Phaseolus vulgaris* L.). *PLoS One*. doi: 10.1371/journal.pone.0189597

Blair, M. W., Cortés, A. J., Penmetsa, R. V., Farmer, A., Carrasquilla-Garcia, N., and Cook, D. R. (2013). A high-throughput Snp marker system for parental polymorphism screening, and diversity analysis in common bean (*Phaseolus vulgaris* L.). *Theor. Appl. Genet.* 126, 535–548. doi: 10.1007/s00122-012-1999-z

Blair, M. W., Cortés, A. J., and This, D. (2016). Identification of an *Erecta* gene and its drought adaptation associations with wild and cultivated common bean. *Plant Sci.* 242, 250–259. doi: 10.1016/j.plantsci.2015.08.004

Blair, M. W., Soler, A., and Cortés, A. J. (2012). Diversification and population structure in common beans (*Phaseolus vulgaris* L.). *PLoS One* 7:e49488. doi: 10.1371/journal.pone.0049488

Bradbury, P. J., Zhang, Z., Kroon, D. E., Casstevens, T. M., Ramdoss, Y., and Buckler, E. S. (2007). Tassel: software for association mapping of complex traits in diverse samples. *Bioinformatics* 23, 2633–2635. doi: 10.1093/bioinformatics/btm308

Broughton, W. J., Hernandez, G., Blair, M., Beebe, S., Gepts, P., and Vanderleyden, J. (2003). Beans (Phaseolus Spp.) - model food legumes. *Plant Soil* 252, 55–128. doi: 10.1023/A:1024146710611

Carlson, C. S., Eberle, M. A., Rieder, M. J., Yi, Q., Kruglyak, L., and Nickerson, D. A. (2004). Selecting a maximally informative set of single-nucleotide polymorphisms for association analyses using linkage disequilibrium. *Am. J. Hum. Genet.* 74, 106–120. doi: 10.1086/381000

Cortés, A. J. (2013). On the origin of the common bean (*Phaseolus vulgaris* L.). *Am. J. Plant Sci.* 4, 1998–2000. doi: 10.4236/ajps.2013.410248

Cortés, A. J. (2015). *On the Big Challenges of a Small Shrub: Ecological Genetics of Salix Herbacea L*. Uppsala: Acta Universitatis Upsaliensis.

Cortés, A. J. (2016). *Environmental Heterogeneity at a Fine Scale: Ecological and Genetic Implications in a Changing World*. Saarbrücken: LAP Lambert Academic Publishing.

Cortés, A. J. (2017a). "Local scale genetic diversity and its role in coping with changing climate," in *Genetic Diversity*, ed. L. Bitz (Rijeka: InTech), 140. doi: 10.5772/67166

Cortés, A. J. (2017b). On how role versatility boosts an STI. *J. Theor. Biol.* 440, 66–69. doi: 10.1016/j.jtbi.2017.12.018

Cortés, A. J. (2018). "Prevalence in MSM is enhanced by role versatility," in *Big Data Analytics in HIV/AIDS Research*, ed. A. Mazari (Hershey: IGI Global), 250.

Cortés, A. J., and Blair, M. W. (2018a). "Lessons from common bean on how wild relatives and landraces can make tropical crops more resistant to climate change," in *Rediscovery of Landraces as a Resource for the Future*, ed. O. Grillo (Rijeka: InTech), 165.

Cortés, A. J., and Blair, M. W. (2018b). "Naturally available genetic adaptation in Common bean and its response to climate change," in *Climate Resilient Agriculture – Strategies and Perspectives*, eds C. Srinivasarao, A. K. Shanker, and C. Shanker (Rijeka: InTech), 133. doi: 10.5772/intechopen.72380

Cortés, A. J., Chavarro, M. C., and Blair, M. W. (2011). Snp marker diversity in common bean (*Phaseolus vulgaris* L.). *Theor. Appl. Genet.* 123, 827–845. doi: 10.1007/s00122-011-1630-8

Cortés, A. J., Chavarro, M. C., Madriñán, S., This, D., and Blair, M. W. (2012a). Molecular ecology and selection in the drought-related *Asr* gene polymorphisms in wild and cultivated common bean (*Phaseolus vulgaris* L.). *BMC Genet.* 13:58. doi: 10.1186/1471-2156-13-58

Cortés, A. J., Liu, X., Sedlacek, J., Wheeler, J. A., Lexer, C., and Karrenberg, S. (2015a). "Maintenance of female-bias in a polygenic sex determination system is consistent with genomic conflict," in *On the Big Challenges of a Small Shrub: Ecological Genetics of Salix herbacea L*, ed. A. J. Cortés (Uppsala: Acta Universitatis Upsaliensis).

Cortés, A. J., Monserrate, F., Ramírez-Villegas, J., Madriñán, S., and Blair, M. W. (2013). Drought tolerance in wild plant populations: the case of common beans (*Phaseolus vulgaris* L.). *PLoS One* 8:e62898. doi: 10.1371/journal.pone.0062898

Cortés, A. J., This, D., Chavarro, C., Madriñán, S., and Blair, M. W. (2012b). Nucleotide diversity patterns at the drought-related *Dreb2* encoding genes in wild and cultivated common bean (*Phaseolus vulgaris* L.). *Theor. Appl. Genet.* 125, 1069–1085. doi: 10.1007/s00122-012-1896-5

Cortés, A. J., Waeber, S., Lexer, C., Sedlacek, J., Wheeler, J. A., Van Kleunen, M., et al. (2014). Small-scale patterns in snowmelt timing affect gene flow and the distribution of genetic diversity in the alpine dwarf shrub *Salix herbacea*. *Heredity* 113, 233–239. doi: 10.1038/hdy.2014.19

Cortés, A. J., and Wheeler, J. A. (2018). "The environmental heterogeneity of mountains at a fine scale in a changing world," in *Mountains, Climate, and Biodiversity*, eds C. Hoorn, A. Perrigo, and A. Antonelli (Hoboken: Wiley), 584.

Cortés, A. J., Wheeler, J. A., Sedlacek, J., Lexer, C., and Karrenberg, S. (2015b). "Genome-wide patterns of microhabitat-driven divergence in the alpine dwarf shrub *Salix herbacea* L," in *On the Big Challenges of a Small Shrub: Ecological Genetics of Salix herbacea L*, ed. A. J. Cortés (Uppsala: Acta Universitatis Upsaliensis).

Des Marais, D. L., Auchincloss, L. C., Sukamtoh, E., Mckay, J. K., Logan, T., Richards, J. H., et al. (2014). Variation in *Mpk12* affects water use efficiency in *Arabidopsis* and reveals a pleiotropic link between guard cell size and Aba response. *Proc. Natl. Acad. Sci. U.S.A.* 111, 2836–2841. doi: 10.1073/pnas.1321429111

Desta, Z. A., and Ortiz, R. (2014). Genomic selection: genome-wide prediction in plant improvement. *Trends Plant Sci.* 19, 592–601. doi: 10.1016/j.tplants.2014.05.006

Ellegren, H., and Galtier, N. (2016). Determinants of genetic diversity. *Nat. Rev. Genet.* 17, 422–433. doi: 10.1038/nrg.2016.58

Elshire, R. J., Glaubitz, J. C., Sun, Q., Poland, J. A., Kawamoto, K., Buckler, E. S., et al. (2011). A robust, simple genotyping-by-sequencing (Gbs) approach for high diversity species. *PLoS One* 6:e19379. doi: 10.1371/journal.pone.0019379

Fischer, M. C., Rellstab, C., Tedder, A., Zoller, S., Gugerli, F., Shimizu, K. K., et al. (2013). Population genomic footprints of selection and associations with climate in natural populations of *Arabidopsis halleri* from the Alps. *Mol. Ecol.* 22, 5594–5607. doi: 10.1111/mec.12521

Forester, B. R., Jones, M. R., Joost, S., Landguth, E. L., and Lasky, J. R. (2016). Detecting spatial genetic signatures of local adaptation in heterogeneous landscapes. *Mol. Ecol.* 25, 104–120. doi: 10.1111/mec.13476

Galeano, C. H., Cortés, A. J., Fernandez, A. C., Soler, A., Franco-Herrera, N., Makunde, G., et al. (2012). Gene-based single nucleotide polymorphism markers for genetic and association mapping in common bean. *BMC Genet.* 13:48. doi: 10.1186/1471-2156-13-48

Gepts, P., and Debouck, D. (1991). "Origin, domestication and evolution of the common bean (*Phaseolus vulgaris* L.)," in *Common Beans: Research for Crop Improvement*, eds A. Van Shoonhoven and O. Voysest (Wallingford: Commonwealth Agricultural Bureau), 7–53.

Glaubitz, J. C., Casstevens, T. M., Lu, F., Harriman, J., Elshire, R. J., Sun, Q., et al. (2014). Tassel-Gbs: a high capacity genotyping by sequencing analysis pipeline. *PLoS One* 9:e90346. doi: 10.1371/journal.pone.0090346

Hamon, W. R. (1961). Estimating potential evapotranspiration. *Proc. Am. Soc. Civil Eng.* 87, 107–120.

Hancock, A. M., Brachi, B., Faure, N., Horton, M. W., Jarymowycz, L. B., Sperone, F. G., et al. (2011). Adaptation to climate across the *Arabidopsis thaliana* Genome. *Science* 334, 83–86. doi: 10.1126/science.1209244

Hart, J. P., and Griffiths, P. D. (2015). Genotyping-by-sequencing enabled mapping and marker development for the Potyvirus resistance allele in common bean. *Plant Genome* 8. doi: 10.3835/plantgenome2014.09.0058

Hermisson, J., and Pennings, P. S. (2005). Soft sweeps: molecular population genetics of adaptation from standing genetic variation. *Genetics* 169, 2335–2352. doi: 10.1534/genetics.104.036947

Hijmans, R. J., Cameron, S. E., Parra, J. L., Jones, P. G., and Jarvis, A. (2005). Very high resolution interpolated climate surfaces for global land areas. *Int. J. Climatol.* 25, 1965–1978. doi: 10.1002/joc.1276

Hoffmann, A. A., and Sgro, C. M. (2011). Climate change and evolutionary adaptation. *Nature* 470, 479–485. doi: 10.1038/nature09670

Kelleher, C. T., Wilkin, J., Zhuang, J., Cortés, A. J., Quintero, Á. L. P., Gallagher, T. F., et al. (2012). Snp discovery, gene diversity, and linkage disequilibrium in wild populations of *Populus tremuloides*. *Tree Genet. Genomes* 8, 821–829. doi: 10.1007/s11295-012-0467-x

Kwak, M., and Gepts, P. (2009). Structure of genetic diversity in the two major gene pools of common bean (*Phaseolus vulgaris* L., Fabaceae). *Theor. Appl. Genet.* 118, 979–992. doi: 10.1007/s00122-008-0955-4

Lasky, J. R., Des Marais, D. L., Mckay, J. K., Richards, J. H., Juenger, T. E., and Keitt, T. H. (2012). Characterizing genomic variation of *Arabidopsis thaliana*: the roles of geography and climate. *Mol. Ecol.* 21, 5512–5529. doi: 10.1111/j.1365-294X.2012.05709.x

Lasky, J. R., Upadhyaya, H. D., Ramu, P., Deshpande, S., Hash, C. T., Bonnette, J., et al. (2015). Genome-environment associations in sorghum landraces predict adaptive traits. *Sci. Adv.* 1:e1400218. doi: 10.1126/sciadv.1400218

Li, H., and Durbin, R. (2007). Fast and accurate short read alignment with burrows-wheeler transform. *Bioinformatics* 25, 1754–1760. doi: 10.1093/bioinformatics/btp324

Little, C. J., Wheeler, J. A., Sedlacek, J., Cortés, A. J., and Rixen, C. (2016). Small-scale drivers: the importance of nutrient availability and snowmelt timing on performance of the alpine shrub *Salix herbacea*. *Oecologia* 180, 1015–1024. doi: 10.1007/s00442-015-3394-3

Madriñán, S., Cortés, A. J., and Richardson, J. E. (2013). Páramo is the world's fastest evolving and coolest biodiversity hotspot. *Front. Genet.* 4:192. doi: 10.3389/fgene.2013.00192

Maher, B. (2008). Missing Heritability. *Nature* 456, 18–21.

Nei, M. (1987). *Molecular Evolutionary Genetics*. New York, NY: Columbia University Press.

Nei, M. (2010). The neutral theory of molecular evolution in the genomic era. *Annu. Rev. Genomics Hum. Genet.* 11, 265–289. doi: 10.1146/annurev-genom-082908-150129

Pedmale, U. V., and Liscum, E. (2007). Regulation of phototropic signaling in Arabidopsis via phosphorylation state changes in the phototropin 1-interacting protein Nph3. *J. Biol. Chem.* 282, 19992–20001. doi: 10.1074/jbc.M702551200

Pluess, A. R., Frank, A., Heiri, C., Lalague, H., Vendramin, G. G., and Oddou-Muratorio, S. (2016). Genome-environment association study suggests local adaptation to climate at the regional scale in *Fagus sylvatica*. *New Phytol.* 210, 589–601. doi: 10.1111/nph.13809

Pritchard, J. K., Pickrell, J. K., and Coop, G. (2010). The genetics of human adaptation: hard sweeps, soft sweeps, and polygenic adaptation. *Curr. Biol.* 20, R208–R215. doi: 10.1016/j.cub.2009.11.055

Rendón-Anaya, M., Montero-Vargas, J. M., Saburido-aìLvarez, S., Vlasova, A., Capella-Gutierrez, S., Ordaz-Ortiz, J. J., et al. (2017). Genomic history of the origin and domestication of common bean unveils its closest Sister Species. *Genome Biol.* 18:60. doi: 10.1186/s13059-017-1190-6

Rosenberg, N. A., Huang, L., Jewett, E. M., Szpiech, Z. A., Jankovic, I., and Boehnk, M. (2010). Genome–wide association studies in diverse populations. *Nat. Rev. Genet.* 11, 356–366. doi: 10.1038/nrg2760

Rossi, M., Bitocchi, E., Bellucci, E., Nanni, L., Rau, D., Attene, G., et al. (2009). Linkage disequilibrium and population structure in wild and domesticated populations of *Phaseolus vulgaris* L. *Evol. Appl.* 2, 504–522. doi: 10.1111/j.1752-4571.2009.00082.x

Savolainen, O., Lascoux, M., and Merilä, J. (2013). Ecological genomics of local adaptation. *Nat. Rev. Genet.* 14, 807–820. doi: 10.1038/nrg3522

Schmutz, J., Mcclean, P. E., Mamidi, S., Wu, G. A., Cannon, S. B., Grimwood, J., et al. (2014). A reference genome for common bean and genome-wide analysis of dual domestications. *Nat. Genet.* 46, 707–713. doi: 10.1038/ng.3008

Schroder, S., Mamidi, S., Lee, R., Mckain, M. R., Mcclean, P. E., and Osorno, J. M. (2016). Optimization of genotyping by sequencing (Gbs) data in common bean (*Phaseolus vulgaris* L.). *Mol. Breed.* 36:6. doi: 10.1007/s11032-015-0431-1

Sedlacek, J., Bossdorf, O., Cortés, A. J., Wheeler, J. A., and Van-Kleunen, M. (2014). What role do plant-soil interactions play in the habitat suitability and potential range expansion of the alpine dwarf shrub *Salix herbacea*? *Basic Appl. Ecol.* 15, 305–315. doi: 10.1016/j.baae.2014.05.006

Sedlacek, J., Cortés, A. J., Wheeler, J. A., Bossdorf, O., Hoch, G., Klapste, J., et al. (2016). Evolutionary potential in the alpine: trait heritabilities and performance variation of the dwarf willow *Salix herbacea* from different elevations and microhabitats. *Ecol. Evol.* 6, 3940–3952. doi: 10.1002/ece3.2171

Sedlacek, J., Wheeler, J. A., Cortés, A. J., Bossdorf, O., Hoch, G., Lexer, C., et al. (2015). The response of the alpine dwarf shrub *Salix herbacea* to altered snowmelt timing: lessons from a multi-site transplant experiment. *PLoS One* 10:e0122395. doi: 10.1371/journal.pone.0122395

Slate, J., Gratten, J., Beraldi, D., Stapley, J., Hale, M., and Pemberton, J. M. (2009). Gene mapping in the wild with SNPs: guidelines and future directions. *Genetica* 136, 97–107. doi: 10.1007/s10709-008-9317-z

Slatkin, M. (2008). Linkage disequilibrium—understanding the evolutionary past and mapping the medical future. *Nat. Rev. Genet.* 9, 477–485. doi: 10.1038/nrg2361

Stinchcombe, J. R., and Hoekstra, H. E. (2008). Combining population genomics and quantitative genetics: finding the genes underlying ecologically important traits. *Heredity* 100, 158–170. doi: 10.1038/sj.hdy.6800937

Strasburg, J. L., Sherman, N. A., Wright, K. M., Moyle, L. C., Willis, J. H., and Rieseberg, L. H. (2011). What can patterns of differentiation across plant genomes tell us about adaptation and speciation? *Philos. Trans. R. Soc. B Biol. Sci.* 367, 364–373. doi: 10.1098/rstb.2011.0199

Tai, A. P. K., Martin, M. V., and Heald, C. L. (2014). Threat to future global food security from climate change and ozone air pollution. *Nat. Clim. Change* 4, 817–821. doi: 10.1038/nclimate2317

Tajima, F. (1989). Statistical method for testing the neutral mutation hypothesis by DNA polymorphism. *Genetics* 123, 585–595.

Thornthwaite, C. W., and Mather, J. R. (1957). Instructions and tables for computing potential evapotranspiration and the water balance. *Climatology* 10, 185–311.

Tiranti, B., and Negri, V. (2007). Selective microenvironmental effects play a role in shaping genetic diversity and structure in a *Phaseolus vulgaris* L. Landrace: implications for on-farm conservation. *Mol. Ecol.* 16, 4942–4955. doi: 10.1111/j.1365-294X.2007.03566.x

Tohme, J., González, O., Beebe, S., and Duque, M. C. (1996). Aflp analysis of gene pools of a wild bean core collection. *Crop Sci.* 36, 1375–1384. doi: 10.2135/cropsci1996.0011183X003600050048x

Turner, T. L., Bourne, E. C., Von Wettberg, E. J., Hu, T. T., and Nuzhdin, S. V. (2010). Population resequencing reveals local adaptation of *Arabidopsis lyrata* to serpentine soils. *Nat. Genet.* 42, 260–263. doi: 10.1038/ng.515

Valdisser, P. A. M. R., Pereira, W. J., Almeida, J. E., MuüLler, B. S. F., Coelho, G. R. C., and de Menezes, I. P. P. (2017). In-depth genome characterization of a Brazilian common bean core collection using dartseq high-density Snp genotyping. *BMC Genomics* 18:423. doi: 10.1186/s12864-017-3805-4

Voronin, D. A., and Kiseleva, E. V. (2008). Functional role of proteins containing ankyrin repeats. *Cell Tissue Biol.* 2, 1–12. doi: 10.1134/S1990519X0801001X

Wakeley, J. (2008). *Coalescent Theory: An Introduction*. Cambridge: Harvard University.

Watterson, G. A. (1975). Number of segregating sites in genetic models without recombination. *Theor. Popul. Biol.* 7, 256–276. doi: 10.1016/0040-5809(75)90020-9

Wheeler, J. A., Cortés, A. J., Sedlacek, J., Karrenberg, S., Van Kleunen, M., Wipf, S., et al. (2016). The snow and the willows: accelerated spring snowmelt

reduces performance in the low-lying alpine shrub *Salix herbacea*. *J. Ecol.* 104, 1041–1050. doi: 10.1111/1365-2745.12579

Wheeler, J. A., Hoch, G., Cortés, A. J., Sedlacek, J., Wipf, S., and Rixen, C. (2014). Increased spring freezing vulnerability for alpine shrubs under early snowmelt. *Oecologia* 175, 219–229. doi: 10.1007/s00442-013-2872-8

Wheeler, J. A., Schnider, F., Sedlacek, J., Cortés, A. J., Wipf, S., Hoch, G., et al. (2015). With a little help from my friends: community facilitation increases performance in the dwarf shrub *Salix herbacea*. *Basic Appl. Ecol.* 16, 202–209. doi: 10.1016/j.baae.2015.02.004

Wolf, J. B., and Ellegren, H. (2016). Making sense of genomic islands of differentiation in light of speciation. *Nat. Rev. Genet.* 18, 87–100. doi: 10.1038/nrg.2016.133

Yeaman, S., Kathryn, A. H., Katie, E., Lotterhos, K. E., Suren, H., and Nadeau, S. (2016). Convergent local adaptation to climate in distantly related conifers. *Science* 353, 1431–1433. doi: 10.1126/science.aaf7812

Yoder, J. B., Stanton-Geddes, J., Zhou, P., Briskine, R., Young, N. D., and Tiffin, P. (2014). Genomic signature of adaptation to climate in *Medicago truncatula*. *Genetics* 196, 1263–1275. doi: 10.1534/genetics.113.159319

Zhang, Z., Ersoz, E., Lai, C. Q., Todhunter, R. J., Tiwari, H. K., Gore, M. A., et al. (2010). Mixed linear model approach adapted for genome-wide association studies. *Nat. Genet.* 42, 355–360. doi: 10.1038/ng.546

Zou, X., Shi, C., Austin, R. S., Merico, D., Munholland, S., Marsolais, F., et al. (2013). Genome-wide single nucleotide polymorphism and insertion-deletion discovery through next-generation sequencing of reduced representation libraries in common bean. *Mol. Breed.* 33, 769–778. doi: 10.1007/s11032-013-9997-7

Conflict of Interest Statement: The authors declare that the research was conducted in the absence of any commercial or financial relationships that could be construed as a potential conflict of interest.

frontiers in Plant Science

ORIGINAL RESEARCH
published: 12 February 2018
doi: 10.3389/fpls.2018.00005

Abiotic Stresses Modulate Landscape of Poplar Transcriptome via Alternative Splicing, Differential Intron Retention, and Isoform Ratio Switching

*Sergei A. Filichkin[1‡], Michael Hamilton[2‡], Palitha D. Dharmawardhana[1], Sunil K. Singh[1†], Christopher Sullivan[3], Asa Ben-Hur[2], Anireddy S. N. Reddy[4] and Pankaj Jaiswal[1]**

[1] Department of Botany and Plant Pathology, Oregon State University, Corvallis, OR, United States, [2] Department of Computer Science, Colorado State University, Fort Collins, CO, United States, [3] Center for Genome Research and Biocomputing, Oregon State University, Corvallis, OR, United States, [4] Department of Biology and Program in Cell and Molecular Biology, Colorado State University, Fort Collins, CO, United States

Abiotic stresses affect plant physiology, development, growth, and alter pre-mRNA splicing. Western poplar is a model woody tree and a potential bioenergy feedstock. To investigate the extent of stress-regulated alternative splicing (AS), we conducted an in-depth survey of leaf, root, and stem xylem transcriptomes under drought, salt, or temperature stress. Analysis of approximately one billion of genome-aligned RNA-Seq reads from tissue- or stress-specific libraries revealed over fifteen millions of novel splice junctions. Transcript models supported by both RNA-Seq and single molecule isoform sequencing (Iso-Seq) data revealed a broad array of novel stress- and/or tissue-specific isoforms. Analysis of Iso-Seq data also resulted in the discovery of 15,087 novel transcribed regions of which 164 show AS. Our findings demonstrate that abiotic stresses profoundly perturb transcript isoform profiles and trigger widespread intron retention (IR) events. Stress treatments often increased or decreased retention of specific introns – a phenomenon described here as differential intron retention (DIR). Many differentially retained introns were regulated in a stress- and/or tissue-specific manner. A subset of transcripts harboring super stress-responsive DIR events showed persisting fluctuations in the degree of IR across all treatments and tissue types. To investigate coordinated dynamics of intron-containing transcripts in the study we quantified absolute copy number of isoforms of two conserved transcription factors (TFs) using Droplet Digital PCR. This case study suggests that stress treatments can be associated with coordinated switches in relative ratios between fully spliced and intron-retaining isoforms and may play a role in adjusting transcriptome to abiotic stresses.

Keywords: western poplar, transcriptome, alternative splicing, abiotic stress, isoform switching, differential intron retention, stress adaptation

OPEN ACCESS

Edited by:
Jose M. Pardo,
Instituto de Bioquímica Vegetal y Fotosíntesis (CSIC), Spain

Reviewed by:
Ping Lan,
Institute of Soil Science (CAS), China
Umesh K. Reddy,
West Virginia State University, United States

****Correspondence:***
Pankaj Jaiswal
jaiswalp@science.oregonstate.edu

†Present address:
Sunil K. Singh,
Department of Biology, University of North Dakota, Grand Forks, ND, United States

‡Co-first authors

Specialty section:
This article was submitted to Plant Abiotic Stress, a section of the journal Frontiers in Plant Science

Received: *20 October 2017*
Accepted: *03 January 2018*
Published: *12 February 2018*

Citation:
Filichkin SA, Hamilton M, Dharmawardhana PD, Singh SK, Sullivan C, Ben-Hur A, Reddy ASN and Jaiswal P (2018) Abiotic Stresses Modulate Landscape of Poplar Transcriptome via Alternative Splicing, Differential Intron Retention, and Isoform Ratio Switching. Front. Plant Sci. 9:5. doi: 10.3389/fpls.2018.00005

INTRODUCTION

Alternative splicing (AS) can increase a complexity of transcriptome and proteome via generating multiple transcripts and protein isoforms from the single gene. Up to 95% of mammalian precursor messenger RNAs (pre-mRNAs) are alternatively spliced (Pan et al., 2008) whereas recent studies in higher plants suggest that AS is fairly conserved (Mei et al., 2017a) and is observed in approximately 42–61% of intron-containing genes (Filichkin et al., 2010; Marquez et al., 2012). Common types of AS include intron retention (IR), exon skipping (ES), the alternative donor (alt 5′) or acceptor (alt 3′) splice site, and mutually exclusive exons (**Figure 1A**). IR is the prevalent mode of AS in plants and represents at least ∼40% of all AS events (Filichkin et al., 2010; Marquez et al., 2012; Shen et al., 2014) whereas ES is considered a predominant mode in animals (Pan et al., 2008). AS resulting in alternative open reading frames may increase proteome diversity. Increasing evidence suggests that AS is involved in regulation of development and cellular responses to environmental stresses in plants (Wang and Brendel, 2006; Barbazuk et al., 2008; Filichkin et al., 2010, 2015a; Vitulo et al., 2014; Li et al., 2016; Mei et al., 2017b). High salinity stress affects AS and IR of ∼49% of all intron-containing *Arabidopsis* genes (Ding et al., 2014). Heat stress triggers widespread IR including specific events in the first line response factors such as heat shock transcription factors (TFs) (Filichkin et al., 2010; Jiang et al., 2017). Drought is another common stress that profoundly perturbs AS patterns. Conversely, a single aberrant ES event in the *Arabidopsis* mRNA encoding *Δ1-pyrroline-5-carboxylate synthase1* reduced plant drought tolerance (Kesari et al., 2012).

Both full IR and alternative donor (Alt 5′) and acceptor (Alt 3′) events often introduce premature termination codons (PTCs) and trigger nonsense-mediated mRNA decay (NMD) in mammals (Maquat, 2005), flies (Nicholson and Muhlemann, 2010), and worms (Casadio et al., 2015). However, despite the presence of such NMD-eliciting features, the majority of *Arabidopsis* transcripts with full IR escape the NMD pathway (Kalyna et al., 2012). In contrast, many Alt 5′ and Alt 3′ events can elicit NMD response (Filichkin and Mockler, 2012; Kalyna et al., 2012; Staiger and Brown, 2013; Filichkin et al., 2015b). One possible explanation of NMD-insensitivity of the full intron-retaining mRNAs is their reversible sequestration (Boothby and Wolniak, 2011; Boothby et al., 2013; Filichkin et al., 2015a). Indeed, Boothby et al. (2013) showed that translation of such masked mRNAs in the male gametophyte of the fern *Marsilea vestita* activated upon introns removal.

In contrast to plants, ES is a predominant type of AS in mammalian cells. However, recent close examination of high coverage RNA-Seq data suggested that IR can affect as many as three-quarters of all mammalian genes with multiple exons (Braunschweig et al., 2014). Significantly, widespread IR is a signature feature of many human cancers (Dvinge and Bradley, 2015) and plays a role in the mechanism of tumor-suppressor inactivation (Jung and Lee, 2015). Even though IR is a prevailing mode of AS in higher plants its functional role(s) during stress adaptation remain unclear.

Western poplar (*Populus trichocarpa*) is a model woody plant and a commercial crop with a potential for bioenergy production. *Populus* species from different geographical zones display remarkably flexible adaptation to diverse environmental conditions (Soolanayakanahally et al., 2015). Increasing evidence suggests that AS is widespread and diversified across *Populus* species and could potentially contribute to the environmental adaptation, development of specialized tissues such as secondary xylem (wood) (Bao et al., 2013). Up to 25% of AS events in poplar (Xu et al., 2014) are estimated to generate protein domain modifications and therefore may contribute to proteome complexity during adaptation to the stresses. However, a comprehensive analysis of global changes in AS events across all main poplar tissues types induced by common abiotic stresses is currently unavailable. Here, we conducted a high resolution survey of AS and IR events in leaf, stem xylem, and root tissues under drought, salt, and temperature stresses. Stress-induced statistically significant IR rates were calculated across all detected IR events. We found that differential intron retention (DIR) is a widespread and often tissue- and/or stress-specific phenomenon in poplar. We identified subsets of transcripts showing similar dynamics of differential IR. Case study of two conserved eukaryotic TFs showed that relative ratios of DIR-harboring isoforms decrease during stress-induced up-regulation of their fully spliced mRNAs and vice versa. Analyses of both RNA-Seq and Iso-Seq (single molecule real time isoform sequencing) datasets generated thousands of novel protein-coding and non-coding gene models including those encoding for stress- and/or tissue-specific transcripts.

MATERIALS AND METHODS

Plant Materials and Growth Conditions

Approximately 3 months old plants of Western poplar (*P. trichocarpa,* clone Nisqually 1) were propagated from stem cuttings and grown in 2 L pots at 12 h day/12 h night photo cycles with light intensity 300 μmoles/m^2/s. For heat stress, plants were treated at 39°C for 12 h (short term) or 7 days (prolonged). For cold stress plants were subjected to 4°C (night) and 12°C (day) for 24 h (short term) or 7 days (prolonged). For drought treatment watering was withheld until the moisture of soil reached 0.1 m^3/m^3 and maintained at the level of 0.06 – 0.1 m^3/m^3. For a short term drought, stress plants were grown for 5 days after water withholding (an initial leaf wilting point) or for 7 days after initial leaf wilting (prolonged treatment, 12 days after withholding water). For high salinity, stress plants were treated with 100 mM sodium chloride solution for 24 h (short term) or for 7 days (prolonged). Root, leaf, and xylem tissues from both short- and long-term treatments were collected each in three independent biological replicates (**Supplementary File 1**). Controls represented the same tissue types of untreated plants. For the high resolution heat-cold stress time course plants were subjected to the 24 h heat treatment (42°C) followed by the 24 h incubation at 4°C. Leaf tissues were collected at 0, 2, 4, 6, 8, 10, and 24 h time points during the interval of each treatment. Leaves, including petioles, were collected from the medium third

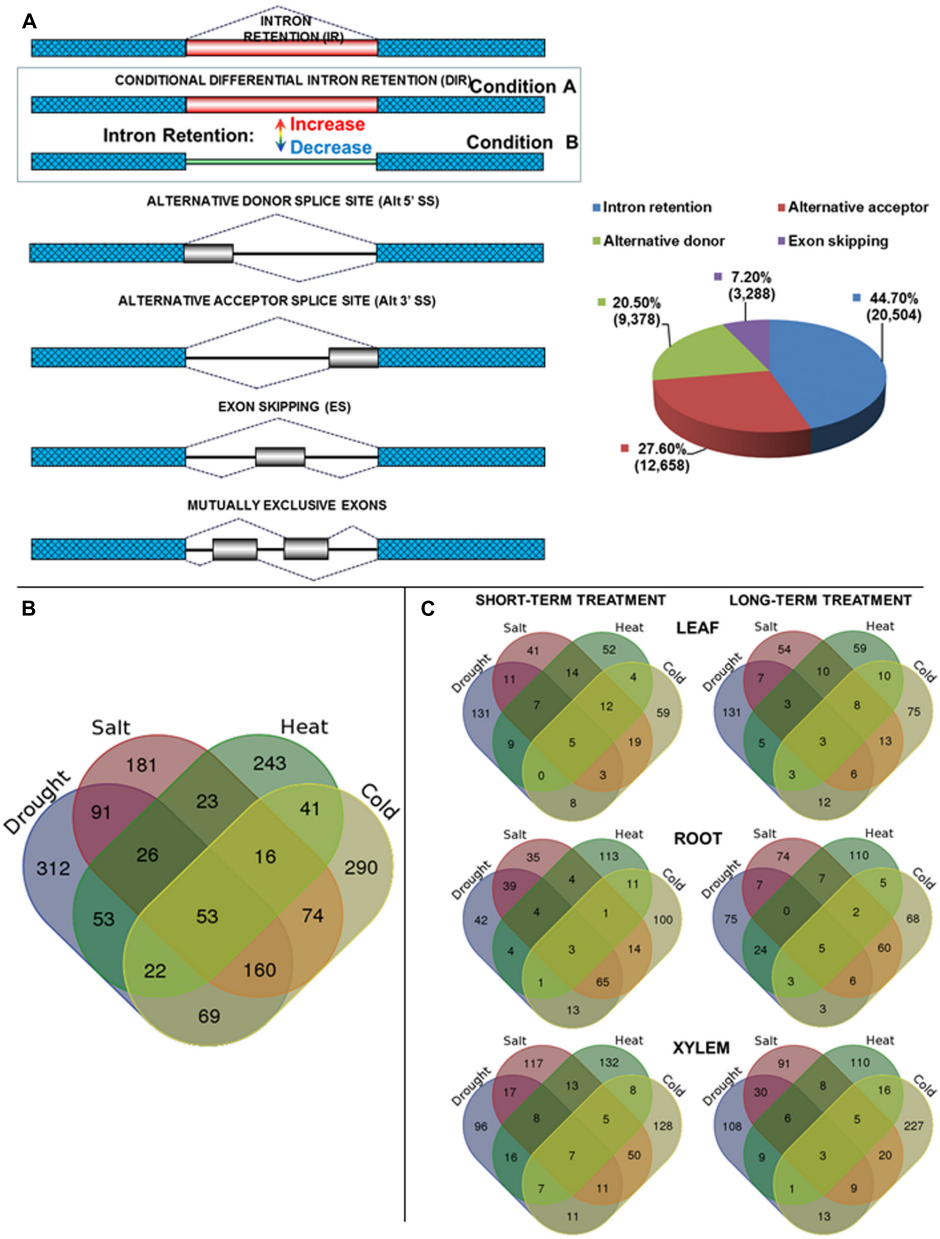

FIGURE 1 | (A) Major classes of alternative splicing (AS) events. Differential intron retention (DIR) is a particular type of the intron retention events characterized by condition-dependent increase or decrease in the degree of retention of certain introns. The pie chart (right) shows distribution of major AS types in *Populus trichocarpa* transcriptome as estimated from Iso-Seq data. Mutually exclusive exons were classified as a subcategory of more general ES class. **(B)** Distribution of genes that encode transcripts harboring stress-regulated differentially retained introns. Venn diagram illustrating intersection between the gene loci associated with stress-regulated DIR events. Lists of DIR-harboring genes were combined across all tissue types. Both short term and prolonged treatments were combined for each stress type. **(C)** Venn diagram showing intersection between DIR-associated genes during the short or prolonged phases of each stress treatment within same tissue type.

portion of the shoot. Stem xylem was isolated from young poplar shoots by making longitudinal cuts and removing surrounding layers of epidermis, bark, cortex, phloem, and cambium. Roots were extensively washed to remove soil and briefly dried using filter paper before freezing in liquid nitrogen. All tissues (with the exception of short term heat stress) were collected at the same time of day 11 am and immediately frozen in liquid nitrogen.

RNA Extraction, Preparation and Sequencing of RNA-Seq Libraries

Total RNA was extracted from each replicate as previously described (Filichkin et al., 2010). 81 individual strand-specific RNA-Seq libraries were prepared using True-Seq kit according to the manufacture's protocols (Illumina, Inc., San Diego, CA, United States). Sequencing was performed at the core facilities

of Oregon State University Center for Genome Research and Biocomputing[1] using paired-end 101cycles runs and Illumina HiSeq 2000 platform.

Initial Analysis of RNA-Seq Datasets

Populus trichocarpa genome assembly (Tuskan et al., 2006) and gene annotations were downloaded from the Phytozome (Goodstein et al., 2012) Version 3.0 database[2]. A total of approximately 10^9 of 101 nt paired-end RNA-Seq reads were aligned against the Version 3.0 poplar genome using STAR (Spliced Transcripts Alignment to a Reference) (Dobin et al., 2013). Only uniquely aligned reads were used in downstream analyses. For the basic expression analysis, RNA-Seq reads were aligned to the poplar V 3.0 genome using TopHat version 2.1.1 with default options. Transcripts were assembled using Cufflinks version 2.2.1 with default parameters as described[3]. The Cufflinks-generated output files in GTF format were loaded for display in Poplar Interactome project web site[4] using the GMOD GBrowse software Version 2.55. Raw RNA-Seq data sets deposited at EMBL-EBI ArrayExpress (accession number E-MTAB-5540). Additional RNA-Seq-associated data available to public through GBrowse at Poplar Interactome project web site[4].

Identification of Differentially Retained Introns

Differential intron retention events (DIRs) were detected and quantified using the iDiffIR software package[5] (Xing et al., 2015). A cutoff of <0.05 for adjusted p-values was used to filter statistically significant DIR events. The adjusted log-fold change of intron coverage was calculated as the log fold change adjusted to a pseudo-count divided by a measure of standard error as described[5]. The best pseudo-count value was calculated using the pseudo-count for which the adjusted log-fold change was minimized. To minimize effects of fluctuating levels of transcript expression on DIR calls only transcripts showing fivefold or less expression change across the treatments were used for DIR value calculation. The relative IR scores were calculated as the average read depth of an intron divided by the number of splice junction reads that flank the intron. The splicing ratio difference for DIRs was calculated as the difference between the ratio scores in the control and the treatment.

Quantification of DIR-Harboring and Fully Spliced Transcript Isoforms

Reverse transcription followed by droplet digital PCR (RT-ddPCR) was performed using Bio-Rad (Bio-Rad, Hercules, CA, United States) iScript Select cDNA synthesis and QX200 EvaGreen ddPCR kits, respectively, according to the manufacturer protocols[6]. SJ-specific primers (see Supplementary Material for primer sequences) were designed using previously described strategy (Filichkin et al., 2010, 2015a).

Production and Analysis of Iso-Seq Libraries

For Iso-Seq libraries equal amounts of total RNA from biological replicates which were used for RNA-Seq libraries were combined to generate six RNA pools: leaf control, leaf stress, root control, root stress, xylem control, xylem stress. Each stress pool included all replicates of stress treatments (e.g., heat, cold, drought, and salt). Complementary DNA (cDNA) was synthesized and Iso-Seq libraries generated according to standard procedures[7]. cDNA from each sample was divided into four fractions (approximately in 1–2, 2–3, 3–6, and 5–10 Kbp ranges) and sequenced using Pacific Biosciences RSII system and Single Molecule, Real-Time (SMRT) Sequencing SMRT cells essentially as described[7]. 1–2 Kbp libraries were run using two SMRT cells whereas libraries from larger fractions were run once. Initial processing of the raw Iso-Seq sequence data assembly was performed at Arizona Genomics Institute essentially as described[8]. Primary Iso-Seq data analysis was performed using the SMRT pipeline (Version 1.87.139483). Initial alignments of Iso-Seq reads to poplar genome for plotting on GMOD GBrowse were produced using STAR aligner V.2.5.2a (Dobin et al., 2013). STAR output files in BAM format were uploaded using GMOD GBrowse tool (V.2.55).

Final analysis of Iso-Seq data was performed as follows. Reads of insert predicted as non-full length by the SMRT Analysis software from Pacific Biosciences that did not exhibit an identifiable poly-(A) tail and 3′ adapter were removed. Finally, Iso-Seq reads were corrected using a hybrid error correction method LoRDEC (Salmela and Rivals, 2014) against a de Bruijn graph constructed from the bulk of RNA-Seq libraries (approximately 10^9 of 101 nt paired-end RNA-Seq reads, see above). These corrected Iso-Seq reads were further aligned to the poplar genome using Transcriptome Analysis Pipeline for Isoform Sequencing (TAPIS) (Abdel-Ghany et al., 2016) pipeline to produce approximately 10^6 aligned reads. Iso-Seq alignments were then assembled into strand-specific clusters and unique splice isoforms were inferred by merging alignments with common splice junctions.

For identification of IR events in miRNA precursors all Iso-Seq read clusters (15,087) were first aligned to the poplar genome assembly V.3.0. Iso-Seq Read clusters that did not overlap any annotated genes were aligned using BLAST search against plant hairpin miRNA from miRBase[9]. Total of 335 of these read clusters showed a significant match (at e-value $< 10e^{-5}$). 192 out of the 335clusters showed a significant match against annotated *P. trichocarpa* miRNAs whereas 123 matched annotated *P. euphratica* miRNAs. Iso-Seq read alignments to the poplar genome and transcript isoform

[1]http://cgrb.oregonstate.edu/core/sequencing

[2]https://phytozome.jgi.doe.gov/pz/portal.html

[3]http://cole-trapnell-lab.github.io/cufflinks/cufflinks/

[4]http://poplar.cgrb.oregonstate.edu/cgi-bin/gb2/gbrowse/poplar/

[5]http://combi.cs.colostate.edu/idiffir/

[6]http://www.bio-rad.com/webroot/web/pdf/lsr/literature/Bulletin_6450.pdf

[7]http://www.pacb.com/products-and-services/pacbio-systems

[8]http://www.genome.arizona.edu/modules/publisher/item.php?itemid=29

[9]http://www.mirbase.org/

models publicly available through Poplar Interactome project web site[10].

RESULTS

Strategy and Computational Approaches Used for Profiling of Stress-Induced Splice Isoforms

To ensure comparable representation of both short- and long-term phases of stress response and provide statistical means of data analysis our experimental design included following key arrangements. 81 RNA-Seq libraries representing triplicates of short term and prolonged phase of each stress treatment for leaf, root, and stem xylem were generated as described in Section "Materials and Methods" (**Supplementary Files 1**, **2**). Both RNA-Seq and Iso-Seq libraries were produced using the same RNA samples. Stress-inducible DIR events and splice junctions were mapped using RNA-Seq datasets whereas Iso-Seq was used for general survey and/or validation of splice isoforms structure predicted by RNA-Seq. Both data sets were used to build independent transcript isoform models (see section "Materials and Methods" and **Supplementary File 1**). Likewise, for quantifying absolute copy numbers of isoforms by Droplet Digital PCR, we employed same RNA samples used for libraries production. A single source of RNA input in all experiments ensured a consistent approach for downstream validation and statistical analyses.

Intron Retention Is a Dominant Class of Alternative Splicing Events across All Tissue Types

To evaluate the distribution of the major classes of AS events we analyzed individual cDNA isoforms from untreated controls or stress-treated tissue samples using Iso-Seq data. The RNA from control or stress-treated tissues types were pooled to produce six Iso-Seq libraries as described in Section "Materials and Methods." First, non-full length reads that did not exhibit an identifiable poly-A tail were removed. Finally, corrected full-length non-chimeric Iso-Seq reads were aligned to the poplar genome to produce approximately 10^6 alignments nearly evenly distributed across tissue types and stress treatments (**Supplementary File 3**). Analysis of these Iso-Seq reads aligned to the annotated poplar genes using TAPIS software (Abdel-Ghany et al., 2016) identified 20,504 isoforms with IR, 12,658 with alternative acceptor (Alt 3′), 9,378 with alternative donor (Alt 5′), and 3,288 with ES (including mutually exclusive exons) events. Among all detected alternatively spliced transcripts intron retaining isoforms occurred with the highest frequency (44.7%) followed by alternative acceptor (27.6%), the alternative donor (20.5%) and ES (7.2%) (**Figure 1A**). Thus, similar to other plants [e.g., *Arabidopsis*, (Filichkin et al., 2010, 2015b)] the IR and ES events in *Populus* species represent the most and the least prevalent classes of AS, respectively. Additional analysis of Iso-Seq reads that aligned to non-annotated genome portions resulted in the discovery of 15,087 novel transcribed regions of which 164 were alternatively spliced (**Supplementary File 4**).

[10]http://poplar.cgrb.oregonstate.edu/cgi-bin/gb2/gbrowse/poplar/

Mapping of Novel Splice Junctions Using High Depth RNA-Seq Coverage

Paired-end Illumina libraries were analyzed for differential splicing events using the following strategy. First, reads mapping to the multiple loci in the genome assembly were removed. Second, potential false-positive splice junctions were filtered using classifier module of SpliceGrapher package (Rogers et al., 2012). Third, putative novel splicing events were predicted using SpliceGrapher software (Rogers et al., 2012). Finally, DIR events were identified using the iDiffIR software (Xing et al., 2015) (also see section "Materials and Methods"). Alignment of 101 nucleotides (nt) paired end reads to the *P. trichocarpa* genome V. 3.0 produced a total of approximately 1.1 billion uniquely aligned reads from 81 libraries from three tissues namely leaf, xylem, and root, each subjected to four stress treatments. Uniquely mapped reads comprised on average 89% per library with a typical mapped length of 196 nucleotides (**Supplementary File 5**). Using the STAR read-mapping software (Dobin et al., 2013) we detected a total of 526,014,279 transcript splice junctions (SJs) of which 15,244,125 were novel when compared with the reference *P. trichocarpa* genome V3.0 annotations. Canonical GT/AG dinucleotide splicing signals constituted a major fraction of the 516,154,103 introns whereas GC/AG and AT/AC signals represented minor proportions with 7,313,526 and 346,044 SJs, respectively.

Abiotic Stresses Trigger Broad Spectrum of Unique and Distinct DIR Events

A total of 4,287 iDiffIR-predicted differentially retained introns showed statistically significant ($P_{adj} < 0.05$) stress-induced IR across all the treatments and tissue types (**Table 1** and **Supplementary Files 6**, **7**). A typical distribution of multivariate analysis data is shown in **Supplementary File 8**. A total of 1,654 unique genes ($P_{adj} < 0.05$) were associated with stress-induced DIR events (**Figure 1B** and **Supplementary Files 9**, **10**) with an average of 1.1 DIRs per gene. Of these, 1021 were induced by cold, 990 by drought, 942 by high salinity, and 651 by heat stress including both short- and prolonged treatment durations combined across leaf, root, and xylem tissues (**Supplementary File 11**). Of these gene sets the largest number of unique DIRs was observed for drought stress with a total of 312 genes, followed by 290 genes for cold, 243 genes for heat, and 181 genes for high salinity stress treatments. Fifty-three DIR-associated genes were observed across all stress treatments and tissue types (**Figure 1B** and **Supplementary File 11**). Drought, high salinity, and cold treatments universally affected 160 common DIR-associated genes. High salinity, heat, and cold treatments shared the lowest proportion of common DIR- associated genes (**Figure 1B** and **Supplementary File 12**). Short- and long-term phases of treatment within the same tissue type induced both unique and common subsets of DIRs (**Figure 1C** and **Supplementary File 13**). Several instances showed that the same

TABLE 1 | Distribution of stress-induced differential intron retention events in poplar tissues.

Tissue	Treatment		Differential intron retention events		
			Unique events	Associated non-redundant loci	Loci associated with multiple DIRs (two or more events per gene)
Leaf	Drought	Short term	195	174	19
		Prolonged	178	170	6
	Salt	Short term	134	112	15
		Prolonged	117	104	11
	Heat	Short term	116	103	11
		Prolonged	110	101	7
	Cold	Short term	117	110	4
		Prolonged	140	130	9 1
Root	Drought	Short term	172	171	1
		Prolonged	137	123	11
	Salt	Short term	166	165	1
		Prolonged	161	161	9
	Heat	Short term	150	141	8
		Prolonged	167	156	8
	Cold	Short term	213	208	5
		Prolonged	154	152	2
Xylem	Drought	Short term	203	173	20
		Prolonged	218	179	28
	Salt	Short term	249	228	18
		Prolonged	221	172	33
	Heat	Short term	222	196	19
		Prolonged	190	158	23
	Cold	Short term	244	227	15
		Prolonged	313	294	16

gene could be associated with multiple DIR events that are regulated by the specific stress treatments in an independent manner.

Switch between Increased or Decreased Intron Retention Specifically Regulated by Stress Type

We further examined if a switch between increasing or decreasing IR levels specifically pre-determined by stress type. Using the iDiffIR software developed for detecting differentially retained introns, we identified a set of 290 genes associated with two or more DIRs induced by broad range of treatments (**Supplementary Files 14**, **15**). On average, each of these genes was associated with ∼2.4 differentially regulated introns. We further examined instances of stress- and/or tissue-dependent regulation of such multiple DIR-harboring mRNAs. For example, an increase or a decrease of IR events in mRNA of *actin-related protein c2b* (*ptAC2B*) gene (*POTRI.010G067100*) in xylem was specifically determined by the type of treatment (**Figure 2A**). The short phase of high salinity stress resulted in an increase of the IR in five out of six DIR events harbored by *ptAC2B* mRNA whereas the prolonged phase caused a substantial decrease in all six events. In contrast, retention of intron seven decreased during the short phase of the treatment suggesting that short- or long-term treatment phases can have an opposite effect on regulation of distinct DIR events in the same mRNA. The structure of intron-retaining transcript models was generally corroborated by both RNA-Seq and Iso-Seq data (see **Figures 2B,C** for *ptAC2B* transcript models and for additional examples in Supplementary Material) providing an additional cross-platform validation of our computational methods. Similar to *ptAC2B*, the retention of six out of ten predicted introns of putative mRNA encoding *glutamate ammonia ligase* (*ptGAL*, *POTRI.004G085400*) in leaf tissues occurred in a differential and stress-specific manner (**Supplementary File 14**). Similar stress type-dependent behavior of DIRs harbored by *ptGAL* mRNA also occurred in xylem tissue (data not shown). We found numerous additional instances where the outcome of a particular IR event specifically regulated by stress type (**Supplementary File 14**).

Retention of Individual Introns in mRNA with Super Stress-Responsive DIRs Can Be Regulated Independently in a Stress-and/or Tissue Specific Manner

Among transcripts harboring multiple DIR events, several mRNAs displayed a broad stress response across all stress treatments (i.e., at least one DIR event was detected during one or more treatments). Such transcripts with highly responsive DIRs across all stress treatments were associated with 21, 6, and 33 genes in leaf, root, and xylem tissues, respectively

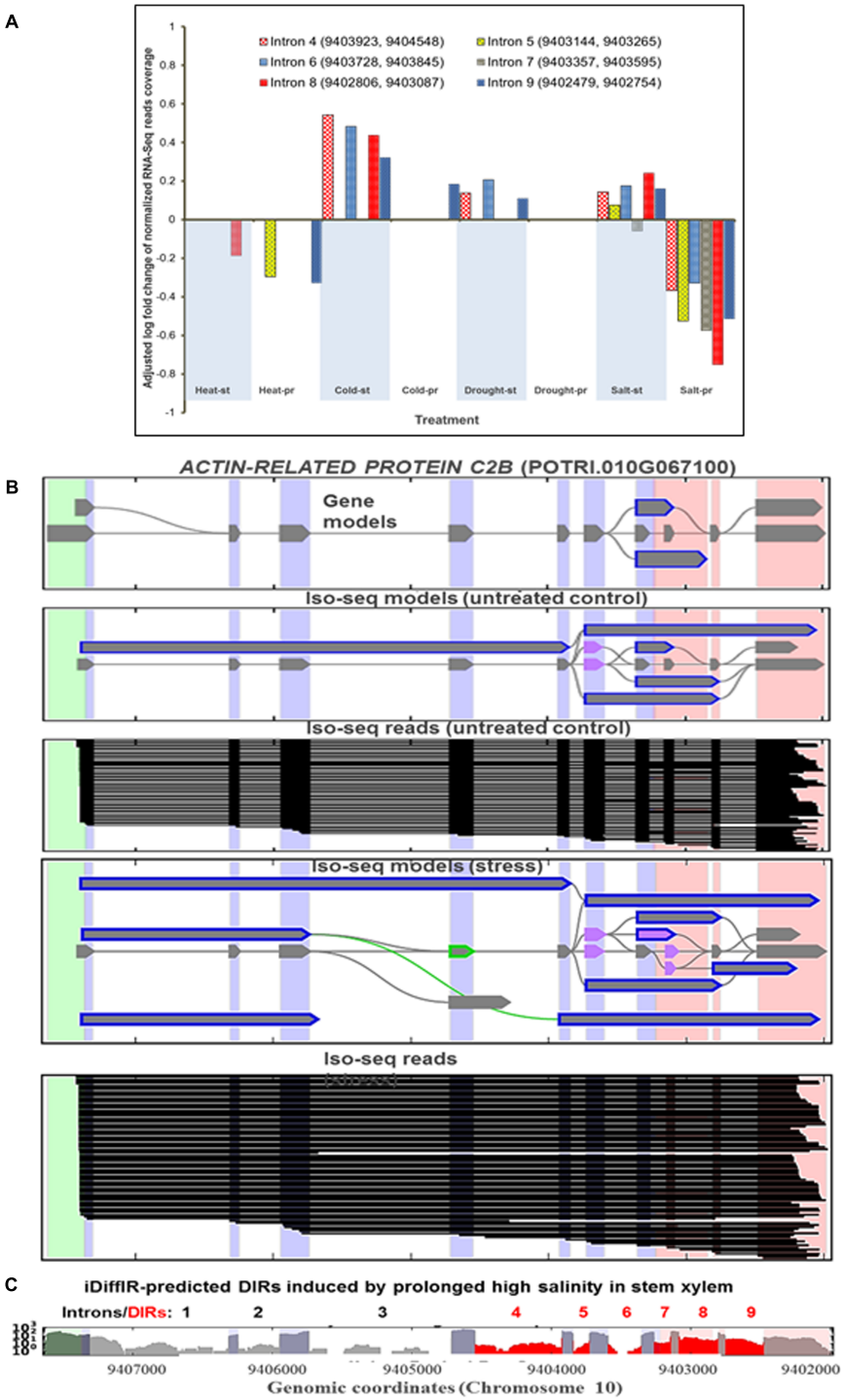

FIGURE 2 | Multiple differential intron retention events can be associated with a single gene and conditionally and differentially regulated within the same tissue type in a stress-specific manner. **(A)** Change in normalized RNA-Seq coverage of DIRs harbored by transcripts derived from *ACTIN-RELATED PROTEIN C2B* gene (*ptAC2B*, *POTRI.010G067100)* in stem xylem. Six out of nine introns DIRs show statistically significant ($P_{adj} < 0.05$) increase or decrease of coverage by normalized RNA-Seq reads in a stress type-dependent manner. Vertical axis shows an adjusted log fold change of normalized RNA-Seq reads coverage of differentially retained introns. Note that five out of six DIRs (except intron 7) can be up- or down-regulated depending on type of stress treatment. **(B)** Iso-Seq splicing models (ribbon drawings) and individual single molecule reads (black lines) of *ptAC2B* mRNA. Iso-Seq models suggest an extensive diversification of splice isoforms under abiotic stress. **(C)** Normalized RNA-Seq coverage of DIR events (shown in red) in *ptAC2B* mRNA. DIR events predicted from the RNA-Seq data using iDiffIR consistently corroborated by Iso-Seq models and individual reads. *ptAC2B* DIR events detected only in xylem but not in other tested tissue types. The vertical axis in denotes log of normalized RNA-Seq reads coverage.

(**Supplementary File 16**). Three genes out of 179 multi-DIR-associated loci responded universally to all tested stress treatment through the retention of one or more introns. Such super stress-responsive genes included orthologs of *Arabidopsis DCD (DEVELOPMENT AND CELL DEATH)* (*POTRI.003G141900*), a *HEAT SHOCK TRANSCRIPTION FACTOR B1* (*POTRI.007G043800*), and a putative *PATATIN-RELATED PHOSPHOLIPASE* (*POTRI.007G040400*). All three super stress-responsive poplar genes are likely to be involved in regulation of stress responses because their *Arabidopsis* orthologs and homologs were also implicated in cellular responses to a broad range of environmental stresses (Huang et al., 2008; Li et al., 2011; Kim et al., 2013). Another *dcd*-related gene, *ptDCD-l* (*POTRI.001G088800*), was among other five genes commonly responsive to drought, cold, and salt (**Supplementary File 16**). Three out of four introns in *ptDCD-l* mRNA were retained in xylem in various arrangements depending on type of stress treatment. Combinatory arrangements and the degree of retention of multiple DIRs associated with transcripts encoding *GLUTAMATE AMMONIA LIGASE* (*POTRI.004G085400*) in leaf tissues were also specifically controlled by the type of treatment (**Supplementary File 14**). Similar to *ptAC2B*, particular DIRs in the *ptDCD-l* mRNA were regulated by several stresses independently of each other (**Supplementary File 14**). *ptAC2B* and *ptGAL* transcripts harbored stress-inducible DIRs only in xylem and leaf, respectively, but not in any other tissues types. These results suggest that up- or downregulation of each event in multi-DIR transcripts in principle can occur independently in a stress- and/or tissue-specific manner.

mRNAs Encoding Key Regulatory Proteins Often Harbor Stress-Induced DIR Events

Numerous stress-induced differentially retained introns were present in the transcripts of key gene families regulating pre-mRNA splicing, general and specific stress-responses, plant development, cell wall metabolism, and circadian rhythms. Of the 101 annotated poplar splicing factors approximately 13% contained DIRs. DIR events in poplar mRNAs encoding orthologs of human general AS regulator SF2/ASF (*ptSF2*) and mammalian splicing factors 9G8 (*ptSRZ22*) harbored complex combinations of DIRs and other AS events in the 3′ portions of the transcripts. DIRs in *ptSF2* and *ptSRZ22* mRNAs were specifically induced by the heat stress and detected only in xylem tissues (**Supplementary File 9**).

At least one DIR per major gene family was found in general regulators of stress-response such as ABA responsive element binding (*AREB*), dehydration responsive element binding (*DREB*) TFs, and 14-3-3 genes (**Supplementary File 10**). DIR events in poplar genes encoding *ptAREB* and *ptDREB* factors were induced primarily by thermal and/or drought stress. Transcripts of numerous heat-shock factors also contained temperature-, drought-, and salt-sensitive DIRs (**Supplementary File 17**). Among key genes controlling plant development, poplar ortholog of *Arabidopsis late embryogenesis abundant 2* displayed a particularly interesting pattern of stress-regulated IR. Retention of a single intron in *ptLEA* transcript was up or down regulated in a stress- and/or tissue-specific manner (**Supplementary File 18**).

Numerous genes regulating cell wall metabolism including cellulose and lignin biosynthesis also harbored DIR events. Among genes involved in cellulose and lignin biosynthesis pathways, we identified seven and three transcripts harboring DIRs, respectively. For instance, an inclusion of the first intron in mRNA encoding GLYCOSYL TRANSFERASE FAMILY 8 PROTEIN (*POTRI.005G218900*, a co-ortholog of *Arabidopsis At1g06780* and *At2g30575* genes) was up-regulated by the prolonged heat treatment (**Supplementary File 19**). Such up-regulation occurred only in stem xylem but not in other tested tissues (data not shown) suggesting that this DIR event is xylem specific. DIR events in the transcripts of several key circadian regulators were regulated by several stress treatments (**Supplementary File 20**). At least 17% of annotated poplar genes from *glycine rich protein-like* family were associated with one or more DIRs.

Stress-Coordinated Modulation of Intron Splicing Ratios in Co-regulated DIR Clusters

To characterize changes in IR rates across the transcriptome we calculated the ratios of intron inclusion in stress treated tissues vs. untreated control samples. The relative IR rates were calculated using the RNA-Seq read coverage of the introns and corresponding splice junctions. The score of relative IR rate was calculated as the average of intron read coverage divided by the number of splice junction reads that are associated with this particular intron. The difference in splicing ratios was calculated as the difference between the ratio scores in the control and the treatment as described in Section "Materials and Methods." Intron splicing ratios of DIRs across all stress treatments for leaf, root, and xylem tissues summarized in **Supplementary Files 20–22**, respectively. Clustering of differential splicing ratios produced 124 DIR events co-regulated across the stress treatments (**Supplementary Files 23–25**). **Figure 3** shows a typical example of a cluster of co-regulated DIR events. The cluster includes mRNAs encoding 40 KDA HEAT SHOCK PROTEIN (*POTRI*.010G036200), SERINE PROTEASE (*POTRI.012G077900*), DYNAMIN (*POTRI*.017G041800) and SAICAR SYNTHASE (*POTRI*.017G051500). A distinct feature of this cluster is that all DIRs localized to the 3′ ends of mRNAs (**Supplementary File 21**). Retention of these introns will result in mRNAs with unusually long 3′ untranslated regions (3′UTR) — potential targets for NMD degradation (Kertész et al., 2006). Splicing ratios of each DIR showed either increase (e.g., a higher proportion of intron-retaining transcript) or decrease (e.g., a lower proportion of transcript with retained intron) across all stress types and tissues (**Figure 3**). Profile similarities for this cluster were especially obvious during short term and prolonged phases of heat (ratio decrease) or cold (ratio increase) stress. Statistically significant ($P < 0.05$) coordinated changes in intron splicing ratios were observed in

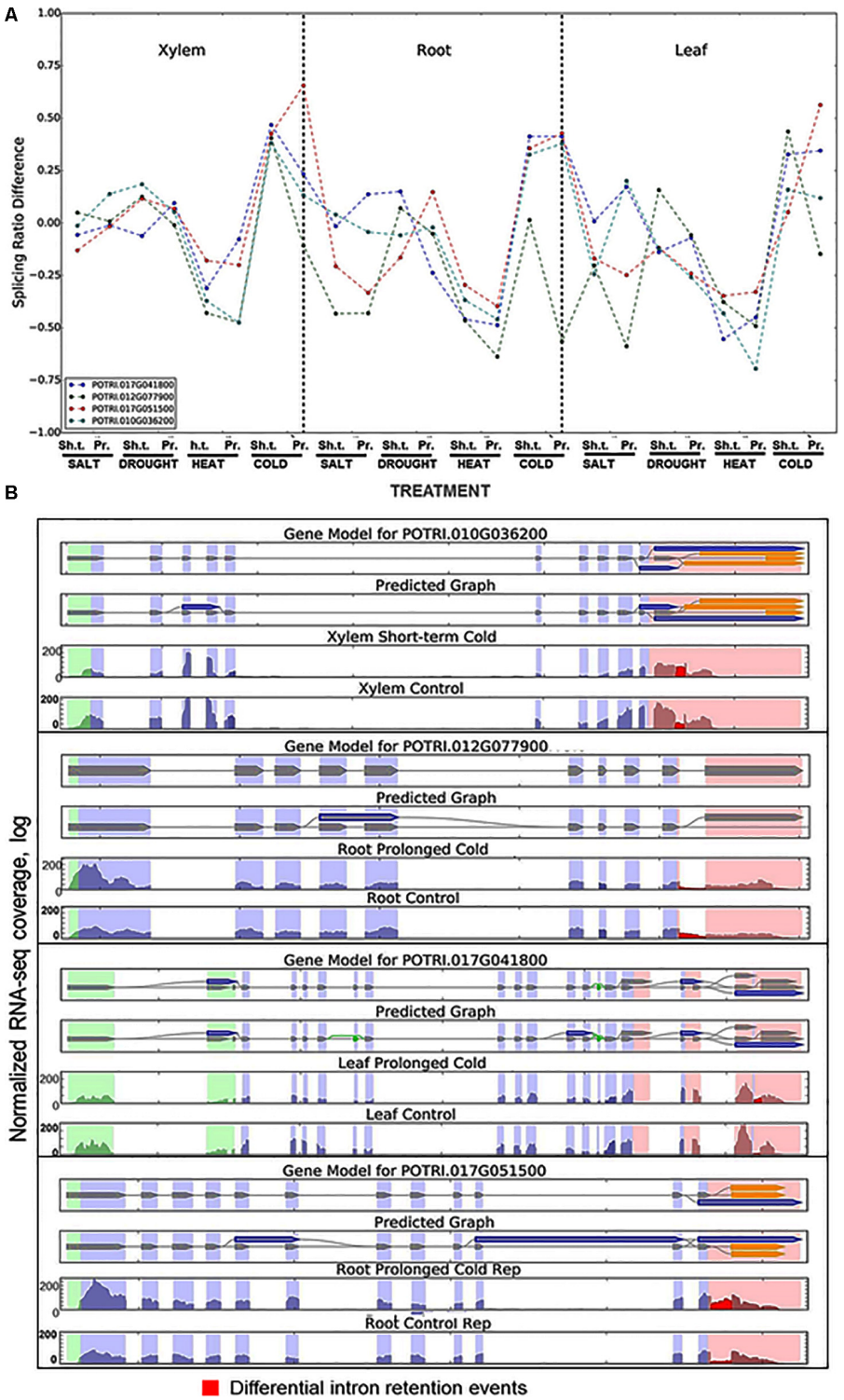

FIGURE 3 | A representative example of DIR events regulated across all the treatments in all tissue types in a coordinated manner. **(A)** Intron splicing ratios show similar profiles across all treatments and tissue types. Differences in intron splicing ratios were calculated as described in Section "Materials and Methods." The cluster includes a *40 KDA HEAT SHOCH PROTEIN* (*POTRI.010G036200*), *SERINE PROTEASE* (*POTRI.012G077900*), *DYNAMIN* (*POTRI.017G041800*), and *SAICAR SYNTHASE* (*POTRI.017G051500*). **(B)** Predicted models and DIR events of the genes in the cluster shown in **(A)**. Note that all DIRs confined to the transcript 3′ end. Retention of these introns will generate transcripts with unusually long (>300 nt) 3′UTRs – potential targets for NMD degradation. Transcript models and DIR events were predicted using SpliceGrapher and iDiffIR software packages, respectively. RNA-Seq read coverage of DIRs depicted in red. Sh.t., short term treatment; Pr., prolonged treatment.

other 124 independent gene clusters (**Supplementary File 26**) suggesting that many DIRs are co-regulated in a stress-specific manner.

Dynamics of DIR-Harboring Isoforms Accumulation

To examine stress-induced changes in quantities of transcript splicing isoforms, we further analyzed IR rates using real-time quantification of individual isoforms copy number. To achieve this, we employed reverse transcription – droplet digital PCR (RT-ddPCR) using event-specific primers as described in Section "Materials and Methods." RT-ddPCR allows quantification of relative proportions of splice variants in the same cDNA sample without the need for a standard curve (Baker, 2012). Using examples of two DIR-harboring mRNAs encoding conserved metazoan TFs we investigated stress-driven shifts in ratios between their fully spliced and intron-retaining isoforms. *ptOCR2-L* (*POTRI.002G102500*) mRNA encodes an ortholog of *Arabidopsis ONCOGENE-RELATED PROTEIN 2*, (*AT4G24380*) whereas *ptTFIIB* mRNA (*POTRI.006G048400*) encodes an ortholog of the conserved eukaryotic *TRANSCIPTION INITIATION FACTOR II SUBUNIT B*. Both *OCR2* and *TFIIB* proteins are involved in regulation of eukaryotic cellular responses to stress (Gong et al., 2001) (Zanton and Pugh, 2006). DIR events in both *ptOCR2-L* and *ptTFIIB* transcripts showed fluctuations in the degree of IR in a stress-specific manner (**Supplementary File 22**). A sharp increase in the levels of *ptOCR2-L* mRNA occurred under specific stress treatments and only in particular tissue types (**Figure 4A**). The inclusion of both or any of the fourth (I4R) and/or fifth (I5R) introns would produce either PTC+ mRNAs or transcripts with abnormally long 3′UTRs which could be potential NMD targets. To examine stress-induced shifts in ratios between intron-retaining and fully spliced transcripts we quantified the accumulation of the I4R and I5R isoforms under drought, high salinity or heat stresses in roots and xylem tissues. The exact quantification of *ptOCR2-L* isoforms using reverse transcription – droplet digital PCR (RT-ddPCR) and event-specific primers revealed that high salinity treatment induced a sharp increase in absolute copy numbers of the fully spliced mRNA in root and xylem. Such an increase was accompanied by a moderate increase in I4R and I5R isoforms copy number (**Figures 4B,C**). However, a sharp increase in spliced transcript copy number was also accompanied by a decrease in the relative abundance of intron-retaining isoforms, calculated as a percentage of absolute copy number of intron-retaining isoform relative to the fully spliced mRNA. Similarly, the copy number of the fully spliced *ptOCR2-L* mRNA and its intron-retaining isoforms were consistently increased in root and xylem tissues under short term heat and prolonged drought stresses (**Figures 4C–E**). In contrast, the relative ratios between both intron-retaining isoforms and spliced mRNA sharply decreased under heat and drought treatments. Thus, for all three types of treatment (e.g., high salt, heat, and drought) a sharp increase in absolute copy numbers of fully spliced *ptOCR2-L* mRNA followed by a decrease in relative ratios of intron-retaining isoforms.

We further examined the stress-driven regulation of isoforms ratios of *ptTFIIB* (POTRI.002G102500), a poplar ortholog of mammalian general TF *TFIIB*. The *ptTFIIB* transcripts showed tissue-specific and/or stress-dependent retention of its first (I1R) and/or the sixth (I6R) introns. Iso-Seq models strongly support such stress-modulated retention of these two introns (**Figure 5A**) (**Supplementary File 22**). Prolonged high salinity and heat treatments sharply increased levels of *ptTFIIB* mRNA in roots. Quantification of individual isoforms using RT-ddPCR showed that the retention of both introns decreased together with stress-induced down-regulation of the spliced mRNA. Conversely, a decrease in the copy number of fully spliced mRNA under heat stress was associated with a sharp increase of relative retention rates for both introns (92 and 95% for the I1R and the I6R events, respectively, see **Figures 5B,C**).

Stress-induced fluctuation of *ptTFIIB* mRNA of such extreme amplitude was observed only in root tissues under specific stress conditions such as prolonged high salinity and heat stresses (**Figures 5B,C**). In contrast to roots, the *ptTFIIB* mRNA levels in leaves showed more moderate changes under temperature stress. We used the leaf tissue to evaluate dynamics of DIR fluctuations in *ptTFIIB* isoforms in more narrow range using high resolution heat-cold stress time course (**Supplementary File 27**). To mimic extreme temperature swings, plants were subjected to the cyclical temperature changes as follows. First, plants were treated at 42°C for 24 h followed by the transition to 4°C for another 24 h. The absolute copy number of the first intron-retaining and fully spliced *ptTFIIB* isoforms was monitored using RT-ddPCR. During a 24-h segment of heat treatment, fully spliced mRNA remained at near constant levels. In contrast, accumulation of the I1R transcript showed a substantial copy number increase. The relative ratio of I1R isoform to the spliced mRNA also showed a considerable increase under heat stress (**Supplementary File 13**). The following 24 h cold treatment segment resulted in a decrease of both the I1R transcript and its ratios relative to the highest copy number observed during heat stress. Thus, the copy number of the fully spliced or intron-retaining isoforms increased or decreased during the heat or cold treatments, respectively. Concomitantly, during heat stress the relative ratio of intron-retaining isoform increased approximately sevenfold. Conversely, the cold treatment segment showed the decrease of both isoforms and reduction of the relative ratios to approximate levels of untreated controls. This result is consistent with a general conclusion of *ptTFIIB* and *ptOCR2-L* case studies that specific stresses induce broad fluctuations in relative ratios of the intron-harboring isoforms to the fully spliced mRNA.

Transcripts of Many Non-protein Coding Genes Alternatively Spliced and Harbor Differentially Retained Introns

A total of 15,087 Iso-Seq read clusters with low protein coding capacity that did not align to any annotated genes in poplar genome assembly (V.3.0) were designated as non-protein coding

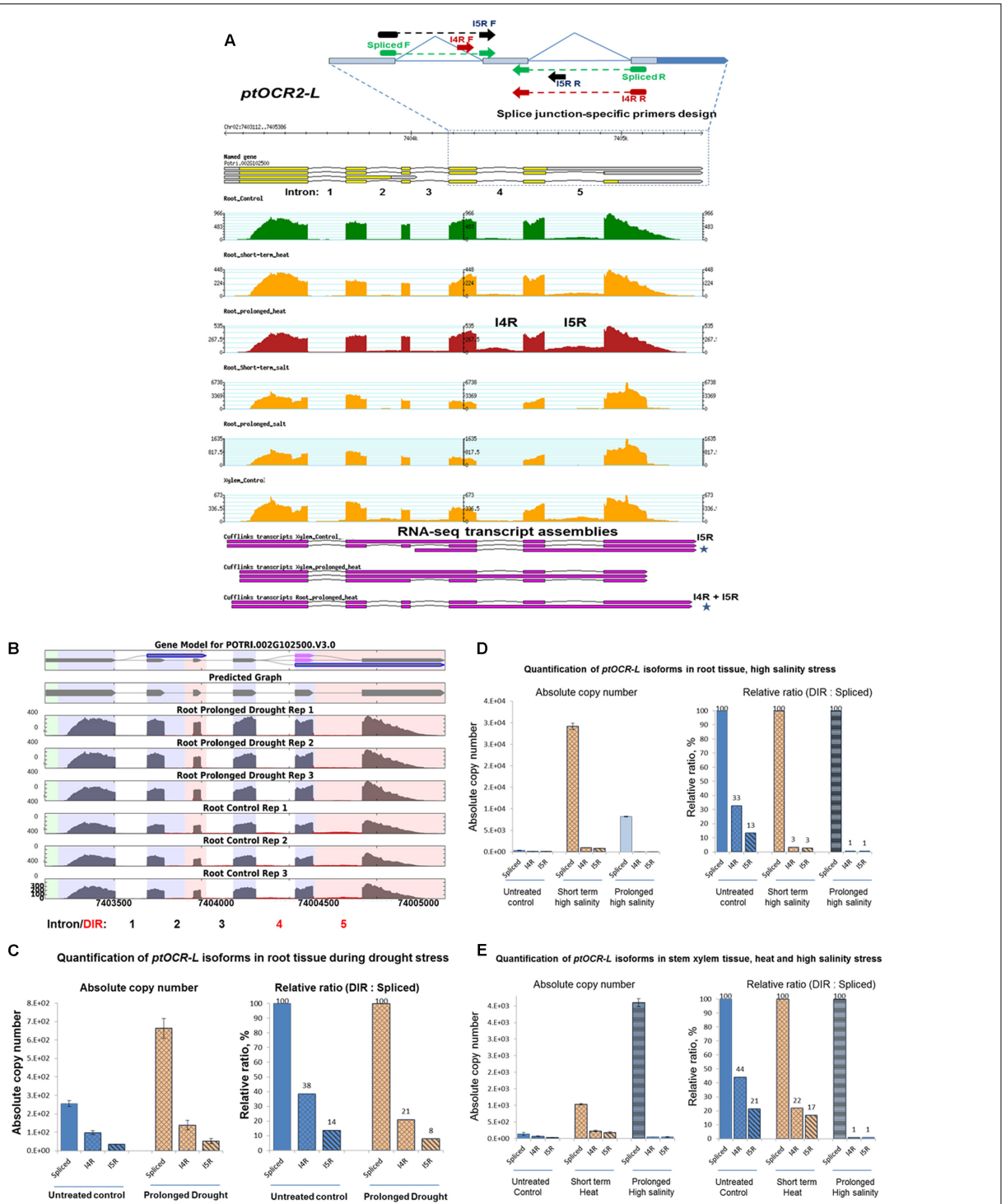

FIGURE 4 | Dynamics of stress-driven IR in mRNA encoding poplar ovarian cancer related transcription factor (*ptOCR2-L*, *POTRI.002G102500*). This example illustrates that stress-induced increase in copy number of the fully spliced *ptocr-lptocr-lptocr2-l* mRNA occurs concomitantly with a decrease in the relative ratios of both retained introns. **(A)** RNA-Seq coverage of *ptocr-lptocr-lptocr2-l* locus and design of splice junction (SJ)-specific primers. Primers designated as "Spliced" detect only the isoform with fully spliced introns 4 and 5 (gene model *POTRI.002G102500.1*); "I4R" – intron 4 is retained whereas intron 5 is spliced (reverse primer spans I4 SJ); "IR5" – I5 is retained whereas I4 is spliced (corresponds to gene model 3; forward primer spans I4 SJ). Stars indicate Cufflinks transcript assemblies supporting retention of both fourth and fifth introns (I4R + I5R) under the heat stress in roots and the fifth intron (I5R) in xylem. *Y*-axis indicates the number of Illumina reads aligned to the genome. **(B)** Gene model and differentially retained introns of *ptOCR2-L* transcripts. **(C–E)** Quantification of mRNA absolute copy number and relative ratios of the differentially retained introns vs. fully spliced transcripts in tissues under various stress treatments. Absolute copy number of mRNA was quantified using reverse transcription – droplet digital PCR (RT-ddPCR) and event-specific primers as described in Section "Materials and Methods."

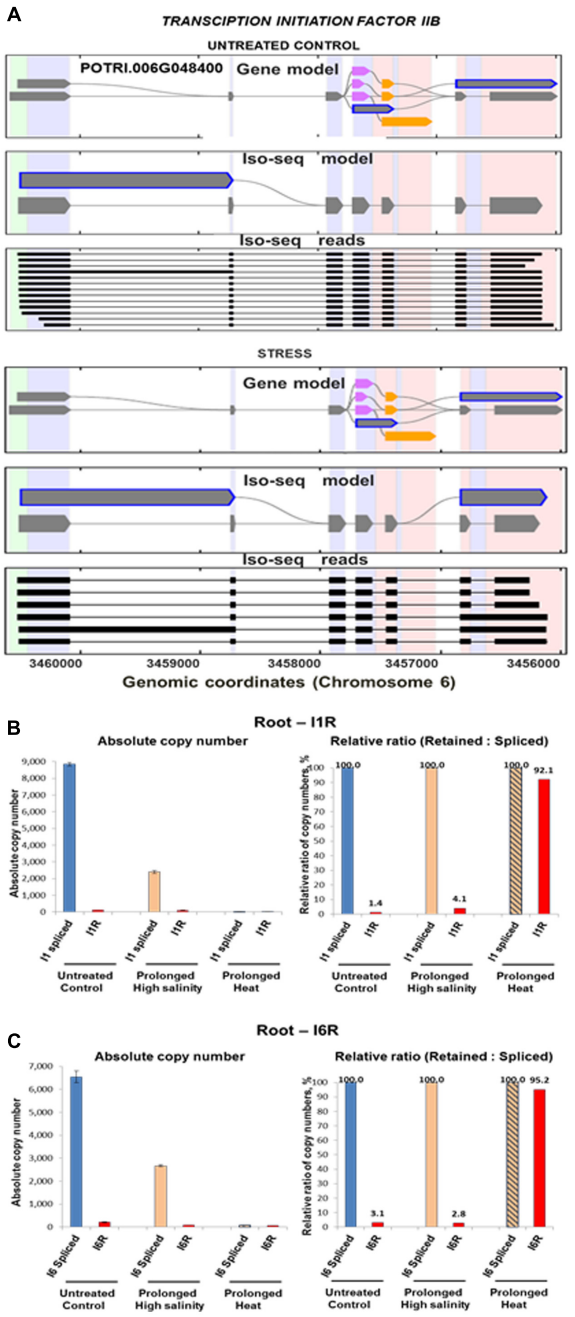

FIGURE 5 | Stress-driven increase of fully spliced *pttfIIB* mRNA accompanied by the switch in relative ratios of intron-retaining isoform. Quantification of absolute copy number of *ptTFIIB* transcript isoforms encoding *P. trichocarpa* general TRANSCIPTION INITIATION FACTOR IIB (*POTRI*.006G048400). **(A)** Iso-Seq isoforms models of mRNA under normal conditions and under abiotic stress (combined treatments). **(B,C)** The degree of retention of the first and sixth introns of the *pttfIIB* mRNA regulated by the prolonged salinity and heat in a stress-specific manner. Both the first and the sixth introns can be partially or completely retained producing isoforms with early PTCs or with unusually long 3′ untranslated regions, respectively. Notably, absolute copy number of isoforms retaining either first (I1R) or sixth (I6R) introns decreased in parallel with the salt- and heat-induced down-regulation of the fully spliced mRNA. However, a decrease of copy number of the fully spliced *pttfIIB* mRNA *(Continued)*

FIGURE 5 | Continued
was accompanied by the increase of relative proportions of both (e.g., I1R and I6R) intron-retaining isoforms. Thus, prolonged heat stress drastically increased the relative ratios of I1R and I6R isoforms to the spliced mRNA despite increase of copy number across all isoforms. Absolute copy number was quantified using reverse transcription – droplet digital PCR and event-specific primers as described in Section "Materials and Methods."

transcripts. Sequence alignments of these reads to hairpin miRNAs from miRBase showed a significant match of 335 reads to annotated plant miRNAs (*e*-value $< 10e^{-5}$). 192 Iso-Seq reads had a significant hit against annotated *P. trichocarpa* miRNAs whereas 123 showed a significant match to *P. euphratica* miRNAs. Mapping splice junctions revealed that many of these primary miRNA transcripts undergo extensive AS including stress-specific IR events. Examples of splicing models for ptc-miR156e and ptc-miR398c are shown in **Supplementary File 28** whereas features of other primary non-coding transcripts can be explored using Poplar Interactome GBrowse[11].

DISCUSSION

High Resolution Survey of Poplar Transcriptome Reveals Thousands of New Stress-Induced Transcript Isoforms of Protein-Coding and Non-protein Coding Genes

We carried out high depth coverage RNA-Seq survey of changes in AS patterns induced by drought, high salinity, heat and cold stress across transcriptomes of leaf, stem xylem and root tissues. Using more than one billion genome-aligned RNA-Seq reads from 81 libraries, we mapped approximately 500 million splice junctions to the *P. trichocarpa* genome (V.3.0). 15,244,125 of these were novel. Majority of the introns had canonical GT/AG splicing signals whereas GC/AG and AT/AC dinucleotide signals represented minor fractions. A parallel analysis of a single molecule real time sequencing (Iso-Seq) data produced about one million genome-aligned reads and showed that IR is a prevalent event across all tissues and treatments (an average of 44.7%). Alternative acceptor and donor events represented 27.6 and 20.5% of all detected AS events, respectively, whereas ES was the more rare class (7.2%).

In addition to protein-coding genes, we identified dozens of novel non-protein coding genes. Analysis of primary miRNA transcripts revealed that many of poplar pri-miRNAs undergo extensive AS including conditional IR. Since introns can be critical for proper biogenesis and processing of some *Arabidopsis* miRNAs (Szarzynska et al., 2009; Bielewicz et al., 2013), the further in-depth investigation is required to establish particular roles of miRNA DIRs in the regulation of stress responses in poplar. Both RNA-Seq and Iso-Seq datasets and catalogs of inferred transcript isoform models present valuable public resources for refining existing poplar

[11] http://poplar.cgrb.oregonstate.edu/cgi-bin/gb2/gbrowse/poplar/

genome annotation and data mining of stress-induced changes in transcriptomes of key poplar tissues. RNA-seq-derived expression data (**Supplementary File 29**) presents an additional public source of data mining to establish possible correlations between mRNA expression and occurrence of particular splicing events.

Stress-Induced Differential Intron Retention Is a Common Phenomenon in Plants

In-depth analysis of the IR events showed that the degree of retention for many introns under abiotic stress is variable, an incident described here as DIR. Comparative analysis of the degree of stress-induced IR events revealed that DIR is widespread across major tissue types of Western poplar. A broad range of intersecting or stress-specific DIR events was triggered by drought, high salinity, heat or cold stress across the leaf, stem xylem and root tissues. Short-term and prolonged treatment produced subsets of intersecting (i.e., common for both phases) or phase-specific DIR events. We identified several subsets of DIRs commonly induced by two or more stress types. The highest number of genes associated with unique DIRs was induced by drought (312) followed by cold (290), heat (243), and high salinity (181). The repertoire of differentially retained introns associated with the same gene was often tissue-specific and varied across the leaf, root, and xylem tissues (**Figure 2**). Detection of transcripts with multiple but independently differentially regulated DIRs suggested that increase or decrease in the degree of IR can be specifically regulated by the type of stress. DIRs were found across main gene families including those involved in regulation of plant stress-responses, development, pre-mRNA splicing, transcription, cell wall metabolism, and circadian rhythms.

Interestingly, transcripts of many key genes involved in regulation of general and specific responses to environmental stresses harbored DIR events. Discovery of numerous stress-inducible DIRs in transcripts encoding poplar splicing factors was consistent with findings that pre-mRNAs of several *Arabidopsis* SR splicing factors undergo extensive AS (Palusa et al., 2007; Filichkin et al., 2010; Palusa and Reddy, 2010; Reddy and Shad Ali, 2011; Thomas et al., 2012; Reddy et al., 2013; Ding et al., 2014). Key regulators of plant stress responses such as TFs encoded by *AREB*, *DREB*, *NAC*, and *14-3-3* gene families alternatively spliced under stress (Nakashima et al., 2009; Lata and Prasad, 2011; Todaka et al., 2012; Zhao et al., 2014; Tian et al., 2015). Our finding that these gene families in poplar are also associated with numerous stress-induced DIR events suggests a potential role that DIR play in regulating stress responses.

Stress-Coordinated Fluctuations of Intron Splicing Ratios Occur at Transcriptome-Wide Scale

We detected statistically significant coordinated fluctuations in intron splicing ratios across 124 independent gene clusters suggesting that many DIRs are co-regulated in a stress-specific manner. Observation of such coordinated stress- and/or tissue-dependent co-regulation across numerous DIRs suggested a broader role of DIR in transcriptome adjustments during adaptation to stresses. We quantified the exact stress-induced changes in IR rates using case studies of two key highly conserved eukaryotic TFs.

Dynamics of Differential Intron Retention in Case Studies Suggest That Shifts in Isoform Ratios Regulated in a Stress-Specific Manner

Quantification of absolute copy number of *ptTFIIB* and *ptOCR2-L* mRNAs revealed a consistent trend in the stress-induced switching of the relative ratios between fully spliced and intron-retaining isoform. Sharp up-regulation of the fully spliced *ptOCR2-L* mRNA occurred in parallel with a decrease in the relative ratio of intron-retaining isoforms under stress. Conversely, lower absolute copy numbers of fully spliced *ptOCR2-L* mRNA in untreated controls paralleled increase of relative ratios of intron-retaining isoforms (**Figures 4C–E**). In contrast to *ptOCR2-L*, prolonged heat and salt treatments resulted in the severe decrease in the copy number of a fully spliced *ptTFIIB* mRNA. Such an extreme decrease of the fully spliced mRNA levels was accompanied by the reduction in relative proportions of intron-retaining *ptTFIIB* isoforms (**Figures 4B,C**). The high resolution heat-cold stress time course of accumulation *ptTFIIB* copies in leaf under consecutive heat/cold treatment showed a similar tendency in changing isoform ratios (**Supplementary File 27**). However, more moderate mRNA fluctuations were associated with less conspicuous changes in isoforms ratios.

Dynamics of IR in these case studies suggested a common relationship between the fully spliced and DIR-harboring mRNA isoforms. Specifically, the decrease in relative ratio of intron-retaining isoform accompanied stress-induced up-regulation of the fully spliced mRNA and vice versa. Additional in-depth studies required to establish if this notion can be applicable at transcriptome-scale level.

Transcriptome Stress Adaptation Associated with Switches in Relative Ratios of Isoforms

About 42–60% of *Arabidopsis* genes alternatively spliced with many events being condition, developmental stage, and/or tissue type-dependent (Filichkin et al., 2010; Marquez et al., 2012). AS events that generate nonsense variants with diminished or abolished protein coding capacity often degraded by NMD [reviewed in (Popp and Maquat, 2013)]. Such splicing outcomes widespread in mammalian cells and described as "unproductive AS" (Lewis et al., 2003). It was proposed that unproductive splicing in eukaryotes play a role in the regulation of transcript abundancy via coupling with NMD pathway (Lareau et al., 2007). In plants, a dominant proportion of alternatively spliced pre-mRNAs harboring PTCs is generated through IR (Filichkin et al., 2010; Filichkin and Mockler, 2012; Kalyna et al., 2012; Marquez et al., 2012) [reviewed in (Reddy and Shad Ali, 2011; Reddy et al., 2013)]. However, a majority of these IR events

with some exceptions generally are not targeted by NMD for degradation (Palusa et al., 2007; Filichkin et al., 2010; Filichkin and Mockler, 2012; Kalyna et al., 2012; Marquez et al., 2012). For instance, an mRNA encoding *CCA1*, the key regulator of plant circadian oscillator, presents a particularly interesting example of DIR. Intron-retaining *CCA1* transcripts are NMD-insensitive (Filichkin and Mockler, 2012; Filichkin et al., 2015a,b). Similar to *ptTFIIB* and *ptOCR2-L*, temperature stresses shift ratio between intron-retaining and fully spliced *CCA* isoforms (Filichkin et al., 2010; Filichkin and Mockler, 2012; Filichkin et al., 2015a). These case studies and detection of numerous gene clusters with coordinated changes in intron splicing ratios suggest that stress-induced shifts of isoforms ratios widespread in plants.

Increasing evidence indicates that translation and degradation by NMD of intron-retaining mRNAs can be prevented via reversible sequestration of splicing intermediates (Boothby et al., 2013; Gohring et al., 2014; Brown et al., 2015; Filichkin et al., 2015b). Intron removal and translation of such masked mRNAs can be triggered by the specific environmental condition (Boothby et al., 2013). Increasing evidence also suggests that the dynamically changing repertoire and extent of IR events modulate mRNA abundance in the mammalian cell (Braunschweig et al., 2014). Altogether, our results broadly consistent with this notion and favor a hypothesis that conditional IR may play a role in posttranscriptional transcriptome adjustments during adaptation to environmental stresses.

AUTHOR CONTRIBUTIONS

SF and PJ conceived the study and the project discussed in this paper. PD and SF carried out the greenhouse experimental setup. SF carried out all the experimental validations. MH developed the iDiffIR and TAPIS software and analyzed the RNA-Seq and Iso-Seq datasets under the supervision of AB-H and AR. MH, SF, and AB-H carried out other computational analyses. CS performed the analysis of basic gene expression, isoform transcripts assembly, and maintenance of the poplar genome browser for the project. SS assisted in RNA extraction and ddPCR experiments. SF, MH, AB-H, AR, and PJ wrote the paper.

FUNDING

We acknowledge the DOE Office of Biological and Environmental Research for supporting this project through Grant No. DE-SC0008570.

ACKNOWLEDGMENTS

We thank Rod Wing, Dave Kudrna, and Dario Copetti from Arizona Genomics Institute for help with SMRT sequencing services and Mark Dasenko from OSU Center for Genome Research, Biocomputing (CGRB) for RNA-Seq services. We also thank Anne-Marie Girard (CGRB) for assistance in ddPCR experiments. We also appreciate Jim Erwin and green house staff for help with poplar growth facilities.

SUPPLEMENTARY MATERIAL

The Supplementary Material for this article can be found online at: https://www.frontiersin.org/articles/10.3389/fpls.2018.00005/full#supplementary-material

FILE 1 | Sampling strategy and flow of data analysis. **(A)** Sample collection strategy and consequent steps of data analyses to detect and validate DIR events. **(B)** Flow of data analysis for detection of splice variants using SpliceGrapher package (Rogers et al., 2012). SpliceGrapher software predicts splicing isoforms using, RNA-Seq data, expressed sequence tags alignments, and information supporting gene models.

FILE 2 | Descriptions of samples and stress treatments.

FILE 3 | Distribution of genome-aligned Iso-Seq reads across libraries and tissues.

FILE 4 | A list of novel transcribed regions identified by the ISO-seq data.

FILE 5 | Distribution of genome-aligned RNA-Seq reads across libraries and tissues.

FILE 6 | Lists of significant ($P_{adj} < 0.05$) DIR events with adjusted log fold change in leaf, root, and xylem across all the treatments.

FILE 7 | Lists of all DIR-associated genes (summarized in **Table 1**). Only unique genes associated with significant DIRs ($P_{adj} < 0.05$) are listed.

FILE 8 | The distribution of DIR events: typical examples of multivariate analysis (MvA) plots. **(A)** Short term root heat stress. **(B)** Prolonged heat stress in root. Colored points represent IR events with statistically significant differential retention values (P*adj* equal or lesser 0.05).

FILE 9 | Examples of temperature-inducible DIRs in transcripts encoding ptSF2 and ptSRZ22 splicing factors. ptSF2 (*POTRI.T134200*, top panel) is an ortholog of a human general/alternative splicing factor SF2/ASF SF2 and co-ortholog of *Arabidopsis* serine/arginine-rich proteins R34/SR1 (*At1g02840*) and SR34B (encoded by *At4g024302*). ptSRZ22 (*POTRI.018G009100*, bottom panel) is an ortholog of a mammalian 9G8 SF and the *Arabidopsis* serine/arginine-rich protein AthRSZp22 (*AT4G31580*). *Y*-axis shows the log of normalized intron coverage by RNA-Seq reads.

FILE 10 | Examples of stress-inducible DIRs in mRNAs of *ABA-responsive element binding factors (AREB) and dehydration-responsive element binding (DREB)* gene families. *Y*-axis shows the log of normalized intron coverage.

FILE 11 | List of genes associated with multiple DIRs.

FILE 12 | Intersect lists of all DIR-associated genes by stress and tissue type.

FILE 13 | Venn diagrams representation of overlaps between the genes associated with DIR events induced by short term or prolonged treatment phases.

FILE 14 | Distribution and examples of genes with multiple DIRs. **(A)** Venn diagrams showing intersect between super stress-responsive genes with associated multiple differential intron retention events across all stress treatments. The gene lists for short term and prolonged treatments for all tissue types (within each treatment) were pooled together to produce four combined lists of DIR-associated genes for drought, salt, heat, and cold treatments. **(B)** An example of the discrete stress-defined variations of multiple DIR events in a super stress-responsive gene. *POTRI.001G088800* gene encodes a homolog of *Arabidopsis* DCD (DEVELOPMENT AND CELL DEATH) domain protein (ptDCD-L). *Y*-axis represents the log of normalized intron coverage by RNA-Seq reads. **(C)** Iso-Seq models of transcript isoforms of *ptdcd-l* mRNA (*POTRI*.001G088800) under normal conditions and under combined abiotic stresses. **(D)** Multiple stress-responsive DIRs in the poplar mRNA encoding ptGAL (GLUTAMATE AMMONIA LIGASE, *POTRI.004G085400*). The top panel in **(D)** shows Iso-Seq models and individual single molecule reads of *ptgal* mRNA isoforms. The bottom

panel shows stress-induced increase or decrease of statistically significant ($P_{adj} < 0.05$) DIRs in *ptgal* mRNA in leaf. Note that the retention of the sixth intron either increases, decreases, or remains unchanged in a stress type-specific manner. *Y*-axis shows the adjusted log fold change of normalized intron coverage by RNA-Seq reads. The numbering of introns and DIRs is depicted in black and red, respectively. Initial alignments of Iso-Seq reads to poplar genome for plotting on GMOD GBrowse were produced using STAR aligner V.2.5.2a (Dobin et al., 2013). with the following parameters: –runMode alignReads –outSAMattributes NH HI NM MD –readName-
Separator space –outFilterMultimapScoreRange 1 –outFilterMismatchNmax 2000 –scoreGapNoncan -20 –scoreGapGCAG -4 –scoreGapATAC -8 –scoreDelOpen -1 –scoreDelBase -1 –scoreInsOpen -1 –scoreInsBase -1 –alignEndsType Local –seedSearchStartLmax 50 –seedPerReadNmax 100000 –seedPerWindow-Nmax 1000 –alignTranscriptsPerReadNmax 100000 –alignTranscriptsPerWindow-Nmax 10000 –runThreadN 10. Iso-Seq models were generated using Transcriptome Analysis Pipeline for Isoform Sequencing (TAPIS) software (Abdel-Ghany et al., 2016).

FILE 15 | Lists of genes associated with multiple DIRs for each specific tissue/treatment.

FILE 16 | Intersect lists of genes associated with super-responsive DIRs.

FILE 17 | Stress-inducible DIR in poplar mRNA encoding heat stress transcription factor ptHSFA2. **(A)** iDiffIR models and RNA-Seq reads coverage of *pthsfA2* mRNA. PCE designates: a poison cassette exon (e.g., an alternative exon introducing premature stop codon). Interestingly, this PCE event in *pthsfA2* mRNA conserved similar to described previously PCE in *Arabidopsis hsfA2* homolog (Filichkin et al., 2015a). *Y*-axis indicates the log of normalized intron coverage by RNA-Seq reads. **(B)** Iso-Seq models and individual cDNA reads. DIR event indicated by arrow, PCE – by asterisk. iDiffIR models were generated using iDiffIR (Xing et al., 2015) and SpliceGrapher (Rogers et al., 2012) software packages as described in Section "Materials and Methods."

FILE 18 | Stress-induced DIR in *ptLEA* mRNA. *ptlea* (*POTRI.002G165000*) is an ortholog of *Arabidopsis late embryogenesis abundant 27* (*At2g46140*), which is a key gene involved in dehydration stress response and embryo development. **(A)** Adjusted log fold change of intron coverage across stress treatments and tissues. Drought, cold, and salt stresses decreased retention of the single *ptlea* intron in all tissues. However, heat stress increased IR in roots whereas there were no significant changes under heat in all other tissues. Note that the retention of the *ptlea* intron increases or decreases in roots under prolonged heat or cold stresses, respectively. It is also decreases consistently under heat, cold salt, and drought stresses in all other tissue types. Therefore, similar to multiple DIRs the retention of a single intron can be modulated in stress- and/or tissue-specific manner. *Y*-axis shows adjusted log fold change of normalized intron coverage by RNA-Seq reads. **(B)** Graphical output of iDiffIR showing normalized coverage of a DIR event in *ptlea* mRNA Y-axis shows the log of normalized intron coverage by RNA-Seq reads. DIR event shown in red.

FILE 19 | Stress-inducible DIR in mRNA encoding a poplar protein homologous to GALACTURONOSYLTRANSFERASE-LIKE and IRREGULAR XYLEM protein families (*POTRI.005G218900*). Note that retention of the first intron by heat stress occurs in xylem only suggesting a tissue specificity of this event. Graphical output of iDiffIR software showing normalized coverage of a DIR event (depicted in red). *Y*-axis: the log of normalized intron coverage.

FILE 20 | Stress-inducible DIR in transcripts of poplar homologs of the key regulators of plant circadian oscillator *ptca1/lhy-l* **(A)** and *ptgrp7-l* **(B)**. IR events in *ptcca1/lhy* (*circadian clock associated1/late elongated hypocotyl-like*; *POTRI.002G180800*) and *ptgrp7* (*glycine rich protein7-like*, *POTRI.009G116400*) mRNAs were differentially regulated by the temperature. This observation is consistent with our previous findings of regulation of similar intron retention events in *Arabidopsis* and *Brachypodium CCA1/LHY* homologs (Filichkin et al., 2010; Filichkin and Mockler, 2012; Filichkin et al., 2015a).

FILE 21 | An example of a cluster of transcripts containing stress co-regulated differential intron retention events (DIRs). Iso-Seq models show mRNAs encoding 40 KDA HEAT SHOCK PROTEIN (*POTRI.010g036200*) **(A)**, SERINE PROTEASE (*POTRI.012G077900*) **(B)**, DYNAMIN (*POTRI.017G041800*) **(C)**, and SAICAR SYNTHASE (*POTRI.017G051500*) **(D)**. The transcript features including all DIRs identified by iDiffIR software (see main **Figure 3**) consistent with the Iso-Seq models and individual reads. Notably, all DIR events in this cluster are located in the 3′ ends of mRNAs. The retention of introns in all four mRNAs will produce unusually long 3′ untranslated regions potentially targeting these transcripts for degradation by the nonsense mediated mRNA decay pathway.

FILE 22 | Iso-Seq models generally support transcript features (including differentially retained introns) predicted by the iDiffIR software using RNA-Seq data. Iso-Seq-predicted models of poplar *oncogene-related protein 2-like* (*ptOCR2-L*) **(A)** and *general transcription factor* II B (*ptTFIIB*) **(B)** mRNAs. **(C)** Coverage of *ptTFIIB* mRNA by RNA-Seq reads under normal conditions and high/low temperature stresses. Image generated using Poplar Interactome project web site (http://poplar.cgrb.oregonstate.edu/cgi-bin/gb2/gbrowse/poplar/). Retention of the 1st and 6th introns was quantified using reverse transcription – droplet digital PCR ((RT-ddPCR) as described in **Figure 5** and Section "Materials and Methods."

FILE 23 | Splicing ratios of all introns in leaf across all stress treatments.

FILE 24 | Splicing ratios of all introns in root across all stress treatments.

FILE 25 | Splicing ratios of all introns in xylem across all stress treatments.

FILE 26 | Distribution of genes with co-regulated clusters of DIRs across all tissues and stress treatments.

FILE 27 | Moderate range temperature stress-driven increase of fully spliced *ptttfIIB* mRNA (encodes GENERAL TRANSCRIPTION FACTOR II B) is accompanied by moderate increase of the relative ratio of the 1st intron-retaining isoform (I1R). **(A)** A time course of accumulation of fully spliced *ptttfIIB* mRNA copies during increasing (heat stress) or decreasing (cold stress) temperature. **(B)** A time course of accumulation of the first intron-retaining *ptttfIIB* mRNA during high or low temperature stresses. Absolute copy number of each isoform was determined using cDNA from reverse transcription reaction followed by the droplet digital PCR (RT-ddPCR) as described in Section "Materials and Methods." RT-ddPCR of the fully spliced *ptttfIIB* mRNA and its first intron-retaining isoform was performed using event-specific primers as described in Section "Materials and Methods." **(C)** Relative ratio of the first intron-retaining isoform to its fully spliced counterpart mostly decreases with the increase of copy number of spliced mRNA and vice versa. Note that during heat stress treatment segment the level of spliced mRNA shows limited changes whereas relative proportion of I1R isoform increased substantially. Young poplar plants were heat treated (42°C) for 24 h followed by the transition to cold temperature (4°C) for another 24 h as described in Section "Materials and Methods." Diagram at the bottom shows fluctuations of temperature during the time course of treatment. Each time point represents 2 h.

FILE 28 | Examples of extensive alternative splicing and multiple intron retention events in primary transcripts of poplar miRNAs ptc-miR156e and ptc-miR398c. Numbers in gray boxes indicate genomic coordinates of splice junctions.

FILE 29 | Normalized gene expression values (RNA-seq reads) across all stress treatments.

REFERENCES

Abdel-Ghany, S. E., Hamilton, M., Jacobi, J. L., Ngam, P., Devitt, N., Schilkey, F., et al. (2016). A survey of the sorghum transcriptome using single-molecule long reads. *Nat. Commun.* 7:11706. doi: 10.1038/ncomms 11706

Baker, M. (2012). Digital PCR hits its stride. *Nat. Methods* 9, 541–544.

Bao, H., Li, E., Mansfield, S. D., Cronk, Q. C., El-Kassaby, Y. A., and Douglas, C. J. (2013). The developing xylem transcriptome and genome-wide analysis of alternative splicing in *Populus trichocarpa* (black cottonwood) populations. *BMC Genomics* 14:359. doi: 10.1186/1471-2164-14-359

Barbazuk, W. B., Fu, Y., and McGinnis, K. M. (2008). Genome-wide analyses of alternative splicing in plants: opportunities and challenges. *Genome Res.* 18, 1381–1392.

Bielewicz, D., Kalak, M., Kalyna, M., Windels, D., Barta, A., Vazquez, F., et al., (2013). Introns of plant pri-miRNAs enhance miRNA biogenesis. *EMBO Rep.* 14, 622–628. doi: 10.1038/embor.2013.62

Boothby, T. C., and Wolniak, S. M. (2011). Masked mRNA is stored with aggregated nuclear speckles and its asymmetric redistribution requires a homolog of mago nashi. *BMC Cell Biol.* 12:45. doi: 10.1186/1471-2121-12-45

Boothby, T. C., Zipper Richard, S., van der Weele, C. M., and Wolniak Stephen, M. (2013). Removal of retained introns regulates translation in the rapidly developing gametophyte of *Marsilea vestita*. *Dev. Cell* 24, 517–529. doi: 10.1016/j.devcel.2013.01.015

Braunschweig, U., Barbosa-Morais, N. L., Pan, Q., Nachman, E. N., Alipanahi, B., Gonatopoulos-Pournatzis, T., et al. (2014). Widespread intron retention in mammals functionally tunes transcriptomes. *Genome Res.* 24, 1774–1786. doi: 10.1101/gr.177790.114

Brown, J. W., Simpson, C. G., Marquez, Y., Gadd, G. M., Barta, A., and Kalyna, M. (2015). Lost in translation: pitfalls in deciphering plant alternative splicing transcripts. *Plant Cell* 27, 2083–2087. doi: 10.1105/tpc.15.00572

Casadio, A., Longman, D., Hug, N., Delavaine, L., Vallejos Baier, R., Alonso, C. R., et al. (2015). Identification and characterization of novel factors that act in the nonsense-mediated mRNA decay pathway in nematodes, flies and mammals. *EMBO Rep.* 16, 71–78. doi: 10.15252/embr.201439183

Ding, F., Cui, P., Wang, Z., Zhang, S., Ali, S., and Xiong, L. (2014). Genome-wide analysis of alternative splicing of pre-mRNA under salt stress in *Arabidopsis*. *BMC Genomics* 15:431. doi: 10.1186/1471-2164-15-431

Dobin, A., Davis, C. A., Schlesinger, F., Drenkow, J., Zaleski, C., Jha, S., et al. (2013). STAR: ultrafast universal RNA-seq aligner. *Bioinformatics* 29, 15–21. doi: 10.1093/bioinformatics/bts635

Dvinge, H., and Bradley, R. K. (2015). Widespread intron retention diversifies most cancer transcriptomes. *Genome Med.* 7:45. doi: 10.1186/s13073-015-0168-9

Filichkin, S. A., Cumbie Jason, S., Dharmawardhana, P., Jaiswal, P., Chang Jeff, H., Palusa Saiprasad, G., et al. (2015a). Environmental stresses modulate abundance and timing of alternatively spliced circadian transcripts in *Arabidopsis*. *Mol. Plant* 8, 207–227.

Filichkin, S. A., and Mockler, T. C. (2012). Unproductive alternative splicing and nonsense mRNAs: a widespread phenomenon among plant circadian clock genes. *Biol. Direct* 7:20. doi: 10.1186/1745-6150-7-20

Filichkin, S. A., Priest, H. D., Givan, S. A., Shen, R., Bryant, D. W., Fox, S. E., et al. (2010). Genome-wide mapping of alternative splicing in *Arabidopsis thaliana*. *Genome Res.* 20, 45–58. doi: 10.1101/gr.093302.109

Filichkin, S. A., Priest, H. D., Megraw, M., and Mockler, T. C. (2015b). Alternative splicing in plants: directing traffic at the crossroads of adaptation and environmental stress. *Curr. Opin. Plant Biol.* 24, 125–135. doi: 10.1016/j.pbi.2015.02.008

Gohring, J., Jacak, J., and Barta, A. (2014). Imaging of endogenous messenger RNA splice variants in living cells reveals nuclear retention of transcripts inaccessible to nonsense-mediated decay in *Arabidopsis*. *Plant Cell* 26, 754–764. doi: 10.1105/tpc.113.118075

Gong, Z., Koiwa, H., Cushman, M. A., Ray, A., Bufford, D., Kore-eda, S., et al. (2001). Genes that are uniquely stress regulated in salt overly sensitive (*sos*) mutants. *Plant Physiol.* 126, 363–375.

Goodstein, D. M., Shu, S., Howson, R., Neupane, R., Hayes, R. D., Fazo, J., et al. (2012). Phytozome: a comparative platform for green plant genomics. *Nucleic Acids Res.* 40, D1178–D1186. doi: 10.1093/nar/gkr944

Huang, D., Wu, W., Abrams, S. R., and Cutler, A. J. (2008). The relationship of drought-related gene expression in *Arabidopsis thaliana* to hormonal and environmental factors. *J. Exp. Bot.* 59, 2991–3007. doi: 10.1093/jxb/ern155

Jiang, J., Liu, X., Liu, C., Liu, G., Li, S., and Wang, L. (2017). Integrating omics and alternative splicing reveals insights into grape response to high temperature. *Plant Physiol.* 173, 1502–1518. doi: 10.1104/pp.16.01305

Jung, H., and Lee, D. (2015). Intron retention is a widespread mechanism of tumor-suppressor inactivation. *Nat. Genet.* 47, 1242–1248. doi: 10.1038/ng.3414

Kalyna, M., Simpson, C. G., Syed, N. H., Lewandowska, D., Marquez, Y., Kusenda, B., et al. (2012). Alternative splicing and nonsense-mediated decay modulate expression of important regulatory genes in *Arabidopsis*. *Nucleic Acids Res.* 40, 2454–2469. doi: 10.1093/nar/gkr932

Kertész, S., Kerényi, Z., Mérai, Z., Bartos, I., Pálfy, T., Barta, E., et al. (2006). Both introns and long 3'-UTRs operate as *cis*-acting elements to trigger nonsense-mediated decay in plants. *Nucleic Acids Res.* 34, 6147–6157.

Kesari, R., Lasky, J. R., Villamor, J. G., Des Marais, D. L., Chen, Y.-J. C., Liu, T.-W., et al. (2012). Intron-mediated alternative splicing of *Arabidopsis P5CS1* and its association with natural variation in proline and climate adaptation. *Proc. Natl. Acad. Sci. U.S.A.* 109, 9197–9202. doi: 10.1073/pnas.1203433109

Kim, M.-H., Sonoda, Y., Sasaki, K., Kaminaka, H., and Imai, R. (2013). Interactome analysis reveals versatile functions of Arabidopsis COLD SHOCK DOMAIN PROTEIN 3 in RNA processing within the nucleus and cytoplasm. *Cell Stress Chaperones* 18, 517–525. doi: 10.1007/s12192-012-0398-3

Lareau, L. F., Inada, M., Green, R. E., Wengrod, J. C., and Brenner, S. E. (2007). Unproductive splicing of SR genes associated with highly conserved and ultraconserved DNA elements. *Nature* 446, 926–929.

Lata, C., and Prasad, M. (2011). Role of DREBs in regulation of abiotic stress responses in plants. *J. Exp. Bot.* 62, 4731–4748. doi: 10.1093/jxb/err210

Lewis, B. P., Green, R. E., and Brenner, S. E. (2003). Evidence for the widespread coupling of alternative splicing and nonsense-mediated mRNA decay in humans. *Proc. Natl. Acad. Sci. U.S.A.* 100, 189–192.

Li, M., Bahn, S. C., Guo, L., Musgrave, W., Berg, H., Welti, R., et al. (2011). Patatin-related phospholipase pPLAIIIβ-induced changes in lipid metabolism alter cellulose content and cell elongation in *Arabidopsis*. *Plant Cell* 23, 1107–1123. doi: 10.1105/tpc.110.081240

Li, S., Yamada, M., Han, X., Ohler, U., and Benfey, P. N. (2016). High-resolution expression map of the *Arabidopsis* root reveals alternative splicing and lincRNA regulation. *Dev. Cell* 39, 508–522. doi: 10.1016/j.devcel.2016.10.012

Maquat, L. E. (2005). Nonsense-mediated mRNA decay in mammals. *J. Cell Sci.* 118(Pt 9), 1773–1776.

Marquez, Y., Brown, J. W. S., Simpson, C., Barta, A., and Kalyna, M. (2012). Transcriptome survey reveals increased complexity of the alternative splicing landscape in *Arabidopsis*. *Genome Res.* 22, 1184–1195. doi: 10.1101/gr.134106.111

Mei, W., Boatwright, L., Feng, G., Schnable, J. C., and Barbazuk, W. B. (2017a). Evolutionarily conserved alternative splicing across monocots. *Genetics* 207, 465–480. doi: 10.1534/genetics.117.300189

Mei, W., Liu, S., Schnable, J. C., Yeh, C.-T., Springer, N. M., Schnable, P. S., et al. (2017b). A comprehensive analysis of alternative splicing in paleopolyploid maize. *Front. plant sci.* 8:694. doi: 10.3389/fpls.2017.00694

Nakashima, K., Ito, Y., and Yamaguchi-Shinozaki, K. (2009). Transcriptional regulatory networks in response to abiotic stresses in *Arabidopsis* and grasses. *Plant Physiol.* 149, 88–95.

Nicholson, P., and Muhlemann, O. (2010). Cutting the nonsense: the degradation of PTC-containing mRNAs. *Biochem. Soc. Trans.* 38, 1615–1620. doi: 10.1042/BST0381615

Palusa, S. G., Ali, G. S., and Reddy, A. S. N. (2007). Alternative splicing of pre-mRNAs of *Arabidopsis* serine/arginine-rich proteins: regulation by hormones and stresses. *Plant J.* 49, 1091–1107.

Palusa, S. G., and Reddy, A. S. N. (2010). Extensive coupling of alternative splicing of pre-mRNAs of serine/arginine (SR) genes with nonsense-mediated decay. *New Phytol.* 185, 83–89. doi: 10.1111/j.1469-8137.2009.03065.x

Pan, Q., Shai, O., Lee, L. J., Frey, B. J., and Blencowe, B. J. (2008). Deep surveying of alternative splicing complexity in the human transcriptome by high-throughput sequencing. *Nat. Genet.* 40, 1413–1415. doi: 10.1038/ng.259

Popp, M. W., and Maquat, L. E. (2013). Organizing principles of mammalian nonsense-mediated mRNA decay. *Annu. Rev. Genet.* 47, 139–165. doi: 10.1146/annurev-genet-111212-133424

Reddy, A. S. N., Marquez, Y., Kalyna, M., and Barta, A. (2013). Complexity of the alternative splicing landscape in plants. *Plant Cell* 25, 3657–3683. doi: 10.1105/tpc.113.117523

Reddy, A. S. N., and Shad Ali, G. (2011). Plant serine/arginine-rich proteins: roles in precursor messenger RNA splicing, plant development, and stress responses. *Wiley Interdiscip. Rev. RNA* 2, 875–889. doi: 10.1002/wrna.98

Rogers, M. F., Thomas, J., Reddy, A. S. N., and Ben-Hur, A. (2012). SpliceGrapher: detecting patterns of alternative splicing from RNA-Seq data in the context of gene models and EST data. *Genome Biol.* 13:R4. doi: 10.1186/gb-2012-13-1-r4

Salmela, L., and Rivals, E. (2014). LoRDEC: accurate and efficient long read error correction. *Bioinformatics* 30, 3506–3514. doi: 10.1093/bioinformatics/btu538

Shen, Y., Zhou, Z., Wang, Z., Li, W., Fang, C., Wu, M., et al. (2014). Global dissection of alternative splicing in paleopolyploid soybean. *Plant Cell* 26, 996–1008. doi: 10.1105/tpc.114.122739

Soolanayakanahally, R., Guy, R., Street, N., Robinson, K., Silim, S., Albrectsen, B., et al. (2015). Comparative physiology of allopatric *Populus* species: geographic clines in photosynthesis, height growth, and carbon isotope discrimination in common gardens. *Front. Plant Sci.* 6:528. doi: 10.3389/fpls.2015.00528

Staiger, D., and Brown, J. W. S. (2013). Alternative splicing at the intersection of biological timing, development, and stress responses. *Plant Cell* 25, 3640–3656. doi: 10.1105/tpc.113.113803

Szarzynska, B., Sobkowiak, L., Pant, B. D., Balazadeh, S., Scheible, W. R., Mueller-Roeber, B., et al. (2009). Gene structures and processing of *Arabidopsis thaliana* HYL1-dependent pri-miRNAs. *Nucleic Acids Res.* 37, 3083–3093. doi: 10.1093/nar/gkp189

Thomas, J., Palusa, S. G., Prasad, K. V. S. K., Ali, G. S., Surabhi, G.-K., Ben-Hur, A., et al. (2012). Identification of an intronic splicing regulatory element involved in auto-regulation of alternative splicing of *SCL33* pre-mRNA. *Plant J.* 72, 935–946. doi: 10.1111/tpj.12004

Tian, F., Wang, T., Xie, Y., Zhang, J., and Hu, J. (2015). Genome-wide identification, classification, and expression analysis of *14-3-3* gene family in *Populus*. *PLOS ONE* 10:e0123225. doi: 10.1371/journal.pone.0123225

Todaka, D., Nakashima, K., Shinozaki, K., and Yamaguchi-Shinozaki, K. (2012). Toward understanding transcriptional regulatory networks in abiotic stress responses and tolerance in rice. *Rice* 5:6. doi: 10.1186/1939-8433-5-6

Tuskan, G. A., Difazio, S., Jansson, S., Bohlmann, J., Grigoriev, I., Hellsten, U., et al. (2006). The genome of black cottonwood, *Populus trichocarpa* (Torr. & Gray). *Science* 313, 1596–1604.

Vitulo, N., Forcato, C., Carpinelli, E. C., Telatin, A., Campagna, D., D'Angelo, M., et al. (2014). A deep survey of alternative splicing in grape reveals changes in the splicing machinery related to tissue, stress condition and genotype. *BMC Plant Biol.* 14:99. doi: 10.1186/1471-2229-14-99

Wang, B.-B., and Brendel, V. (2006). Genomewide comparative analysis of alternative splicing in plants. *Proc. Natl. Acad. Sci. U.S.A.* 103, 7175–7180.

Xing, D., Wang, Y., Hamilton, M., Ben-Hur, A., and Reddy, A. S. (2015). Transcriptome-wide identification of RNA targets of *Arabidopsis* SERINE/ARGININE-RICH45 uncovers the unexpected roles of this RNA binding protein in RNA processing. *Plant Cell* 27, 3294–3308. doi: 10.1105/tpc.15.00641

Xu, P., Kong, Y., Song, D., Huang, C., Li, X., and Li, L. (2014). Conservation and functional influence of alternative splicing in wood formation of *Populus* and *Eucalyptus*. *BMC Genomics* 15:780. doi: 10.1186/1471-2164-15-780

Zanton, S. J., and Pugh, B. F. (2006). Full and partial genome-wide assembly and disassembly of the yeast transcription machinery in response to heat shock. *Genes Dev.* 20, 2250–2265.

Zhao, Y., Sun, J., Xu, P., Zhang, R., and Li, L. (2014). Intron-mediated alternative splicing of WOOD-ASSOCIATED NAC TRANSCRIPTION FACTOR1B regulates cell wall thickening during fiber development in *Populus* species. *Plant Physiol.* 164, 765–776. doi: 10.1104/pp.113.231134

Conflict of Interest Statement: The authors declare that the research was conducted in the absence of any commercial or financial relationships that could be construed as a potential conflict of interest.

frontiers in Plant Science

ORIGINAL RESEARCH
published: 17 January 2018
doi: 10.3389/fpls.2017.02269

Improvement of Salt Tolerance Using Wild Rice Genes

Ruidang Quan[1,2], Juan Wang[1,2], Jian Hui[3], Haibo Bai[3], Xuelian Lyu[3], Yongxing Zhu[3], Haiwen Zhang[1,2], Zhijin Zhang[1,2], Shuhua Li[3]* and Rongfeng Huang[1,2]**

[1] Biotechnology Research Institute, Chinese Academy of Agricultural Sciences, Beijing, China, [2] National Key Facility of Crop Gene Resources and Genetic Improvement, Beijing, China, [3] Ningxia Academy of Agriculture and Forestry Sciences, Yinchuan, China

Salt stress causes significant reductions in rice production worldwide; thus, improving salt tolerance is a promising approach to meet the increasing food demand. Wild rice germplasm is considered a valuable genetic resource for improving rice cultivars. However, information regarding the improvement of salt tolerance in cultivated rice using wild rice genes is limited. In this study, we identified a salt-tolerant line Dongxiang/Ningjing 15 (DJ15) under salt-stress field conditions from the population of a salt tolerant Dongxiang wild rice × a cultivated rice variety Ningjing16 (NJ16). Genomic resequencing analysis of NJ16, DJ15 and Dongxiang wild rice revealed that the introgressed genomic fragments were unevenly distributed over the 12 chromosomes (Chr.) and mainly identified on Chr. 6, 7, 10, and 11. Using quantitative trait locus (QTL) mapping, we found 9 QTL for salt tolerance (qST) at the seedling stage located on Chr. 1, 3, 4, 5, 6, 8, and 10. In addition, sequence variant analysis within the QTL regions demonstrated that SKC1/HKT8/HKT1;5 and HAK6 transporters along with numerous transcriptional factors were the candidate genes for the salt tolerant QTL. The DJ15/Koshihikari recombinant inbred lines that contained both qST1.2 and qST6, two QTL with the highest effect for salt tolerance, were more tolerant than the parental lines under salt-stress field conditions. Furthermore, the qST6 near-isogenic lines with IR29 background were more tolerant than IR29, indicating that qST1.2 and qST6 could improve salt tolerance in rice. Overall, our study indicates that wild rice genes could markedly improve the salt tolerance of cultivated rice.

Keywords: wild rice, cultivated rice, salt tolerance, QTL, gene introgression

OPEN ACCESS

Edited by:
Jose M. Pardo,
Instituto de Bioquímica Vegetal y Fotosíntesis (CSIC), Spain

Reviewed by:
Keisuke Nagai,
Nagoya University, Japan
Ahmad Arzani,
Isfahan University of Technology, Iran

****Correspondence:***
Ruidang Quan
quanruidang@caas.cn
Shuhua Li
shuhua.l@163.com
Rongfeng Huang
rfhuang@caas.cn

Specialty section:
This article was submitted to Plant Abiotic Stress, a section of the journal Frontiers in Plant Science

Received: *19 October 2017*
Accepted: *27 December 2017*
Published: *17 January 2018*

Citation:
Quan R, Wang J, Hui J, Bai H, Lyu X, Zhu Y, Zhang H, Zhang Z, Li S and Huang R (2018) Improvement of Salt Tolerance Using Wild Rice Genes. Front. Plant Sci. 8:2269. doi: 10.3389/fpls.2017.02269

INTRODUCTION

Rice is one of the most important staple crops worldwide. The global demand for staple crops, including rice, increases with the continuous increase of human population. However, the production of staple crops is threatened by abiotic stresses including salt, drought and high/low temperature (Arzani and Ashraf, 2016; Calanca, 2017). Therefore, improving the productivity of crops in salt-stressed areas is considered essential to meet the increasing food demand.

Compared with wheat, barley and cotton, rice is a more salt sensitive crop (Chinnusamy et al., 2005). Salt tolerance in rice changes with age; it is salt sensitive at the seedling stage, becomes moderately salt tolerant at the vegetative stage, and highly sensitive at reproductive stage (Lutts et al., 1995; Zeng et al., 2002). Additionally, the salt tolerance is genotype-dependent; i.e., the *Oryza*

sativa Indica cultivar Nona Bokra is highly salt tolerant, the *O. sativa* Japonica cultivar Nipponbare is moderately salt tolerant, while the *O. sativa* Japonica cultivar Koshihikari is highly salt sensitive (Kurotani et al., 2015). Salt stress often causes photosynthesis decrease, plant growth inhibition, biomass loss, and partial sterility, all of which lead to yield reduction (Khatun and Flowers, 1995; Pardo, 2010; Munns, 2011; Todaka et al., 2012).

Salt tolerance is a polygenic trait controlled by several quantitative loci (QTL) (Ismail and Horie, 2017).From a mapping population derived from a *indica/indica* cross, 11 QTL for Na^+ uptake, K^+ uptake, and Na^+/K^+ selectivity in rice were mapped to regions on chromosomes (Chr.) 1, 4, 6, and 9, and the QTL for Na^+ and K^+ uptake were on different linkage groups (Koyama et al., 2001). In a population derived from a cross between Nona Bokra and Koshihikari, 11 QTL for salt tolerance were identified on Chr. 1, 4, 6, 7, and 9, of which two major QTL, qSNC-7 for shoot Na^+ concentration and qSKC-1 for shoot K^+ concentration, explained more than 40% of the total phenotypic variance (Lin et al., 2004). The major QTL Saltol, for shoot K^+/Na^+ homeostasis in the salt tolerant cultivar Pokkali on Chr. 1 (10.7–12.2 Mb), explained 43% of the variation for seedling shoot Na^+/K^+ ratio in a RIL population between indica varieties IR29 and Pokkali (Bonilla et al., 2002; Mohammadi-Nejad et al., 2008; Thomson et al., 2010). And 13 QTL for salt tolerance at seedling stage in the salt tolerantcultivar Changbai10 on Chr. 1, 5, 6, and 7 were identified by linkage mapping, of which 6 QTL were validated by association analysis of 341 japonica rice accessions (Zheng et al., 2015). Although numerous QTL for salt tolerance in rice have been identified, only SKC1, encoding an HKT-type transporter, was cloned by map-based cloning in the qSKC-1 region of Chr. 1 (Lin et al., 2004; Ren et al., 2005). Therefore, further research is needed to characterize genes for salt tolerance in rice.

Wild rice germplasm is considered a valuable source of genes for tolerance to biotic and abiotic stresses, which can be potentially used in rice breeding (Zhang and Xie, 2014; Arzani and Ashraf, 2016; Brozynska et al., 2016; Mishra et al., 2016; Menguer et al., 2017). A previous study identified 13 QTL associated with salt tolerance in the wild rice species *O. rufipogon* Griff. (Tian et al., 2011). Introgression of *PcINO1* gene that encodes L-myoinositol 1-phosphate synthase in the wild rice species *O. coarctata* was introgressed into *O. sativa* Indica cultivar and improved its salt tolerance (Das-Chatterjee et al., 2006). *OsHKT1* (high-affinity potassium transporter), *OsHKT7,* as well as numerous transcription factor genes, including zinc finger proteins (ZFPs), NAC (NAM, ATAF, and CUC), MYB, and AP2/ERF (APETALA2/ethylene response factor) are differentially expressed in Dongxiang wild rice under salt stress conditions (Zhou et al., 2016), suggesting that multiple genes are responsible for salt tolerance in wild rice.

From 1970s wild rice genes have been introgressed into cultivated rice, and most of these studies focused on the improvement resistance/tolerance to biotic stresses (Brar and Khush, 1997; Zamir, 2001; Hajjar and Hodgkin, 2007; Dempewolf et al., 2017). Therefore, information regarding the improvement of salt tolerance in cultivated rice using wild rice genes is limited.

We previously identified several genes regulating plant abiotic stress tolerance in Arabidopsis, tobacco and rice (Quan et al., 2007, 2010, 2017; Wan et al., 2011; Zhang et al., 2011). In this study, we isolated a salt tolerant introgression line Dongxiang/Ningjing 15 (DJ15) from the population of the salt-tolerant wild rice line Dongxiang (*O. rufipogon* Griff.) (Song et al., 2005; Tian et al., 2011; Zhou et al., 2016) hybridized to a cultivated rice variety (*O. sativa* ssp. japonica) Ningjing16 (NJ16). Our objectives were to (1) investigate the distribution pattern of genomic fragments introgressed into DJ15, (2) map QTL for salt tolerance, and (3) utilize newly identified QTL in rice breeding for improving salt tolerance.

MATERIALS AND METHODS

Plant Materials

Dongxiang wild rice, which was the northernmost population of common wild rice naturally grown in Jiangxi Province, China (N28.14) (Gao et al., 2000; Liu et al., 2017), was crossed to a cultivated japonica rice Ningjing16 (NJ16) four times (**Figure 1**). The salt tolerance of introgression lines was evaluated against NJ16 and a reference cultivar 96D10, which was widely planted in North China. Based on the method (**Figure 1**), the salt tolerant introgression line Dongxiang/Ningjing 15 (DJ15) was selected for further study.

Determination of Rice Salt Tolerance

Two hundred rice seeds of each sample were exposed to 45°C for 3 days, then soaked in water containing 0, 100, and 150 mM NaCl at 25°C overnight, and placed at 35°C for 3 days. And the germination rate was calculated.

Rice seeds were treated at 45°C for 3 days, soaked in water at 25°C overnight, and placed at 35°C for 3 days. Forty uniformly germinated seeds were sown on metal meshes floating on Yoshida solution (Yoshida et al., 1976) and grown at 26°C. Seedlings at 10-days stage were transferred to Yoshida solution containing 0, 100, and 150 mM NaCl for comparison among DJ15, NJ16 and 96D10, and 120 mM NaCl for $F_{2:4}$ population. The number of wilted/dead leaves was counted 7 days later (Gao and Lin, 2013).

One-month rice seedlings were transferred to saline field [electrical conductivity of saturated soil extract (ECe) = 5.7 dS m^{-1}, pH 8.45], and 1-month later the survival rates were checked. When seeds matured, agronomic parameters, including tillering number, plant height and panicle number, were determined, and the yield was calculated after harvest. ECe was determined every week, and controlled to a range of 5.7–5.9 dS m^{-1} by the irrigation of fresh water or saline water as required.

Analysis of the Distribution of Single Nucleotide Polymorphism (SNP)/ Insertion or Deletion (Indel) Variants

Genomic resequencing of DJ15 and NJ16 was conducted by a high-throughput sequencing platform (Hiseq2500, Illumina, Inc.; San Diego, CA, U.S.), and the resequencing data were deposited in the National Center for Biotechnology Information Sequence Read Archive (NCBI SRA) under the accession numbers SRR6423773 and SRR6423774. The resequencing data

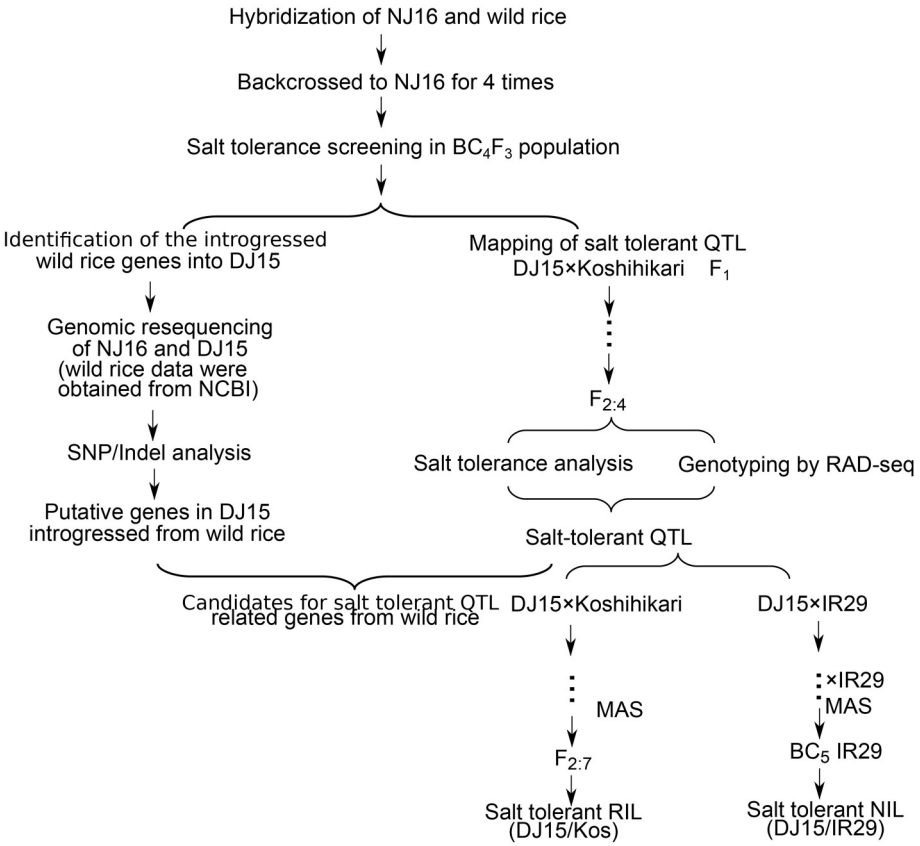

FIGURE 1 | Flowchart that describes the study. Abbreviations: BC, backcross; Kos, Koshihikari; MAS, marker-assisted selection; RAD-seq, restriction-site-associated DNA sequencing.

of Dongxiang wild rice was obtained from NCBI SRA accession SRX158100. The pair-end reads were mapped to Nipponbare rice reference genome (MSU Rice Genome Annotation Project Release 7) (Kawahara et al., 2013) by BWA (Li and Durbin, 2009). Then SNP/Indel variants were called using GATK (McKenna et al., 2010; DePristo et al., 2011). Finally, SNP/Indel density was calculated from the variation data by VCFtools (Danecek et al., 2011).

To verify the Indel variants derived from resequencing analysis, we designed specific PCR primers for randomly selected Indel variants with 3bp or more difference, spreading over the 12 chromosomes (Table S1). PCR amplification was conducted using genomic DNA isolated from NJ16, DJ15 and Dongxiang wild rice as templates. And the PCR products were separated by electrophoresis in 4% agarose gel.

Generation of QTL Mapping Population

DJ15 was crossed with the salt sensitive and late maturing Japonica cultivar Koshihikari. F_3 and F_4 were obtained by harvesting separately from responding F_2 parents, which were named as $F_{2:3}$ and $F_{2:4}$, respectively.

DJ15 was backcrossed to a salt sensitive indica rice variety IR29 (recurrent parent) five times, along with the confirmation of QTL in the offspring by marker assisted screening at each generation.

Population Genotyping by Restriction-Site-Associated DNA Sequencing (RAD-Seq)

Genomic DNA was extracted from 103 $F_{2:4}$ lines and the two parental lines using the cetyl trimethylammonium bromide (CTAB) method (Murray and Thompson, 1980). Sequencing libraries were constructed from the genomic DNA using the method modified from previous description (Sun et al., 2013). In brief, genomic DNA was incubated at 37°C with *Mse*I, T4 DNA ligase, ATP and *Mse*I adapter. After heat-inactivation of the restriction/ligation reactions at 65°C, the samples were digested with *Rsa*I and *Hpy*166II, then the subsequent steps for library construction were carried out as detailed in previous description (Sun et al., 2013). Then, pair-end sequencing was performed using a high-throughput sequencing platform (Hiseq2500, Illumina, Inc.; San Diego, CA, U.S.). Finally, specific-locus amplified fragments (SLAFs) were processed to obtain the SLAF genotype of each sample (Sun et al., 2013).

QTL Analysis

A total of 5,472 polymorphic SLAFs was obtained from the RAD-seq data of DJ15 and Koshihikari. Using HighMap method as described by Liu et al. (2014), a high density linkage map was constructed from the SLAF genotyping data of 103 $F_{2:4}$ lines.

Next, QTL were identified by the composite interval mapping method using Windows QTL Cartographer (Silva et al., 2012). The LOD threshold of QTL significance was determined by a permutation test (1,000 replications) at $P < 0.05$.

Identification of Candidate Genes for Salt Tolerance in QTL

The genomic resequencing data of Koshihikari was obtained from NCBI (DRX002963). After aligning of the pair-end reads to rice reference genome (MSU Rice Genome Annotation Project Release 7) (Kawahara et al., 2013) using BWA (Li and Durbin, 2009), SNP/Indel variants were called using GATK (McKenna et al., 2010; DePristo et al., 2011). The different SNP/Indel variants of DJ15, Koshihikari, NJ16, and Dongxiang were processed with GATK (McKenna et al., 2010; DePristo et al., 2011), and annotated with SnpEff (Cingolani et al., 2012). Candidate genes for salt tolerance in the QTL regions were obtained after filtering out transposons and pseudogenes.

RESULTS

Evaluation of DJ15 for Salt Tolerance

The salt-tolerant introgression line DJ15 was selected by lab screening and field evaluating the populations of Dongxiang/Ningjing16 (Ningjing16 as the recurrent parent) at backcross2 (BC_2) to BC_4 generations (**Figure 1**). Under non-stress conditions, the germination rate of DJ15 was not significantly different from that of the parental variety NJ16 and the control variety 96D10 (**Figure 2A**). However, at the 150 mM NaCl treatment, the germination rate of DJ15 was reduced by

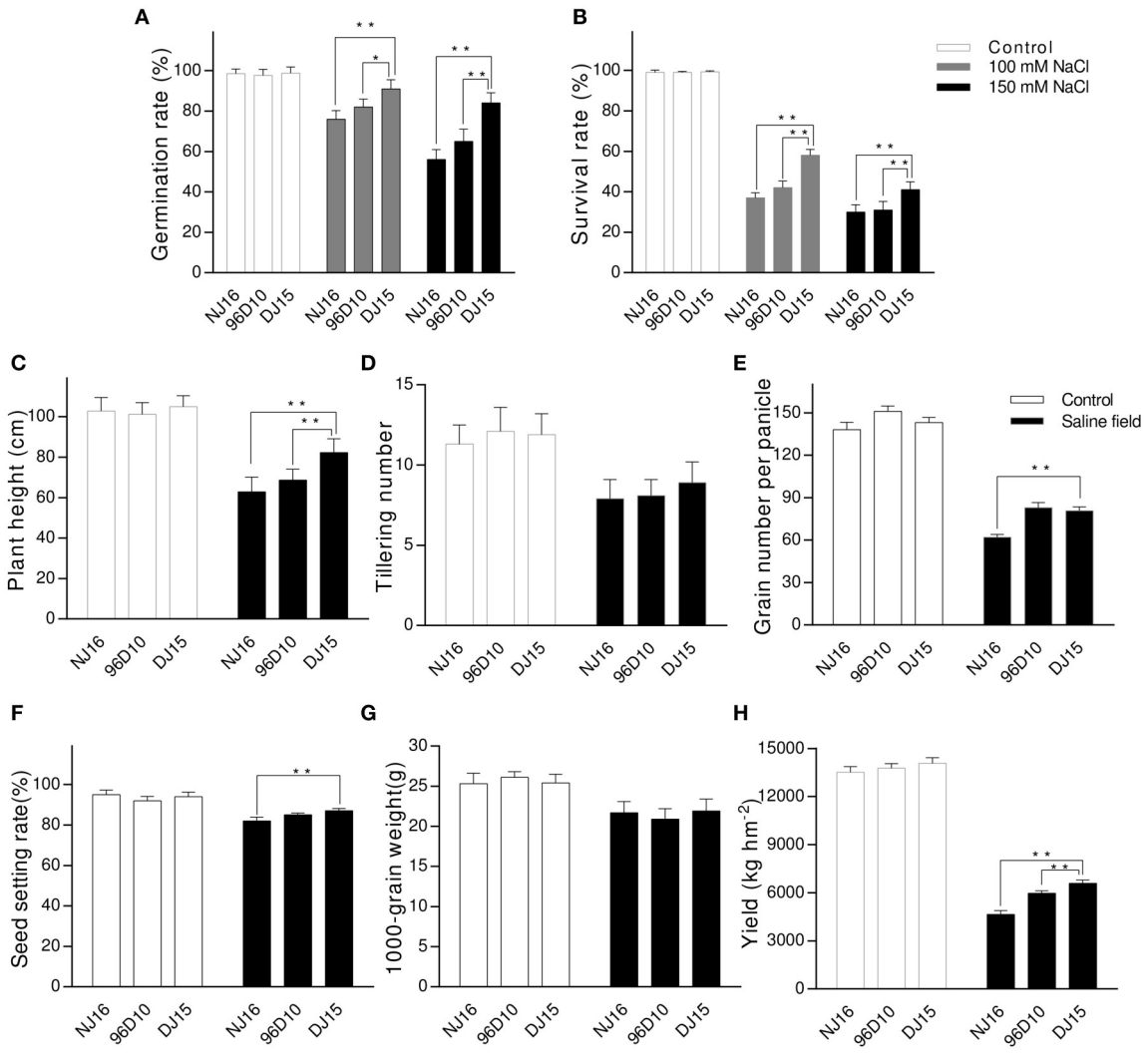

FIGURE 2 | Salt tolerance evaluation of introgression line DJ15. **(A)** Germination rate of rice seeds after treatment at 0, 100, and 150 mM NaCl for 3 days at 35°C. **(B)** Survival rate of 10-day-old seedlings after treatment at 0, 100, and 150 mM for 10 days and subsequent recovery for 7 days. **(C–H)** Field performance of rice under non-stress field conditions (ECe = 1.3 dS m^{-1}, pH 7.01) and under salt-stress field conditions (ECe = 5.7 dS m^{-1}, pH 8.45). *Indicates significant difference at $P < 0.05$ in Tukey's multiple comparisons test after ANOVA; **Indicates significant difference at $P < 0.01$ in Tukey's multiple comparisons test after ANOVA.

16%, of NJ16 by 44% and of 96D10 by 35%, suggesting that DJ15 was more salt tolerant than NJ16 and 96D10 at the germination stage.

At the 100 and 150 mM NaCl treatment, the percentage of wilted/dead leaves was 59 and 42% for DJ15, 37 and 30% for NJ16, and 41 and 31% for 96D10, respectively, indicating that DJ15 was also more salt tolerant than NJ16 and 96D10 at the seedling stage (**Figure 2B**).

Under non-stress field conditions (ECe = 1.3 dS m^{-1}, pH 7.01), the yield of DJ15 was slightly higher than that of NJ16 and 96D10; however, plant height, 1,000-grain weight, grain number per panicle, and effective tillering per plant were not significantly different among DJ15, NJ16 and 96D10. Under salt-stress field conditions (ECe = 5.7 dS m^{-1}, pH 8.45), the yield of DJ15 was markedly higher than that of NJ16 and 96D10, possibly due to its higher plant height and effective tillering number, grain number and seed setting rate (**Figures 2C–H**).

Therefore, these results suggested that DJ15 was more salt tolerant than NJ16 and 96D10 at the germination, seedling and mature stages (**Figure 2**).

Identification of Introgressed Genomic Fragments in DJ15

By comparing SNP/Indel variants of DJ15, NJ16 and Dongxiang wild rice, we found 642,349 SNP/Indel variants between DJ15 and NJ16 across the 12 chromosomes, among which 265,862 variants might be obtained from Dongxiang wild rice (**Table 1**). More than 97% of 617,227 SNP/Indel variant effects were in intergenic, intron, downstream and upstream of the coding regions, whereas only 2.3% in exons (**Table 2**).

PCR amplification using specific primers for 52 randomly selected Indel variants showed that different fragments were amplified from the genomic DNA of DJ15, NJ16, and Dongxiang (**Figure 3A**, Figure S1; Table S1). This result indicated that the identified variants from high-throughput sequencing were accurate.

The rate of variants between NJ16 and Dongxiang wild rice was one variant for every 194 bases, which was markedly higher than that between NJ16 and DJ15 (one variant for every 581 bases). Therefore, the genomic regions introgressed from Dongxiang wild rice into DJ15 were probably enriched with SNP/Indel variants. The regions of high density in SNP/Indel variants between DJ15 and NJ16 (receipt line) distributed unequally over the 12 rice chromosomes, within which four large regions of high density were located in Chr. 6, 7, 10, and 11 (**Figure 3B**). The distribution pattern of SNPs/Indels was identical between DJ15 and Dongxiang wild rice, different between NJ16 and Dongxiang, and similar between DJ15 and NJ16. These results indicated that the regions of high density in SNP/Indel variants identified in DJ15 might be large DNA fragments introgressed from Dongxiang wild rice.

QTL Mapping

QTL for salt tolerance were mapped in an $F_{2:4}$ population (n = 103) derived from a cross between DJ15 and a salt sensitive japonica rice variety Koshihikari. Lab and field screening for salt tolerance showed that the survival rate of DJ15 seedlings was 75%, whereas that of Koshihikari was 37%. Curve fitting by Gaussian method showed that the distribution of salt tolerance in $F_{2:4}$ lines was close to normal with a slight skewness to the salt sensitivity side, since 61% of the lines congregated between DJ15 and Koshihikari, 15% of the lines were more salt sensitive than Koshihikari, and 24% of the lines were more salt tolerant than DJ15 (**Figure 4A**).

We used restriction-site-associated DNA sequencing to determine the genotype of DJ15, Koshihikari and the $F_{2:4}$ lines. DJ15 and Koshihikari were sequenced at an average depth of 23.98 ×, whereas $F_{2:4}$ lines were sequenced at an average depth of 4.18 ×. We found a total of 136,724 specific-locus amplified fragments (SLAFs), of which 5.49% were polymorphic SLAFs (Tables S2, S3).

Mapping SLAFs to the rice reference genome (MSU Rice Genome Annotation Project Release 7, http://rice.plantbiology.msu.edu/) showed that they were nearly equally distributed over

TABLE 1 | Number of SNP/Indel variants in the *O. rufipogon* line Dongxiang, the *O. sativa Japonica* variety Ningjing16 (NJ16), and the salt-tolerant introgression line DJ15.

Chromosome	DJ15 vs. NJ16	(DJ15 = Dongxiang) vs. NJ16
1	29,164	11,550
2	41,189	12,497
3	14,797	6,090
4	22,665	13,017
5	34,779	9,396
6	156,245	85,301
7	62,336	21,950
8	25,905	11,802
9	18,535	9,817
10	64,841	19,714
11	158,873	59,294
12	13,020	5,434
Total	642,349	265,862

TABLE 2 | Number of SNP/Indel effects by genomic region.

Type (alphabetical order)	Count	Percent(%)
Downstream	138,852	22.496
Exon	14,534	2.355
Intergenic	217,168	35.184
Intron	33,819	5.479
Splice_site_acceptor	39	0.006
Splice_site_donor	32	0.005
Splice_site_region	805	0.13
Transcript	53,643	8.691
Upstream	145,527	23.578
Utr_3_prime	7,861	1.274
Utr_5_prime	4,947	0.801
Total	617,227	100%

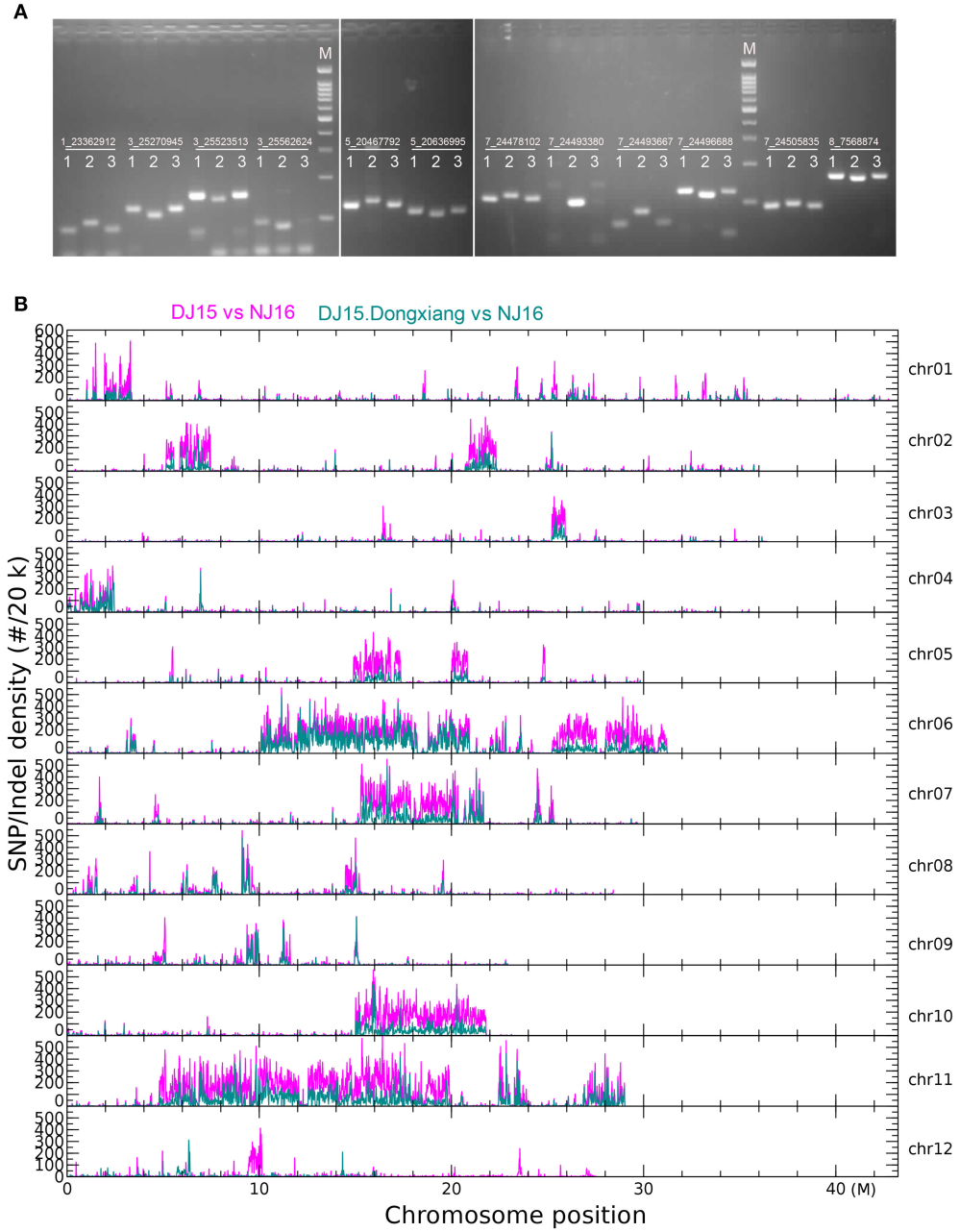

FIGURE 3 | Distribution of single nucleotide polymorphism (SNP)/insertion or deletion (Indel) variants in rice genome. **(A)** PCR verification of Indels with 3 bp or more difference among the *O. rufipogon* line Dongxiang (1), the *O. sativa Japonica* variety Ningjing16 (2), and the salt-tolerant introgression line DJ15 (3). M. 100 bp ladder. **(B)** Density of SNP/Indel variants in rice genome. "DJ15 vs. NJ16" indicates SNP/Indel variants between DJ15 and NJ16; "DJ15.Dongxiang vs. NJ16" indicates SNP/Indel variants identical between DJ15 and Dongxiang, but different from NJ16.

the 12 rice chromosomes. However, polymorphic SLAFs were unequally distributed over the chromosomes and condensed to six regions of high density on Chr. 2, 5, 6, 7, 10, and 11 (**Figures 4B,C**).

After filtering SLAFs with sequencing depth under 10 × or heterozygous in parents, we obtained 5,479 polymorphic SLAFs. Then using HighMap software (Liu et al., 2014), we constructed a high density linkage map from SLAF-seq genotyping data of DJ15 × Koshihikari $F_{2:4}$ lines. After filtering makers with MLOD < 5, we arranged 5,472 of 5,479 SLAF markers to 12 linkage groups, with an average distance of 0.34 cM between two adjacent markers. The linkage map was consistent with the rice reference physical map as revealed by mapping SLAFs to the rice reference genome and finding a Spearman's correlation

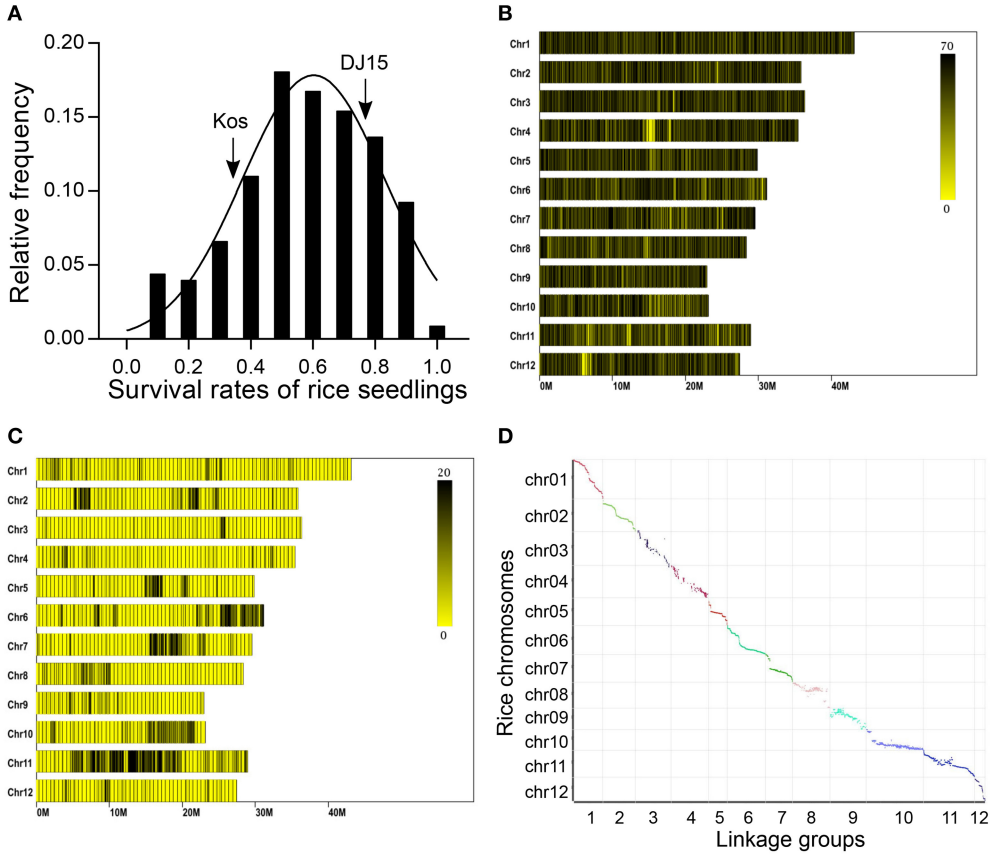

FIGURE 4 | Salt tolerance screening and genotyping of DJ15 × Koshihikari $F_{2:4}$ rice population. **(A)** Survival rate of 2-week rice seedlings after treatment at 120 mM NaCl for 10 d. Arrows indicate the survival rate of DJ15 and Koshihikari (Kos), respectively. **(B)** Distribution of specific-locus amplified fragments (SLAFs) in the rice reference genome. **(C)** Distribution of polymorphic SLAFs between DJ15 and Koshihikari in rice reference genome. Color bars indicate the SLAF number in the rice genome within 1 M window. **(D)** Comparison of the linkage map constructed from DJ15 × Koshihikari $F_{2:4}$ population with the rice reference physical map.

coefficient of approximately one (**Figure 4D**). Thus, the marker positions on the linkage map were valid and the genotyping results were accurate.

Using composite interval mapping, we found 9 QTL for salt tolerance spreading over 7 chromosomes with an LOD cutoff > 3.0 (**Table 3**). The positive additive effects of 7 QTL were derived from DJ15 alleles, and the total phenotypic variance explained by each QTL was 8.81–22.10%. Of these, qST6 accounted for 19.38% of the total phenotypic variance, and had an additive effect of 0.12 for increasing survival rate derived from DJ15 allele.

TABLE 3 | QTL for salt tolerance identified in DJ15 × Koshihikari $F_{2:4}$ segregating population.

QTL	Chromosome	Chromosome position (M)	Peak LOD	Additive effect[a]	R^2(%)[b]
qST1.1	1	40.3	4.90	0.017	22.10
qST1.2	1	10.6	3.30	0.038	10.00
qST3	3	6.2	3.61	0.022	14.27
qST4.1	4	29.6	3.65	0.15	9.79
qST4.2	4	23.4	3.55	−0.096	8.81
qST5	5	16.5	3.98	−0.11	12.67
qST6	6	25.6	4.12	0.12	19.38
qST8	8	21.7	4.33	0.019	15.80
qST10	10	17.2	3.68	0.13	11.35

[a] *Additive effect on the DJ15 allele.*
[b] *Percentage of total phenotypic variance explained by the QTL.*

Candidate Genes for Salt Tolerance in QTL

To identify candidate genes for salt tolerance in the QTL regions, we analyzed the sequence variants of NJ16, DJ15, Koshihikari and Dongxiang wild rice in the 9 QTL regions (Table S4). Among the candidate genes, we found *Os01g0307500* (*OsSKC1*) located in the qST1.2 region and *Os01g0932500* (*OsHAK6*) located in the qST1.1 region. Other QTL candidates included several transcription factors (MYB, zinc finger and AP2/ERF) and protein kinases, which might stimulate plant salt stress tolerance by transcriptional regulation and kinase pathways (Golldack et al., 2014). These results indicated that the identified QTL might enhance rice salt tolerance via ionic homeostasis maintenance, gene transcription and kinase signaling pathways.

TABLE 4 | Agronomic traits of DJ15/Koshihikari recombinant inbred lines (RILs) carrying $qST6^{DJ15}$ under salt-stress field conditions (ECe = 4.0 dS m^{-1}, pH 8.5).

RIL	Tillering No.	Panicle No.	Plant height(cm)	Heading date	Yield (kg hm^{-2})
YD7	10.2	9.2	94.7	Aug 1	11,743
YD8	9.2	7.8	93.6	Aug 2	11,411
YD22	13.0	11.0	97.2	Aug 5	10,085
YD23	12.0	11.0	94.0	Aug 4	10,275
YD28	14.4	12.2	98.4	Aug 8	10,511
YD44	10.0	9.4	97.3	Aug 2	10,606
DJ15	13.8	11.6	88.7	Jul 28	9,521
Koshihikari	16.4	14.4	94.3	Aug 9	7,386

Application of QTL for Improvement of Salt Tolerance in Cultivated Rice

As DJ15 is a salt tolerant and early maturing introgression line which is only suitable for Ningxia but not suitable for planting in other areas of Northeast China, we investigated if it would be possible to identify a highly salt-tolerant and late maturing line by hybridization of DJ15 to a salt sensitive but late maturing rice variety Koshihikari. By marker-assisted screening, we identified 55 lines carrying $qST1.2^{DJ15}$ and $qST6^{DJ15}$ from 980 DJ15/Koshihikari recombinant inbred lines (RILs). Under salt-stress field conditions (ECe = 4.0 dS m^{-1}), the heading dates of 6 (YD7, 8, 22, 23, 28, 44) of 55 lines were about 4–11 days later than that of DJ15, and their yields were 8–23% more than that of DJ15 or 36–59% more than that of Koshihikari (**Table 4**). Therefore, the 6 salt tolerant, high yielding and late maturing lines might be used for developing new rice varieties.

qST1.2 and qST6 were two QTL that showed the highest effect for salt tolerance in DJ15, and SKC1 might be one major effect gene for qST1.2 (Ren et al., 2005). Among the 9 newly identified QTL for salt tolerance, qST6 was a novel QTL in a region of high SNP/Indel variant density; thus, we backcrossed DJ15 to IR29 5 times and screened the offspring by qST6 linked markers to select IR29 near-isogenic line $(NIL)^{DJ15}$. Under non-stress conditions, no significant differences were found in the seedling growth of IR29 and IR29 NIL^{DJ15} (**Figure 5**). Lab screening under salt stress conditions (80 mM NaCl) for 10 d, IR29 NIL^{DJ15} seedlings demonstrated higher survival rate, plant height, and biomass compared with IR29, indicating that IR29 NIL^{DJ15} was more tolerant to salt stress (**Figure 5**). These results suggested that qST1.2 and qST6 could be utilized in rice breeding for improving salt tolerance.

DISCUSSION

O. sativa and *O. glaberrima* are the only two domesticated species within the genus *Oryza*, and thus the genetic diversity of cultivated rice is limited. *Oryza* contains more than 20 wild species, which are considered a significant source of genetic diversity (Atwell et al., 2014) since they compose a valuable pool of genes for disease or abiotic stress resistance/tolerance (Brar and Khush, 1997; Zamir, 2001; Hajjar and Hodgkin, 2007; Maxted et al., 2012; Mishra et al., 2016; Dempewolf et al., 2017; Wang et al., 2017). Pest/disease resistance is the most well studied trait that can be improved by introgression of wild rice genes (Hajjar and Hodgkin, 2007). In addition, the genome of wild rice contains tolerant alleles of abiotic stress genes. For example, submerge tolerant *O. rufipogon* and *O. nivara* accessions carry the *SUB1A-1* allele for submergence tolerance (Niroula et al., 2012). An accession of wild rice (*O. rufipogon*) from Yunnan Province of China contains 13 QTL for salt tolerance QTL (Tian et al., 2011). Dongxiang wild rice changes the expression of more than 6,800 genes related to salt stress, including numerous transcription factor genes, such as ZFP, NAC, MYB, and ERF, indicating that these transcription factors might regulate multiple regulatory pathways under salt stress conditions (Zhou et al., 2016). However, information regarding the improvement of salt tolerance in cultivated rice using wild genes is limited. In this study, we demonstrate that wild rice genes could enhance the salt tolerance of cultivate rice.

NJ16 is a commercial variety widely cultivated in the Yellow-river irrigating region of Ningxia Province in China. However, the yield is negatively affected by salt stress due to the widespread saline soil in this region. In the present study, we introgressed wild rice fragments into a rice cultivar, and obtained an introgression line with improved salt tolerance after several rounds of selection. These results demonstrated that wild rice genes could be used to improve salt tolerance in cultivated rice.

AtHKT1 promotes Na^+ unloading from the xylem and increases salt tolerance in Arabidopsis (Davenport et al., 2007; Møller et al., 2009). OsSKC1 (Ren et al., 2005) is a HKT-like protein, namely HKT8/HKT1;5 (Garciadeblás et al., 2003; Hauser and Horie, 2010). OsSKC1 is not primarily a K^+ transporter but is a Na^+ selective transporter, which regulates Na^+/K^+ levels in shoots by recirculating Na^+ from shoots to roots, thus affecting the shoot K^+ content indirectly (Ren et al., 2005). Furthermore, Immuno-staining and $^{22}Na^+$ tracer experiments suggested that OsHKT1;5 protein contributes to Na^+ exclusion in the phloem, in addition to xylem Na^+ unloading, to prevent Na^+ transfer to young leaf blades (Kobayashi et al., 2017). K^+ transporter OsHAK1 mediates K^+ uptake in roots and K^+ translocation to shoots, which could enhance salt tolerance (Bañuelos et al., 2002; Chen et al., 2015). Similarly, OsHAK5 enables K^+ uptake by roots under external K^+ nutrient limitation and saline conditions (Yang et al., 2014). Therefore, OsHAK6 in qST1.1 might mediate salt tolerance as the OsHAKs mentioned above.

Salt tolerance is a complex trait controlled by many genetic loci. For example, eleven QTL related to salt tolerance are located on 5 chromosomes from the F_3 population of Nona Bokra and Koshihikari (Ren et al., 2005). And 13 of 15 QTL on six chromosomes from wild rice improve salt tolerance in Teqing background (Tian et al., 2011). Compared with salt tolerance QTL identified from wild rice *O. rufipogon* (Tian et al., 2011), in this study the position of qST1.2 is close to qSTS1, and the other 5 QTL for salt tolerance are novel. Up to now, only *SKC1* localized in qST1.2 region has been cloned by mapping (Ren et al., 2005). Therefore, the function of other candidate genes for salt tolerant QTL remains to be explored in future studies.

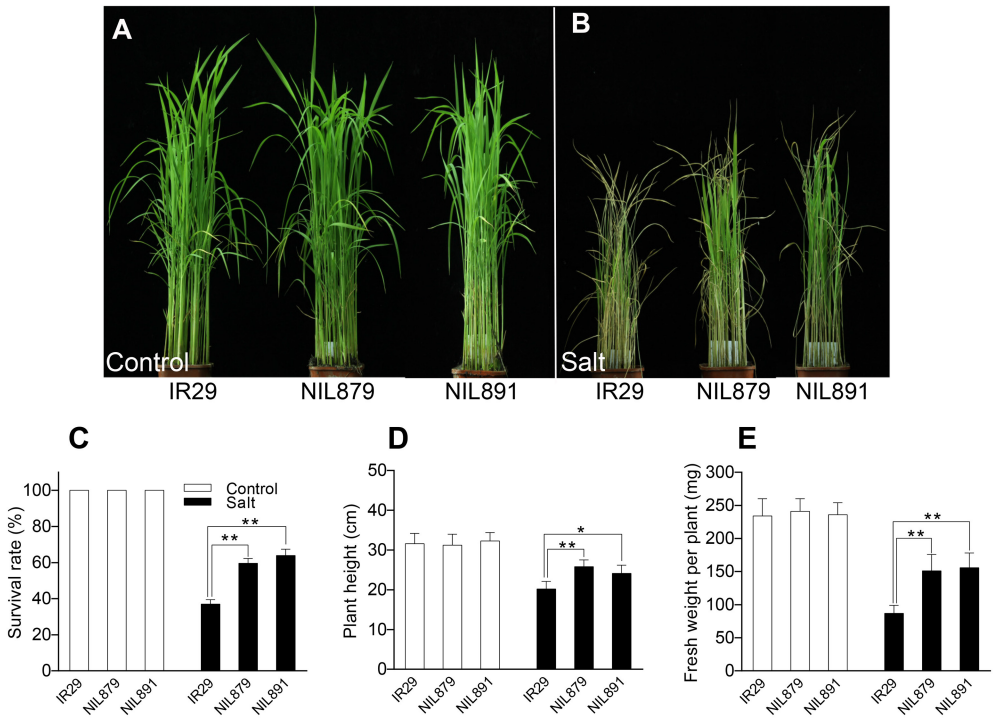

FIGURE 5 | Salt tolerance of qST6^{DJ15} near isogenic lines. **(A–E)** Survival rate, plant height, and fresh weight of 2-week-old IR29 and qST6^{DJ15} NILs (NIL879 and NIL891) seedlings after treatment at 80 mM NaCl for 10 days and subsequent recovery for 5 days. *Indicates significant difference at $P < 0.05$ in Tukey's multiple comparisons test after ANOVA; **Indicates significantly difference at $P < 0.01$ in Tukey's multiple comparisons test after ANOVA.

Although several QTL for salt tolerance have been identified from wild rice (Tian et al., 2011), their physiological function has not been confirmed under salt-stress field conditions. In the present study, we obtained 6 salt-tolerant DJ15/Koshihikari RILs, carrying both qST1.2^{DJ15} and qST6^{DJ15}, via marker-assisted screening. These RILs showed a lower tillering and panicle number than Koshihikari and DJ15, but a higher yield, under salt-stress field conditions, which might result from the relatively higher seed setting rate of RILs. Additionally, IR29 NIL^{DJ15} was more salt tolerant than IR29 at the seedling stage and showed higher yield per plant in a preliminary study. However, more research is needed to elucidate the underlying regulating mechanism of yield in relation to qST6^{DJ15} under salt stress conditions.

As DJ15 and the salt tolerant RILs demonstrate variation in growth duration, the growth adaptability in saline field of Dongying (Shandong Province, E118.7, N37.6) and Panjin (Liaoning Province, E122.0, N41.0), other than Yinchuan (Ningxia Province, E106.2, N38.5) in North China, is under investigation. And we hope to release these salt tolerant lines to the public in the near future. Overall, our results demonstrated that wild rice genes could be successfully used in rice breeding programs to develop varieties with markedly improved salt tolerance.

AUTHOR CONTRIBUTIONS

RH conceived the project. SL, JH, HB, XL, and YZ constructed wild rice introgression lines to isolate DJ15, and performed saline field tests. JW performed salt tolerance determination by hydroponics in $F_{2:4}$ population. RQ performed the rest of experiments and analyzed data. HZ and ZZ analyzed the data. RQ wrote the manuscript.

ACKNOWLEDGMENTS

This work was supported by the National Key Research and Development Program of China (2016YFD0100604), National Natural Science Foundation of China (31771706), Ministry of Agriculture of China (2016ZX08009-003-005), and Ningxia Hui Autonomous Region of China (2013NYY Z0302).

SUPPLEMENTARY MATERIAL

The Supplementary Material for this article can be found online at: https://www.frontiersin.org/articles/10.3389/fpls.2017.02269/full#supplementary-material

REFERENCES

Arzani, A., and Ashraf, M. (2016). Smart engineering of genetic resources for enhanced salinity tolerance in crop plants. *Crit. Rev. Plant Sci.* 35, 146–189. doi: 10.1080/07352689.2016.1245056

Atwell, B. J., Wang, H., and Scafaro, A. P. (2014). Could abiotic stress tolerance in wild relatives of rice be used to improve *Oryza sativa*? *Plant Sci.* 215–216, 48–58. doi: 10.1016/j.plantsci.2013.10.007

Bañuelos, M. A., Garciadeblas, B., Cubero, B., and Rodríguez-Navarro, A. (2002). Inventory and functional characterization of the HAK potassium transporters of rice. *Plant Physiol.* 130, 784–795. doi: 10.1104/pp.007781

Bonilla, P., Dvorak, J., Mackill, D., Deal, K., and Gregorio, G. (2002). RFLP and SSLP mapping of salinity tolerance genes in chromosome 1 of rice (*Oryza sativa* L.) using recombinant inbred lines. *Philipp. Agric. Sci.* 85, 68–76.

Brar, D., and Khush, G. (1997). Alien introgression in rice. *Plant Mol. Biol.* 35, 35–47. doi: 10.1023/A:1005825519998

Brozynska, M., Furtado, A., and Henry, R. J. (2016). Genomics of crop wild relatives: expanding the gene pool for crop improvement. *Plant Biotechnol. J.* 14, 1070–1085. doi: 10.1111/pbi.12454

Calanca, P. P. (2017). "Effects of abiotic stress in crop production," in *Quantication of Climate Variability, Adaptation and Mitigation for Agricultural Sustainability*, eds M. Ahmed and C. O. Stockle (Cham: Springer International Publishing), 165–180. doi: 10.1007/978-3-319-32059-5_8

Chen, G., Hu, Q., Luo, L., Yang, T., Zhang, S., Hu, Y., et al. (2015). Rice potassium transporter OsHAK1 is essential for maintaining potassium-mediated growth and functions in salt tolerance over low and high potassium concentration ranges. *Plant Cell Environ.* 38, 2747–2765. doi: 10.1111/pce.12585

Chinnusamy, V., Jagendorf, A., and Zhu, J.-K. (2005). Understanding and improving salt tolerance in plants. *Crop Sci.* 45, 437–448. doi: 10.2135/cropsci2005.0437

Cingolani, P., Platts, A., Wang, L. L., Coon, M., Nguyen, T., Wang, L., et al. (2012). A program for annotating and predicting the effects of single nucleotide polymorphisms, SnpEff: SNPs in the genome of *Drosophila melanogaster* strain w^{1118}; *iso*-2; *iso*-3. *Fly* 6, 80–92. doi: 10.4161/fly.19695

Danecek, P., Auton, A., Abecasis, G., Albers, C. A., Banks, E., DePristo, M. A., et al. (2011). The variant call format and VCFtools. *Bioinformatics* 27, 2156–2158. doi: 10.1093/bioinformatics/btr330

Das-Chatterjee, A., Goswami, L., Maitra, S., Dastidar, K. G., Ray, S., and Majumder, A. L. (2006). Introgression of a novel salt-tolerant L-*myo*-inositol 1-phosphate synthase from *Porteresia coarctata* (*Roxb.*) Tateoka (*PcINO1*) confers salt tolerance to evolutionary diverse organisms. *FEBS Lett.* 580, 3980–3988. doi: 10.1016/j.febslet.2006.06.033

Davenport, R. J., Muñoz-Mayor, A., Jha, D., Essah, P. A., Rus, A., and Tester, M. (2007). The Na^+ transporter AtHKT1;1 controls retrieval of Na^+ from the xylem in *Arabidopsis*. *Plant Cell Environ.* 30, 497–507. doi: 10.1111/j.1365-3040.2007.01637.x

Dempewolf, H., Baute, G., Anderson, J., Kilian, B., Smith, C., and Guarino, L. (2017). Past and future use of wild relatives in crop breeding. *Crop Sci.* 57:1070. doi: 10.2135/cropsci2016.10.0885

DePristo, M. A., Banks, E., Poplin, R., Garimella, K. V., Maguire, J. R., Hartl, C., et al. (2011). A framework for variation discovery and genotyping using next-generation DNA sequencing data. *Nat. Genet.* 43, 491–498. doi: 10.1038/ng.806

Gao, J.-P., and Lin, H.-X. (2013). "QTL analysis and map-based cloning of salt tolerance gene in rice," in *Rice Protocols, Methods in Molecular Biology*, Vol. 956, ed Y. Yang (Totowa, NJ: Humana Press), 69–82. doi: 10.1007/978-1-62703-194-3_6

Gao, L., Chen, W., Jiang, W., Song, G. E., Hong, D., and Wang, X. (2000). Genetic erosion in northern marginal population of the common wild rice *Oryza rufipogon* Griff. and its conservation, revealed by the change of population genetic structure. *Hereditas* 133, 47–53. doi: 10.1111/j.1601-5223.2000.00047.x

Garciadeblás, B., Senn, M. E., Bañuelos, M. A., and Rodríguez-Navarro, A. (2003). Sodium transport and HKT transporters: the rice model. *Plant J.* 34, 788–801. doi: 10.1046/j.1365-313X.2003.01764.x

Golldack, D., Li, C., Mohan, H., and Probst, N. (2014). Tolerance to drought and salt stress in plants: unraveling the signaling networks. *Front. Plant Sci.* 5:151. doi: 10.3389/fpls.2014.00151

Hajjar, R., and Hodgkin, T. (2007). The use of wild relatives in crop improvement: a survey of developments over the last 20 years. *Euphytica* 156, 1–13. doi: 10.1007/s10681-007-9363-0

Hauser, F., and Horie, T. (2010). A conserved primary salt tolerance mechanism mediated by HKT transporters: a mechanism for sodium exclusion and maintenance of high K^+/Na^+ ratio in leaves during salinity stress. *Plant Cell Environ.* 33, 552–565. doi: 10.1111/j.1365-3040.2009.02056.x

Ismail, A. M., and Horie, T. (2017). Genomics, physiology, and molecular breeding approaches for improving salt tolerance. *Annu. Rev. Plant Biol.* 68, 405–434. doi: 10.1146/annurev-arplant-042916-040936

Kawahara, Y., de la Bastide, M., Hamilton, J. P., Kanamori, H., McCombie, W. R., Ouyang, S., et al. (2013). Improvement of the *Oryza sativa* Nipponbare reference genome using next generation sequence and optical map data. *Rice* 6:4. doi: 10.1186/1939-8433-6-4

Khatun, S., and Flowers, T. J. (1995). Effects of salinity on seed set in rice. *Plant Cell Environ.* 18, 61–67. doi: 10.1111/j.1365-3040.1995.tb00544.x

Kobayashi, N. I., Yamaji, N., Yamamoto, H., Okubo, K., Ueno, H., Costa, A., et al. (2017). OsHKT1;5 mediates Na^+ exclusion in the vasculature to protect leaf blades and reproductive tissues from salt toxicity in rice. *Plant J.* 91, 657–670. doi: 10.1111/tpj.13595

Koyama, M. L., Levesley, A., Koebner, R. M., Flowers, T. J., and Yeo, A. R. (2001). Quantitative trait loci for component physiological traits determining salt tolerance in rice. *Plant Physiol.* 125, 406–422. doi: 10.1104/pp.125.1.406

Kurotani, K., Yamanaka, K., Toda, Y., Ogawa, D., Tanaka, M., Kozawa, H., et al. (2015). Stress tolerance profiling of a collection of extant salt-tolerant rice varieties and transgenic plants overexpressing abiotic stress tolerance genes. *Plant Cell Physiol.* 56, 1867–1876. doi: 10.1093/pcp/pcv106

Li, H., and Durbin, R. (2009). Fast and accurate short read alignment with Burrows–Wheeler transform. *Bioinformatics* 25, 1754–1760. doi: 10.1093/bioinformatics/btp324

Lin, H. X., Zhu, M. Z., Yano, M., Gao, J. P., Liang, Z. W., Su, W. A., et al. (2004). QTLs for Na^+ and K^+ uptake of the shoots and roots controlling rice salt tolerance. *Theor. Appl. Genet.* 108, 253–260. doi: 10.1007/s00122-003-1421-y

Liu, D., Ma, C., Hong, W., Huang, L., Liu, M., Liu, H., et al. (2014). Construction and analysis of high-density linkage map using high-throughput sequencing data. *PLoS ONE* 9:e98855. doi: 10.1371/journal.pone.0098855

Liu, S., Zheng, X., Yu, L., Feng, L., Wang, J., Gong, T., et al. (2017). Comparison of the genetic structure between *in situ* and *ex situ* populations of Dongxiang wild rice (*Oryza rufipogon* Griff.). *Crop Sci.* 57:3075. doi: 10.2135/cropsci2017.01.0015

Lutts, S., Kinet, J., and Bouharmont, J. (1995). Changes in plant response to NaCl during development of rice (*Oryza sativa* L.) varieties differing in salinity resistance. *J. Exp. Bot.* 46, 1843–1852. doi: 10.1093/jxb/46.12.1843

Maxted, N., Kell, S., Ford-Lloyd, B., Dulloo, E., and Toledo, A. (2012). Toward the systematic conservation of global crop wild relative diversity. *Crop Sci.* 52, 774–785. doi: 10.2135/cropsci2011.08.0415

McKenna, A., Hanna, M., Banks, E., Sivachenko, A., Cibulskis, K., Kernytsky, A., et al. (2010). The Genome Analysis Toolkit: a MapReduce framework for analyzing next-generation DNA sequencing data. *Genome Res.* 20, 1297–1303. doi: 10.1101/gr.107524.110

Menguer, P. K., Sperotto, R. A., and Ricachenevsky, F. K. (2017). A walk on the wild side: *Oryza* species as source for rice abiotic stress tolerance. *Genet. Mol. Biol.* 40, 238–252. doi: 10.1590/1678-4685-gmb-2016-0093

Mishra, S., Singh, B., Misra, P., Rai, V., and Singh, N. K. (2016). Haplotype distribution and association of candidate genes with salt tolerance in Indian wild rice germplasm. *Plant Cell Rep.* 35, 2295–2308. doi: 10.1007/s00299-016-2035-6

Møller, I. S., Gilliham, M., Jha, D., Mayo, G. M., Roy, S. J., Coates, J. C., et al. (2009). Shoot Na^+ exclusion and increased salinity tolerance engineered by cell type-specific alteration of Na^+ transport in *Arabidopsis*. *Plant Cell* 21, 2163–2178. doi: 10.1105/tpc.108.064568

Mohammadi-Nejad, G., Arzani, A., Rezai, A., Singh, R., and Gregorio, G. (2008). Assessment of rice genotypes for salt tolerance using microsatellite markers associated with the saltol QTL. *Afr. J. Biotechnol.* 7, 730–36.

Munns, R. (2011). "Plant adaptations to salt and water stress: differences and commonalities," in *Plant Responses to Drought and Salinity Stress Developments*

in a Post-genomic Era, Vol 57 of Advances in Botanical Research, ed I. Turkan (London: Academic Press), 1–32. doi: 10.1016/B978-0-12-387692-8.00001-1

Murray, M. G., and Thompson, W. F. (1980). Rapid isolation of high molecular weight plant DNA. *Nucleic Acids Res.* 8, 4321–4325. doi: 10.1093/nar/8.19.4321

Niroula, R. K., Pucciariello, C., Ho, V. T., Novi, G., Fukao, T., and Perata, P. (2012). *SUB1A*-dependent and -independent mechanisms are involved in the flooding tolerance of wild rice species. *Plant J.* 72, 282–293. doi: 10.1111/j.1365-313X.2012.05078.x

Pardo, J. M. (2010). Biotechnology of water and salinity stress tolerance. *Curr. Opin. Biotechnol.* 21, 185–196. doi: 10.1016/j.copbio.2010.02.005

Quan, R., Hu, S., Zhang, Z., Zhang, H., Zhang, Z., and Huang, R. (2010). Overexpression of an ERF transcription factor TSRF1 improves rice drought tolerance. *Plant Biotechnol. J.* 8, 476–488. doi: 10.1111/j.1467-7652.2009.00492.x

Quan, R., Lin, H., Mendoza, I., Zhang, Y., Cao, W., Yang, Y., et al. (2007). SCaBP8/CBL10, a putative calcium sensor, interacts with the protein kinase SOS2 to protect *Arabidopsis* shoots from salt stress. *Plant Cell* 19, 1415–1431. doi: 10.1105/tpc.106.042291

Quan, R., Wang, J., Yang, D., Zhang, H., Zhang, Z., and Huang, R. (2017). EIN3 and SOS2 synergistically modulate plant salt tolerance. *Sci. Rep.* 7:44637. doi: 10.1038/srep44637

Ren, Z. H., Gao, J. P., Li, L. G., Cai, X. L., Huang, W., Chao, D. Y., et al. (2005). A rice quantitative trait locus for salt tolerance encodes a sodium transporter. *Nat. Genet.* 37, 1141–1146. doi: 10.1038/ng1643

Silva, L. D. C. E., Wang, S., and Zeng, Z.-B. (2012). "Composite interval mapping and multiple interval mapping: procedures and guidelines for using Windows QTL Cartographer," in *Quantitative Trait Loci (QTL): Methods and Protocols, Methods in Molecular Biology*, Vol. 871, ed Y. Yang (New York, NY: Humana Press), 75–119. doi: 10.1007/978-1-61779-785-9_6

Song, Z., Li, B., Chen, J., and Lu, B. (2005). Genetic diversity and conservation of common wild rice (*Oryza rufipogon*) in China. *Plant Species Biol.* 20, 83–92. doi: 10.1111/j.1442-1984.2005.00128.x

Sun, X., Liu, D., Zhang, X., Li, W., Liu, H., Hong, W., et al. (2013). SLAF-seq: an efficient method of large-scale *de novo* SNP discovery and genotyping using high-throughput sequencing. *PLoS ONE* 8:e58700. doi: 10.1371/journal.pone.0058700

Thomson, M. J., de Ocampo, M., Egdane, J., Akhlasur Rahman, M., Godwin Sajise, A., Adorada, D. L., et al. (2010). Characterizing the saltol quantitative trait locus for salinity tolerance in rice. *Rice* 3, 148–160. doi: 10.1007/s12284-010-9053-8

Tian, L., Tan, L., Liu, F., Cai, H., and Sun, C. (2011). Identification of quantitative trait loci associated with salt tolerance at seedling stage from *Oryza rufipogon*. *J. Genet. Genomics* 38, 593–601. doi: 10.1016/j.jgg.2011.11.005

Todaka, D., Nakashima, K., Shinozaki, K., and Yamaguchi-Shinozaki, K. (2012). Toward understanding transcriptional regulatory networks in abiotic stress responses and tolerance in rice. *Rice* 5:6. doi: 10.1186/1939-8433-5-6

Wan, L., Zhang, J., Zhang, H., Zhang, Z., Quan, R., Zhou, S., et al. (2011). Transcriptional activation of OsDERF1 in OsERF3 and OsAP2-39 negatively modulates ethylene synthesis and drought tolerance in rice. *PLoS ONE* 6:e25216. doi: 10.1371/journal.pone.0025216

Wang, C., Hu, S., Gardner, C., and Lübberstedt, T. (2017). Emerging avenues for utilization of exotic germplasm. *Trends Plant Sci.* 22, 624–637. doi: 10.1016/j.tplants.2017.04.002

Yang, T., Zhang, S., Hu, Y., Wu, F., Hu, Q., Chen, G., et al. (2014). The role of a potassium transporter OsHAK5 in potassium acquisition and transport from roots to shoots in rice at low potassium supply levels. *Plant Physiol.* 166, 945–959. doi: 10.1104/pp.114.246520

Yoshida, S., Forno, D., Cock, J., and Gomez, K. (1976). *Laboratory Manual for Physiological Studies of Rice, 3rd Edn*. Manila: International Rice Research Institute.

Zamir, D. (2001). Improving plant breeding with exotic genetic libraries. *Nat. Rev. Genet.* 2, 983–989. doi: 10.1038/35103590

Zeng, L., Shannon, M., and Grieve, C. (2002). Evaluation of salt tolerance in rice genotypes by multiple agronomic parameters. *Euphytica* 127, 235–245. doi: 10.1023/a:1020262932277

Zhang, F., and Xie, J. (2014). "Genes and QTLs resistant to biotic and abiotic stresses from wild rice and their applications in cultivar improvements," in *Rice - Germplasm, Genetics and Improvement*, eds W. Yan and J. Bao (Rijeka: InTech), Chapter 02. doi: 10.5772/56825

Zhang, L., Li, Z., Quan, R., Li, G., Wang, R., and Huang, R. (2011). An AP2 domain-containing gene, *ESE1*, targeted by the ethylene signaling component EIN3 is important for the salt response in *Arabidopsis*. *Plant Physiol.* 157, 854–865. doi: 10.1104/pp.111.179028

Zheng, H., Zhao, H., Liu, H., Wang, J., and Zou, D. (2015). QTL analysis of Na^+ and K^+ concentrations in shoots and roots under NaCl stress based on linkage and association analysis in *japonica* rice. *Euphytica* 201, 109–121. doi: 10.1007/s10681-014-1192-3

Zhou, Y., Yang, P., Cui, F., Zhang, F., Luo, X., and Xie, J. (2016). Transcriptome analysis of salt stress responsiveness in the seedlings of Dongxiang wild rice (*Oryza rufipogon* Griff.). *PLoS ONE* 11:e0146242. doi: 10.1371/journal.pone.0146242

Conflict of Interest Statement: The authors declare that the research was conducted in the absence of any commercial or financial relationships that could be construed as a potential conflict of interest.

Advantages of publishing in Frontiers

OPEN ACCESS
Articles are free to read for greatest visibility and readership

FAST PUBLICATION
Around 90 days from submission to decision

HIGH QUALITY PEER-REVIEW
Rigorous, collaborative, and constructive peer-review

TRANSPARENT PEER-REVIEW
Editors and reviewers acknowledged by name on published articles

Frontiers
Avenue du Tribunal-Fédéral 34
1005 Lausanne | Switzerland

Visit us: www.frontiersin.org
Contact us: info@frontiersin.org | +41 21 510 17 00

REPRODUCIBILITY OF RESEARCH
Support open data and methods to enhance research reproducibility

DIGITAL PUBLISHING
Articles designed for optimal readership across devices

FOLLOW US
@frontiersin

IMPACT METRICS
Advanced article metrics track visibility across digital media

EXTENSIVE PROMOTION
Marketing and promotion of impactful research

LOOP RESEARCH NETWORK
Our network increases your article's readership